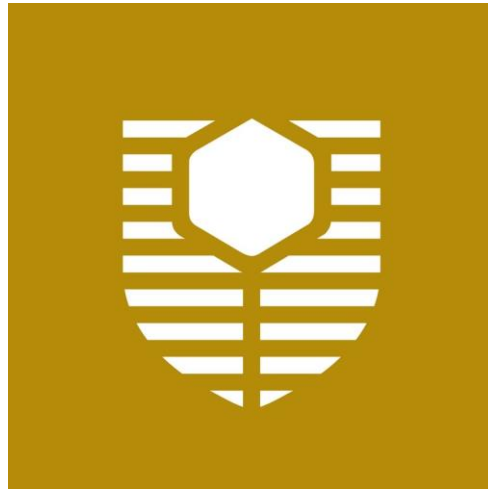


**Bacteriophage therapy for multi-drug
resistant *Staphylococcus aureus* infections
within the airways**



Curtin University: School of Population Health

Joshua James Iszatt

December 2023

Thesis declaration

This thesis has been produced during the enrolment period of this degree. It does not contain materials which have been submitted for award by any other institution nor will it, in future, be used for submission in my name for an award without the consent of Curtin University or its potential collaborators.

This thesis does not contain previously published data written by another person(s) except where due reference has been included and in the author declarations below.

All research involving human and animal resources has been approved by the Curtin University Human Resources Ethics Committee (HREC) and the telethon kids Animal Ethics Committee (AEC). Ethics approval letters can be located within the appendices (Appendices A-E).

The approval details are as follows:

Ethics committee	Description	Approval number
SJOG HREC	St John of God human research ethics committee approval	901
Curtin HREC	Curtin reciprocal human research ethics committee approval	HRE2019-0086
AEC	Animal ethics committee (TKI)	P2267
Curtin reciprocal AEC	Reciprocal animal ethics (Curtin)	ARE2023-15

This thesis contains work published and/or prepared for publication, all of which have been co-authored. The details of these works, its authors, and their approval/signatures can be found below under authorship declarations.

Name: Joshua James Iszatt

Signature: _____  _____ Date: ___18/12/2023_____

COPYRIGHT STATEMENT

I have obtained permission from the copyright owners to use any third-party copyright material reproduced in the thesis (e.g. questionnaires, artwork, unpublished letters), or to use any of my own published work (e.g. journal articles) in which the copyright is held by another party (e.g. publisher, co-author).

ABSTRACT

The emergence of multi-drug resistant (MDR) bacteria is recognised as one of the great challenges to public health. An especially dangerous bacterial pathogen, considered a high priority by the World Health Organisation, is *Staphylococcus aureus* (*S. aureus*), the MDR strains of which are known as methicillin-resistant *S. aureus* (MRSA). Whilst MRSA is associated with increased morbidity and mortality across many diseases, ranging from skin and soft tissue to blood and respiratory infections, prevalence is high in patients with cystic fibrosis (CF). As pathogens continue to develop resistance towards traditional antimicrobials, antibiotic development research has not been able to provide sufficient new options. Yet there has been an alternative solution existing within nature. Bacteriophages (phage) are obligate intracellular viruses that infect, replicate within, and often terminally lyse their host bacterium. Importantly, bacteriophages active against *S. aureus* have been isolated previously but their isolation frequency, when compared to bacteriophages targeting other prominent pathogens, is lower [1]. . Furthermore, safety profiles of bacteriophage in general have not been fully established, especially in the context of pulmonary infections. This project was established with the goal of addressing these points through two hypotheses. Hypothesis 1 was that bacteriophage can be isolated from the environment and exhibit *in vitro* activity against *Staphylococcus aureus*. Hypothesis 2 was that appropriately prepared bacteriophages do not induce cell death or inflammation when applied to *in vitro* and *in vivo* models of the airway.

Bacteriophages active against *S. aureus* were first isolated from samples of wastewater and breastmilk using a panel of *S. aureus* clinical isolates. Upon isolation, a pre-screen of activity against a subset of respiratory *S. aureus* was used to determine the host range of each phage. gDNA extractions were performed and samples sent for whole genome sequencing (WGS) using the Illumina short reads platform. Phage genomes were *de novo* assembled and screened for markers of virulence and integration to identify therapeutic candidates appropriate for phage therapy. High Pressure Liquid Chromatography (HPLC) was performed to purify the top 2 candidates, which were then used to conduct extended host range activity assays using MRSA and methicillin-sensitive *S. aureus* (MSSA) isolates from a range of clinical manifestations. Temperature and pH stability experiments were performed to complement phage characterisation profiles, followed by aerosolisation studies to

determine phage stability post-aerosolisation. Preclinical *in vitro* safety studies were conducted using a fully differentiated airway cell model whereby cellular damage, oxidative stress and inflammatory effects were all measured post phage delivery. Finally, *in vivo* safety and toxicity studies were performed whereby phages were administered to adult C57BL/6J mice via intranasal inoculation and mice were assessed for changes in weight, behaviour, and wellbeing. In addition, cellular inflammation in the mouse airways was quantitated via total and differential cell counts, and mediator production assessed using a Bio-Plex assay. Blood samples were analysed for gases, chemistry and other haematological parameters and necropsy performed to visually inspect the anatomy and key organs including the lungs post phage treatment.

Results: Hypothesis 1:

From these phage isolation efforts, there were a total of 38 bacteriophage from wastewater and a single bacteriophage from breastmilk active against a range of MRSA and MSSA isolates from the respiratory tract. Two of the 38 bacteriophages were genetically distinct and passed the genomics screening checks (Chapter 3). Both were predicted to have lytic lifecycles and to have broad host ranges making them attractive for phage therapy. Phages were given the following names: Koomba kaat 1 and Biyabeda mokiny 1. When examined using phylogenomic analyses it was found that both phages belong to the family *Herelleviridae*, from which many phages have been previously characterised for therapeutic activity. Both bacteriophage genomes were verified as complete genomic assemblies with high coverage (>500 X). Colinear comparisons showed that phage genomes had a similar genomic architecture to its closest relatives. Biyabeda mokiny 1 belongs to the well-studied *Kayvirus* genus (n = 107) and Koomba kaat 1 belongs to the more recently discovered *Silviavirus* genus (n = 31), the latter known for their exceptional ranges of activity.

Koomba kaat 1 and Biyabeda mokiny 1 were able to maintain effective plaque forming units for 1 year across three storage conditions (4°C, -20°C, and -80°C), with 4°C the optimal storage condition due to significantly better preservation of plaque forming units per mL

(PFU/mL). Both phages were resilient towards changes across pH 5 to pH 7 and also survived high temperatures up to 70°C. Transmission electron microscopic images of both Biyabeda mokiny 1 and Koomba kaat 1 confirmed a morphotype expected of their genus classification. When aerosolised, neither bacteriophage exhibited a significant reduction in PFU/mL ($p=0.05$, <0.1% titre drop). When phages were investigated for lytic activity against an in house *S. aureus* repository, it was found that both phages demonstrated lytic activity against >40% of isolates, irrespective of antibiotic resistance phenotype.

Results: Hypothesis 2:

In the safety analysis conducted, pseudostratified primary airway epithelial cells were challenged with Koomba kaat 1 and Biyabeda mokiny 1, as well as two heat inactivated respiratory MRSA strains SA1 and SA9. IL-8 ELISAs revealed that neither phage induced an inflammatory response from airway epithelial cells in either the apical or basolateral compartments. Using LDH assays it was further confirmed that the phages were nontoxic to airway epithelial cells. Together, these results demonstrate that phage would not be directly disruptive to the airway epithelium.

In the animal model study, intranasal administration of Koomba kaat 1 for two weeks caused small but significant increases of three mediators in the airway: IL-12(p40), IL-17, and IFN- γ , when compared with mock treatment but was not observed for Biyabeda mokiny 1. The remaining mediators did not differ between phage and control treatment groups. There was no significant effect of phage treatment on weight change, general health or behaviour, and no significant differences were observed in blood glucose, blood gasses, or mineral concentrations (iCa, K, Na) between phage groups and controls. Differential cell counts for macrophages or neutrophils found no significant difference between phage treatment groups and controls.

In summary, phages were successfully isolated that exhibit different but effective activity against *S. aureus* bacteria. Koomba kaat 1 and Biyabeda mokiny 1 were verified as safe therapeutic candidates with rigorous *in vitro* and *in vivo* safety analyses demonstrating

neither phage triggered harmful biological responses. Overall, this thesis expands upon prior work by identifying novel *S. aureus* bacteriophage that can be used for potential therapeutic application. More importantly, this work has highlighted the potential of phage therapy for the treatment of *S. aureus* infections within a pulmonary context and provided a representative pipeline of *in vitro* and *in vivo* models for assess safety of therapeutic phages.

Authorship declaration: Co-author publications:

This thesis contains work published and/or prepared for publication, all of which have been co-authored. The details of these works, its authors, and their approval/signatures can be found in the table below.

Title: Phage Therapy for Multi-Drug Resistant Respiratory Tract Infections

Description:

This manuscript reviews the current evidence supporting bacteriophage therapy as a treatment for multi-drug resistant bacterial infections. Specific focus is given to treatment within the respiratory context and the challenges which are associated. This includes delivery methods, current developments in animal models, and a summary of clinical trials performed to date. This work highlights the potential of bacteriophage therapy for respiratory infections and specifies the need for quality preclinical assessment within this field.


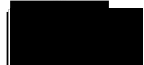




Location: This manuscript constitutes **Chapter One** of this thesis

Publication:

Iszatt, J. J., Larcombe, A. N., Chan, H.-K., Stick, S. M., Garratt, L. W., & Kicic, A. (2021). "Phage Therapy for Multi-Drug Resistant Respiratory Tract Infections". In: *Viruses* 13.9 (2021). issn: 1999-4915 (Electronic) 1999-4915 (Linking). doi: 10.3390/v13091809. [url:https://www.ncbi.nlm.nih.gov/pubmed/34578390](https://www.ncbi.nlm.nih.gov/pubmed/34578390).

Student contribution:

JJI was responsible for the manuscript's conception, creation, data generation, graphics illustration, and final editing including reviewer feedback. (70%).

Name	Sign	Date
Joshua J Iszatt		1/12/23
Alexander N Larcombe		26/07/2023
Hak-Kim Chan		26/07/2023
Stephen M Stick		26/07/2023
Luke W Garratt		26/07/2023
Anthony Kicic		26/07/2023

I, Benjamin Mullins certify that the student's statements regarding their contribution to each of the works listed above are correct.

Coordinating Chair's signature and date:
Page | VII



1/12/23

Authorship declaration: Co-author publications:

Title: Genome Sequences of Two Lytic *Staphylococcus aureus* Bacteriophages Isolated from Wastewater

Description:

This resource announcement described two lytic double-stranded (dsDNA) bacteriophages belonging to the family *Herelleviridae*. These were isolated from wastewater as part of this project and determined to be suitable therapeutic candidates for further analysis. The work within this paper demonstrates how data generated from whole genome sequencing (WGS) analysis can be used to guide the identification of lytic bacteriophage using previously published data as a guide.







Location: This manuscript constitutes **Chapter Three** of this thesis

Publication:

Iszatt, J. J., Larcombe, A. N., Garratt, L. W., Stick, S. M., Agudelo-Romero, P., Kicic, A. (2022). Genome Sequences of Two Lytic *Staphylococcus aureus* Bacteriophages Isolated from Wastewater. *Microbiology Resource Announcements*. 11(12): p. e0095422.

Student contribution:

JJI was responsible for the manuscript's conception, creation, data generation, graphics illustration, and final editing including reviewer feedback. (70%).

Name	Sign	Date
Joshua J Iszatt		1/12/23
Alexander N Larcombe		26/07/2023
Luke W Garratt		26/07/2023
Stephen M Stick		26/07/2023
Patricia Agudelo Romero		26/07/2023
Anthony Kicic		26/07/2023

I, Benjamin Mullins certify that the student's statements regarding their contribution to each of the works listed above are correct.

Coordinating Chair's signature and date:



1/12/23

Authorship declaration: Co-author publications:

Title: Genome Sequence of a Lytic *Staphylococcus aureus* Bacteriophage Isolated from Breast Milk

Description:

This Genome announcement is for Biyabeda mokiny 1, a lytic dsDNA bacteriophage isolated from breastmilk samples that test positive for the presence of *S. aureus* bacteria. This bacteriophage belongs to the Genus *Kayvirus* within the Family *Herelleviridae* and is one of the most effective bacteriophages isolated within this study.

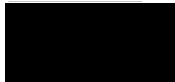


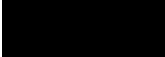



Location: This manuscript constitutes **Chapter Three** of this thesis

Publication:

Iszatt, J. J., Larcombe, A. N., Garratt, L. W., Trend, S., Stick, S. M., Agudelo-Romero, P., & Kicic, A. (2022). Genome Sequence of a Lytic *Staphylococcus aureus* Bacteriophage Isolated from Breast Milk. *Microbiology Resource Announcements*. 11(12): p. e0095322.

Student contribution:

JJI was responsible for the manuscript's conception, creation, data generation, graphics illustration, and final editing including reviewer feedback. (70%).

Name	Sign	Date
Joshua J Iszatt		1/12/23
Alexander N Larcombe		26/07/2023
Luke W Garratt		26/07/2023
Stephanie Trend		28/07/2023
Stephen M Stick		26/07/2023
Patricia Agudelo Romero		26/07/2023
Anthony Kicic		26/07/2023

I, Benjamin Mullins certify that the student's statements regarding their contribution to each of the works listed above are correct.

Coordinating Chair's signature and date:



1/12/23

List of figures

Number	Description	Page
1.1	Phage lifecycle	13
3.1	Plaque morphology	72
3.2	Average nucleotide identity scores for phages passing QC checkpoints	76
3.3	TEM images of BMP1, P1, and P7	82
4.1	Storage stability profiles for Koomba kaaat 1 and Biyabeda mokiny 1	99
4.2	Temperature and acid-base stability profiles for Koomba kaat 1 and Biyabeda mokiny 1	101
4.3	Host range activity against <i>S. aureus</i> isolates collected from different clinical sites	103
4.4	Dosage curves against host clinical isolates	105
4.5	Anti biofilm activity including biofilm disruption (panel A) and biofilm infection (panel B)	107
4.6	Phylogenetics network graph produced by vContact2	110
4.7	Phylogenetic tree using Unweighted Pair Group Method with Arithmetic Mean (UPGMA)	111
4.8	Co-linear alignment of Koomba kaat 1 against closest BLASTn relatives	114
4.9	Co-linear alignment of Biyabeda mokiny 1 against closest BLASTn relatives	115
4.10	Co-linear alignment of Koomba kaat 1 and Biyabeda mokiny 1 alongside <i>Staphylococcus</i> phages with known receptor binding proteins	117
5.1	Barrier integrity (TEER) assessments 24 hours post-exposure. to phages Koomba kaat 1 and Biyabeda mokiny 1	137
5.2	Alcian blue was quantified after 24 hours post-exposure	138
5.3	Haematoxylin and eosin-stained primary AECs collected from children and cultured at the air liquid interface	139
5.4	Alcian blue stained primary AECs collected from children and cultured at the air liquid interface	140
5.5	Quantification of LDH from the apical washings (A) and basolateral media (B) compartments of the primary AEC air-liquid interface cultures	142
5.6	Quantification of IL-8 in the apical washings (A) and basolateral media (B) compartments of the primary AEC air-liquid interface cultures	143
5.7	Weight change in male and female mice between day 1 and day 15 of treatment	145
5.8	Differential cell counts obtained from stained cytospin samples of BALf collected from mice	153
5.9	Quantification of total protein from mouse BALf.	154

List of tables

Number	Description	Page
2.1	Bacterial isolates	24
3.1	Positive hits from phage positive wastewater and breastmilk samples collected between January 2020 and November 2021	68
3.2	Phenotypic characterisations for each phage plaque isolation	70
3.3	Extracted gDNA samples, quality control metrics, and raw reads generated	73
3.4	Summary of contigs that passed assembly quality control checks and were extracted for further analysis	75
3.5	Phages identified as unique and the reasons why.	77
3.6	Annotation summary and coding capacity percentages for each phage genome.	78
3.7	Summary of the lysogeny warnings flagged within each phage genome.	79
3.8	Dimensions of phages BMP1, P1, and P7 as measured using TEM images	81
3.9	Host genome assembly statistics and prophage content.	83
4.1	Aerosol stability characteristics for Koomba kaat 1 and Biyabeda mokiny 1.	102
4.2	Phylogenetics analysis data from vContact2 for phages Koomba kaat 1 and Biyabeda mokiny 1	108
4.3	Closest relative genome statistics for Biyabeda mokiny 1 and Koomba kaat 1	112
5.1	Total average water and food consumption per day (mL/mouse per day and grams/mouse per day).	146
5.2	Mouse organ weights for the liver, spleen, and both kidneys.	148
5.3	Mouse blood and gas chemistry parameters across experimental groups and controls separated by sex	150
5.4	Mouse cytokine mediators across experimental groups and controls separated by sex	156

List of abbreviations:

AEC	Airway epithelial cells
AGRF	Australian Genomics Research Facility
ALI	Air-liquid interface
AMR	Antimicrobial resistance
ANI	Average nucleotide identity
ANOVA	Analysis of variance
AREST CF	Australian Respiratory Early Surveillance Team for Cystic Fibrosis
ASL	Airway surface liquid
ATCC	American Type Culture Collection
ATP	Adenosine triphosphate
AUC	Area under the curve
BAL	Bronchoalveolar lavage
BCA	Bicinchoninic acid
BCC	<i>Burkholderia cepacia</i> complex
BEBM	Bronchial epithelial basal medium
BSA	Bovine serum albumin
CCM	Conditionally reprogrammed culture media
CDC	Centers for Disease Control and Prevention
CDS	Coding sequence
CEB	Cell extraction buffer
CF	Cystic fibrosis
<i>CFTR</i>	Cystic fibrosis transmembrane conductance regulator
CFU	Colony forming unit
CFWA	Cystic Fibrosis Western Australia
CLSI	Clinical and Laboratory Standards Institute
COMET	Characterisation of Milk after preterm birth
COPD	Chronic obstructive pulmonary disease
CV	Column volumes
DMEM	Dulbecco's Modified Eagle Medium
DMSO	Dimethyl sulfoxide
EDTA	Ethylenediaminetetraacetic acid
EGF	Epidermal growth factor
EGTA	Ethylene glycol-bis(β -aminoethyl ether)-N,N,N',N'-tetraacetic acid
ELISA	Enzyme-linked immunosorbent assay
EOP	Efficiency of plating
EVOM	Transepithelial volt/ohm meter
FCS	Foetal calf serum
FPF	Fine particle fraction
GAS	Group A Streptococci

GBS	Group B Streptococci
GC	Guanine-cytosine content
GMP	Good manufacturing practice
HBSS	Hank's balanced salt solution
HC	Hydrocortisone
HEPES	4-(2-hydroxyethyl)-1-piperazineethanesulfonic acid
HMM	Hidden Markov Model
HPLC	High pressure liquid chromatography
HREC	Human Research Ethics Committee
ICTV	International Committee on Taxonomy of Viruses
IFN	Interferon
IL	Interleukin
KC	Kill curves
LB	Luria-Bertani broth
LDH	Lactate dehydrogenase assay
LTA	Lipoteichoic acids
LRTI	Lower respiratory tract infection
MDR	Multi-drug resistant
MGE	mobile genetic element
MIC	minimum inhibitory concentration
MOI	Multiplicity of infection
MRSA	Methicillin-resistant <i>Staphylococcus aureus</i>
MSSA	Methicillin-sensitive <i>Staphylococcus aureus</i>
NATA	National Association of Testing Authorities
NBF	Neutral buffered formalin
NCBI	National Centre for Biotechnology Information
OD	Optical density
OGTR	Office of the gene technology regulator
ONC	Overnight cultures
ORF	Open reading frame
PBP2	Penicillin binding protein 2
PBS	Phosphate buffered saline
PCR	Polymerase chain reaction
PEV	Peak expiratory volume
PFU	Plaque forming units
PGFE	Pulsed field gel electrophoresis
PHROG	Prokaryotic Virus Remote Homologous Groups
QC	Quality control
RBP	Receptor binding protein
RT	Room temperature
SJOG	Saint John of God
SNP	Single nucleotide polymorphism

TEER	Trans-Epithelial Electrical Resistance
TEM	Transmission electron microscopy
TKI	Telethon Kids Institute
TSA	Tryptic soy agar
TSB	Tryptic soy broth
UPGMA	Unweighted paired group mean analysis
UV	Ultraviolet
VISA	Vancomycin intermediate <i>S. aureus</i>
VRSA	Vancomycin resistant <i>S. aureus</i>
VSSA	Vancomycin sensitive <i>S. aureus</i>
WAERP	Western Australian Epithelial Research Program
WGS	Whole genome sequencing
WHO	World Health Organisation
WTA	Wall teichoic acids

Presentations arising from this project:

2020:

Iszatt JJ, Vaitekenas A, Larcombe AN, Garratt LW, and Kicic A on behalf of WAERP, and AREST-CF. Can bacteriophage therapy provide an alternative treatment for *Staphylococcus aureus* infections in patients with Cystic Fibrosis?

National conference poster presentation: Australian Institute of Medical Scientists (AIMS) / Australian Society for Microbiology (ASM) Joint Scientific Meeting. November, 2020

2021:

Iszatt JJ, Garratt LW, Larcombe AN, Chang B, Tai A, Stick SM, and Kicic A on behalf of WAERP, and AREST-CF. Novel bacteriophage active against *Staphylococcus aureus* from individuals with Cystic Fibrosis exhibit variable lytic capabilities.

International oral presentation: Australasian Cystic Fibrosis (ACF) conference, May 2021.

Iszatt JJ, Ng R, Vaitekenas A, Poh MWP, Laucirica DL, Mclean S, Hillas J, Garratt LW, Larcombe AN, Stick SM, and Kicic A on behalf of WAERP, and AREST-CF. Improved isolation yields for bacteriophage active against *Staphylococcus aureus*. (Published ECFS 2021 abstracts: P151, *Journal of Cystic Fibrosis*, 2021; doi:10.1016/S1569-1993(21)01177-2).

International conference poster presentation: European Cystic Fibrosis Society (ECFS), June 2021.

Iszatt JJ, Garratt LW, Larcombe AN, and Kicic A on behalf of WAERP, and AREST-CF. Can bacteriophage treat *Staphylococcus aureus* infections in people with Cystic Fibrosis? *Respirology*, 2021. 26(S2): p. 88-21-122. <https://doi.org/10.1111/resp.14021>

National conference presentation: The Thoracic Society of Australia and New Zealand (TSANZ). Annual Scientific Meeting, May 2021.

Iszatt JJ, Garratt LW, Larcombe AN, Stick SM, and Kicic A on behalf of WAERP, and AREST-CF. Improved isolation yields for bacteriophage active against *Staphylococcus aureus* bacteria from children with Cystic Fibrosis. *Journal of Cystic Fibrosis*, 2021. 20: p. S85.

National poster presentation: The Thoracic Society of Australia and New Zealand Western Australia (TSANZ-WA). Annual Scientific Meeting, July 2021

Iszatt JJ, Larcombe AN, Garratt LW, and Kicic A on behalf of WAERP, and AREST-CF. Addressing antimicrobial resistance with Bacteriophage Therapy.

Local oral presentation: Telethon Kids Seminar Series, August 2021.

Iszatt JJ, Garratt LW, Larcombe AN, and Kicic A on behalf of WAERP, and AREST-CF. Can bacteriophage infect MRSA biofilms?

Local oral presentation: Telethon Kids Institute Student Symposium, November 2021

2022:

Iszatt JJ, Agudelo-Romero P, Ng R, Vaitekenas A, Garratt LW, Larcombe AN, and Kicic A on behalf of WAERP, and AREST-CF. Characterisation of a *Staphylococcus aureus* bacteriophage (SAB9) with therapeutic potential. *Respirology*, 2022. 27(S1): p. 88-220.

National conference e-poster presentation. The Thoracic Society of Australia and New Zealand Annual Scientific Meeting, March 2022.

Iszatt JJ, Garratt LW, Larcombe AN, and Kicic A on behalf of WAERP, and AREST-CF. Characterisation of therapeutic bacteriophage candidates.

Local conference poster presentation: The Thoracic Society of Australia and New Zealand Western Australia (TSANZ-WA). Annual Scientific Meeting, August 2022

Iszatt JJ, Larcombe AN, Garratt LW, and Kicic A. In-silico Characterisation of a novel bacteriophage endolysin K1EN2.

Local conference oral presentation: Perth Protein Group (PPG), Annual General Meeting, October 2022.

Iszatt JJ, Larcombe AN, Garratt LW, and Kicic A. Can bacteriophage remove MRSA biofilms?

Local oral presentation: New Investigator Award (NIA): Wal-yan Scientific Retreat, Rottneest, October 2022.

Iszatt JJ, Garratt LW, Larcombe AN, Agudelo-Romero P, and Kicic A on behalf of WAERP, and AREST-CF. Bacteriophage Cocktail for Multi-drug Resistant *Staphylococcus aureus*.

International conference poster presentation: International Congress of Antimicrobial Chemotherapy (ICC), November 2022.

2023:

Iszatt JJ, Larcombe AN, Garratt LW, and Kicic A. Identification of appropriate *Staphylococcus aureus* bacteriophages for the pulmonary environment.

Community presentation: CFWA Parents Retreat (Bunbury), March 2023.

Iszatt JJ, Larcombe AN, Garratt LW, and Kicic A. Phage genomics at the Telethon Kids Institute.

Community presentation: CFWA Annual General Meeting, June 2023.

Funding sources:

2020: Curtin International Postgraduate Research Scholarship (CIPRS) and Research Stipend Scholarship: This is a three-year fee offset and base stipend scholarship awarded before the confirmation of PhD candidature by Curtin University, Perth, Western Australia, Australia.

2020: Golf PhD Top Up Scholarship: This was awarded by Cystic Fibrosis Western Australia, Perth, Western Australia, Australia.

Awards:

2022: New Investigator Award: Wal-yan Scientific Retreat, Rottnest, October 2022.

2022: Runner up, Best Presentation: Perth Protein Group (PPG), Annual General Meeting, October 2022.

Acknowledgments

Professional

I would like to acknowledge the study participants and their families who have supported and participated the WAERP study. I want to acknowledge the staff at St John of God hospital including the doctors and nurses' contributions towards sample collection. I would also like to thank Dr Angela Fuery, Dr Elizabeth Kicic-Starceвич and Ms Amy Greenly for participant recruitment. I would also like to thank Dr Patricia Agudelo-Romero for her patience in teaching our team bioinformatics analysis concepts and applications. I would also like to thank the Water Corporation of Western Australia for providing wastewater samples from the Subiaco Wastewater Treatment Plant. I am grateful towards: Dr Anna Tai, Dr Papanin Putsathit, Professor Scott Bell, Dr Tim Barnet, Dr Lucy Furfaro, Professor Geoffrey Coombs, and Associate Professor Christopher Peacock for their donation of the bacterial clinical isolates used in this study.

For the epithelial team members, I would like to extend my thanks in welcoming me to Australia when I first arrived. I have received the utmost support from every member of the team and weekly feedback at the team meetings.

For my supervisors, Associate Professor Anthony Kicic, Dr Luke Garratt, and Associate Professor Alexander Larcombe, I would like to express my thanks in helping me in so many ways to complete this journey. Specifically, I would like to thank Associate Professor Anthony Kicic for starting me on this journey and for setting an incredible example for work ethic. Without this PhD; I would have been stuck in the UK during the worst of the COVID-19 pandemic, so I would also like to thank you for facilitating my Brexit early. My sincerest thanks to Dr Luke Garratt, whose patience in helping me perform unfamiliar tasks has helped me to build my skillset and understand cell culture models from a practical perspective. In speaking of unfamiliar tasks, I would like to thank Associate Professor Alexander Larcombe for training me in the multitude of tasks required to conduct the animal experiments.

Familial

To Alexia Foti and the family, thank you for being the most unconditionally kind people I have ever met. I am lucky to be welcomed to Sunday lunch each week, and I'm sincerely thankful for the board games, endless coffee (sometimes with ice cream...?), and chats that come with it.

To Andrew Vaitekenas, I was unsure whether to place you into the professional or familial... for sake of argument, here we are... (kidding!). I'm glad you've been able to put up with my madness for so long. I genuinely appreciate it. I think my favourite memories of us will always include heading to various parties dressed as bacteria, phages, power puff girls, and even Snow White.

To Ruben Pineiro Sanchez, thank you for being my coach throughout this time and getting me through two of the most intense fights I've ever had. You have a true understanding of what it means to believe in yourself and it's simply inspiring to be around. Thank you.

To Jonyar, Chris, and Sara back home, I cannot thank you enough for staying in contact and checking in. You are the greatest friends I could ask for and I cannot wait to tell you all about the adventures I've had here in Australia. We'll play some speed runners and watch some Vikings when I'm back!

To my lifelong friends Fred and Tyler, it's hard to express how grateful I am that you guys have always been there for me. We have been through so much together and I am fortunate to have you. One day soon I know we'll crack open a case of brew dog, chat about the memories we share, and plan for more each year.

To Jess, you have always supported me in the pursuit of my goals, regardless of what they are. Whilst this applies to many members of our family, and I am sincerely grateful... the reason I made it here to Australia is because of you. I just sometimes wish you wouldn't set the bar so high each year... but I'm always happy you do. For this and much more, I am truly proud to be your brother.

Table of Contents

Chapter 1: Literature review	- 1 -
1.1. The Antimicrobial Resistance Crisis	- 1 -
1.1.1. Introduction: the not so ‘Silent pandemic’	- 1 -
1.1.2. Priority pathogens.....	- 2 -
1.2. Respiratory tract infections.....	- 4 -
1.2.1. Infection sites within the respiratory system	- 4 -
1.2.2. Cystic fibrosis.....	- 5 -
1.3. <i>Staphylococcus aureus</i>	- 7 -
1.3.1. Overview: Diversity and pathogenesis	- 7 -
1.3.2. Adaptation to the respiratory tract.....	- 8 -
1.4. Current research and development pipelines.....	- 9 -
1.4.1. Immunotherapies: Vaccines and Monoclonal antibodies.....	- 10 -
1.4.2. Nanoparticles	- 12 -
1.5. Phage therapy for <i>Staphylococcus</i> bacteria	- 12 -
1.5.1. Preclinical data generation	- 14 -
1.5.2. Pulmonary implementation	- 15 -
1.5.3. Modelling phage activity within the airways	- 18 -
1.5.4. Clinical uses of phage against <i>Staphylococcus aureus</i>	- 22 -
1.5.5. Summary	- 22 -
1.5.6. Hypotheses	- 23 -
Chapter 2: Materials and methods	- 24 -
2.1. Bacterial isolates:.....	- 24 -
2.2. General equipment:	- 27 -
2.2.1. Pipettes:	- 27 -
2.2.2. Pipettor:	- 27 -
2.2.3. Biosafety cabinets:.....	- 28 -
2.2.4. Fumigation hoods:	- 28 -
2.2.5. Flasks and Schott bottles:	- 28 -
2.2.6. Heating blocks:.....	- 28 -
2.2.7. Centrifuges:	- 29 -
2.2.8. Scales and balances:	- 29 -
2.2.9. Microscopes:.....	- 29 -
2.2.10. Calibration: pH:	- 29 -

2.2.11.	Plate readers:.....	- 29 -
2.2.12.	Orbital shakers and stirring:.....	- 30 -
2.2.13.	Water baths:	- 30 -
2.2.14.	NanoDrop 2000:	- 30 -
2.2.15.	Electrophoresis:	- 30 -
2.2.16.	Qubit™ fluorometer:	- 31 -
2.2.17.	Bead beating:	- 31 -
2.2.18.	Bacterial incubator:.....	- 31 -
2.2.19.	Dry oven for molten overlay agar:.....	- 31 -
2.2.20.	Mesh nebuliser:.....	- 31 -
2.2.21.	High Pressure Liquid Chromatography:	- 32 -
2.2.22.	Transepithelial volt/ohm meter (EVOM):.....	- 32 -
2.2.23.	Blood gas and chemistry:.....	- 32 -
2.2.24.	Anaesthesia delivery system:.....	- 32 -
2.2.25.	Mechanical ventilation:.....	- 33 -
2.2.26.	Long read sequencing:	- 33 -
2.2.27.	Gamma cell Irradiation:	- 33 -
2.3.	Consumables:.....	- 33 -
2.3.1.	Coating Buffer (AECs):	- 33 -
2.3.2.	Cryopreservation Solution:	- 33 -
2.3.3.	Foetal Calf Serum (FCS):	- 34 -
2.3.4.	FCS-Based Trypsin Neutralising Solution:.....	- 34 -
2.3.5.	Fibronectin Coating Buffer:	- 34 -
2.3.6.	NIH-3T3 Co-Culture Growth Medium:.....	- 34 -
2.3.7.	Conditionally-Reprogrammed Culture Medium (CCM):	- 35 -
2.3.8.	Penicillin/Streptomycin:	- 35 -
2.3.9.	ROCK Inhibitor:	- 35 -
2.3.10.	Subculture Reagent Pack:	- 35 -
2.3.11.	Trypan Blue Solution (0.05% v/v):.....	- 36 -
2.3.12.	Anaesthetics:.....	- 36 -
2.3.13.	SM buffer:.....	- 36 -
2.3.14.	Tryptic Soy broth (TSB) preparations:	- 36 -
2.3.15.	Tryptic Soy agar (TSA) preparation:	- 37 -
2.3.16.	Tryptic Soy overlay (0.5% w/v) agar (TS-overlay agar):	- 37 -

2.3.17.	Magnesium chloride (MgCl ₂ : 1 M) solution:	- 37 -
2.3.18.	Calcium chloride (CaCl ₂ : 1 M) solution:.....	- 37 -
2.3.19.	Phosphate buffer solution (PBS) (Cell culture):.....	- 38 -
2.3.20.	Bacteriological petri dishes:	- 38 -
2.3.21.	Tissue culture plastic materials:.....	- 38 -
2.3.22.	Double deionized water (ddH ₂ O):	- 38 -
2.3.23.	Bovine Serum Albumin (BSA):.....	- 38 -
2.3.24.	Ethanol (70% v/v):	- 39 -
2.3.25.	Glycerol (50% v/v):.....	- 39 -
2.3.26.	Hank's Balanced Salt Solution (HBSS):.....	- 39 -
2.3.27.	Hydrochloric Acid (HCl: 1 M):	- 39 -
2.3.28.	Neutral Buffered Formalin (NBF: 10% v/v):	- 39 -
2.3.29.	Sodium Deoxycholate Solution (10% w/v):.....	- 40 -
2.3.30.	Sodium Hydroxide Solution (0.2 M):.....	- 40 -
2.3.31.	Sodium Hydroxide Solution (1 M):.....	- 40 -
2.3.32.	Tris Buffered Saline (TBS):.....	- 40 -
2.3.33.	Tris(hydroxymethyl)aminomethane hydrochloride (Tris-HCl: 1 M):	- 41 -
2.3.34.	Triton-X-100 Solution (10% v/v):	- 41 -
2.3.35.	Cell extraction buffer (CEB):	- 41 -
2.4.	Methods:	- 41 -
2.4.1.	Glycerol stock preparations for bacterial isolates:.....	- 41 -
2.4.2.	Bacterial Culturing:	- 42 -
2.4.3.	Overnight cultures (ONCs):	- 42 -
2.4.4.	Measurement of Bacterial Density Using OD _{600nm} :.....	- 42 -
2.4.5.	Measurement of Viable Bacterial Load Using Colony Forming Units per Millilitre (CFU/mL):.....	- 42 -
2.4.6.	Preparation of inoculated Overlay Agar plates:.....	- 43 -
2.4.7.	Wastewater pre-processing	- 43 -
2.4.8.	Phage Enrichment (stepwise process)	- 43 -
2.4.9.	Phage isolation rounds (stepwise process)	- 44 -
2.4.10.	Short Read DNA Extraction and Sequencing:.....	- 44 -
2.4.11.	Host range assay	- 45 -
2.4.12.	Phage Propagation: plate elution method (stepwise process).....	- 45 -
2.4.13.	Phage titration (stepwise process):	- 46 -
2.4.14.	Efficiency of Plating (EOP):.....	- 47 -

2.4.15.	Kill-curves / Dosage curves:.....	- 47 -
2.4.16.	NIH-3T3 Cell Line:	- 47 -
2.4.17.	Irradiation of Fibroblasts:	- 47 -
2.4.18.	Cell Line Recovery:	- 48 -
2.4.19.	Cell Line Subculture:	- 48 -
2.4.20.	Cell Counts and Viability:.....	- 49 -
2.4.21.	Primary airway epithelial cell storage.....	- 49 -
2.4.22.	Primary airway epithelial cell recovery	- 49 -
2.4.23.	Mycoplasma Testing of cell lines and pAECs	- 50 -
2.4.24.	BCA assay:.....	- 50 -
2.4.25.	High Pressure Liquid Chromatography	- 50 -
2.4.26.	Anion-exchange column cleaning.....	- 51 -

Chapter 3: Identification and genomic screening of *Staphylococcus* bacteriophages with therapeutic potential against respiratory isolates of *Staphylococcus aureus* bacteria - 52 -

3.1.	Introduction:.....	- 52 -
3.2.	Materials and methods:	- 54 -
3.2.1.	Bacterial strains used for the isolation of <i>S. aureus</i> bacteriophage:.....	- 54 -
3.2.2.	Wastewater processing:.....	- 54 -
3.2.3.	Direct plating method (unenriched).....	- 54 -
3.2.4.	Enrichment of potential phages in wastewater	- 54 -
3.2.5.	Visual indication of phage	- 55 -
3.2.6.	Phage purifications via plaque excision.....	- 55 -
3.2.7.	Plaque characterisations.....	- 55 -
3.2.8.	Phage isolations from breastmilk:.....	- 56 -
3.2.9.	Phage DNA extraction	- 56 -
3.2.10.	Sequencing.....	- 57 -
3.2.11.	Phage assembly pipeline	- 57 -
3.2.12.	Manual curation of phage assembly data.....	- 60 -
3.2.13.	Genome annotation and reordering.....	- 61 -
3.2.14.	Lifecycle analysis.....	- 61 -
3.2.15.	Screening for virulence factors	- 61 -
3.2.16.	Assessment of microdiversity / population diversity.....	- 62 -
3.2.17.	Taxonomic classification:	- 62 -
3.2.18.	Transmission electron microscopy:.....	- 62 -
3.2.19.	Host genome analysis:	- 63 -

3.2.20.	Host contamination.....	- 65 -
3.2.21.	Generalised transduction	- 65 -
3.3.	Results	- 65 -
3.3.1.	Phage isolation.....	- 65 -
3.3.2.	Plaque morphology.....	- 66 -
3.3.3.	DNA extraction.....	- 67 -
3.3.4.	Phage genomes	74
3.3.5.	Average nucleotide identity (%) scores	76
3.3.6.	Unique phage identification.....	77
3.3.7.	Therapeutic checkpoints: lifecycle, virulence, gene content	78
3.3.8.	Annotation	78
3.3.9.	Lifecycle analysis	79
3.3.10.	Population diversity:.....	80
3.3.11.	Phage taxonomy and morphotype	80
3.3.12.	Host genome analysis	83
3.3.13.	Phage naming	83
3.4.	Discussion:	84

Chapter 4: Characterising Koomba kaat 1 and Biyabeda mokiny 1 phages for respiratory implementation against *Staphylococcus aureus* from cystic fibrosis..... 91

4.1.	Introduction:	91
4.2.	Materials and methods:.....	92
4.2.1.	Bacterial isolates and phage propagation	92
4.2.2.	High Pressure Liquid Chromatography	92
4.2.3.	Stability assessments	93
4.2.4.	Lytic activity assessment	94
4.2.5.	Comparative genomics analysis	96
4.2.6.	Statistical analysis	98
4.3.	Results	98
4.3.1.	Storage.....	98
4.3.2.	High temperature	101
4.3.3.	pH.....	101
4.3.4.	Nebulisation.....	103
4.3.5.	Lytic activity assessments.....	104
4.3.6.	Antibiofilm activity	107
4.3.7.	Comparative genomics analyses.....	109

4.3.8.	Identification of receptor binding proteins.....	117
4.3.9.	Machine learning RBP detection	117
4.3.10.	Comparison and alignment to phages with known RBPs	117
4.4.	Discussion.....	119
Chapter 5: Preclinical safety assessment of Koomba kaat 1 and Biyabeda mokiny 1 phages		126
5.1.	Introduction:.....	126
5.2.	Materials and methods:.....	127
5.2.1.	Bacterial isolates and phage propagation.....	127
5.2.2.	High Pressure Liquid Chromatography	128
5.2.3.	Preparation of <i>S. aureus</i> for primary airway epithelial cell exposure	128
5.2.4.	Enterotoxin screen	129
5.2.5.	WAERP Participant demographics	129
5.2.6.	Primary airway epithelial cell collection	129
5.2.7.	Primary airway epithelial cell processing	130
5.2.8.	Primary airway epithelial cell co-culture	130
5.2.9.	Primary airway epithelial growth at the air liquid interface	131
5.2.10.	Primary airway epithelial cell exposures	131
5.2.11.	Primary airway epithelial cell staining and histology	132
5.2.12.	Quantification of Alcian Blue Stain.....	133
5.2.13.	Transepithelial Electrical Resistance	133
5.2.14.	Cell viability (LDH assay).....	133
5.2.15.	IL-8 ELISA	134
5.2.16.	Mouse exposure model	134
5.2.17.	<i>In vivo</i> sample collection and analysis.....	135
5.2.18.	Statistical analyses	136
5.3.	Results:.....	137
5.3.1.	Phages Koomba kaat 1 and Biyabeda mokiny 1 phages were successfully purified using HPLC.	137
5.3.2.	Primary airway epithelial cell integrity is not adversely affected by Koomba kaat 1 or Biyabeda mokiny 1 phages.....	137
5.3.	Primary airway epithelial cell mucus production is not influenced by Koomba kaat 1 or Biyabeda mokiny 1 phages.	139
5.4.	Phages Koomba kaat 1 and Biyabeda mokiny 1 are nontoxic and noninflammatory towards airway epithelial cells <i>in vitro</i>	142
5.4.2.	Airway implementation of Koomba kaat 1 and Biyabeda mokiny 1 does not induce pathology in a respiratory mouse model.	145

5.4 Discussion	159
Chapter 6: General discussion	168
6.1. Thesis summary:.....	168
6.1.1. Genomics: whole genome sequencing	169
6.1.2. Sample purification and storage	170
6.1.3. Therapeutic phages: safety	172
6.1.4. Data: storage and manipulation	173
6.2. Phages for <i>Staphylococcus</i> species:.....	174
6.2.1. Phage training.....	175
6.2.2. Genetically modified phages	176
6.3. How can bottlenecks in phage characterisation be addressed?	177
6.3.1. High throughput study design.....	178
6.3.2. Predictive capacity: Machine learning	179
6.4. Preclinical models of phage activity.....	180
6.4.1. Biofilms and Intracellular switches	182
6.4.2. How can challenges in modelling phage interactions be overcome?	183
6.5. Translation of phages into clinical care	184
6.6. Phage resistance.....	186
6.7. Study progressions and limitations.....	188
6.8. Contributions to the field.....	189

Chapter 1: Literature review

1.1. The Antimicrobial Resistance Crisis

1.1.1. Introduction: the not so ‘Silent pandemic’

Bacteria and other microorganisms can evolve resistance to medications (antimicrobials) which is primarily driven by prolonged or inappropriate use of antimicrobials. Antimicrobial resistance (AMR) is a global, multifaceted issue which has been termed a ‘silent pandemic’ due to the lack of public interest and general ineffectual calls to action [2, 3]. The rise of AMR has been facilitated by economic factors making antimicrobials attractive to use in multiple industries, the ‘inefficiencies’ of preparing for future scenarios of resistance that may never eventuate [4], and a lack of public interest [5, 6], which may reflect a failure in producing coherent narratives concerning AMR definitions, priorities, thresholds, and global indicators of success [7]. The predominant narrative concerning AMR is that the current treatments are becoming ineffective and, without coordinated efforts to prevent rise of resistance, commonly treatable infections will become life threatening once more [8, 9]. Exacerbating the issue further is that in the age of global pandemics, targeting the spread of AMR requires a coordinated global effort. Yet less economically developed countries present a triple threat to AMR including a lack of surveillance for resistance, availability of antimicrobial compounds without the need for prescription [8], and the allocation of resources based on purchasing capacity [4].

A widely discussed global review of AMR, commissioned in the UK in 2014 [10], examined the results from two global research teams to provide data concerning the growing economic burdens of AMR [11]. Despite the concerning and widely cited figures, with the primary implications predicting 10 million deaths per year by the year 2050, many medical professionals consider the secondary effects of AMR to be of greater risk [10, 11]. Secondary implications include decreased efficacy of prophylactic antibiotic usage during surgical procedures and chemotherapy, needed to prevent infections at the surgical site and in scenarios where the host immune system is suppressed [10]. Essentially, if antibiotics become ineffective, these procedures will greatly affect populations regardless of economic

Page | - 1 -

climate and once again, infections will be the greatest cause of human death. Whilst a future such as this sounds dystopic, a lack of actionable support in the face of compounding evidence to date has supported the rise of AMR over the last two decades [12-14] and reflect an ongoing general failure to recognise enormity of the situation [15]. The COVID-19 pandemic demonstrated the global capacity for fast, deliberate, and yet highly disruptive actions in response to an immediate threat to public health and simultaneously underscored the complete lack of true pandemic preparedness [4, 16]. In an ironic twist, efforts to address AMR development such as antibiotic stewardship were also negatively impacted by the overprescription of antibiotics during the COVID-19 pandemic [17].

Collectively, the ‘silent pandemic’ of AMR continues to grow, and the world continues to remain unprepared. To address this, the World Health Organisation (WHO) and the Centres of Disease Control and Prevention (CDC) have published lists of priority pathogens [18, 19]. As the human population is estimated to rise to 9.7 billion by the year 2050 [20], such population density is expected to contribute to the number of epidemics and pandemics and the need for innovative solutions is unlikely to decline. Our ability to ‘outwit’ the natural world is being tested; the use of antimicrobial compounds (natural and artificial) in healthcare and agricultural settings in response to diseases and unsanitary conditions is the highest it has ever been and their use is expected to continue to grow [21, 22].

1.1.2. Priority pathogens

In the most recent comprehensive AMR report released by Murray et al in 2022, it was estimated that there were 4.95 million deaths annually associated with bacterial AMR [14]; further supporting previous predictions published in 2014 [10]. Six major bacterial pathogens were identified in the report as collectively causing the highest number of AMR related deaths (929,000) [14]: *Escherichia coli*, *Staphylococcus aureus*, *Klebsiella pneumoniae*, *Streptococcus pneumoniae*, *Acinetobacter baumannii*, and *Pseudomonas aeruginosa*. In terms of resistant phenotypes, these bacteria are commonly associated with resistance to multiple classes of antibiotics, and are frequently termed multi-drug resistant (MDR)

pathogens [9]. These species also feature amongst the 12 species of bacteria categorised by WHO in 2017 [23] warranting urgent development of novel antimicrobials. These initiatives served to frame the allocation of resources and efforts by the medical and pharmaceutical community [14] and identify target objectives for improvement [24]. These improvements include infection control via sanitation in health care facilities and the community, better antibiotic stewardship, research and development of new antimicrobials and diagnostic tools, awareness and education, and surveillance of pathogens through national and global surveillance systems [24]. It is also essential to understand genetic adaptations that enable MDR. To support these efforts and facilitate effective collaboration, the WHO introduced the Guiding Principles for Pathogen Genome Data Sharing [25]. This framework offers guidance to researchers, epidemiologists, and public health officials on how to share pathogen genome data in ‘as close to real time as possible’ [25]. Fortunately, the growing accessibility to cost effective genetic sequencing techniques is serving to be a key tool in the battle against MDR seen in emerging resistant pathogens.

However, MDR infections are not equally distributed across sites within the body; instead, infections within the respiratory system (including thorax), bloodstream, and intra-abdominal regions collectively accounted for 78.8% of deaths attributed to AMR in 2019, with lower respiratory infections alone responsible for approximately 31.5% (400,000) of deaths attributable to resistance [14]. Interestingly, despite the expectation that higher antibiotic consumption in high-resource settings (more economically developed countries) would correspond to a greater burden of bacterial AMR, the highest rates of death were found in sub-Saharan Africa and south Asia [14]. This discrepancy is due to a combination of resistance prevalence and the frequency of infection within the lower respiratory tract, bloodstream, and intra-abdominal area, which tend to be more prevalent in these regions [14].

1.2. Respiratory tract infections

1.2.1. Infection sites within the respiratory system

The respiratory tract has emerged as an especially susceptible site for MDR bacterial infections. The components of the respiratory system can be broadly separated into upper and lower airways, or the nasopharynx and lungs respectively [26]. Currently, lower respiratory tract infections (LRTIs) are the 4th leading cause of death worldwide and are the greatest communicable form of disease on the planet [27]. Of the total 2,604,000 deaths caused by respiratory infections in 2019, 2,593,000 (99.58%) of these were infections in the lower respiratory tract [27]. In addition to mortality, LRTIs cause severe decreases in respiratory quality of life, estimated at 103 million LRTI disability adjusted life-years [12, 28]. The trajectory of these statistics is not improving, and an estimate suggests that the median number of attributable deaths caused by MDR respiratory infections has more than doubled from 2007 to 2015 [13]. This rise in antibacterial resistance has occurred in parallel with dramatic decreases in the number of promising antibiotic pipelines; likely due to the lack of pharmaceutical investment into products that may become obsolete within short timeframes [4, 29].

As for all communicable diseases, some cohorts are at greater risk of infection. Any form of immunocompromised phenotype, whether from a muco-obstructive disorder, organ transplant, or chemotherapy, increases the chances of acquiring bacterial respiratory tract infections [30]. As well as greater risk of acquisition, lung infections in immunocompromised individuals can persist to months or longer, which provides the organisms additional opportunities to employ or develop resistance mechanisms to standard antibiotic treatments [31]. Chronic respiratory tract infection and subsequent inflammatory exacerbations are a major concern for individuals with conditions such as Chronic Obstructive Pulmonary Disease (COPD), a condition that resulted in the deaths of over 3 million people in 2019 [27, 32]. Beyond COPD, the rare but severe disease cystic fibrosis (CF) is also characterised by great risk of acquiring AMR respiratory infections and this population is uniquely vulnerable to the benefits and risks of antibiotic treatment.

1.2.2. Cystic fibrosis

Cystic fibrosis is an autosomal recessive genetic disorder which is characterised by cystic fibrosis transmembrane conductance regulator (*CFTR*) dysfunction, and whilst this can arise from a number of different mutations that cause *CFTR* abnormalities, the most common mutation is *Phe508del* [33, 34]. Unfortunately, this disorder is lethal and affects approximately 80,000 people worldwide [33]. The highest prevalence of CF is in Europe, Australia, and North America due to the genetic ties these populations have with northern Europe. The *CFTR* protein is a chloride ion channel that contributes to normal ion flow across epithelial cell surfaces. When disrupted, a thickening of mucosal surfaces in organs such as the lungs creates an environment that is beneficial to bacteria and obstructive to effective host immunity [35]. Progressive lung failure is the major cause of mortality and improvements in survival thus far have been achieved by managing chronic pulmonary infections, which are the predominant drivers of lung function decline. Appropriate strategies have been built upon understanding the muco-obstructive nature of CF, the importance of aiding airway clearance using mucolytic agents and treating infections aggressively and from a young age. Today CF patients are aided by multidisciplinary teams and this effective care strategy along with new *CFTR* specific medications has led to increasing number of adults surviving with CF [35, 36].

CF lung pathology is noted to follow a predictable course of infection with the predominant organisms being *S. aureus* and *Haemophilus influenzae* first detected during early childhood, followed by persistent infections with *P. aeruginosa* and other gram negative bacteria [36]. Infection susceptibility is due to *CFTR* dysfunction that impairs ion transport and alters the composition of airway surface liquid (ASL) in the lungs. As the hydrated layer of mucus that forms a barrier between airway epithelial cells and the environment, the ASL acts as both a liquid, which is important to spread and cover the airways, and an elastic substance that enables cilia to beat and push mucus out via mucociliary clearance [37]. Two key factors which differ between CF ASL and healthy ASL are the composition of mucins (MUC5AC and MUC5AB) and the level of hydration, both of which are important in determining

viscoelastic properties of mucous [38]. These alterations cause muco-obstruction within CF airways and this in turn favours the growth of certain pathogens such as *S. aureus* and *P. aeruginosa*, as they make use of nutrients derived from host-compounds such as cytokines, defensins, and mucins [39]. Over time, persistent infections drive chronic inflammation of the airway and long term tissue damage [38, 40]. Prominent is neutrophil migration into the site of infection, which release a range of oxidants and proteases such as neutrophil elastase to combat the organism. However, persistent release also damages the airway epithelium [41] and perpetual epithelial remodelling further exacerbates inflammation with continuous production of inflammatory mediators such as Interlukin-13 (IL-13) and transforming growth factor alpha (TGF α) [41].

Overall, CF is a severe, life limiting disorder hallmarked by chronic respiratory infection with *S. aureus* and *P. aeruginosa*, that predominate the early and late stages of life respectively. Early life interventions that can alter the course of lung function decline are highly desirable to preserve lung function as long as possible and this includes antimicrobial therapy. However, for *S. aureus* clinical care, debate surrounds the most effective use of both old and new drugs to target this pathogen [42]. Points of debate include the prescription of prophylactic anti-staphylococcal antibiotics and the most effective way to implement new or old treatment strategies [43, 44]. Prior work has shown that prophylactic use of anti-staphylococcal antibiotics in infants reported no significant lung function preservation at age 6 years [45]. More recent data suggest that *de novo* acquisition of *S. aureus* at age 3 is associated with later bronchiectasis at 5-6 years of age [46]. In the long term, AMR of *S. aureus* remains an acute concern for people with CF, as it is noticeably associated with progressive lung function decline in later life [33, 42]. The next section will delve deeper into the history of *S. aureus* antimicrobial resistance.

1.3. Staphylococcus aureus

1.3.1. Overview: Diversity and pathogenesis

Antimicrobial resistance in *Staphylococcus aureus* (*S. aureus*) has become a major concern to public health and is currently considered a high risk bacterial pathogen by the World Health Organisation [18]. The AMR variants of *S. aureus* are commonly known as methicillin-resistant *S. aureus* (MRSA) and the antibiotic susceptible phenotypes are known as methicillin-sensitive *S. aureus* (MSSA). One of the latest reports describes *S. aureus* as one of the six leading pathogens responsible for deaths attributable to AMR [14]. To clarify for the purposes of this thesis; the term MRSA has remained a common term referring to MDR *S. aureus* since the first detection of methicillin resistance. However, methicillin itself was almost immediately superseded as a treatment by oxacillin due to the acid stability of oxacillin [47].

The majority of MRSA infections are still able to be treated [12] but the concern is that the acquisition and development of resistance in MRSA is notoriously fast [47, 48]. For persistent bacterial infections, MRSA is able to mutate in the presence of antibiotics *in situ*, making MRSA especially dangerous for those with underlying compromised immunity such as CF [49]. Other states commonly associated with MRSA infection that include persistent bacteraemia, infective endocarditis, and other various lung diseases such as COPD and non-CF bronchiectasis [9, 50].

Prospectively, the issue of AMR across MRSA isolates remains a priority as the last anti-staphylococcal discovery was daptomycin in 1987 [48]. One of the most commonly used antibiotics to treat recalcitrant MRSA infections is the glycopeptide vancomycin, although resistance to vancomycin also forms within the bacterial genome over time [51]. To assist clinical treatments, *S. aureus* clinical isolates are categorised into Clinical and Laboratory Standards Institute (CLSI) categories based on their minimum inhibitory concentration (MIC) values: vancomycin intermediate strains have an MIC of 4-8 $\mu\text{g mL}^{-1}$ whilst vancomycin-susceptible *S. aureus* (VSSA) have an MIC of $\leq 2 \mu\text{g mL}^{-1}$ [47]. Currently, the

presence of vancomycin resistance (Combination of VRSA, VSSA, VISA) has been reported across all major continents [52]. The authors reported that in some studies, the high rate of *vanA* positive VRSA strains (as measured via PCR) indicated that resistance was acquired from vancomycin resistant *Enterococci* species [47, 48, 53, 54]. This is of concern since the mobility of vancomycin resistance genes (*van* operon) has been shown to be via the use of mobile genetic elements, making the spread of resistance from this pathogen to other strains or species of bacteria more difficult to control [53, 55]. If vancomycin resistance is transferred between different bacterial species, it may further complicate infection control measures. Hospitals and healthcare facilities often implement strict protocols to prevent the spread of antibiotic-resistant bacteria and the emergence of strains with resistance acquired from other species may require adjustments to these protocols to effectively control resistance spread.

1.3.2. Adaptation to the respiratory tract

S. aureus utilises multiple adaptations to survive in the respiratory microenvironment [56, 57], encoded by a large number of regulatory genetic elements, transcription factors, and regulatory RNAs present within the genome [58]. Recently, transcriptomics analysis revealed how *S. aureus* can regulate up to 29 distinct sets of genes to facilitate infection of different tissue sites [59-61]. The study of *ex vivo* nasal samples [57] identified how a small group of virulence network regulators, including *agr*, *sae*, *sigB*, *graRS*, and *WalKR* were influential in enabling persistent colonisation in individuals [57]. Timing of their expression is also important; for example, *WalKR* is an essential two-component system of *S. aureus* that controls cell wall metabolism and autolysis and early expression of *WalKR* has been shown to facilitate virulence [62].

As mentioned, *S. aureus* can be detected in the airways of young children with CF [46]. When characterised using Whole genome sequencing (WGS) techniques to map distribution of isolates within the population, *S. aureus* isolates collected longitudinally within the CF paediatric population often displayed the ability to transmit from person to person within

domestic settings [63]. In addition, key findings from pangenome analysis reveal that the diversity of gene content amongst CF respiratory isolates of *S. aureus* is in an ‘open state’; the expansion of the pangenome is not predicted to reach an asymptote as more clinical isolates are added to the pool (n = 21,358 genes) [63]. On an individual scale, MRSA status is dynamic, and many lineages of *S. aureus* (n = 89/383) contain at least one MRSA isolate, many of which (19.1%) are related via descent. These data demonstrate the ability for MSSA isolates to readily transition towards a resistant phenotype regardless of genetic background [63]. In addition, the choice of antibiotics and their dosage regimes change based on the MRSA status of isolates with which they are colonised [33, 46, 64]. It should also be noted that the concept of a single clonal strain driving infections has been challenged by higher resolution sequencing techniques, that instead suggests polyclonality and dynamic gene acquisition does occur *in situ* [63].

Overall, these findings highlight how *S. aureus* is an especially diverse microbe. The combination of genetic flexibility, an open pangenome, and high numbers of tightly regulated regulation systems have resulted in an incredibly versatile pathogen. The dogmatic approach previously used to define microbiological isolates, such as the clonal view of *S. aureus* genomics, has been challenged and should be considered when assessing the potential of novel alternative treatment strategies.

1.4. Current research and development pipelines

With reports of growing prevalence of MRSA resistance to antibiotics such as vancomycin [53], the need for new therapeutics is urgent. Whilst new antibiotics targeting *S. aureus* are being developed, many of these are variations of existing treatments and are designed to act in a similar manner to traditional antibiotics [65, 66]. Furthermore, several research and development pipelines involving vaccines, monoclonal antibodies, nanoparticles, phages, and many more are striving to fill the antibiotic void [66]. Still, development pipelines

against Gram positive pathogens such as *S. aureus* are comparatively neglected compared to the preclinical development pipelines for Gram negative bacterial species.

1.4.1. Immunotherapies: Vaccines and Monoclonal antibodies

Immunotherapy seeks to leverage one of medicine's most successful treatments, vaccination. The traditional method of producing *S. aureus* vaccines involves the use of recombinant proteins and polysaccharides to induce an immune response [67]. In fact, two of the most popular attempts at vaccine creation utilised chemically conjugated capsular polysaccharides of *S. aureus* to carrier proteins, these were Nabi's StaphVax and Pfizer's SA4Ag [67]. In a phase 3 clinical trial (www.clinicaltrials.gov, clinical trial registration: NCT00071214) a single dose of StaphVax demonstrated partial protection within 40 weeks but showed no activity past 1 year [68, 69]. The fact that many clinical isolates causing infection do not produce a capsule *in vivo* may have contributed to these vaccine failures [67, 70]. Pfizer's SA4Ag was also found to be ineffective despite inducing antibody responses within a clinical trial designed to prevent postoperative bloodstream infection using a single dose of SA4Ag (www.clinicaltrials.gov, clinical trial registration: NCT02388165) [71]. The results of these trials may indicate a lack of research elucidating the pathogenic determinants of *S. aureus*, as after Pfizer's SA4Ag vaccine trial was discontinued, hindsight reports discussed how the preclinical studies before the trial could not sufficiently estimate a prediction of clinical efficacy [72]. Compounding this issue is a lack of relevant models of invasive *S. aureus* disease. Host interactions are further complicated by the 'occasionally' commensal nature of the bacterium that leads to a percentage of the population with detectable sera levels of anti-staphylococcal antibodies regardless of healthy or diseases states [73]. Interestingly, antibodies active against distinct antigens of *S. aureus*, such as fibrinogen binding proteins, are depleted in both infected patients and carriers [73], perhaps a function of the capacity for *S. aureus* to manipulate the adaptive host immune responses and underscores the need for innovative strategies to combat this pathogen [74].

Outer membrane vesicles are another potential vaccination agent. Outer membrane vesicles are commonly associated with Gram negative bacteria, however the generation of these by Gram positive bacteria, including *S. aureus* has been reported [75]. With regards to respiratory infection focused applications, outer membrane vesicles have been trialled as vaccine agents in rodent models and protected mice against lethal doses of *S. aureus* administered, with lung infection prevented through Th1 cell mediated immunity [76]. Whilst promising vaccine research is still underway, unfortunately there are still no effective vaccines against *S. aureus* that have made it through clinical trials to date [67].

Immunotherapeutic approaches have also specifically targeted key proteins and toxins required for survival and propagation of *S. aureus* within the host [77, 78]. Antibodies that can bind to *S. aureus* clumping factor B (ClfB) were previously used *in vivo* to significantly reduce the amount of *S. aureus* in the nares of mice using 300 µg administered 10 hours prior to bacterial inoculation [79]. Another key advantage of using monoclonal antibodies is their high specificity that can be leveraged to use as a vehicle to carry antimicrobial compounds to the target. This has been shown using two human monoclonal antibodies that recognise *S. aureus* biofilms (via wall teichoic acids) *in vitro* and *in vivo* [77]. As mentioned previously, the ability for *S. aureus* to be both a commensal and an infectious pathogen has led to a scenario where antibody patterns within a population become extremely diverse leading to difficulties in forming a clear pattern and forming targeted therapeutic antibodies [80]. Previous reports have also demonstrated levels of heterogeneity amongst bacteraemia patients infected with similar (PGFE-identical) *S. aureus* strains and have surmised that monovalent immunotherapies targeting a single antigen is unlikely to be effective [81]. In light of this, a monoclonal antibody-centyrin fusion protein termed SM1B74 or “mAbtyrin” recently demonstrated multivalent activity, able to target multiple bacterial adhesins and subvert its degradation via *S. aureus* produced protease GluV8 and immunoglobulin binding proteins SpA and Sbi [82]. Key findings from this study include SM1B74s efficacy within different models of *S. aureus* infection including a neutrophil lysis model that demonstrated a 75% reduction in neutrophil lysis when in the presence of SM1B74 when compared to an IgG control, and mouse models of therapeutic intervention and prophylaxis that both demonstrated the ability for SM1B74 to significantly reduce bacterial load and kidney

abscess formation [82]. For respiratory *S. aureus*, the safety and efficacy of monoclonal antibodies is still being studied within clinical trials; the SAATELLITE study currently includes two monoclonal antibodies Suvratoxumab (www.clinicaltrials.gov, clinical trial registration: NCT05331885) and MEDI4893 (www.clinicaltrials.gov, clinical trial registration: NCT02296320). A Phase 3 trial for Suvratoxumab is currently ongoing and investigating the ability of this antibody to prevent nosocomial pneumonia caused by *S. aureus*. Similarly, MEDI4893 is being developed to also prevent pneumonia; this antibody binds to *S. aureus* [83].

1.4.2. Nanoparticles

Nanoparticles and nanoparticle-based delivery mechanisms are more novel strategies to enhance efficiency of antimicrobial compound delivery [84]. Relevant to the treatment of AMR pathogens, previous data have shown that sodium citrate-capped gold nanoparticles conjugated to ampicillin could effectively overcome the beta lactamase antibiotic resistance mechanisms in multiple bacteria, including MRSA species [85]. For intracellular treatment of *S. aureus*, nanoparticles might be used to great effect as previous data have demonstrated the ability to ‘ferry’ antimicrobials into mammalian cells *in vitro* [86]. Currently, the utilisation of nanoparticles and vancomycin (‘nano conjugated vancomycin’) is being investigated *in vitro* as an effective drug delivery mechanism, aiming to understand the mechanisms by which nanoparticles significantly improved vancomycin activity against VRSA strains when compared to vancomycin alone [87, 88].

1.5. Phage therapy for *Staphylococcus* bacteria

Bacteriophages (phages) have also emerged as a promising alternative therapy in response to the AMR crisis [89, 90]. To stem the increases in morbidity caused by AMR today, widespread implementation of alternative medicines is urgently required and phages have gained traction in recent years due to their successful use on compassionate grounds [91-93]. As such, phages may represent an alternative treatment with the potential for faster translation to therapy than newly developed therapies due to the previous history of use in

human medicine. Implementation of phage within the clinic is not without its hurdles [94], however, the need for alternative treatments to combat the AMR crisis has led to the rapid development of numerous phage institutions worldwide that seek to tackle these hurdles (with an Australian example being [PhageAustralia](#)).

Phage therapy refers to the therapeutic administration of virulent phage to treat bacterial infections and dates to the early 1930s, when it was considered a potential alternative treatment to serum injections [90, 95]. Phage preparations typically involve high titres ($>1 \times 10^9$ PFU/mL) of virulent and adequately characterised phage to ensure clearance of the bacterial infections [96]. The delivered phage infect, replicate within, and lyse bacterial cells to release phage progeny (Figure 1.1) and this process results in a rapid decrease in specific bacterial populations.

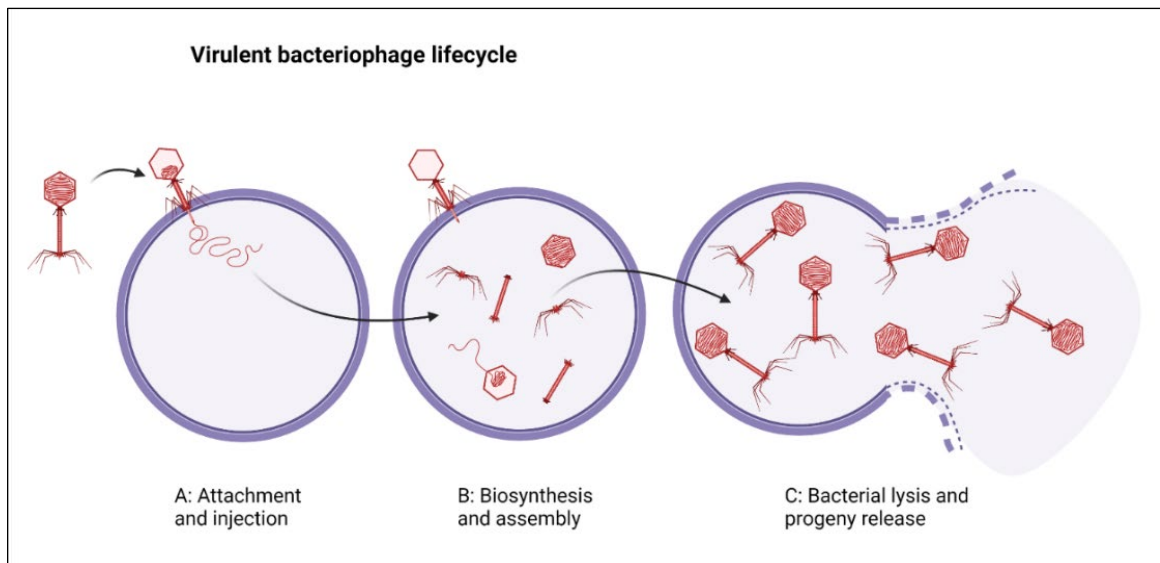


Figure 1.1: A) Phage (depicted in red) attachment and injection of its genome into a host bacterium (circular purple cell). B) Bacterial cellular machinery is used to synthesise and assemble new phage progeny. C) Progeny are released due to bacterial cell lysis. Created with BioRender.com.

Phages have several clinically relevant advantages over antibiotics and, more importantly, are able to rapidly reduce bacterial populations in situations of antibiotic resistance [91, 92, 96]. In lieu of increasing antibacterial resistance, phage therapy is one of the most promising potential alternatives to antibiotics based on this ability to eradicate multi-drug resistant (MDR) bacterial infections [92, 97]. However, despite the demonstrated efficacy of fully characterised phages against MDR infections administered on compassionate grounds, there are still many factors that require further investigation for usage within the respiratory milieu. These include accurately discerning the optimal pulmonary delivery mechanisms and the continued development of appropriate pre-clinical models [98].

1.5.1. Preclinical data generation

Preclinical data generation for phages follows a general trend from the isolation of phage, from environmental and/or clinical sources, through to microbial characterisations of efficacy and safety validations in animal models [1, 99]. It has been stated that phage therapy has not yet made its way into standard care due to the lack of consistent efficacy and safety data and a lack of knowledge surrounding bacterial-host interactions [100, 101]. Preclinical data generated against ‘in house’ libraries of bacteria are often insufficient to identify potential long-term implications of widespread phage implementation. There is also a need to develop new strategies to characterise phages in a way that enables the data generated within teams to be extrapolated to a larger scale. This may be achieved by producing standardised bacterial panels for clinically relevant bacterial species that are accessible to the scientific community. A similar resource has proved very beneficial to metagenomic studies looking at the pan-genomic repertoire of target bacterial species [102, 103]. Such data integration could facilitate small-scale phage applications, such as compassionate cases, being modelled and then trialled by the wider scientific community.

Also required for phage to move from preclinical studies into larger clinical trials is *in vitro* data centred on measurements of infectivity, manufacturing quality and safety confirmations. These data are becoming more commonplace, with recent examples of phage products made

according to GMP standards for the major MDR pathogens, *S. aureus* and *P. aeruginosa* [104], that satisfy criteria for a phase 1 clinical trials [93, 105]. In-depth characterisations of phage for applications broader than compassionate use include genome sequencing to confirm the absence of virulence and antibiotic resistance genes within the phage, morphological verification of the expected virion particles, and infectivity measurements against relevant and representative bacterial species [104, 105].

1.5.2. Pulmonary implementation

While phage therapy for bacterial infections has not yet made its way into standard care due to insufficient pre-clinical data, phages have a long history of use on compassionate and investigational grounds with few reports of adverse events [91, 93, 100, 106]. Many of these cases have been for patients with MDR or even pan-drug resistant bacterial lung infections where all other therapeutic options for eradication had been exhausted [91, 92]. The use of phages on compassionate grounds targets organisms that are prone to becoming drug resistant, so the most frequent cases are for *S. aureus*, *P. aeruginosa* and *E. coli* [106]. To date, pulmonary phages have been predominantly applied in CF and other cohorts of mucobstructive lung diseases like non-CF bronchiectasis, primary ciliary dyskinesia, and COPD [38]. Indeed, many compassionate uses of phages for lung infections have been for CF sufferers who are at end stage lung disease and have exhausted all other eradication options [91, 92, 107].

In terms of application, most phage use involves a combination of phages mixed into a single preparation called a phage cocktail. The isolation and characterisation of each contributing phage is considered time consuming and laborious to complete on an ‘ad hoc’ basis [92, 107-109]. One study investigated the probabilities of isolating phage “on-demand” active against various MDR pathogens such as *S. aureus*, *E. coli*, *K. pneumoniae*, and *P. aeruginosa* [1]. Their results indicated variable densities of infectious phage within their samples and that phages that were able to infect MRSA were particularly scarce [1]. Furthermore, individual phages demonstrate highly variable stability, which is consistent throughout literature

published so far [1, 110, 111] and has important consequences to generating amounts of phage required for therapeutic application.

Creating a cocktail necessitates access to multiple phages that are readily able to infect and lyse the target diverse bacterium isolates. The feasibility of using phage cocktails in treating bacterial respiratory infections this way to solve urgent needs is in question as this approach presents many challenges, including phage availability. There have been ongoing efforts to expand the repertoire of novel phages for cocktail combinations. Careful selection of phages is required to ensure both safety and efficacy. Attributes such as adsorption, replication, and distribution at the site of infection should be modelled in addition to acquiring full genomic and morphological characterisations for each phage within a cocktail [96, 112]. Since phage preparation practices and buffer systems in which phage are stored have an impact on the application of phage and patient safety, these must first be reviewed prior to application [28, 109]. Currently, the lag times between the current need for an approved treatment and the earliest foreseeable approvals for alternative antimicrobials are troublesome, with newly approved therapies taking approximately 12 years to arise from preclinical studies in the USA [113]. Phages may be an exception, as their safety for use in humans as an adjunct therapy has already been demonstrated on compassionate grounds [91, 92].

Whilst bactericidal activity is an important aspect, there are other important considerations when using virulent phage to clear infections. One relates to the delivery method, which may take the form of nebulised liquid suspensions, inhalable dry powders, or hydrogels to transport phage directly to the organ surface [114, 115]. Even though the use of hydrogels as a delivery method has produced promising results thus far, this method would be unsuitable to pulmonary delivery as it is designed for topical applications [115]. Delivery formulations of phage have provided both an efficacy and stability challenge for researchers and phage preparations in early clinical trials involved stabilising agents such as glycerol [108, 109]. Nebulisation is widely utilised in respiratory medicine to deliver therapeutics to the deepest airway passages, using vibrating mesh, compressed air (jet nebulisation), or ultrasound to produce aerosols from liquid suspensions [116]. Nebulisation methods have been shown to

reduce infectivity, measured by titre decrease, which correlated to morphological damage to the phages [116, 117]. Furthermore, air-jet nebulisation was reported to damage the structural integrity of phages more than mesh nebulisation, and the extent of this damage was associated with tail length [117].

A study comparing the efficacy of two different delivery methods (intraperitoneal injection and aerosol inhalation) in an animal model of MDR *Burkholderia cepacia* complex (BCC), illustrated that aerosolised phages can be significantly more effective at treating respiratory infections [118]. This method was able to deliver phage at high titres (10^7) directly into the respiratory tract using a jet-nebuliser and inhalation device. Phage delivered this way caused statistically significant reductions in BCC in the lungs of mice whereas similar reductions were not seen in mice injected intraperitoneally [117, 118]. The stability of phage post nebulisation is phage dependent and demonstrates the need to evaluate *in vitro* propagation to high titres before moving onto more costly *in vivo* models.

An alternative to nebulisation is dry powder inhalation, a method that sprays dried phage into sugar containing particles that are then stored as a dry powder [119, 120]. The dry powder phage preparations produced this way have been assessed for stability and delivery efficacy over a range of conditions at 4°C with minor drops in viable titre after 12 months [120]. This demonstrates a major advantage over liquid suspensions concerning ease of transport. In addition to storage considerations, measurements of aerosol performance also need to be assessed for pulmonary delivery. Chang *et al* (2017) reported good phage aerosol performance as measured by the fine particle fraction (FPF) of their PEV20 phage formulation, far exceeding the FPF values of most commercial inhalers [121].

Overall, phage delivery methods have been developed to the minimum standard required for compassionate use of phage in targeting pulmonary MDR infections. There remains significant further work to refine these processes to reduce variability in preparation delivery and thus improve the feasibility of clinical trials comparing phage to existing treatments.

Appropriate *in vitro* assessments of aerosol performance should be performed following the isolation of novel phages to assess suitability for delivery. However, the ability to infer these characteristics depends on the models used to recapitulate the airway milieu in a robust manner.

1.5.3. Modelling phage activity within the airways

In the context of phage to treat respiratory infections, developing appropriate *in vitro* models that can accurately recapitulate the human airway is vital in understanding how novel phages will interact with airway surface liquid, mucous and biofilm [122]. This is especially relevant in the face of new data demonstrating the impact of mucus on phage activity [123]. Whilst previous studies have demonstrated the influences of cocktail design and resistance development, or antibiotics and potential for synergy, there is a lack of data discerning the effects of mucus composition on phage efficacy [124-126]. Interestingly, data from the gut microenvironment has shown that some phages adapt to the mammalian mucosal environment when ‘trained’ *in vitro* and exhibit competitive advantages when compared to their wild-type counterparts [127]. Whilst the known and suggested interactions between phages and mucin / mucin like domains are discussed in depth elsewhere [128]; for *Staphylococcus* infecting phages specifically, there are no published reports of mucin specific effects on phage activity.

Many *in vitro* models of the lung epithelium thus far have used immortalised cell lines of human pulmonary epithelial cells, including NCI-H441 and A549 [129]. A significant drawback of using these transformed or immortalised cells is their limited ability to truly generate the complex cellular stratification and physiology of the lung epithelium [130]. This, in conjunction with their inability to produce a phenotype marked by persistent inflammation and mucous production mean they do not represent a chronically infected epithelial layer. Primary airway epithelial cells (AECs) cultured at the air liquid interface (ALI) [131] are better able to recapitulate these features of airway physiology by proper pseudo-stratification into multiple cell types with mucous production [94, 131, 132].

One concern for phage is that it may induce or exacerbate inflammation in the airways. To determine this, inflammatory biomarkers produced by the above models in response to phage can be measured [122]. The effects of phage on inflammatory immune cells such as the neutrophil, which is often as a key driver of airway damage in obstructive pulmonary diseases [33], is less well known. To the authors knowledge, the only publication measuring the effects of phage on neutrophilic migration was conducted using wild-type and hyper-inflamed *cfr* loss-of-function zebrafish embryo models [133]. This study observed that a four-phage cocktail had immunomodulatory effects via the downregulation of pro-inflammatory cytokines and reduced neutrophil migration in response to acute inflammatory induction by tailfin amputation [133]. Recently, the development of a transepithelial migration model has enabled researchers to measure the polymorphonuclear neutrophilic migration through epithelial monolayers at ALI in response to a stimulus such as purified airway supernatants from CF patients [134]. Utilising this model to determine how phage exposure might affect the function of dynamically active neutrophils recruited into the airways may help to increase the amount of relevant preclinical data supporting the safety of phages for pulmonary infection. This could provide a significant improvement upon the previously mentioned zebrafish model due to the closer recapitulation of the airway environment and use of human AECs.

Following *in vitro* testing, the use of animal models is a necessary component in assessing the safety and efficacy of new therapeutics within a fully functional biological system. As mentioned previously, one safety concern with bactericidal agents, such as antibiotics and lytic phage, is the release of bacterial endotoxin upon cell lysis [135]. Fortunately, many of the results generated *in vitro* have been reflected *in vivo* thus far [136, 137]. For example, Dufour and colleagues reported that phage causing rapid bacterial lysis did not cause as much endotoxin release as various Beta-lactam antibiotics using an *in vitro* model [138]. Similarly, an acute pneumonia murine infection model showed that phage treatment was associated with lower levels of inflammation than antibiotics [139]. These results are also supported across other *in vivo* studies with different bacteria isolated including MDR *P. aeruginosa* and *S. aureus*, common respiratory pathogens [140, 141].

Existing *in vivo* models of phage therapy have been typically designed to study phage efficacy in response to an acute infection in which animals are challenged with lethal doses of bacteria [101, 118, 142-145]. While providing a plethora of useful safety and efficacy data, this does not accurately reflect a chronic infection status in humans. As such, a model in which longer-term infection can be maintained and studied has been developed [146]. Such studies have not yet been described using *S. aureus* bacteria in an *in vivo* model of long-term infection, however this has been achieved for other respiratory bacteria such as *P. aeruginosa*. Fothergill et al [146] described a mouse inhalation model in 2014 whereby *P. aeruginosa* is introduced intranasally and colonises the nasopharynx, followed by migration towards the lungs causing a lower respiratory tract infection over the course of 28 days. This enables comparison of *P. aeruginosa* isolated at both early and late stages of infection. Interestingly, their analysis of isolates taken at various timepoints indicated that the bacteria became resistant to tobramycin in the absence of antibiotic pressure [146]. The importance of this study towards pulmonary phage therapy is evident as despite the phenotypic similarities between the original *P. aeruginosa* isolate and two isolates collected from the same mouse at day 21, a re-challenge experiment with these isolates confirmed that post-infective *P. aeruginosa* was far more adept at colonising the lower respiratory tract *in vivo* [146]. In comparison to previous studies utilising beads impregnated with bacteria to mimic a chronic infection, this model more accurately represents the natural development route of a persistent infection brought about by stable colonisation of the nasopharynx followed by migration to the lower respiratory tract after adequate adaptations have been acquired [146]. In understanding the dynamic nature of *S. aureus* bacteria, regardless of clonal complex / lineage, it may be important to revisit such models and suggest the production of dynamic models for bacteria that are known to be genomically versatile [63]. Using a rodent model of skin infection, Muller and colleagues elucidate the well-studied antibiotic resistance factor in MRSA PBP2a; the authors found that β -lactam antibiotic treatments are both ineffective and proinflammatory when used to treat MRSA bacteria [147]. This arises from the structural changes in peptidoglycan when the arrest of PBP2 induces the activities of PBP2a; the downstream effects of which are increased inflammation within the host [147].

The dominant delivery route used in these models is intranasal administration and overall this delivery route of phage therapy has demonstrated bacterial reductions using both curative and preventative doses of phage [145, 148]. Whilst easy to perform, this method is not without disadvantages, as a *lux* tagged strain of *P. aeruginosa* MR299 was visualised from 2-8 hours post intranasal administration and found to be localised in the head and stomach of the mice in addition to the lung target [148]. Still, the study was able to demonstrate the efficacy tolerability of phages, significantly reducing *P. aeruginosa* biomass over the course of 24 hours. Further studies have performed intratracheal administration of phage preparations to address the variability of intranasal administration, for example demonstrating safety and efficacy of dry powdered formulations which retain bactericidal activity (0.3-log₁₀ titre drop) and demonstrate good aerosol performance *in vitro* (FPF 51.6%) [121].

Though many animal models used thus far have demonstrated the safety and efficacy of phage therapy, the majority of these studies incorporated a single bacterial species and a high dose of phage specific for treatment [139, 140, 143, 145]. To date, there is a paucity of data on the efficacy of phage against polymicrobial infections, and the models developed thus far do not translate this polymicrobial aspect into their models. Despite the lack of polymicrobial contexts in preclinical data generation, phages have been used to clear a polymicrobial bone infection caused by *K. pneumoniae* and *A. baumannii* and, whilst successful, the phages were administered in conjunction with the antibiotics Colistin and Meropenem [149]. The importance of incorporating polymicrobial aspects into *in vivo* models is required to further support the safety of phages when used to treat various infection scenarios. This is emphasised by publications indicating that phage implementation may cause adverse consequences in scenarios where complex microbial communities exist, as is often the case in the lungs [150]. Furthermore, preclinical data generation for specific phage preparations must represent the clinical scenario in which it is used as accurately as possible. Expansion of models which enable establishment of LRTIs over a longer time period, representing chronic infections more accurately, should be a priority for pulmonary phage therapy aimed at the usual clinical scenarios of patients whose case history has exhausted all other treatment options [91, 92, 146].

1.5.4. Clinical uses of phage against *Staphylococcus aureus*

There will always be caveats when using animal models to represent human conditions, but it is promising that human clinical trials involving phages have reported no adverse events, aligning with results of *in vivo* animal models [93, 101, 151]. The small number of clinical trials conducted to date have demonstrated the safety and tolerability of phage preparations when administered intravenously or topically for otitis media, or wound sites [93, 108, 109]. Outside of the respiratory context, a phase 1 clinical trial demonstrated safe topical applications of phages to venous leg ulcers with no reports of adverse events [108]. In addition to this, another clinical trial (Trial registration: NCT03395769) was conducted in an Australian hospital which used intravenously administered phage as an adjunctive therapy [93], also with no adverse events reported. These phage preparations were designed according to good manufacturing practice (GMP) standards and, whilst promising for phage therapy in general, have not administered nebulised phages directly to the lungs [93, 108, 109, 152]. Regardless of delivery route, general safety parameters have been established by these uses of phage, a more in-depth review of clinical trials and the regulatory hurdles they face are described by Furfaro and colleagues 2018 [100]. Unfortunately, the number of clinical trials that utilise phage for respiratory infections are few and many of these studies have not yet completed or published the findings.

1.5.5. Summary

Phages represent a unique opportunity in combating multi-drug resistant bacterial pathogens. The escalating prevalence of chronic lung infections attributed to antibiotic resistant *S. aureus* poses a growing concern [14], particularly among individuals with CF [33]. Notably, young children with CF commonly exhibit chronic *S. aureus* infections that set them on a path towards increased lung function decline in later life [153, 154], marked by the pathogen's ability to successfully evade both host immune defences and conventional antibiotic treatments [57, 155, 156]. Whilst the isolation of phages has rekindled interest in addressing bacterial infections, there remains a gap in exploring the potential of isolating phages specifically targeting *S. aureus* from environmental and clinical sources.

Furthermore, the establishment of gold standards for the preclinical evaluation of phages is an ongoing process marked by many processes pertaining to genomics and microbiological analyses unique to phages [157, 158]. Regarding genomic screening, there is a lack of strict guidelines and procedures determining which phages are acceptable for use in humans [159-161]. Furthermore, there is a lack of data concerning direct pulmonary application, its safety, and the optimal phage administration factors such as dose and timing [162, 163]. The absence of standardised preclinical safety data complicates cross-literature comparisons and hampers the integration of phage therapy into standard clinical practices [164]. Despite the promise that phages have in combatting persistent *S. aureus* infections [93, 165, 166], their full potential remains unrealised without further preclinical investigations.

1.5.6. Hypotheses

Phage studies performed in recent years have demonstrated that whilst *Staphylococcus* phages are generally regarded as safe, they are also highly diverse and difficult to isolate from environmental sources [1]. Furthermore, there is a paucity of safety data concerning the application of *Staphylococcus* phages to airway epithelial surfaces. To address these gaps, this study aimed test the following hypotheses:

1. Phages can be isolated from the environment and will exhibit *in vitro* activity against *S. aureus* bacterial pathogens.
2. Phages active against *S. aureus* will be non-toxic and non-inflammatory when applied to *in vitro* and *in vivo* safety models of the airways.

Chapter 2: Materials and methods

This chapter contains the equipment, materials, and methods used to conduct work within this thesis. Methods specific to each chapter are generally kept within the chapter but may be expanded on here and referenced within the chapter.

2.1. Bacterial isolates:

Table 2.1: Bacterial isolates obtained and stocked as part of this thesis.

<i>Microorganism</i>	<i>Bacterial ID</i>	<i>Phenotype</i>	<i>State</i>	<i>Provided by</i>
<i>Staphylococcus aureus</i>	ATCC29213	MSSA		
<i>Staphylococcus aureus</i>	ATCC25923	MSSA		
<i>Staphylococcus aureus</i>	ATCC6538	MSSA		
<i>Staphylococcus aureus</i>	RN4420	MSSA		
<i>Staphylococcus aureus</i>	SA1	MRSA	QLD	Professor Scott Bell
<i>Staphylococcus aureus</i>	SA2	MRSA	QLD	Professor Scott Bell
<i>Staphylococcus aureus</i>	SA3	MRSA	QLD	Professor Scott Bell
<i>Staphylococcus aureus</i>	SA4	MRSA	QLD	Professor Scott Bell
<i>Staphylococcus aureus</i>	SA5	MRSA	QLD	Professor Scott Bell
<i>Staphylococcus aureus</i>	SA6	MRSA	QLD	Professor Scott Bell
<i>Staphylococcus aureus</i>	SA7	MRSA	QLD	Professor Scott Bell
<i>Staphylococcus aureus</i>	SA8	MRSA	QLD	Professor Scott Bell
<i>Staphylococcus aureus</i>	SA9	MRSA	QLD	Professor Scott Bell
<i>Staphylococcus aureus</i>	SA10	MSSA	QLD	Professor Scott Bell
<i>Staphylococcus aureus</i>	SA11	MSSA	QLD	Professor Scott Bell
<i>Staphylococcus aureus</i>	SA12	MSSA	QLD	Professor Scott Bell
<i>Staphylococcus aureus</i>	SA13	MSSA	QLD	Professor Scott Bell
<i>Staphylococcus aureus</i>	SA14	MSSA	QLD	Professor Scott Bell
<i>Staphylococcus aureus</i>	SA15	MSSA	QLD	Professor Scott Bell
<i>Staphylococcus aureus</i>	SA16	MSSA	QLD	Professor Scott Bell
<i>Staphylococcus aureus</i>	SA17	MSSA	QLD	Professor Scott Bell
<i>Staphylococcus aureus</i>	SA18	MSSA	QLD	Professor Scott Bell
<i>Staphylococcus aureus</i>	SA19	MSSA	QLD	Professor Scott Bell
<i>Staphylococcus aureus</i>	SA20	MRSA	WA	Professor Geoffrey Coombs
<i>Staphylococcus aureus</i>	SA21	MSSA	WA	Professor Geoffrey Coombs
<i>Staphylococcus aureus</i>	SA22	MSSA	WA	Professor Geoffrey Coombs
<i>Staphylococcus aureus</i>	SA23	MSSA	WA	Professor Geoffrey Coombs
<i>Staphylococcus aureus</i>	SA24	MRSA	NSW	Professor Geoffrey Coombs
<i>Staphylococcus aureus</i>	SA25	MRSA	WA	Professor Geoffrey Coombs
<i>Staphylococcus aureus</i>	SA26	MRSA	NSW	Professor Geoffrey Coombs

<i>Staphylococcus aureus</i>	SA27	MRSA	QLD	Professor Geoffrey Coombs
<i>Staphylococcus aureus</i>	SA28	MRSA	NSW	Professor Geoffrey Coombs
<i>Staphylococcus aureus</i>	SA29	MRSA	VIC	Professor Geoffrey Coombs
<i>Staphylococcus aureus</i>	SA30	MRSA	NSW	Professor Geoffrey Coombs
<i>Staphylococcus aureus</i>	SA31	MRSA	VIC	Professor Geoffrey Coombs
<i>Staphylococcus aureus</i>	SA32	MRSA	NT	Professor Geoffrey Coombs
<i>Staphylococcus aureus</i>	SA33	MRSA	VIC	Professor Geoffrey Coombs
<i>Staphylococcus aureus</i>	SA34	MRSA	QLD	Professor Geoffrey Coombs
<i>Staphylococcus aureus</i>	SA35	MRSA	WA	Professor Geoffrey Coombs
<i>Staphylococcus aureus</i>	SA36	MRSA	NT	Professor Geoffrey Coombs
<i>Staphylococcus aureus</i>	SA37	MRSA	VIC	Professor Geoffrey Coombs
<i>Staphylococcus aureus</i>	SA38	MRSA	TAS	Professor Geoffrey Coombs
<i>Staphylococcus aureus</i>	SA39	MRSA	WA	Professor Geoffrey Coombs
<i>Staphylococcus aureus</i>	SA40	MSSA	ACT	Professor Geoffrey Coombs
<i>Staphylococcus aureus</i>	SA41	MSSA	ACT	Professor Geoffrey Coombs
<i>Staphylococcus aureus</i>	SA42	MSSA	NSW	Professor Geoffrey Coombs
<i>Staphylococcus aureus</i>	SA43	MSSA	NSW	Professor Geoffrey Coombs
<i>Staphylococcus aureus</i>	SA44	MSSA	NT	Professor Geoffrey Coombs
<i>Staphylococcus aureus</i>	SA45	MSSA	NT	Professor Geoffrey Coombs
<i>Staphylococcus aureus</i>	SA46	MSSA	QLD	Professor Geoffrey Coombs
<i>Staphylococcus aureus</i>	SA47	MSSA	QLD	Professor Geoffrey Coombs
<i>Staphylococcus aureus</i>	SA48	MSSA	SA	Professor Geoffrey Coombs
<i>Staphylococcus aureus</i>	SA49	MSSA	SA	Professor Geoffrey Coombs
<i>Staphylococcus aureus</i>	SA50	MSSA	TAS	Professor Geoffrey Coombs
<i>Staphylococcus aureus</i>	SA51	MSSA	TAS	Professor Geoffrey Coombs
<i>Staphylococcus aureus</i>	SA52	MSSA	VIC	Professor Geoffrey Coombs
<i>Staphylococcus aureus</i>	SA53	MSSA	VIC	Professor Geoffrey Coombs
<i>Staphylococcus aureus</i>	SA54	MSSA	WA	Professor Geoffrey Coombs
<i>Staphylococcus aureus</i>	SA55	MSSA	WA	Professor Geoffrey Coombs
<i>Staphylococcus aureus</i>	SA56	MRSA	QLD	Professor Geoffrey Coombs
<i>Staphylococcus aureus</i>	SA57	MRSA	VIC	Professor Geoffrey Coombs
<i>Staphylococcus aureus</i>	SA58	MRSA	NSW	Professor Geoffrey Coombs
<i>Staphylococcus aureus</i>	SA59	MRSA	NSW	Professor Geoffrey Coombs
<i>Staphylococcus aureus</i>	SA60	MRSA	WA	Professor Geoffrey Coombs
<i>Staphylococcus aureus</i>	SA61	MRSA	WA	Professor Geoffrey Coombs
<i>Staphylococcus aureus</i>	SA62	MRSA	VIC	Professor Geoffrey Coombs
<i>Staphylococcus aureus</i>	SA63	MRSA	QLD	Professor Geoffrey Coombs
<i>Staphylococcus aureus</i>	SA64	MRSA	VIC	Professor Geoffrey Coombs
<i>Staphylococcus aureus</i>	SA65	MRSA	QLD	Professor Geoffrey Coombs
<i>Staphylococcus aureus</i>	SA66	N/A	WA	Professor Geoffrey Coombs
<i>Staphylococcus aureus</i>	SA67	N/A	WA	Professor Geoffrey Coombs
<i>Staphylococcus aureus</i>	SA68	N/A	WA	Professor Geoffrey Coombs
<i>Staphylococcus aureus</i>	SA69	N/A	WA	Professor Geoffrey Coombs
<i>Staphylococcus aureus</i>	SA70	N/A	WA	Professor Geoffrey Coombs

<i>Staphylococcus aureus</i>	SA71	N/A	WA	Professor Geoffrey Coombs
<i>Staphylococcus aureus</i>	SA72	N/A	WA	Professor Geoffrey Coombs
<i>Staphylococcus aureus</i>	SA73	N/A	WA	Professor Geoffrey Coombs
<i>Staphylococcus aureus</i>	SA74	N/A	WA	Professor Geoffrey Coombs
<i>Staphylococcus aureus</i>	SA75	N/A	WA	Professor Geoffrey Coombs
<i>Staphylococcus aureus</i>	SA76	MRSA	SA	Professor Geoffrey Coombs
<i>Staphylococcus aureus</i>	SA77	MRSA	NSW	Professor Geoffrey Coombs
<i>Staphylococcus aureus</i>	SA78	MRSA	NSW	Professor Geoffrey Coombs
<i>Staphylococcus aureus</i>	SA79	MRSA	NSW	Professor Geoffrey Coombs
<i>Staphylococcus aureus</i>	SA80	MRSA	NSW	Professor Geoffrey Coombs
<i>Staphylococcus aureus</i>	SA81	MRSA	QLD	Professor Geoffrey Coombs
<i>Staphylococcus aureus</i>	SA82	MRSA	NSW	Professor Geoffrey Coombs
<i>Staphylococcus aureus</i>	SA83	MRSA	NSW	Professor Geoffrey Coombs
<i>Staphylococcus aureus</i>	SA84	MRSA	NSW	Professor Geoffrey Coombs
<i>Staphylococcus aureus</i>	SA85	MRSA	NSW	Professor Geoffrey Coombs
<i>Staphylococcus aureus</i>	SA86	MRSA	QLD	Professor Geoffrey Coombs
<i>Staphylococcus aureus</i>	SA87	MRSA	NT	Professor Geoffrey Coombs
<i>Staphylococcus aureus</i>	SA88	MRSA	VIC	Professor Geoffrey Coombs
<i>Staphylococcus aureus</i>	SA89	MRSA	QLD	Professor Geoffrey Coombs
<i>Staphylococcus aureus</i>	SA90	MRSA	QLD	Professor Geoffrey Coombs
<i>Staphylococcus aureus</i>	SA91	MRSA	WA	Professor Geoffrey Coombs
<i>Staphylococcus aureus</i>	SA92	MRSA	VIC	Professor Geoffrey Coombs
<i>Staphylococcus aureus</i>	SA93	MRSA	WA	Professor Geoffrey Coombs
<i>Staphylococcus aureus</i>	SA94	MRSA	QLD	Professor Geoffrey Coombs
<i>Staphylococcus aureus</i>	SA95	MRSA	QLD	Professor Geoffrey Coombs
<i>Staphylococcus aureus</i>	SA96	MRSA	NSW	Professor Geoffrey Coombs
<i>Staphylococcus aureus</i>	SA97	MRSA	NSW	Professor Geoffrey Coombs
<i>Staphylococcus aureus</i>	SA98	MRSA	NSW	Professor Geoffrey Coombs
<i>Staphylococcus aureus</i>	SA99	MRSA	WA	Professor Geoffrey Coombs
<i>Staphylococcus aureus</i>	SA100	MRSA	WA	Professor Geoffrey Coombs
<i>Staphylococcus aureus</i>	SA101	MRSA	SA	Professor Geoffrey Coombs
<i>Staphylococcus aureus</i>	SA102	MRSA	SA	Professor Geoffrey Coombs
<i>Staphylococcus aureus</i>	SA103	MRSA	WA	Professor Geoffrey Coombs
<i>Staphylococcus aureus</i>	SA104	MRSA	WA	Professor Geoffrey Coombs
<i>Staphylococcus aureus</i>	SA105	MRSA	NT	Professor Geoffrey Coombs
<i>Staphylococcus aureus</i>	SA106	MRSA	NSW	Professor Geoffrey Coombs
<i>Staphylococcus aureus</i>	SA107	MRSA	NSW	Professor Geoffrey Coombs
<i>Staphylococcus aureus</i>	SA108	MRSA	NSW	Professor Geoffrey Coombs
<i>Staphylococcus aureus</i>	SA109	MRSA	SA	Professor Geoffrey Coombs
<i>Staphylococcus aureus</i>	SA110	MRSA	NSW	Professor Geoffrey Coombs
<i>Staphylococcus aureus</i>	SA111	MRSA	NSW	Professor Geoffrey Coombs
<i>Staphylococcus aureus</i>	SA112	MRSA	QLD	Professor Geoffrey Coombs
<i>Staphylococcus aureus</i>	SA113	MRSA	WA	Professor Geoffrey Coombs
<i>Staphylococcus aureus</i>	SA114	MRSA	VIC	Professor Geoffrey Coombs

<i>Staphylococcus aureus</i>	SA115	MRSA	VIC	Professor Geoffrey Coombs
<i>Staphylococcus aureus</i>	SA116	MRSA	NSW	Professor Geoffrey Coombs
<i>Staphylococcus aureus</i>	SA117	MRSA	NSW	Professor Geoffrey Coombs
<i>Staphylococcus aureus</i>	SA118	MRSA	WA	Professor Geoffrey Coombs
<i>Staphylococcus aureus</i>	SA119	MRSA	VIC	Professor Geoffrey Coombs
<i>Staphylococcus aureus</i>	SA120	MRSA	VIC	Professor Geoffrey Coombs
<i>Staphylococcus aureus</i>	SA121	MRSA	QLD	Professor Geoffrey Coombs
<i>Staphylococcus aureus</i>	SA122	N/A	WA	Professor Geoffrey Coombs
<i>Staphylococcus aureus</i>	SA123	N/A	WA	Professor Geoffrey Coombs
<i>Staphylococcus aureus</i>	SA124	N/A	WA	Professor Geoffrey Coombs
<i>Staphylococcus aureus</i>	SA125	N/A	WA	Professor Geoffrey Coombs
<i>Staphylococcus aureus</i>	SA126	N/A	WA	Professor Geoffrey Coombs
<i>Staphylococcus aureus</i>	SA127	N/A	N/A	A/Prof Chris Peacock
<i>Staphylococcus aureus</i>	SA128	N/A	N/A	A/Prof Chris Peacock
<i>Staphylococcus aureus</i>	SA129	N/A	N/A	A/Prof Chris Peacock
<i>Staphylococcus aureus</i>	SA130	N/A	N/A	A/Prof Chris Peacock
<i>Staphylococcus aureus</i>	SA131	N/A	N/A	A/Prof Chris Peacock
<i>Staphylococcus aureus</i>	SA132	N/A	N/A	A/Prof Chris Peacock
<i>Staphylococcus aureus</i>	SA133	N/A	N/A	A/Prof Chris Peacock

2.2. General equipment:

2.2.1. Pipettes:

For liquid volumes 1000 μ L and under, single channel pipettes from Axygen were used (Adelab Scientific, Thebarton SA5031, South Australia). For work requiring multiple channels, a Pipetman L multichannel pipettes (Gilson Inc., Middleton, WI, USA) and F1-ClipTip™ multichannel pipettes (Thermo Fisher Scientific, Waltham, MA, USA) were used.

2.2.2. Pipettor:

For liquid volumes exceeding 1mL, transferring fluids were measured using S1 Pipet Fillers from Thermo Fisher Scientific (Waltham, MA, USA).

2.2.3. Biosafety cabinets:

For processes requiring a sterile environment, Lab culture® Class II Type A2 biosafety cabinets (Esco Micro Pte. Ltd, Singapore), compliant with the regulations of the Office of the Gene Technology Regulator (OGTR) were used. Accreditation of which was received from the National Association of Testing Authorities (NATA) certified biological safety cabinet.

2.2.4. Fumigation hoods:

For processes requiring a sterile environment and requiring the user to have additional chemical and vapour protection, a Smoothflow TOUCH Ducted Fume Cupboard compliant with the Office of the Gene Technology Regulator (OGTR) was used. Accreditation of which was received from the National Association of Testing Authorities (NATA) in compliance with ISO/IEC 17025 testing.

2.2.5. Flasks and Schott bottles:

All glassware used in the laboratory was from Schott (Frenchs Forest, NSW, Australia). All used glassware was soaked overnight in Liquid Pyroneg (Diversey Australia, Smithfield, NSW, Australia) and cleaned with an INNOVA® M5/M5-ISOGlasswarewasher (BHT Hygienetechnik, Gersthofen, Germany).

2.2.6. Heating blocks:

Buffers and samples were heated above room temperature using a Ratek 1 Block Digital Dry Block Heater (Ratek Instruments Pty Ltd, Boronia, VIC, Australia).

2.2.7. Centrifuges:

For centrifugation of samples, the small benchtop Eppendorf® 5415D minicentrifuge (Eppendorf, Hamburg, Hamburg, Germany) and larger Eppendorf® 5810R swing-bucket rotor centrifuges were used (Eppendorf, Hamburg, Hamburg, Germany).

2.2.8. Scales and balances:

All reagents were measured using the OHAUS SP602 Scout pro Compact Bench scale (OHAUS, Port Melbourne, VIC, Australia), OHAUS Explorer Balance (OHAUS, Port Melbourne, VIC, Australia), or the A&D Weighing GC-600 Precision Scale (Fisher Biotec, Wembley, WA 6904, Australia).

2.2.9. Microscopes:

Visual assessment of all cell cultures was performed using the Nikon Eclipse TS100 microscope (Tochigi Nikon Precision Co., Ltd. 760, Midori, Otawara). Visual assessment of animal cells was performed using a DM/LS Leica Microscope GmbH (Wetzlar, Hesse, Germany).

2.2.10. Calibration: pH:

All pH measurements were performed using an edge® Dedicated pH/ORP Meter from Hanna Instruments Inc. (Woonsocket, Rhode Island, USA). Calibration standards and solutions were obtained from Scharlau (Barcelona, Catalonia, Spain).

2.2.11. Plate readers:

Spectrophotometry measurements were performed using the following equipment: BioTek™ Synergy™ Mx Multi Detection Top Monochromator Based Microplate Reader with Gen5
Page | - 29 -

Software (Thermo Fisher Scientific, Waltham, MA, USA), CLARIOstar Plus Plate Reader (BMG LabTech, Ortenberg, Germany). Optical density measurements of all bacterial cultures were performed using an Eppendorf Fluorescent BioSpectrometer® (Eppendorf, Hamburg, Hamburg, Germany).

2.2.12. Orbital shakers and stirring:

Solutions requiring agitation and mixing were achieved using magnetic stirrers from Industrial Equipment and Control Pty Ltd (Melbourne, VIC, Australia), or a Ratek shaker (Ratek Instruments Pty Ltd, Boronia, VIC, Australia), or a Stuart® rocking platform from Barloworld Scientific Laboratory Group (Rochester, NY, USA) when needed.

2.2.13. Water baths:

To heat solutions, buffers, and perform freeze-thawing of frozen samples, a heated water bath from Ratek Instruments Pty Ltd (Boronia, VIC, Australia) was used.

2.2.14. NanoDrop 2000:

Extracted DNA were assessed using a NanoDrop 2000c spectrophotometer (Eppendorf, Hamburg, Hamburg, Germany). Specifically, a volume of 1 µL of DNA eluate was spectrophotometrically measured at 260 and 280 nm wavelengths. The purity of the eluted DNA was determined by calculating the absorbance ratio of 260/280 nm, which should fall within the range of 1.8-2.0.

2.2.15. Electrophoresis:

Gel electrophoresis was performed using a PowerPac™ basic power supply (Bio-Rad Laboratories, Hercules, CA, USA).

2.2.16. Qubit™ fluorometer:

All extracted DNA was quantified using a Qubit 4 fluorometer from Thermo Fisher Scientific (Waltham, MA, USA).

2.2.17. Bead beating:

For gDNA extraction pre-treatments, bacterial lysates were produced using a Precellys 24 tissue homogenizer (Bertin Technologies, Rockville, Maryland 20850, United States).

2.2.18. Bacterial incubator:

All bacterial cultures were incubated and maintained in a Heratherm™ incubator (ThermoFisher Scientific, Waltham, MA, USA) under atmospheric air conditions. Established cell cultures were maintained in a Heracell™ VIOS 160i CO₂ (Thermo Fisher Scientific, Waltham, MA, USA) incubator with a 5% CO₂/95% air atmosphere.

2.2.19. Dry oven for molten overlay agar:

All sterilised bacterial culture media were kept molten at 55°C in the Memmert UL30 dry oven (Mettler Toledo, Schwabach, Germany).

2.2.20. Mesh nebuliser:

To aerosolise liquid samples, a Vitrocell chamber was used in conjunction with the Aeroneb Lab control module (Kent Scientific, Torrington, CT 06790, United States) and a Standard VMD Nebuliser Unit with Filler cap (Aerogen Ltd, Dangan, Galway, Ireland). This apparatus achieves a flow rate of approximately 0.3 mL/min and a particle size of 4.0 – 6.0 µM.

2.2.21. High Pressure Liquid Chromatography:

Phage purifications for use within *in vitro* and *in vivo* experiments were performed using the ÄKTA pure™ chromatography system (Cytiva, Pimpri-Chinchwad, Maharashtra 411057, India).

2.2.22. Transepithelial volt/ohm meter (EVOM):

Trans-epithelial electrical resistance (TEER) measurements were then taken across the airway layers using an Epithelial Volt/Ohm Meter (World Precision Instruments, Sarasota, Florida, USA).

2.2.23. Blood gas and chemistry:

Analysis of blood gases, haematology, and chemistry (sodium, potassium, ionised calcium, glucose, haematocrit, haemoglobin, pH, PCO_2 , PO_2 , TCO_2 , HCO_3 , base excess and sO_2 using the -STAT Alinty (Abbott laboratories, Chicago, IL, USA) in combination with i-STAT CG8+ cartridges.

2.2.24. Anaesthesia delivery system:

To deliver isoflurane (Covetrus Isothesia NXT), a SomnoSuite Low-Flow Anaesthesia System (Kent Scientific, Torrington, CT 06790, United States) was used.

2.2.25. Mechanical ventilation:

Mice were mechanically ventilated at ~300 breaths/min with a tidal volume of 8 mL/kg and 2 cmH₂O of positive-end expiratory pressure using a HSE Harvard Minivent (Hugo Sachs Harvard Elektronik, March-Hugstetten, Germany).

2.2.26. Long read sequencing:

Bacterial gDNA were sequenced using a MinION 10.4.1 flow cell (Oxford Nanopore Technologies, Oxford, Gosling Building, Edmund Halley Road, Oxford Science Park, United Kingdom) and rapid barcoding kit (SQK-RBK114.24) to generate long reads.

2.2.27. Gamma cell Irradiation:

The NIH-3T3 cell line was irradiated with 3000 cGy of γ -radiation using a Gammacell 3000 Elan (Nordion, Oxfordshire, UK).

2.3. Consumables:

2.3.1. Coating Buffer (AECs):

The coating buffer for inserts consisted of type 1 rat tail collagen diluted to a final concentration of 0.03 μ g/mL in 1X PBS. A volume of 100 μ L was aliquoted into each well of a 24-well plate (Corning Co-star plates).

2.3.2. Cryopreservation Solution:

The cryopreservation solution for AECs consisted of 90% (v/v) HI-FCS, 10% (v/v) DMSO, and 1 μ L of ROCK inhibitor.

2.3.3. Foetal Calf Serum (FCS):

To obtain FCS with low endotoxin levels: a commercially purchased aliquot from Thermo Fischer Scientific (Waltham, MA, USA) and heat-inactivated FCS aliquots at 56°C for 2 hours prior to usage. It was referred to as HI-FCS.

2.3.4. FCS-Based Trypsin Neutralising Solution:

To neutralise trypsin activity following monolayer cell line detachment, an FCS-based trypsin neutralising solution (TNS) was prepared by supplementing DMEM with 5% (v/v) HI-FCS. This solution was stored at 4°C until required.

2.3.5. Fibronectin Coating Buffer:

Fibronectin coating buffer was prepared by dissolving 1 mg of fibronectin in 10 mL of BEBM™ at 37°C for 1 hour to dissolve the powder completely. Once dissolved, 1 mL of collagen type 1 (rat tail) and 10 mL of BSA stock were added to the buffer. The fibronectin coating buffer was then supplemented with 0.2% (final concentration, v/v) gentamicin and 0.125 µg/mL amphotericin B. The final solution was filter-sterilised using 0.22 µm syringe filters and stored at 4°C away from direct light exposure until use.

2.3.6. NIH-3T3 Co-Culture Growth Medium:

NIH-3T3 cell lines were maintained in Dulbecco's Modified Eagle Medium (DMEM) supplemented with 10% (v/v) HI-FCS and 1% (v/v) penicillin/streptomycin. The medium was prepared in a sterile manner and stored at 4°C until needed.

2.3.7. Conditionally-Reprogrammed Culture Medium (CCM):

Aliquots of CCM were created by blending Han's F-12 Nutrient Mix with Dulbecco's Modified Eagle Medium (DMEM) (2:1 ratio). Then, 500 mL of complete F-medium, enriched with ROCK inhibitor, was combined using 5% HI-FCS (refer to 2.3.3), 24 µg/mL adenine, 8.4 ng/mL cholera toxin, 0.4 µg/mL hydrocortisone, 0.5 µg/mL insulin, 10 ng/mL EGF, and 10 µM/L ROCK inhibitor (refer to 2.3.9). Resulting media were then filtered using 0.22 µm bottle-top filters and was stored at 4°C until required.

2.3.8. Penicillin/Streptomycin:

A penicillin/streptomycin solution containing 10,000 µg/mL of penicillin and 10,000 µg/mL of streptomycin was used to supplement Pneumacult ALI growth media and NIH-3T3 cells.

2.3.9. ROCK Inhibitor:

To make a 10 mM stock solution of rho-associated protein kinase (ROCK) inhibitor (Y-27632), 25 mg of ROCK inhibitor powder was dissolved in 7.8 mL of ddH₂O, filter-sterilised using a 0.22 µm syringe filter, and stored at -20°C in 50 µL aliquots until needed.

2.3.10. Subculture Reagent Pack:

Commercially available subculture reagent packs were purchased from Lonza™ (Basel, Switzerland) for primary cells, including HEPES-buffered saline solution, Trypsin-EDTA, and Trypsin Neutralising solution (TNS), were thawed and stored in 10 mL aliquots at -20°C. Once thawed, the reagents were stored at 4°C until used.

2.3.11. Trypan Blue Solution (0.05% v/v):

To make a 0.05% (v/v) Trypan Blue solution, 5 mL of commercially available Trypan Blue 0.4% (w/v) cell culture-grade solution was diluted in 35 mL of 1X PBS. The prepared solution was filter-sterilized using a 0.22 µm syringe filter and stored at room temperature until required.

2.3.12. Anaesthetics:

Mice were anaesthetised at a dose of 0.1 mL/10 g of body weight with ketamine (40 mg/mL; Troy Laboratories, New South Wales, Australia) and xylazine (2 mg/mL; Troy Laboratories, New South Wales, Australia) diluted in sterile saline.

2.3.13. SM buffer:

To produce 1 L of SM buffer, 5.8 g of sodium chloride (NaCl; 100 mM), 0.96 g of magnesium sulfate anhydrous (MgSO₄; 8 mM), and 50 mL of 1 M Tris-HCl (pH 7.4; 50 mM) were added to 950 mL of ddH₂O to achieve a final volume of 1 L. The reconstituted SM buffer was sterilized in an autoclave at 121°C for 40 min.

2.3.14. Tryptic Soy broth (TSB) preparations:

To make 500 mL of Tryptic Soy broth, 15 g of dehydrated media powder (BD Micro, New Jersey, USA) was rehydrated with 500 mL of ddH₂O. To produce double and triple strength TSB, the required ratio of dehydrated media powder to ddH₂O were manipulated appropriately. All media was sterilised in an autoclave at 121°C for 40 min.

2.3.15. Tryptic Soy agar (TSA) preparation:

To make 500 mL of Tryptic Soy agar, 20 g of dehydrated media powder (BD Micro, New Jersey, USA) was rehydrated with 500 mL of ddH₂O. The media was sterilised in an autoclave at 121°C for 40 min. TSA plates were prepared by dispensing 18 mL of sterile molten TS agar into a sterile Petri dish. Once dry (5-10 minutes at room temperature) TSA plates were stored at 4°C and used within 1 month.

2.3.16. Tryptic Soy overlay (0.5% w/v) agar (TS-overlay agar):

To make 500 mL of TS overlay agar, 2.5 g of bacteriological agar (BD Micro, New Jersey, USA) was combined with 15 g of TS broth media powder and rehydrated with 500 mL of ddH₂O. The solution was supplemented with 500 µL of 1 M CaCl₂ and 1 M MgCl₂ to achieve final concentrations of 1 mM each. The overlay agar was sterilised in an autoclave at 121°C for 40 min and kept molten in a dry oven at 55°C.

2.3.17. Magnesium chloride (MgCl₂: 1 M) solution:

To make 100 mL of MgCl₂ solution, 9.5211 g of MgCl₂·6H₂O crystals (Sigma Aldrich, North Ryde, NSW, Australia) were rehydrated with 100 mL of ddH₂O. The MgCl₂ solution was filter-sterilised by passing through a 0.22 µm syringe filter (Cytiva Whatman™ Uniflo™ PES membrane, USA) and stored at room temperature until needed.

2.3.18. Calcium chloride (CaCl₂: 1 M) solution:

To make 100 mL of CaCl₂ solution, 11.098 g of calcium chloride·6H₂O crystals (Sigma Aldrich, North Ryde, NSW, Australia) were rehydrated with 100 mL of ddH₂O. The CaCl₂ solution was filter-sterilised by passing through a 0.22 µm syringe filter (Cytiva Whatman™ Uniflo™ PES membrane, USA) and stored at room temperature prior to use.

2.3.19. Phosphate buffer solution (PBS) (Cell culture):

To make a 1X solution of PBS, tablets of dehydrated PBS (Thermo Fisher Scientific, Waltham, MA, USA) were dissolved in 1 L of ddH₂O. The solution was autoclaved and stored at room temperature until use.

2.3.20. Bacteriological petri dishes:

Disposable plastic bacterial culture Petri dishes were obtained from Greiner Bio-One (Kremsmünster, Austria).

2.3.21. Tissue culture plastic materials:

All disposable plastic and tissue culture equipment was obtained from Nunc™ (Thermo Fisher Scientific, Waltham, MA, USA).

2.3.22. Double deionized water (ddH₂O):

Double-deionised water was prepared by passing distilled water through a Milli-Q water purification system (Purelab® Ultra, Elga Veolia, Kewdale, WA, Australia).

2.3.23. Bovine Serum Albumin (BSA):

To make a 1 mg/mL BSA solution, 100 mg of BSA powder (Sigma-Aldrich, St. Louis, MO, USA) was dissolved in 100 mL of 1X PBS. The prepared solution was filter-sterilised using a 0.22 µm syringe filter and stored at 4°C until use.

2.3.24. Ethanol (70% v/v):

To make a 70% (v/v) ethanol solution, 700 mL of absolute ethanol (Sigma-Aldrich, St. Louis, MO, USA) was added to 300 mL of ddH₂O and stored at room temperature until required.

2.3.25. Glycerol (50% v/v):

To make a 50% (v/v) glycerol solution, 50 mL of glycerol stock (Univar, Ingleburn, NSW, Australia) solution was added to 50 mL of ddH₂O, autoclaved, and stored at room temperature until use.

2.3.26. Hank's Balanced Salt Solution (HBSS):

To make HBSS, the following components were dissolved in 900 mL of ddH₂O: 0.185 g of CaCl₂, 0.097 g of MgSO₄, 0.4 g of KCl, 0.06 g of KH₂PO₄, 8 g of NaCl, 0.047 g of Na₂HPO₄, and 1 g of glucose. The solution was adjusted to pH 7.4 with 1 M HCl (VWR International, UK) and made up to 1 L with ddH₂O. The prepared solution was autoclaved and stored at room temperature until use.

2.3.27. Hydrochloric Acid (HCl: 1 M):

To make a 1 M HCl solution, 10 mL of 32% HCl (VWR International, UK) was added to 90 mL of ddH₂O to achieve a final volume of 100 mL. The solution was stored at room temperature until required.

2.3.28. Neutral Buffered Formalin (NBF: 10% v/v):

To make 10% (v/v) NBF, 900 mL of ddH₂O was added to 100 mL of formalin (Sigma-Aldrich, St. Louis, MO, USA). Then, 4 g of NaH₂PO₄ (Sigma-Aldrich, St. Louis, MO, USA)

and 6.5 g of Na₂HPO₄ (Sigma-Aldrich, St. Louis, MO, USA) were added. The prepared NBF was stored away from direct light at 4°C until required for cell fixing.

2.3.29. Sodium Deoxycholate Solution (10% w/v):

To make a 10% (w/v) sodium deoxycholate solution, 10 g of sodium deoxycholate was dissolved in 100 mL of ddH₂O, filter-sterilized by passing through a 0.22 µm syringe filter (Cytivas Whatman™ Uniflo™ PES membrane, USA), and stored at room temperature until use.

2.3.30. Sodium Hydroxide Solution (0.2 M):

To make a 0.2 M sodium hydroxide (NaOH) solution, 80 mg of NaOH was dissolved in 10 mL of ddH₂O and stored at room temperature until needed.

2.3.31. Sodium Hydroxide Solution (1 M):

To make a 1 M sodium hydroxide (NaOH) solution, 40 g of NaOH was dissolved in 1 L of ddH₂O and stored at room temperature until used.

2.3.32. Tris Buffered Saline (TBS):

To make a 10x stock solution of Tris Buffered Saline (TBS), 80 g of NaCl, 2 g of KCl, and 30 g of Trizma base were dissolved in 800 mL of ddH₂O. The solution was adjusted to pH 7.4 with 1 M HCl and stored at room temperature. Before use, the stock solution was diluted 1:10 in ddH₂O.

2.3.33. Tris(hydroxymethyl)aminomethane hydrochloride (Tris-HCl: 1 M):

To make 500 mL of 1 M Tris-HCl, 60.57 g of Tris was reconstituted in 400 mL of ddH₂O. The prepared solution was adjusted to a pH of 7.4 by adding approximately 70 mL of 1 M HCl, and then the volume was adjusted to 500 mL. The 1 M Tris-HCl was filter-sterilized by passing it through a 0.22 µm syringe filter (Cytivas Whatman™ Uniflo™ PES membrane, USA) and dispensed into 50 mL aliquots, which were stored at room temperature until needed.

2.3.34. Triton-X-100 Solution (10% v/v):

To make a 10% (v/v) Triton-X-100 solution, 10 mL of Triton-X stock solution was added to 90 mL of 1X PBS. Prepared Triton-X-100 solutions were stored away from direct light at room temperature until needed.

2.3.35. Cell extraction buffer (CEB):

To make CEB, the following solutions were combined with dH₂O to a volume of 80mL order to a final concentration of: Tris-HCl (10 mM, pH6.8), NaCl (100mM), EDTA (1 mM), EGTA (1 mM), NaF (1 mM), sodium pyrophosphate (20 mM), sodium orthovanadate (2mM). This solution was pH adjusted using HCl to pH 7.4 and then the following were added: Triton X-100 (1%), glycerol (10%), SDS (0.1%), and sodium deoxycholate (0.5%). This was then stored frozen at -20°C until required for use.

2.4.Methods:

2.4.1. Glycerol stock preparations for bacterial isolates:

Bacterial cultures grown from a single colony were propagated in and stored using appropriate media supplemented to a final concentration of 25% (v/v) glycerol and stored at -80°C after one hour of incubation at room temperature.

2.4.2. Bacterial Culturing:

Glycerol stocks stored at -80°C were quadrant streaked onto plate of appropriate agar media and incubated overnight at 37°C to obtain single colonies.

2.4.3. Overnight cultures (ONCs):

To make overnight cultures, a single colony was inoculated into the appropriate growth medium and incubated overnight at 37°C . Overnight culture growth is a minimum of 16 hours and a maximum of 24 hours.

2.4.4. Measurement of Bacterial Density Using OD_{600nm}:

Bacterial optical density (OD) was measured using an Eppendorf Fluorescent BioSpectrometer®. Bacterial cultures were diluted 1:10 and measured at a wavelength of 600 nm (OD_{600nm}) in 4cm cuvettes.

2.4.5. Measurement of Viable Bacterial Load Using Colony Forming Units per Millilitre (CFU/mL):

Bacterial overnight cultures were prepared as described above. Bacterial optical density was adjusted to OD_{600nm} 1.0 as the starting inoculum. The adjusted bacterial culture was serially diluted in appropriate broth and 100 μL of each dilution was spread onto appropriate agar plates. The plates were incubated overnight at 37°C , and colonies were enumerated on plates containing 30-300 colonies.

2.4.6. Preparation of inoculated Overlay Agar plates:

Overlay agar plates inoculated with bacteria are used for numerous processes such as isolation, propagation, and enumeration. To imbue an overlay agar plate with bacteria ready for usage: combine 100 μL of the target bacteria (from ONCs made the night before) and add 3-4 mL of molten overlay agar of the appropriate media. The inoculated overlay agar was then poured onto a solid agar plate and gently swirled to ensure even distribution of overlay. Plates are left to solidify at room temperature and then incubated statically at the appropriate growth conditions for the target bacteria.

2.4.7. Wastewater pre-processing

Water samples collected were enriched and screened for phages that could infect *Staphylococcus aureus* bacteria. Briefly, water samples were filtered through a 0.22 μm bottle-top filter (Nalgene™ Rapid-Flow™, Thermo Fisher Scientific, Waltham, MA, USA) or a 0.22 μm syringe filter (Cytivas Whatman™ Uniflo™ PES membrane, USA). The supernatant was supplemented with 1M CaCl_2 and 1M MgCl_2 to a final concentration of 1-5 mM.

2.4.8. Phage Enrichment (stepwise process)

Phage enrichments were performed by supplementing source materials with variable concentrations of 1M CaCl_2 and 1M MgCl_2 (ranging from 1-5 mM) based on the isolation method described in Chapter 3. This step was performed to achieve the desired CaCl_2 and MgCl_2 concentrations for subsequent phage enrichment. Incubation Conditions: For phage enrichment, an enriched culture was prepared by combining 5 mL of double-strength TS broth, supplemented with 1 mM CaCl_2 and 1 mM MgCl_2 , 5 mL of the pre-processed wastewater filtrate, and 100 μL of overnight *S. aureus* cultures. The enriched culture was then incubated for 24-48 hours at 37°C under aerobic conditions and agitation at 50 rpm. Enumeration: After the incubation period, the enriched TS broth was centrifuged at 3220 x g for 10 minutes at room temperature. The resulting supernatants were filtered through a 0.22

µm syringe filter to remove any remaining debris or bacterial cells. To determine the presence of phages, 200 µL of the resulting filtrate were used to produce double agar overlays imbued with the *S. aureus* isolates used for initial enrichment. The agar plates were then incubated under aerobic conditions at 37°C for 24-72 hours. Phage presence was assessed by visually observing the clearance zones (lytic activity) on the bacterial streaks, indicating the presence of phages.

2.4.9. Phage isolation rounds (stepwise process)

To purify previously visualised and identified phages, three rounds of plaque purification were conducted. Initially, the enriched cultures were filtered, and their concentration was determined using titrations before proceeding with purification. To ensure the formation and observation of individual plaques, a double agar overlay technique was employed using the filtered enriched cultures at an appropriate dilution factor, which had exhibited positive lytic activity against the target bacteria. The inoculated double agar overlays were then incubated overnight at 37°C. After the incubation period, plates were carefully examined for the presence of distinct plaques and their morphology. Plaques exhibiting distinct characteristics were chosen for further purification. The middle region of the selected plaque was collected using a sterile Pasteur pipette, and the overlay agar was aspirated before transferring it into 1 mL of SM buffer. The resulting solution containing the phages was filtered using a 0.22 µm syringe filter. This process was repeated for each selected plaque during the final round of purification. Purified phages were stored in SM buffer at 4°C to maintain their stability and viability for subsequent analysis and experimentation.

2.4.10. Short Read DNA Extraction and Sequencing:

Phage genomic DNA (gDNA) was purified from filtered high-titre (1×10^9) phage lysate using 0.22µm syringe filters and sequenced using the Illumina paired-end platform. Briefly, gDNA was extracted using the DNeasy Blood and Tissue kit (QIAGEN, Hilden Germany) following a previously published protocol [167]. The purified extractions were prepared for

whole-genome sequencing (WGS) using the Nextera-XT library preparation kit and sequenced using the Illumina NovaSeq 6000 platform.

Bacterial gDNA was also purified from the propagating hosts of Biyabeda-mokiny 1 and Koomba-kaat 1 phages using bacterial overnight cultures. Bacterial pellets were resuspended in 180µL of enzymatic lysis buffer and incubated for 1 hour at 37°C. DNA extractions were performed via column purification using the DNeasy Blood and Tissue Kit protocols (Qiagen).

2.4.11. Host range assay

Spot tests were performed to determine host range activity using a target bacterial isolate [168]. Bacteria were added to an overlay agar plate of appropriate media, which was then allowed to solidify in a biosafety cabinet for 15 minutes. Activity was measured by spot testing 10 µL of the phage lysate onto the inoculated overlay agar. The spotted phage lysate was left to air-dry in the biosafety cabinet, and the plates were subsequently incubated overnight at 37°C under ambient air conditions. After the incubation period, the plates were visually examined, and the results were recorded based on the presence of clear, turbid, or negative lysis zones as a '1', '2', or a '3' within raw data.

2.4.12. Phage Propagation: plate elution method (stepwise process)

To prepare the phage-bacterial mixture, an equal amount of phage suspension and overnight bacterial culture were combined in a 1:2 ratio, with 100 µL of phage and 200 µL host bacteria added to 3 mL of molten TS overlay agar. The mixture was thoroughly mixed and then poured onto a TS agar plate, allowing it to solidify for 15 minutes in a biosafety cabinet. The plates were incubated overnight at 37°C without movement. After the incubation period, the agar plates were removed from the incubator, and bacterial clearance was visually examined. To recover the phage suspensions, 5 mL of sterile SM buffer was added to each agar plate. The plates were then placed on a platform orbital shaker, set at 50 rpm, and incubated for 15 minutes. Following this, the SM buffer was collected from each plate using a sterile Pasteur

pipette and transferred into 15 mL conical tubes. To remove any remaining cell debris, the conical tubes containing the SM buffer and phage suspension mixture were centrifuged at 4000 rpm for 10 minutes. After centrifugation, the supernatants were carefully collected, avoiding disturbing the pellet, and filtered into a sterile conical tube using a 0.22 μm syringe filter. The filtered phage suspensions were then enumerated, meaning their concentrations were determined, and stored at 4°C for further use. It is assumed that the host bacterial isolate from the isolation process is used unless reason is given to change propagation host.

2.4.13. Phage titration (stepwise process):

To determine phage concentrations, serial dilutions of the phage suspension were performed at a ratio of 1:10. TS agar plates were divided into sections representing different dilution factors. Using an inoculated TS overlay agar containing the host bacteria or bacteria of interest, 10 μL of each serially diluted phage suspension in SM buffer was spot tested onto the corresponding dilution factor section of the agar plate. The plates were left to dry in the biosafety cabinet for approximately 30 minutes, or until the spotted phages were dry, and then incubated statically overnight at 37°C. After the overnight incubation, agar plates were visually inspected for the presence of bacterial growth and/or lytic activity. Phages were enumerated by counting the number of plaques observed at various dilution factors, with a limit of up to 20 plaques per spot. Alternatively, for whole-plate assays, phage suspensions were serially diluted 1:10 using 1.5 mL Eppendorf tubes. An equal volume (100 μL) of the serially diluted phage suspension and overnight bacterial cultures were added to 3 mL of molten overlay agar. This mixture was then poured onto TS agar plates. The agar plates were allowed to dry in the biosafety cabinet for approximately 30 minutes, or until the spotted phages were dry, and subsequently incubated statically overnight at 37°C. Following the overnight incubation, the plates were visually inspected for bacterial growth and/or lytic activity. Phages were enumerated by quantifying the number of plaques observed at various dilution factors ranging from 30 to 300 plaques per plate.

2.4.14. Efficiency of Plating (EOP):

To assess the efficiency of plating (EOP) a previously published method was used [168]. Briefly, a tenfold serial dilution was performed using the host bacterial isolate. These dilutions, from 10^2 to 10^9 were then plated against the target bacterial isolate. The effective plaque forming units (PFU/mL) were determined using both the host strain used for propagation and the specific bacterial isolate of interest by counting plaques using a dilution that produces a whole plate overlay containing 30-300 plaques. The average number of plaque-forming units (PFUs) formed against the target bacteria was divided by the average PFUs on the propagating host bacteria to calculate the EOP.

2.4.15. Kill-curves / Dosage curves:

To assess bactericidal kinetics in liquid media, a previously published method was adapted [158]. Briefly, phages were added to their host bacterial cultures, and the overall bacterial growth was measured using OD_{600nm} at 30-minute time intervals. The lytic activity of the phages was determined using overall bacterial growth (OD_{600nm}) and viable bacterial load enumerated using CFU/mL.

2.4.16. NIH-3T3 Cell Line:

The NIH-3T3 cell line, a mouse fibroblast, was obtained from the American Type Culture Collection (ATCC) (Manassas, VA, USA). It is used for establishing and maintaining conditionally reprogrammed primary airway epithelial cells. The NIH-3T3 cell line originated from desegregated NIH Swiss mouse embryo fibroblasts by George Todaro and Howard Green [169].

2.4.17. Irradiation of Fibroblasts:

Before using fibroblasts to establish a primary AEC culture, NIH-3T3 fibroblasts were subcultured and exposed to 3000 cGy γ -radiation using a Gammacell 3000 Elan (Nordion, Page | - 47 -

Oxfordshire, UK). Total cell count and viability were determined using trypan blue solution and a hemacytometer. Irradiated cells were then seeded at a density of 5,000 cells per cm² into a fibronectin-coated tissue culture flask.

2.4.18. Cell Line Recovery:

NIH-3T3 cells were revived from long-term storage in dimethyl sulfoxide (DMSO) by rapid thawing in a 37°C water bath. They were immediately diluted in RPMI-1640 (1:10 v/v) and centrifuged at 500 x g for 7 minutes at 4°C. The cell pellet was then resuspended in 1 mL of growth medium. Total cell count and viability were determined using trypan blue solution and a haemocytometer. The revived NIH-3T3 cells were seeded into a 25 cm² tissue culture flask with a total volume of 5 mL of growth medium. The cell culture was maintained at 37°C in a Heracell™ VIOS 160i incubator, dedicated to cell lines. Regular mycoplasma testing was conducted to certify the cell cultures as mycoplasma-free.

2.4.19. Cell Line Subculture:

When cells reached approximately 90% confluency, they were serially passaged. Monolayer cells were rinsed once with 1X phosphate-buffered saline (PBS) and then incubated with 0.25% Trypsin-EDTA solution for 7 minutes at 37°C in 5% CO₂/95% air. The trypsin was neutralised using foetal calf serum (FCS)-based trypsin neutralizing solution. The cell suspension was washed with 1X PBS to collect residual cells. The collected cell suspension was centrifuged at 500 x g for 7 minutes at 4°C, and the pellet was resuspended in 1 mL of growth medium. A total cell count and viability were determined using trypan blue solution and a hemacytometer. The cell suspension was then seeded into a new tissue culture flask at an appropriate cell density of 5,000 cells per cm² and maintained at 37°C in 5% CO₂/95% air in a Heracell™ VIOS 160i incubator dedicated to cell lines.

2.4.20. Cell Counts and Viability:

Total cell counts and viability were assessed using trypan blue solution and a haemocytometer. Briefly, 10 μL of cell suspension was mixed with 10 μL of trypan blue stain solution. Then, 10 μL of the resulting solution was added to the haemocytometer chamber and examined under a microscope. The total cell count was determined by averaging the cell numbers from four grids, considering the dilution factor and suspension density. Viable cells, which remained unstained, were counted, and represented as a percentage of the total cell count to determine cell viability. Non-viable cells, stained blue by trypan blue, indicated damaged cell membranes.

2.4.21. Primary airway epithelial cell storage

For cryopreservation, cells were enumerated and aliquot into tubes containing 0.5×10^6 cells/mL along with 1 mL of cryopreservation buffer (refer to section 2.3.2). The cryovials were frozen in a Mr Frosty cryo-container at a controlled rate of -1°C per minute prior to long-term storage at -180°C in liquid nitrogen.

2.4.22. Primary airway epithelial cell recovery

Primary AECs were retrieved from -180°C liquid nitrogen storage and thawed rapidly at 37°C in a water bath. Following thawing, cells were suspended in 9X volumes of Dulbecco's Modified Eagle Medium supplemented with 10% HI-FCS (refer to section 2.3.3). Subsequently, they were centrifuged at $500 \times g$ for 7 minutes at 4°C . The resulting supernatant was discarded, and the cell pellet resuspended in 1 mL of growth medium. Assessments of total cell count, and viability were performed using a haemocytometer and trypan blue solution prior to establishing co-cultures.

2.4.23. Mycoplasma Testing of cell lines and pAECs

All cell cultures were routinely tested for mycoplasma contamination using the MycoAlert™ PLUS assay (Lonza, Basel, Switzerland). The presence of mycoplasma was determined based on the ratio of ATP levels before and after the addition of MycoAlert™ PLUS substrate. All cell cultures used in this study were tested and verified to be mycoplasma contamination-free by appropriately trained staff.

2.4.24. BCA assay:

Total protein levels were quantified with the Pierce BCA Protein Assay Kit which was performed using the manufacturer's instructions (Thermo Fisher Scientific). Once the assay was complete, results were obtained by measuring the optical density at 520nm and interpolating sample values against a standard curve. This process was used for both the apical cell free supernatants and on cell protein extractions both diluted 1:5 in PBS.

2.4.25. High Pressure Liquid Chromatography

Phage purifications for all experiments originate from a single batch of filter-sterilised, high titre phage preparation. Purifications were performed using phage lysate filtered through 0.22 µm filters to remove bacterial debris prior to HPLC purification. Filtered phage lysates were passed through a HiTrap BIA Monolithic Column (BIA Separations, Ajdovščina, Slovenia) using the ÄKTA M2 pure™ HPLC platform (Cytiva Life Sciences, Marlborough, MA, USA). Initially, the column was prepared using 10-column volumes (CV) of deionized water (ddH₂O) at a flow rate of 10 mL/min to remove any remaining storage solution (20% ethanol) within the system. Then, the equilibration process included another 10 column volumes of equilibration buffer (50 mM Tris, pH 7) passed through at 10 mL/min followed by priming the column with approximately 6 mL of phage lysate, and another 10 mL applied onto the resin bed of the column at 10 mL/min. Finally, phage elution was performed by washing the column with elution buffer (50 mM Tris, 1 M NaCl, pH 7) that effectively removes any phages attached to the column. Phages were collected in 5 mL fractions using a fraction

collector and chosen based on the UV measurements with highest peaks at 280 nm. Phage enumeration was determined using phage titrations (described in section 2.4.13) and purified fractions were stored at 4°C.

2.4.26. Anion-exchange column cleaning

The cleaning process for the HiTrap BIA Monolithic Column (BIA Separations, Ajdovščina, Slovenia) involved passing 10 column volumes (CV) of cleaning buffer solution (2 M NaCl), then 10 CV of equilibration buffer, followed by 10 CV of ddH₂O and a final incubation with 1 M NaOH for 30 min. Following this, 10 CV of 1 M NaOH solution and ddH₂O was pumped through the column at 10 mL/min sequentially. Columns were then stored in 20 % (v/v) ethanol at 4°C until required.

Chapter 3: Identification and genomic screening of *Staphylococcus* bacteriophages with therapeutic potential against respiratory isolates of *Staphylococcus aureus* bacteria

3.1. Introduction:

The use of phages is a possible solution to the issue of antibiotic resistance [170]. Fortunately, phages are found wherever their bacterial host species grow [171] and their isolation from various environmental sources has been well documented [1, 172-175]. Most phages have been derived from environments with high bacterial populations, with wastewater being a prominent example, likely owing to the abundance and accessibility of wastewater [176, 177]. With the advent of genomics analyses, the true diversity of phages has become apparent and following this came the idea to isolate specific phages that are highly effective against antibiotic resistant bacteria. The potential for phage as alternative therapeutic options is quickly becoming realised, although achieving ‘on demand’ selection for individual clinical use cases is still in its infancy [1]. Furthermore, the diversity of phages targeting each bacterial species within environmental sources, to date, remains understudied and may be significantly different based on the target pathogen [1].

Once isolated, phages must undergo a lengthy process of characterisation to ensure their suitability for therapeutic application [157]. Whilst there are many characteristics that are considered desirable for phage therapy, such as a broad host range or the ability to disrupt biofilms, these are not considered mandatory. Generally, phages that are suitable for phage therapy must be both obligately lytic so they cannot integrate into the bacterial genome and must also not contain any phage or host derived virulence factors. A crucial aspect of characterising phages includes investigating the genome sequence of isolated phages. Fortunately, the widespread implementation of high throughput sequencing technologies [178-180] has led to the creation of numerous open access tools that can be used to assemble genomes without a reference in a process called *de novo* genome assembly [181-183].

Interactions between the phages and their host are also complex and unique and may include prophages encoded within the bacterial genome that will parasitise the infecting phage to package its own genome in a process called molecular piracy [184]. As this is a known phenomenon within *S. aureus* phage-host interactions [185], it is an important parameter to address using WGS methodology. Currently, information regarding the host organism and levels of prophage induction are often neglected.

Currently, lytic phages identified against *S. aureus* are less diverse than phages active against prominent respiratory pathogens such as *P. aeruginosa*, nearly all of which belong to the Genus *Kayvirus*. This chapter specifically tested the hypothesis that phages fit for therapeutic use could be obtained from environmental and clinical sources. The first aim was to capture a diverse range of phages that were able to target *S. aureus* bacteria specifically isolated using clinical respiratory isolates of MSSA and MRSA. Isolations were performed using a panel of these respiratory isolates in addition to three commonly used laboratory strains of *S. aureus*. The second aim was to create and use a WGS pipeline to *de novo* assemble genomes of the phage isolated and filter out phages considered inappropriate for phage therapy. Finally, the third aim was to determine the safety of phage preparations when grown using clinical host isolates of previously uncharacterised bacteria to ensure that phages grown in their host isolation strain were free of contaminating or dangerous genomic factors.

3.2. Materials and methods:

3.2.1. Bacterial strains used for the isolation of *S. aureus* bacteriophage:

Laboratory control cultures (ATCC-6538 and RN4420) of *S. aureus* were purchased from the American Type Culture Collection (ATCC) and used alongside clinical isolates. De-identified clinical cultures (n=19) of respiratory *S. aureus* bacteria were kindly provided by Professor Scott Bell (QIMR Berghofer Medical Research Institute, Queensland., Queensland, Australia). All isolations were performed using the same panel of 19 clinical respiratory *S. aureus* isolates, consisting of MRSA (n=9) and MSSA (n=10) in addition to two commonly used laboratory strains mentioned above.

3.2.2. Wastewater processing:

Wastewater samples (n=16) were collected from the Subiaco Wastewater Plant located in Shenton Park, Western Australia from 21/01/2020 to 9/11/2021. These samples were immediately filtered to remove macroscopic debris and bacteria using Nalgene bottle top 0.22 µm filters.

3.2.3. Direct plating method (unenriched)

Unenriched wastewater filtrate was screened for *S. aureus* phage using two different methods: 1) three 10 µL volumes of unenriched wastewater dropped onto double agar overlay plates for each bacterial isolate, 2) 100 µL of unenriched wastewater applied as a whole plate overlay on a separate agar plate for each bacterial isolate.

3.2.4. Enrichment of potential phages in wastewater

Wastewater was combined with double strength TS broth at a 1:1 (v/v) ratio and split into three tubes per bacterial isolate. Each tube was incubated for a different amount of time (12, 24, or 48 hours) to optimise the incubation period for *S. aureus* phage propagation. A second

enrichment for each wastewater sample was also attempted with a higher concentration of cations (3 mM CaCl₂ and 3 mM MgCl₂ versus the original 1mM CaCl₂ and 1mM MgCl₂) using the same growth conditions as the previous enrichment method.

3.2.5. Visual indication of phage

The presence of bacteriophage activity, from either unenriched or enriched sources, was assessed by observing plaques after formation on bacterial overlay agar plates incubated overnight for 16 hours. Plaques with potential bacteriophage were selected for further purification.

3.2.6. Phage purifications via plaque excision

Plaques from phage positive samples were randomly selected if plaque sizes were the same across the plate, otherwise a small, medium, and large sized plaque from the plate were selected to capture potential diversity. These were excised from whole plate overlay using a pipette tip to pull some of the phage from the plate. This was then transferred to 500 µL of SM buffer (100mM NaCl, 8mM MgSO₄·7H₂O, 50mM Tris-HCl, pH 7.4, 1 litre dH₂O) and used to produce another whole plate overlay, effectively repeating the process. This was done three times to isolate a homogenous phage population. Upon the final purification process phages were propagated to high titre. Stocks of purified phages were maintained in SM buffer at 4°C until further purifications were required.

3.2.7. Plaque characterisations

Purified phages were morphologically characterised based on four parameters: size, shape, presence of a halo, and the plaque turbidity on a black background. To characterise each plaque, a titration was performed followed by a whole plate overlay to obtain countable numbers (30-300) of plaques on a single plate. Plates with plaques were imaged using the ChemiDoc (BioRad, Hercules, CA, USA). Ten plaques from each plate were chosen and measured using ImageJ (v1.54d) [186] software to generate averages. The diameters of the plaques were averaged, and plaque size categorised as small (<1 mm), medium (1-2 mm), or

Page | - 55 -

large (>2mm) based on the mean value. Colonies were also visually inspected for the presence of a halo (Negative | Positive), lysis type (Clear | Turbid), and shape (Round | Irregular).

3.2.8. Phage isolations from breastmilk:

Biological samples (breastmilk) were also provided from the Characterisation Of Milk after preterm birth (COMET) study (courtesy of Dr. Stephanie Trend, University of Western Australia, Perth, Australia, ethics approval number 2055EW, Appendix F) and thawed for 1 hour on ice. Breastmilk samples were pooled to a total volume of 25-50 mL in a 50 mL Falcon tube and then supplemented with a final concentration of 1 mM CaCl₂ and MgCl₂ using 1 M stock solutions. Fat was removed via centrifugation at 3,224 x g for 20 minutes at 4°C. The aqueous layer was then removed using a 19G needle attached to a 10 mL syringe followed by filtration via 0.22 µm filters. The remaining fat layers were collected and combined with SM buffer at a 1:1 v/v ratio. These diluted fat layers were vortexed for 15 seconds to dislodge any potential phages from the fat and then the centrifugation process repeated to obtain the aqueous layer and discard the fat. Filtrate were then ready for enrichment or direct unenriched plating as described (refer to 3.2.3 and 3.2.4).

3.2.9. Phage DNA extraction

DNA was extracted from phage that had undergone three successful rounds of plaque excision were considered pure. Here, phage gDNA extraction was performed using the DNeasy Blood & Tissue Kit from QIAGEN, using the manufacturer's instructions. In brief, 450 µL of each phage solution was incubated with 50 µL of DNase I 10x buffer, 1 µL of DNase I (1 U/µL) from Thermo Fisher Scientific (Waltham, MA, USA), and 1 µL of RNase A (10 mg/mL) obtained from QIAGEN (Hilden, Germany) at 37°C under ambient air conditions for 2 hours. Subsequently, DNase I and RNase A were deactivated by adding 20 µL of 0.5 M Ethylenediaminetetraacetic acid (EDTA), resulting in a final EDTA concentration of 20 mM. Phage capsids were then broken down using 1.25 µL of Proteinase K (QIAGEN, Hilden, Germany) at 56°C under ambient air conditions for another 2 hours.

DNA quality was determined by measuring absorbance at A260/A280 using a NanoDrop 2000c Spectrophotometer and DNA quantification performed using a Qubit™ dsDNA HS and BR Assay Kit (Thermo Fisher Scientific, Waltham, MA, USA) following the manufacturer's recommendations. Gel electrophoresis was performed using a 1% agarose gel to visualise the DNA. Gels were prepared by dissolving 0.5 g of agarose in 50 mL of 1X TAE (40 mM Tris-acetate 1 mM EDTA, pH 8.3) buffer, and 5 µL of SYBR™ Safe. The mixture was poured into an agarose gel container and solidified at room temperature for approximately 10 minutes. Samples as well as a 1 Kb Plus DNA Ladder were then prepared by mixing 5 µL of the sample DNA with 1 µL of 6x DNA Gel Loading Dye and loaded into each well of the gel. Electrophoresis was conducted at 100 volts (V) for 30-60 minutes and the gel visualised and imaged using the ChemiDoc (BioRad, Hercules, CA, USA).

3.2.10. Sequencing

Sequencing was performed by the Australian Genomics Research Facility (AGRF) (Melbourne, Australia). A Nextera Flex preparation kit (Illumina Inc., San Diego, CA, USA) was used for library preparation, fragmenting and tagging DNA fragments prior to removing any unused adaptors. Libraries were then sequenced using the Novaseq Illumina platform to produce, paired end (PE), 150 bp raw reads.

3.2.11. Phage assembly pipeline

The following pipeline for reads processing (adaptor trimming, quality trimming, and subsampling), *de novo* assembly, assembly verification (Completeness using CheckV), and read mapping ([BBTools](#)) were placed into a docker container for portability. This pipeline was predominantly written in the Python programming language (89.9% of total git repository storage). Code development and logging were tracked using git and stored on GitHub. A wrapper script to utilise the container was uploaded to the Python Package Index.

3.2.11.1. Reads QC and subsampling

The BBTools tool suite [187] released by the Joint Genome Institute were utilised to pre-process the raw sequencing reads for assembly. Firstly, read adaptors were detected and trimmed using the ‘tbo=t’ flag where adaptors are found based on where paired reads overlap, then the first and last 12 bases for each PE read were removed and reads filtered to a minimum average read quality (Q score) of 15, with all trimming performed using bbduk (v38.18). Duplicate reads were then removed using dedupe (v38.18) and resulting reads considered to be Quality Controlled reads (QC reads). Prior to initial assembly, reads were subsampled (normalised) using bbnorm (v38.18) to a target coverage of 400 X. The resulting subsampled QC reads were quality checked using fastQC (v0.11.9) [188] for signs of QC reads processing errors.

3.2.11.2. SPAdes de novo assembly

The SPAdes genome assembler (v3.15.4) [181] was used to assemble reads into contiguous segments of DNA (contigs). The stringent assembly parameter ‘—careful’ was used in the assembly and the output files kept in multifasta format if more than one contig was produced with no internal assembly filtering of any kind. The resulting contigs were then formatted using reformat.sh (v38.18) and contigs below 1 kb were removed.

3.2.11.3. CheckV assessment

Filtered contigs resulting from the initial assembly of subsampled QC reads were analysed using CheckV [189] for genome completeness, quality, and contamination using the latest CheckV database (‘checkv-db-v1.5’, accessed on the 15th March 2023). Using this analysis phage contigs were classified into ‘Complete’, ‘High-quality’, ‘Medium-quality’, ‘Low-quality’ or ‘Genome-fragment’ based on internal metrics. The confidence level for each contig that potentially represents a genome was based on the estimated completeness from amino acid identity scores of complete genomes within its database or hidden Markov model-

based approaches: high confidence ($\geq 90\%$ completeness), medium confidence (80–90% completeness) or low confidence ($< 80\%$ completeness) [189].

3.2.11.4. Read mapping

Mapping reads back to phage contigs was performed using bbmap (v38.18) to generate per base coverage statistics, per contig coverage statistics (average coverage across contigs), and per contig read mapping statistics (number of reads mapping to each contig, and percentage of ambiguity). Ambiguous reads were considered as those that map to more than one of the contigs returned in the assembly process. If an assembled host genome was made available and specified as input into the assembly pipeline, QC phage reads were also mapped to the propagating host to analyse the number of mapped reads, their distribution across the genome, and coverage. These data were collated and used to assess samples for signs of generalised transduction downstream.

3.2.11.5. Putative phage contig extraction and genome verification

Using outputs from CheckV (v1.0.1) analysis and read mapping statistics, putative phage contigs were identified and extracted from the assembly output if they were classified as ‘Complete’ or ‘High-quality’. Average read mapping statistics from mapping subsampled reads were used to indicate whether putative phage contigs had signs of contamination; contigs with an average coverage of at least 80% of the target coverage (320 X) were flagged with a warning for further manual inspection. Samples containing more than one putative phage contig that passed contamination checks were labelled as ‘contaminated’, samples with a single contig were labelled as ‘clean’. Putative phage contigs from clean samples were then extracted using Biopython (v1.78) modules and QC reads mapped back to the genome to obtain absolute (maximal) read coverage using bbmap.sh (v38.18). Per base coverage statistics from the mapped QC reads were visualised using Python’s (v3.11.0) internal Matplotlib module and used for manual curation. At this point; QC reads were also separated into mapped and unmapped reads that were both assembled using SPAdes [181] as described above.

3.2.12. Manual curation of phage assembly data

Using outputs from the assembly pipeline, phage genomes were manually curated for their completeness, assessment of contamination (if any), and lifecycle.

3.2.12.1. *Genome completeness*

Putative phage contigs were considered verified phage genomes based on previously published viral assembly standards for sequencing data [190]. Genomes were classified as ‘complete’ if there were no gaps in the sequence, the terminal repeats were successfully identified, the QC mapped per base coverage statistics were above 100 X, and a genome of the same exact size is able to be produced from reads that were mapped to the initial phage contig (assembly is the same across differing numbers of reads) [157, 190]. The genomes were classified as ‘finished’ if the viral genomes also obtained a per base coverage over 400 X required for the detection of population level variation [157, 190] downstream.

3.2.12.2. *Contamination analysis*

Phage samples were classified as ‘contaminated’ if there were more than one verified genome identified within the sample and excluded from further analysis. Contigs assembled from the QC reads that did not map to phage genome (unmapped reads) were assembled and used to detect prophage induction/contamination events in the phage samples. Contigs that were longer than 1 kb were extracted and queried against the Inphared phage database [191] (accessed 1st May 2023) containing 20,185 phage genomes using BLASTn (v2.5.0) command line tools [192]. Genomes identified, via high scoring hits, as belonging to known prophages were considered contaminants and the phage sample labelled as contaminated with prophage; these samples were also excluded from further analysis. Phage QC reads were mapped to the putative phage contig, signs of general contamination were flagged if the percentage of reads mapping to the phage genome were below 90%.

3.2.13. Genome annotation and reordering

As per previously published guidelines [159, 161], genomes that had passed the assembly curation process were annotated and reordered based on the small or large terminase subunits. Genome annotations were performed using Prokka [193] in conjunction with the PHROGs database (accessed May 2023) [194] to provide initial annotations for each coding sequence (CDS) within the genome using their pre-built Hidden Markov Model (HMM) database. Coding capacity was calculated from Prokka outputs and is the sum of the length of all coding features divided by the total genome length.

3.2.14. Lifecycle analysis

To determine lifecycle, lysogeny associated genes were searched for within the annotation data. Lysogeny associated proteins include integrases, excisionases, recombinases, transposases, repressors, ParA, and ParB [195, 196]. The presence of any of these within the genomes of phages were flagged as lysogens. Next, each coding sequence, regardless of annotation, was subject to BLASTp (v2.5.0) analysis against all proteins extracted from the Inphared database [191] (accessed 1st May 2023) containing 1,799,354 proteins in total. Parameters included 10 maximum target sequences and a coverage of at least 50%. If any of the resulting hits, per CDS, were lysogeny associated proteins, the sample was investigated further as a potential lysogen.

3.2.15. Screening for virulence factors

Identification of antibiotic resistance genes was carried out using internal databases available through ABRicate v1.0.1 [197]. In addition, the NCBI Antimicrobial Resistance Gene Finder Plus [198, 199] (AMRFinderPlus) version 3.11.20 was used to download the latest published databases from NCBI (Database version: 2023-09-26.1) and screen both genomes for the presence of AMR related genes.

3.2.16. Assessment of microdiversity / population diversity

Genomic variation within phage samples was assessed using a rapid haploid variant calling and core genome alignment program Snippy (v4.6.0).

3.2.17. Taxonomic classification:

Phage genomes were queried against the Inphared phage database [191] (accessed 1st May 2023) containing 20,185 phage genomes using BLASTn (v2.5.0) command line tools [192] to generate high scoring matches. Genomes identified by their accession number were then extracted from the database and subject to pairwise comparisons. Pairwise comparison scores of phage genomes were calculated using ANIclustermap (v1.2.0) using default parameters to determine the average nucleotide identity percentages (ANI%) of each phage and 20 of its closest relatives identified using BLASTn (v2.5.0). Images were produced in Python (v3.11.0), using Matplotlib and Seaborn modules.

3.2.18. Transmission electron microscopy:

Phage samples that were verified as ‘complete’ or ‘finished’, free of contamination, lysogenic proteins, and absent of any virulence associated factors were sent for imaging via transmission electron microscopy (TEM). Five microliters of high titre (1×10^9 PFU/mL) phage sample were sent to Dr. Christopher Leigh at the University of Adelaide who aliquoted samples onto formvar coated grids for 2 minutes, and then subsequently stained then with 2% (v/v) aqueous uranyl acetate, before washing with 5 μ L of ddH₂O. Images were taken using a Tecnai G2 Spirit 120kV electron microscope. The acceleration voltage was set at 100 kV to enhance image contrast. Images were recorded using an AMT Nanosprint 15 camera equipped with accompanying software V7.0.1. Phage dimensions such as head length, head diameter, tail length, and tail width were measured using Image J (v1.54d). From these measurements the phage were classified into the following morphotypes: Myovirus, Podovirus or Siphovirus [200].

3.2.19. Host genome analysis:

3.2.19.1. Bacterial short read DNA extraction and sequencing

To generate short reads, gDNA was extracted using the DNeasy Blood & Tissue Kit from QIAGEN, following an adaptation of the manufacturer's instructions as published [201]. Pretreatment steps were as follows: 1×10^9 CFU/mL of bacterial cells were pelleted from an overnight culture and resuspended in 180 μ L of enzymatic lysis buffer (Tris-HCl 20mM, Na-EDTA 2mM, Triton X-100 1%, Rnase A 2mg/mL, Mutanolysin 0.075mg/mL) and incubated for 30 minutes at 37°C to lyse the bacterial cells. Next, 25 μ L of proteinase K and 200 μ L of Buffer AL were added and mixed by vortexing before incubating at 56°C for 30 minutes. DNA precipitation was performed using 200 μ L of ethanol added to the sample and mixed by vortexing. Remaining steps were followed as per the DNeasy Blood & Tissue Kit (QIAGEN, Hilden, Germany) instructions for Spin-Column purification.

The quality and quantity of extracted gDNA were assessed using a combination of methods. Firstly, the quality of DNA samples was determined by measuring absorbance at A260/A280 using the NanoDrop 2000c Spectrophotometer using 1 μ L of extracted sample. Subsequently, DNA quantification was performed using a Qubit™ dsDNA HS and BR Assay Kit following the manufacturer's recommendations. Gel electrophoresis using a 1% (w/v) agarose gel was performed. For gel preparation, 0.5 g of agarose was dissolved in 50 mL of 1X TAE (40 mM Tris-acetate 1 mM EDTA, pH 8.3) buffer, and 5 μ L of SYBR™ Safe was added. The mixture was poured into an agarose gel container and solidified at room temperature for approximately 10 minutes. Five μ L of 1 Kb Plus DNA Ladder was used to indicate DNA fragment sizes and aliquot 5 μ L of the sample DNA mixed with 1 μ L of 6x DNA Gel Loading Dye into each well of the gel. Gel electrophoresis was conducted at 100 volts (V) for 45 minutes. The gel was visualised using the ChemiDoc (BioRad, Hercules, CA, USA) to assess the final DNA quality. Sequencing was performed at the AGRF (Melbourne, Australia). For library preparation, the Nextera Flex preparation kit (Illumina Inc., San Diego, CA, USA) was used to prepare for sequencing by fragmenting and tagging DNA fragments prior to

removing any unused adaptors. Libraries were then sequenced using the Novaseq Illumina platform to produce, paired end, 150 bp reads.

3.2.19.2. Bacterial long read DNA extraction and sequencing

DNA extraction and sequencing for long reads was performed by Dr Samuel Montgomery (Telethon Kids Institute, Perth, Australia). Briefly, genomic DNA was extracted from overnight cultures of bacteria taken from a single colony using MetaPolyzyme (Sigma) as a pre-treatment step, followed by DNA precipitation using ethanol and extraction using the Puregene tissue kit (QIAGEN (Hilden, Germany) [202]. Concentrations (ng/ μ L) were determined via Qubit fluorometer (Thermo Fisher Scientific, Waltham, MA, USA), and quality scores (260/280) were checked using a Nanodrop 2000 instrument (Thermo Fisher Scientific, Waltham, MA, USA). The extracted bacterial gDNA were sequenced using a MinION 10.4.1 flow cell and rapid barcoding kit (SQK-RBK114.24) to generate long reads. Sequencing data were assessed for quality using FastQC (v0.11.9) and NanoPlot (v1.41.6) [35, 36].

3.2.19.3. Bacterial genome analysis

Raw long reads were *de novo* assembled using Flye (v2.9.2) [203] into a single, fully resolved, chromosome of expected size (~2.79 MB) and separate mobile genetic elements (MGEs) of varying length. Remaining contigs were polished using Pilon [204] using the short reads from Illumina. Genome assembly statistics were generated using QUAST (v5.2.0).

Bacterial genomes were checked for completeness and subject to marker gene comparative analyses using the CheckM tool suite (v1.2.2) [38-40]. Genomes and accompanying MGEs were annotated using Bakta (v1.5.1) [41] using the full database in combination with the antimicrobial resistance finder database (v2023-04-17.1) [42].

3.2.20. Host contamination

Phage QC reads were mapped to the host genome, if the percentage of QC reads mapped back to the host genome was more than 5% [157]. Phage samples breaching this value were flagged as host contaminated and excluded from further analysis.

3.2.21. Generalised transduction

Phage QC reads were mapped to the host genome; signs of transduction were assessed using per base coverage statistics across the host genome. Reads mapping to the host genome were assessed for even coverage and regions exceeding 5 kb at low sequencing depth [18]. If these regions were present, phage samples were considered a transduction risk and excluded from further analysis.

3.3. Results

3.3.1. Phage isolation

Over the course of this project, 16 wastewater samples were collected from the Subiaco Wastewater treatment plant (Shenton Park, Perth, Australia) and four breastmilk samples from the COMET study. A total of 14 positive hits were obtained (Table 3.1) from which purifications were attempted for 40 prospective wastewater bacteriophages collected from whole plate overlays. Of the 14 positive hits, 4 were obtained using enrichment conditions that enabled the purification of 11 prospective phage samples, and 10 were obtained using a modified enrichment condition that contained an added timepoint (12h), increased cations (3 mM CaCl₂ + 3 mM MgCl₂), increased incubation speed (80 rpm), and an additional 35 clinical bacterial isolates (SA20 to SA55): enrichments under these conditions enabled the purification of 21/29 (72%) more prospective phage samples, 8 of which could not be recovered after three rounds of purification due to drops in phage concentration.

In total, 32 prospective purified phage samples were isolated using a set of both MSSA (n = 10) and MRSA (n = 9) respiratory clinical isolates. More phages were obtained using MSSA (n = 29) respiratory isolates than MRSA (n = 12) isolates. The modified enrichment protocol increased the number of hits obtained from wastewater samples; however, some of the prospective phages from these samples were unable to be purified (n = 8). In addition, 3 of these phages were obtained using a commonly used laboratory strain of *S. aureus* (ATCC-6538), and a further 6 were isolated using MRSA from a wound (SA20) and MSSA from a blood culture (SA48). Of the four pooled breastmilk samples, a single positive hit was found (breastmilk: Group 2) active against an MRSA (SA01) respiratory isolate, a single plaque was purified from this sample. Attempts were made to obtain phages from the separated breastmilk fat but no positive enrichments were seen.

Breastmilk samples were taken (BMG1-4) and pooled from 107 samples obtained from the COMET study that had varying amounts of *Staphylococcus* bacteria as inferred by 16s sequencing. A single phage was obtained from breastmilk pooled group 2 (table 3.1).

In summary a total of 33 (32 from wastewater and 1 from breastmilk) prospective phage samples could be maintained and grown to high concentrations for DNA extraction (Table 3.3).

3.3.2. Plaque morphology

Phage samples did not maintain consistent morphology when performing consecutive whole plate overlays required for plaque purification (Figure 3.1). Despite undergoing three rounds of plaque isolation, whole plate overlays of the final prospective phage samples against their host bacterial strain of *S. aureus* revealed the presence of multiple plaques with different sizes. The plaque morphologies across the samples were a mixture of clear (n = 17) and turbid (n = 16) types of various sizes (small: 4, medium: 13, large: 16). All plaques identified were round and absent of a halo (Table 3.2).

3.3.3. DNA extraction

Phage gDNA of adequate quality for DNA sequencing and further analysis were able to be extracted from 22 / 33 of the purified phage samples that were able to be propagated to high concentrations (Table 3.3). Extractions were deemed insufficient in quantity if they were under 1 ng in yield or of inappropriate quality if the nanodrop 260/280 values were outside of 1.8-2.0. Samples that passed these checks were sent to the AGRF where further examinations of quality were performed prior to sequencing.

Table 3.1: Positive hits from phage positive wastewater and breastmilk samples collected between January 2020 and November 2021.

Source	Positive hits	Timepoint collected (hours)	Enrichment conditions	Sample ID	Host bacteria	Purified from enrichment
Wastewater: Trap 78	PH1	24	1mM CaCl ₂ + 1mM MgCl ₂ , 50rpm	P1	MSSA (SA19)	Yes
				P2	MSSA (SA19)	Yes
				P3	MSSA (SA19)	Yes
Wastewater: Trap 79	PH2	24	1mM CaCl ₂ + 1mM MgCl ₂ , 50rpm	P4	MSSA (SA17)	Yes
				P5	MSSA (SA17)	Yes
				P6	MSSA (SA17)	Yes
Wastewater: Trap 81	PH3	48	1mM CaCl ₂ + 1mM MgCl ₂ , 50rpm	P7	MRSA (SA09)	Yes
				P8	MRSA (SA09)	Yes
				P9	MRSA (SA09)	Yes
Wastewater: Trap 83	PH4	48	1mM CaCl ₂ + 1mM MgCl ₂ , 50rpm	P10	MRSA (SA06)	Yes
				P11	MRSA (SA06)	Yes
Wastewater: Trap 86	PH5	24	3mM CaCl ₂ + 3mM MgCl ₂ , 80rpm	P12	MSSA (SA19)	Yes
				P13	MSSA (SA19)	Yes
				P14	MSSA (SA19)	Yes
	PH6	12	3mM CaCl ₂ + 3mM MgCl ₂ , 80rpm	P15	MSSA (SA15)	Yes
				P16	MSSA (SA15)	Yes
				P17	MSSA (SA15)	Yes
Wastewater: Trap 87	PH7	12	3mM CaCl ₂ + 3mM MgCl ₂ , 80rpm	P18	ATCC-6538	Yes
				P19	ATCC-6538	Yes
				P20	ATCC-6538	Yes

Wastewater: Trap 88	PH8	24	3mM CaCl ₂ + 3mM MgCl ₂ , 80rpm	P21	MSSA (SA13)	Yes
				P22	MSSA (SA13)	Yes
				P23	MSSA (SA13)	Yes
Wastewater: Trap 89	PH9	12	3mM CaCl ₂ + 3mM MgCl ₂ , 80rpm	P24	MRSA (SA09)	No
				P25	MRSA (SA09)	No
				P26	MRSA (SA09)	No
				P27	MSSA (SA16)	No
	PH10			P28	MSSA (SA16)	No
Wastewater: Trap 90	PH11	12	3mM CaCl ₂ + 3mM MgCl ₂ , 80rpm	P29	MSSA (SA48)	Yes
				P30	MSSA (SA48)	Yes
				P31	MSSA (SA48)	Yes
Wastewater: Trap 91	PH12	12	3mM CaCl ₂ + 3mM MgCl ₂ , 80rpm	P32	MRSA (SA06)	No
				P33	MRSA (SA06)	No
				P34	MRSA (SA06)	No
Wastewater: Trap 92	PH13	12	3mM CaCl ₂ + 3mM MgCl ₂ , 80rpm	P35	MSSA (SA18)	Yes
				P36	MSSA (SA18)	Yes
				P37	MSSA (SA18)	Yes
	PH14	24	3mM CaCl ₂ + 3mM MgCl ₂ , 80rpm	P38	MSSA (SA20)	Yes
				P39	MSSA (SA20)	Yes
				P40	MSSA (SA20)	Yes
Breastmilk: Group 2	PH15	24	3mM CaCl ₂ + 3mM MgCl ₂ , 80rpm	BMP1	MRSA (SA01)	Yes

Table 3.2: Phenotypic characterisations for each phage. Plaque size distribution was calculated by randomly selecting 20 plaques across a whole plate overlay, categorising their sizes as small (<1 mm), medium (1-2 mm), or large (>2 mm), then calculating the mean (SD).

	Host bacterial species (isolate ID)	Shape (Round / irregular)	Presence of 'halo' (Yes / No)	Plaque clearance (Clear / Turbid)	Plaque size	
					category	Mean (\pm SD) mm
P1	MSSA (SA19)	Round	No	Turbid	Medium	1.83 (\pm 0.77)
P2	MSSA (SA19)	Round	No	Turbid	Large	2.20 (\pm 0.54)
P3	MSSA (SA19)	Round	No	Turbid	Medium	1.52 (\pm 0.68)
P4	MSSA (SA17)	Round	No	Clear	Medium	1.83 (\pm 0.82)
P5	MSSA (SA17)	Round	No	Clear	Large	2.20 (\pm 0.86)
P6	MSSA (SA17)	Round	No	Clear	Large	2.45 (\pm 0.82)
P7	MRSA (SA09)	Round	No	Clear	Large	2.97 (\pm 0.73)
P8	MRSA (SA09)	Round	No	Clear	Large	3.17 (\pm 0.83)
P9	MRSA (SA09)	Round	No	Clear	Large	2.85 (\pm 0.89)
P10	MRSA (SA06)	Round	No	Turbid	Large	2.47 (\pm 0.74)
P11	MRSA (SA06)	Round	No	Turbid	Large	2.45 (\pm 0.87)
P12	MSSA (SA19)	Round	No	Clear	Large	2.68 (\pm 0.42)
P13	MSSA (SA19)	Round	No	Clear	Large	2.08 (\pm 0.60)
P14	MSSA (SA19)	Round	No	Clear	Large	2.25 (\pm 0.60)
P15	MSSA (SA15)	Round	No	Turbid	Medium	1.78 (\pm 0.67)

P16	MSSA (SA15)	Round	No	Clear	Large	2.12 (± 0.63)
P17	MSSA (SA15)	Round	No	Turbid	Large	2.67 (± 0.58)
P18	ATCC-6538	Round	No	Clear	Large	2.87 (± 0.68)
P19	ATCC-6538	Round	No	Clear	Large	3.11 (± 0.71)
P20	ATCC-6538	Round	No	Clear	Large	3.39 (± 0.67)
P21	MSSA (SA13)	Round	No	Turbid	Small	0.93 (± 0.21)
P22	MSSA (SA13)	Round	No	Turbid	Medium	1.29 (± 0.34)
P23	MSSA (SA13)	Round	No	Turbid	Medium	1.35 (± 0.40)
P29	MSSA (SA48)	Round	No	Clear	Medium	1.60 (± 0.33)
P30	MSSA (SA48)	Round	No	Clear	Medium	1.89 (± 0.52)
P31	MSSA (SA48)	Round	No	Clear	Medium	1.68 (± 0.54)
P35	MSSA (SA18)	Round	No	Turbid	Small	0.99 (± 0.29)
P36	MSSA (SA18)	Round	No	Turbid	Medium	1.06 (± 0.46)
P37	MSSA (SA18)	Round	No	Turbid	Medium	1.25 (± 0.40)
P38	MSSA (SA20)	Round	No	Turbid	Small	0.93 (± 0.25)
P39	MSSA (SA20)	Round	No	Turbid	Small	0.80 (± 0.32)
P40	MSSA (SA20)	Round	No	Turbid	Medium	1.09 (± 0.21)
BMP1	MRSA (SA01)	Round	No	Clear	Medium	1.65 (± 0.59)

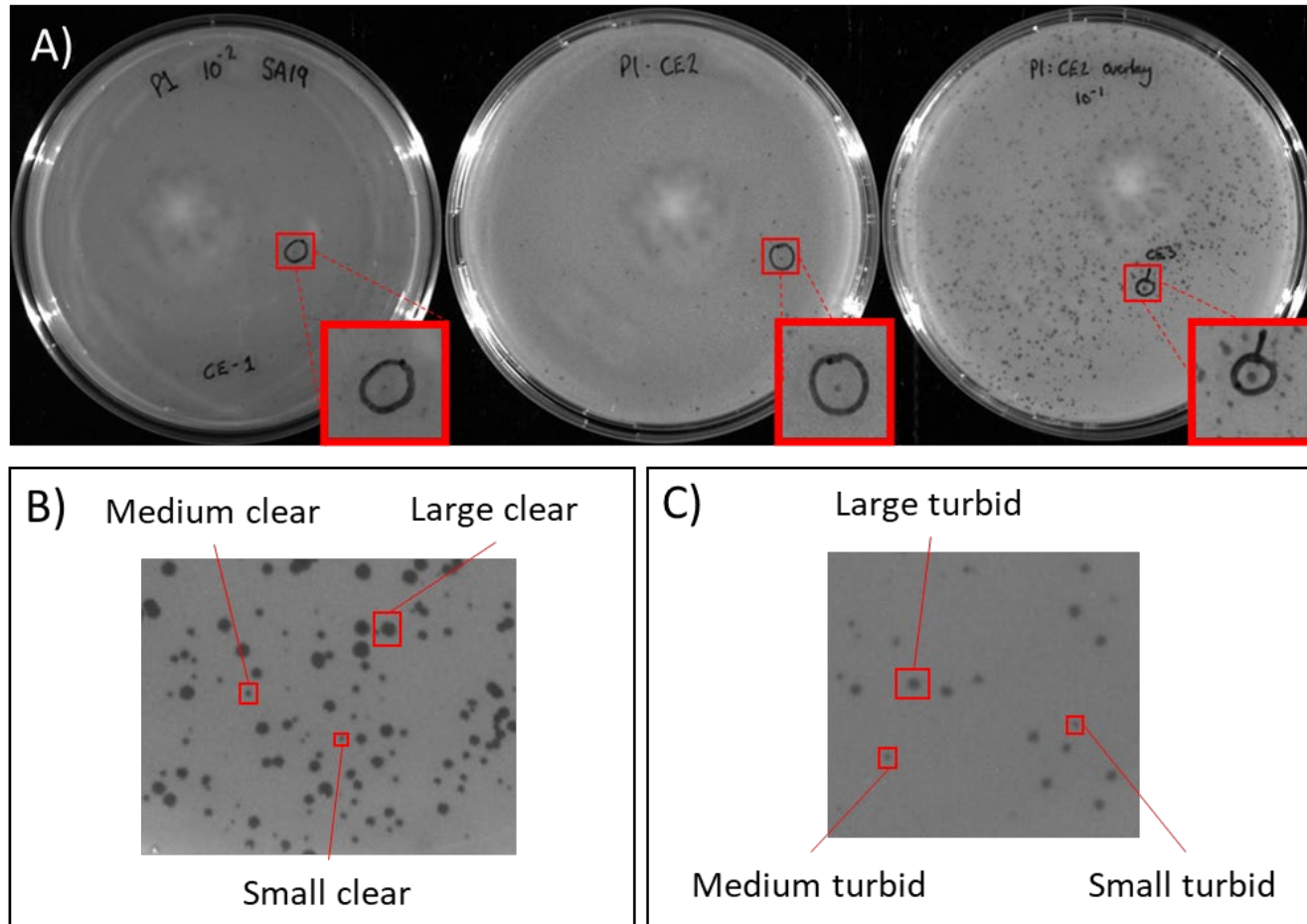


Figure 3.1: Plaque morphology visualised using double agar overlays imbued with phages and their host bacterial strains. Panel A shows positive phage activity for phage P1 against its host MSSA, bacterial isolate SA19. Plaque formation is shown across all three rounds of plaque purification indicating a successful phage isolation process. Panel B shows a plate image with various plaque sizes, the image here is of a phage that produces clear plaques of various sizes against its host. Panel C shows a phage that produces turbid plaques of various sizes against its host isolate.

Table 3.3: Extracted gDNA samples were subject to internal quality control (QC) checks through the AGRF facility in Melbourne. All samples that passed QC checks were sequenced and the following data generated for *de novo* assembly.

Phage	DNA concentration (ng/μL)	Total DNA extracted (ng)	150bp Paired end reads	Data yield (Gb)
P1	15.4	384	4,522,462	1.37
P2	22.5	562	5,902,133	1.78
P3	8.1	282	4,655,001	1.41
P4	16.83	505	2,341,004	0.71
P6	4.4	132	2,299,380	0.69
P7	10.9	328	3,492,780	1.05
P8	4.9	132	3,080,963	0.93
P9	12.2	328	2,162,486	0.65
P10	6.3	188	2,828,158	0.85
P12	7.45	201	4,981,901	1.50
P13	6.51	176	5,167,555	1.56
P15	12.9	321	3,777,999	1.14
P16	21.7	543	4,474,088	1.35
P17	12.2	365	4,632,239	1.40
P18	3.5	94	4,690,987	1.42
P19	8.6	215	3,930,213	1.19
P20	7.0	188	3,829,524	1.16
P29	6.2	166	3,368,591	1.02
P30	18.9	509	3,387,926	1.02
P31	16.1	434	3,889,807	1.17
P38	0.91	27.36	2,980,137	0.90
BMP1	7.1	192	3,690,362	1.11

3.3.4. Phage genomes

To assess whether the phage contigs were phage genomes, each sample assembly result was assessed for completeness using CheckV. A total of 16 samples were used for genome extraction, 14 of these contained a single genome classified as “complete” or “high-quality” by CheckV analysis. Of the remaining potentially contaminated samples, a total of 50 contigs were present, these were curated to assess the quantity of reads that mapped to each contig present within the samples. When mapping QC reads to the total number of contigs from each of the potentially contaminated samples, it was revealed that two of these samples had a single contig that had >95% reads mapped unambiguously to it, P38: 96.4% and P3: 96.6% (Table 3.4). This was an indication that either: the contaminating DNA was very minor, or the ambiguous mapping of reads is a result of microdiversity within the sample. These contigs, in addition to the clean sample contigs were extracted for further analysis (Table 3.4). Each of the extracted phage genomes (n = 16) had a lowest per base coverage and average coverage value above 400 X (Table 3.4). However, when QC mapped reads were reassembled, only genomes over 130 kb (n = 9) assembled into genomes of the exact same size. These genomes were: P1, P3, P7, P8, P9, P18, P19, P20, BMP1. The remaining 7 genomes, P15, P16, P17, P38, P29, P30, P31 were unable to be reassembled into contigs of exact same size from the QC mapped reads. For phage samples that had their host propagating organism sequenced and assembled, phage QC reads were mapped to the assembly and no regions across the genome >5 kb were covered. In addition, less than 5% of phage QC reads (ambiguous + unambiguous) mapped to the host genome for every host pairing. From this, there appeared no signs of generalised transduction for any of these phage genomes when grown with their initial isolation host [157, 195]. To summarise, of the 14 genomes at this point, 7 were between 43-46 kb and expected to be proviral sequences of the Siphovirus morphotype and the other 7 were between >125 kb, typical of lytic myoviruses active against *S. aureus* [205].

Table 3.4: Summary of contigs that passed assembly QC checks (n = 16) and were extracted for further analysis. Subsampled (normalised) reads counts were performed using fastQC (v0.11.9). CheckV version v1.0.1 was used to detect terminal repeats and assess completeness of putative phage contigs. Read mapping statistics were generated using bmap.sh (v38.18) and genome extractions and GC% calculations were performed using Biopython (v1.78) modules.

Sample	Genome length (bp)	GC (%)	Subsampled read count	Subsampled read coverage (X)	Phage QC reads mapped to phage contig (%)
P15	43875	35.2	234280	673	99.1
P16	43875	35.2	261146	748	99.0
P17	43875	35.2	240408	689	98.7
P1	140772	30.4	1409232	590	90.9
P38	44996	33.4	294484	682	96.4
P3	140772	30.4	784878	609	96.6
P18	135421	30.1	701492	648	96.2
P19	135421	30.1	687882	636	95.8
P20	135421	30.1	677516	627	96.2
P29	43943	35.3	253858	721	96.6
P30	44038	35.3	258784	729	97.4
P31	44038	35.3	261112	736	96.1
P7	135423	30.1	672876	625	97.2
P8	135423	30.1	678160	631	97.2
P9	135421	30.1	694268	639	93.6
BMP1	141063	30.4	712676	635	96.9

3.3.5. Average nucleotide identity (%) scores

The average nucleotide identity scores revealed that phages clustered into two main groups; the first were larger genomes >125 kb and the second contained the smaller genomes between 43 and 46 kb. The Y axis in Figure 3.2 shows the sample name in addition to the genome length (bp). The following genomes: P7, P8, P9, P18, P19, and P20 all scored >99.9% between them. This clades closest related genomes consisted of BMP1, P1, and P3. Whilst P1 and P3 were identical in terms of ANI% and length, BMP1 was ~2% different. Of the smaller genomes (n=7), P15, P16, and P17 share >99.8% ANI similarity. P29, P30, and P31 share 99.9% similarity, and P38 stands as an outlier to the rest, sharing a maximum of 84% ANI with the other genomes within this clade (Figure 3.2).

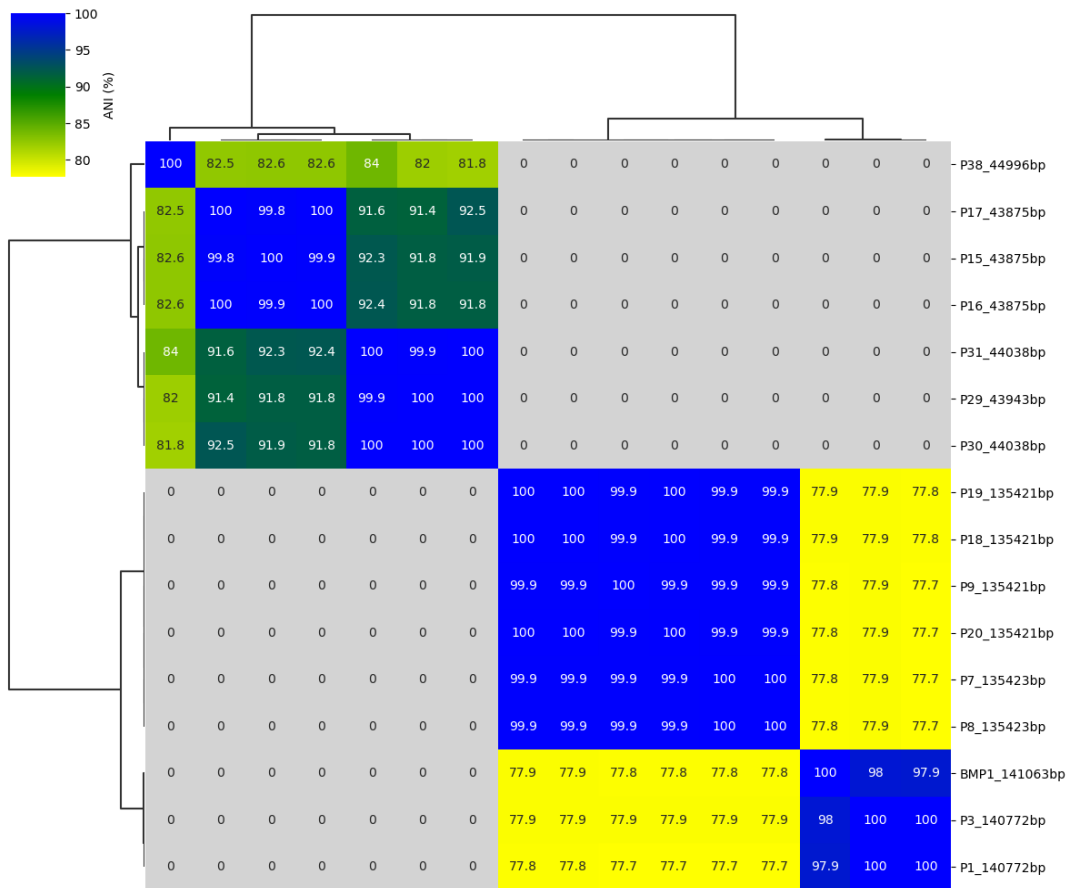


Figure 3.2: Average nucleotide identity scores for all phages passing the assembly QC checkpoints produced using ANIclustermap (v1.2.0). There are 5 clades that form with >5% ANI difference between them. These clades are indicated in blue squares where values do not drop below 95%.

3.3.6. Unique phage identification

Using a combination of metrics generated from the analysis of each phage genome from assembly (size and GC %) and pairwise comparisons (ANI%), phages were classified as the same if any two of the following pairwise conditions were met: the genome sizes were within 100bp of each other, the GC % were the exactly the same, the average nucleotide identity of each phage was >99% similar.

Table 3.5: Phages identified as unique or identical to others isolated. Phage genomes with no reason stated are singletons and satisfied all criteria when compared with all other genomes isolated within this study. The consensus sequence was the sequence used to represent each group for downstream analysis at this point.

Phages	Reason identified as same genome	Consensus sequence used
P1, P3	100% ANI similarity, same genome size and GC content	P1
P7, P8, P9, P18, P19, P20	Genomes above 99% similar via ANI, all genomes within 100bp of each other, all genomes have the same GC%.	P7
P15, P16, P17	Genomes above 99% similar via ANI, all genomes are the exact same size, all genomes have the same GC%.	P15
P29	-	P29
P30, P31	100% ANI similarity, same genome size and GC content	P30
P38	-	P38
BMP1	-	BMP1

3.3.7. Therapeutic checkpoints: lifecycle, virulence, gene content

Amongst the unique phages (n = 7) identified, further analysis was used to determine their therapeutic potential. Phage were considered appropriate and useable for downstream experimentation if they contained no genes associated with AMR or virulence and were not likely to have a lysogenic lifecycle. Screening for resistance genes using AMRFinderPlus (v3.11.20) [198] and ABRicate (v1.0.1) [197] revealed no antimicrobial resistance genes within the genomes of any contigs produced by BMP1, P1, P7, P15, P29, P30, and P38.

3.3.8. Annotation

All genomes were successfully annotated and reordered based on the small terminase subunits. Data shown are from the reordered genomes and values were matched to the raw assembly values to check no errors were introduced in the reordering process (Table 3.6). The genomes: P15, P29, P30, and P38 all contained a CDS for Panton-Valentine leukocidin (Appendices G4, G5, G6, G7).

Table 3.6: Annotation summary and coding capacity percentages for each phage genome. The PHROGs database (accessed May 2023) [194] were used in conjunction with Prokka [193] to provide standardised annotations and calculate coding capacity.

Genome	Total CDS	Hypothetical proteins	Coding capacity (%)	tRNAs
BMP1	224	140	90.17	Trp, Phe, Asp
P1	220	135	90.82	Phe, Asp
P7	187	107	88.67	-
P15	64	24	93.63	-
P29	71	33	93.93	-
P30	71	33	93.96	-
P38	64	24	93.17	-

3.3.9. Lifecycle analysis

Lifecycle analysis revealed that the following phages contained genes that were associated with lysogeny: P15, P16, P17, P29, P30, P31, and P38 (Table 3.7). The lifecycle of each phage genome was also determined using Bacphlip that predicted the likelihood of these phages having a lysogenic lifecycle >50% (>0.5). Phages BMP1, P1, and P7 were all predicted to have a lytic lifecycle (<0.5) (Table 3.7).

Table 3.7: Summary of the lysogeny warnings flagged within each phage genome. Bacphlip (v0.9.6) were used to predict the lifecycle of each phage genome. BLASTp (v2.5.0) were used to query all CDS from these genomes against all proteins extracted from the Inphared database [191] (accessed 1st May 2023).

Genome	BACPHLIP lysogeny score	BLASTp search for lysogeny associated genes	
		Query CDS	Product
BMP1	0.1	-	-
P1	0.125	-	-
P7	0.1125	-	-
P15	1	P15_00007	Arc-like repressor
		P15_00030	integrase
		P15_00031	excisionase
		P15_00033	transcriptional repressor
		P15_00035	ParB-like partition nuclease
		P15_00036	ParB-like partition protein
		P15_00040	anti-repressor
P29	0.925	P29_00007	Arc-like repressor
		P29_00030	integrase
		P29_00034	transcriptional repressor
		P29_00036	anti-repressor Ant

		P29_00039	anti-repressor
P30	0.925	P30_00007	Arc-like repressor
		P30_00030	integrase
		P30_00034	transcriptional repressor
		P30_00036	anti-repressor Ant
		P30_00039	anti-repressor
P38	0.9875	P38_00025	integrase

3.3.10. Population diversity:

Phages deemed to have lytic lifecycles by genome analysis were assessed for microdiversity within the sample. Phages BMP1, P1, and P7 were all found to have zero single nucleotide polymorphisms (SNPs).

3.3.11. Phage taxonomy and morphotype

Phage genomes (n = 3) that passed all QC checks through assembly, were identified as unique, and contained no resistance factors (via ABRicate or AMRfinderPlus) or known lysogeny associated products. These genomes were used for BLASTn analysis to obtain taxonomic information from the closest hits and sent for morphotype identification via TEM imaging. The closest relatives (n = 20) for these phages were also collected and used to infer taxonomic information. From this, the top matches for both phages BMP1 and P1 all belonged to the same genus *Kayvirus* and the top matches for phage P7 were classified as *Silviavirus* phages.

The morphotype of phages BMP1, P1, and P7 were all determined by visually inspecting the TEM images. All three phages were found to belong to the myovirus morphotype (no longer genomically classified [200]). Each phage had a typical sized icosahedral head and a long contractile tail (Figure 3.3). Whilst the dimensions of the head length, head diameter and tail

diameter were similar across all phages, P7 had a much shorter tail length (164.1 nm) than BMP1 and P1 phages (202.1 nm and 208.8 nm respectively).

Table 3.8: Dimensions of phages BMP1, P1, and P7 as measured using TEM images.

Phage	Head length (nm)	Head diameter (nm)	Tail length (nm)	Tail diameter (nm)
BMP1	94.6 (\pm 1.4)	96.8 (\pm 0.9)	202.1 (\pm 4.3)	20.2 (\pm 1.3)
P1	100.5 (\pm 1.7)	99.0 (\pm 1.3)	208.8 (\pm 3.7)	21.3 (\pm 1.0)
P7	93.8 (\pm 1.7)	91.4 (\pm 3.6)	164.1 (\pm 5.7)	26.1 (\pm 0.9)

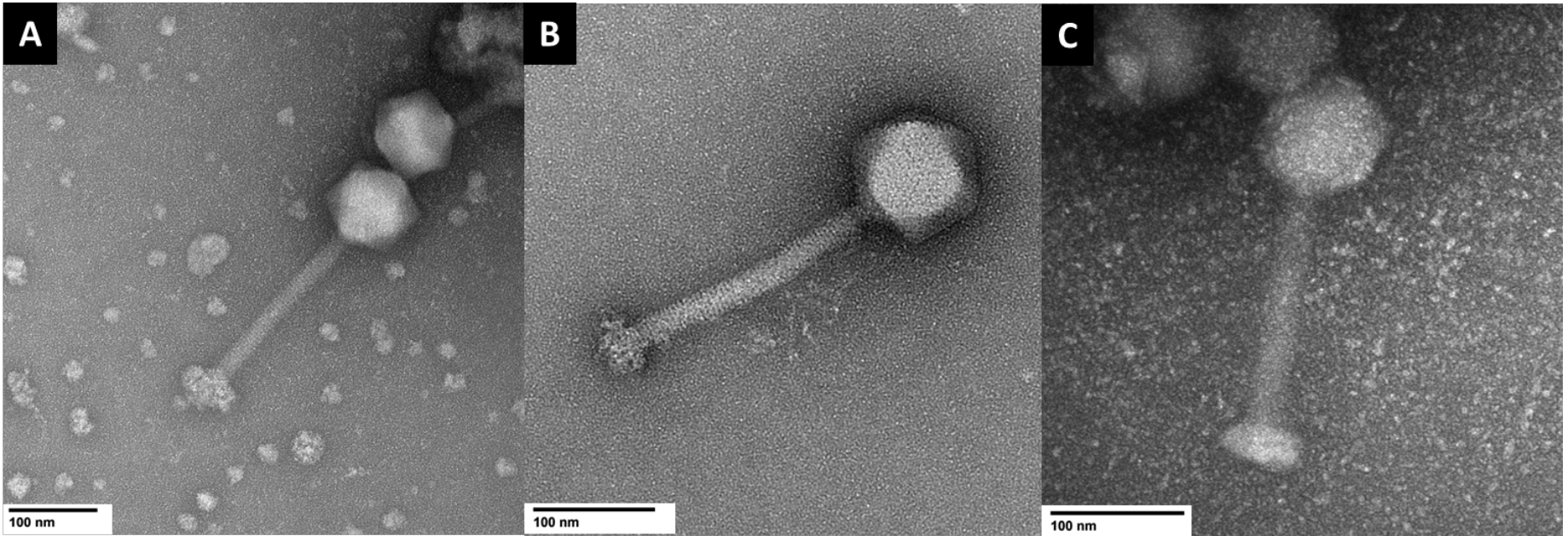


Figure 3.3: Transmission electron micrographs of phages BMP1 (panel A), P1 (panel B), and P7 (panel C). Phages were stained with 2% (v/v) aqueous uranyl acetate for visualisation and imaged using a NANOSPRT15 camera (Exposure: 400 ms). Each bacteriophage had an icosahedral head and a long contractile tail. Scale bars on each image are 100nm.

3.3.12. Host genome analysis

The host genomes for BMP1 (SA01), P1 (SA19), and P7 (SA09) were sent for sequencing and assembled into genome sizes expected for *S. aureus* bacteria. Analysis of the host bacterial genomes, SA01, SA09, and SA19 verify that all isolates belong to *Staphylococcus aureus*. Metrics such as genome length, GC%, and coding density all fit within normal ranges for *S. aureus* and completeness scores were all >90% completeness which is considered the highest ‘formal’ quantitative measurement of completeness (“near complete”) that isn’t 100% [206]. When phage QC reads were mapped to the host genome for each phage, no region above 5 kb were covered. However, the percentage of reads mapping to the host genome for P1 (SA19) were 7.58% mapped unambiguous reads. For BMP1, this value was 0.04%, and for P7 this was 0.03%.

Table 3.9: Host genome assembly statistics. Read mapping statistics were generated using bbmap.sh (v38.18). Assembly statistics were generated using QUAST (v5.2.0). Completeness was determined using CheckM tool suite (v1.2.2).

Host	Genome size (bp)	Coverage (X)	GC %	CheckM completeness (%)	CheckM contamination (%)
SA01	2,810,685	75	32.81	97.88	0.22
SA19	2,814,725	74	32.83	96.60	1
SA09	2,910,757	45	32.79	98.29	0.22

3.3.13. Phage naming

Phages BMP1, P1, and P7 passed all QC checks throughout the genome assembly and analysis steps described above. In recognition of the first nation ownership of the land (Whadjuk Noongar Boodjar), these phages were renamed in collaboration with the Noongar language centre, who were provided the TEM images to produce descriptive names for the

phages in the Noongar language, the following names were assigned: Biyabeda mokiny 1 (BMP1), Biyabeda mokiny 2 (P1), and Koomba kaat 1 (P7).

The assembled and annotated genomes were made available through GenBank under these names, using the accession numbers OP263967 (BMP1), OP263968 (P1) and OP263969 (P7), BioProject number PRJNA862682.

3.4. Discussion:

Within this chapter, a panel of 19 clinical *S. aureus* isolates were used to isolate numerous phages from wastewater and a single phage from clinical breastmilk samples. The majority of these phages were temperate, and bioinformatics pipelines were successfully utilised to screen the phage genomes to identify therapeutic candidates and rule out contaminated samples. Two novel phages were identified as part of this process as belonging to the lytic phage genera: *Kayvirus* and *Silviavirus*. These phages are absent of any genes associated with virulence, antibiotic resistance or lysogeny. To provide a comprehensive foundation from which to perform further characterisations, the host bacterial *S. aureus* genomes were assembled using long reads to resolve a complete genome of expected size. These were used to assess the phage samples for signs of general transduction and prophage contamination from the host; within this analysis, both phages were found to be safe when grown using their initial host isolation strain [157, 161]. To corroborate the genomics analysis, structural dimensions were measured using TEM images of each phage; both phages were confirmed to have Myovirus morphotypes. Phages may offer a promising alternative to antibiotics for *S. aureus* isolated from various clinical sites [99, 207] and the development of phage products against *S. aureus* infections could offer a much-needed solution to the limitations of current antibiotic pipelines. This chapter represents the first step towards generating a phage library involving the isolation and screening processes required to identify phages with the desired traits for therapeutic phages.

For characterisation, plaque morphology has been traditionally used as a tool to infer phage diversity [158, 208], a high standard deviation and overlapping plaque sizes were seen (Table

3.2) amongst the plaque size categories (small, medium, and large). This variation may be attributed to the presence of multiple plaque sizes on each plate, irrespective of the number of purification rounds used to produce a homogenous phage sample. In hindsight, plaque morphology data provide a crude indication of lytic activity, as the frequency of larger, clearer plaques (as opposed to turbid ones) suggested stronger lytic potential. However, due to limited diversity, (since most phages generating the plaque data were genomically identical), any differences observed may have been more likely a result of the combined variability arising from experimental conditions, including static plate incubation periods, temperature fluctuations, and batch differences in agar preparations. Plaque morphology is a characteristic known to be influenced by various factors such as media composition and plating conditions [208]; unfortunately, the phage utilised within this study was a Siphovirus, making broader comparisons difficult for lytic *Staphylococcus* phages that belong to Myoviral morphotypes.

From these 15 bacterial enrichments, approximately 40 plaques were chosen to undergo three rounds of plaque purification for which 32 were stable throughout. Of these, gDNA was successfully extracted from 22 samples, with the remaining not passing quality control standards prior to WGS analysis. A possible reason for this was the low ($<10^7$ PFU/mL) concentrations of phage in many of the final preparations. This could be due to numerous factors including inadequate physiochemical stability profiles or inherent resistance of the bacterial isolate making effective phage propagation difficult [111, 209]. To address these issues, it may be pertinent to add stabilising agents known to preserve the concentrations of phage over time such as glycerol or perform growth optimisations to maximise effective titre prior to WGS [111, 209]. Another suggestion could be to perform efficiency of plating for newly isolated phages at this stage to identify the most efficient host bacterial strain for any given bacteria. Compared to the only (to the authors knowledge) study reporting isolation success against *S. aureus*, results generated in this chapter were as expected; as low hit rates have been found when phages are sourced from a single wastewater sample [1]. More research is required to determine whether low hit rates are due to bias within enrichment techniques, which have remained largely unchanged since their inception [158].

From the 22 sequenced phage samples, the target coverage of 400 X was achieved for 14 of the samples that assembled into contigs that passed internal assembly QC checks. A single sample (P10) failed to produce any contigs that were considered complete or high quality, and upon examination of the data it was confirmed that the assembly was heavily fragmented into 187 contigs from 1 kb to 100 kb long. Of the remaining 21 samples, 7 were deemed contaminated due to the presence of more than one contig labelled as complete by CheckV analysis within the same sample. Every sample contained numerous DNA fragments that were assessed using mapping statistics to determine the cause of contamination, whether proviral, host bacterial, or an unknown or indiscernible contaminant introduced during the extraction or handling procedures prior to sequencing. Irrespective of this, the analyses performed filtered the genomes obtained according to previously published guidelines for the quality assessment of phages [157].

Fragmented assemblies arise due to the presence of multiple genomes or host bacterial DNA contamination [157, 161]. Seven samples identified in this chapter as contaminated had multiple viral contigs with viral genes present as determined by CheckV [189]. This is unsurprising due to the diversity and number of prophages within *S. aureus* bacteria [210, 211]. Comparing these data to the numerous phage characterisation papers released for *Staphylococcus* phages is difficult due to the number of these with uncharacterised hosts [212-215], or the absence of mapping statistics from which lysogen induction or signs of transduction may be determined [195]. From the extracted genomes (n = 16); seven were determined to be unique based on their genomic characteristics (Table 3.5). These seven phages were assessed using vConTACT2 [216] and prospectively belong to 4 known genera of *Staphylococcus* infecting bacteriophages: *Kayvirus*, *Silviavirus*, *Phietavirus*, and *Triavirus*. Whilst we assessed the lifecycle of these phages in a ‘classification independent’ manner first, two of these Genera (*Phietavirus* and *Triavirus*) identified are known to contain phages that have a lysogenic lifecycle, exhibit a Siphovirus morphotype, and reside predominantly within *S. aureus* bacteria [210].

Despite finding low abundances of phages within the samples, the isolation process did yield three bacteriophage candidates that belong to the family Herelleviridae. Many members of this family have already been extensively characterised for therapeutic applications [99, 112, 212, 217]. In the Inphared database (accessed on May 1st 2023), 574 Staphylococcal phages were identified with 217 belonging to the family Herelleviridae. Notably, ~50% of these *Herelleviridae* phages were Kayviruses (n = 107), members of which have been previously characterised and utilised for therapeutic applications in humans [93, 165]. Members of the genus *Silviavirus* were more recently discovered and have not seen use in humans [217]; they are less well studied than their *Kayvirus* relatives and may require stringent safety assessments before making their way into clinic. Currently, numerous members of the *Silviavirus* genus are being characterised for therapeutic purposes [212, 217] owing to their exceptional ranges of activity against MRSA. However, without a fully characterised reference panel of *S. aureus* isolates; the differences seen within host range data are still often limited by the bacterial diversity used within the assay.

This chapter demonstrated that *Staphylococcus* phages appropriate for phage therapy may be isolated using clinical respiratory isolates of *S. aureus*. Whilst phages for this pathogen are low in abundance from wastewater sources and may take time to initially accumulate batches of positive hits for sequencing, once isolated and extracted for WGS, high throughput screening pipelines can be initiated to identify phages that are lytic, absent of lysogenic markers, and meet previously published cutoff points for genome completeness and contamination assessment [157, 161, 190]. To place this into context, the wastewater samples were collected for over a year, and isolation events (positive hits) were infrequent throughout (Table 3.1); however, once sequences were obtained, the process runtime from receiving raw sequencing reads to assembled and extracted genomes with read mapping statistics (read coverage and % ambiguity), completion status (CheckV), contamination status (>1 'Complete' contig per sample), took approximately 4 hours in total. This time included separating and assembling the QC mapped and unmapped reads to each phage contig to enable assembly curations such as the confirmation of a genome of exact same size produced from the mapped reads (A metric ensuring the robustness of the initial assembly which is produced from subsampled reads) and the detection any low-level induction of prophages

from the sample that may be missed in the initial assembly due to subsampling [161]. By identifying genomically safe candidates from these data and filtering out contaminated samples, the allocation of resources may be prioritised effectively; this is especially important in the case of *Staphylococcus* infecting phages being isolated using clinical strains with unknown prophage content.

Data were also provided to support the safety of using the initial isolation hosts (clinical isolates) as the host propagating strains for these particular phages. Using these data, in addition to previous warnings flagged throughout the genome assembly pipeline, Biyabeda mokiny 2 was removed from downstream analysis due to transduction risk. Despite the genome itself being of appropriate quality and meeting the automated coverage checkpoint of >90% phage mapped reads to the assembly, this was a borderline value and a more stringent cutoff point of 95% is suggested [157]. In addition, the unmapped reads that were assembled formed multiple large contigs that were likely from host contamination. An obvious limitation of this procedure is the need to re-purify and characterise phages within different isolation hosts, or use a prophage removed strain of *S. aureus* such as RN4420, however the efficiency of phage replication within this strain was noticeably lower (data not shown). It has been demonstrated previously that the use of RN4420 can be used as a high efficiency propagation strain using an adapted growth protocol to improve lytic efficiency and provide homogenous populations of phages [218]. Whilst this might be useful in producing prophage contaminant free samples, if the target phage is able to lyse *S. aureus* RN4420 bacteria efficiently, for analysis this process may require phages to be recharacterised once the host has been changed. This is because the host bacteria may impart a selection pressure onto the phage or, more deliberately, impart epigenetic changes to the phage genome that will affect its ability to infect other *S. aureus* bacteria effectively [219].

Finally, the high sequencing coverage across the phage genomes enabled assessment of the population diversity, also called microdiversity [161], within the phage preparations. Despite the purification of homogenous phage samples from a single plaque (3x purified), DNA is extracted from phage populations within a sample. This, in conjunction with the

hypermutable of phages gives justification to assess the amount of variation within phage samples by detecting single nucleotide polymorphisms (SNPs), the accurate detection of which requires sequencing to a high depth / read coverage (>400 X) [157]. From data generated, it was confirmed that phage populations grown to high concentration using these propagation hosts, had no detectable SNPs at the time of sequencing. However, over time this may change as each phage is grown to form a new stock. A major limitation currently seen in phage literature is the lack of data surrounding this microdiversity within phage samples, and, to the authors knowledge, no results of this kind have been published and are freely available for benchmarking despite the number of publications recommending it [157, 161, 190].

One of the limitations of the utilised analyses included the use of a transposon-based library preparation kit; which rely on transposon mediated shearing and ligation [220] and are avoided for use in sequencing phage genomes. Unfortunately, this was detected in hindsight and, due to this, genome ends were unable to be defined in an automated manner by looking for buildups of start reads that occur when using reads generated with a ligation-based library preparation or by using tools such as PhageTerm [221]. To account for this, genomes were reordered based on the small terminase subunit (standard practice [159, 161]) which was annotated and found for all genomes that passed assembly QC checks. This effectively orientates genomes in terms of the forward and reverse strands and enables accurate downstream analyses to be performed such as colinear alignments to observe genomic synteny.

Whilst the isolation of Koomba kaat 1 and Biyabeda mokiny 1 itself adds to the number of genomically distinct phages within public databases [191, 192], a strength of the work conducted within this chapter lies in the reproducibility and automation of processes involved. This work focuses on using previously published parameters as ‘best practice’ in the absence of strict guidelines for parameters such as host contamination cutoff points [157, 161, 190]. These data form a strong foundation from which to safely perform further characterisations with assurances of sample purity. To highlight the potential of automated

bioinformatic pipelines, addressing the lack of *Staphylococcus* phage diversity may include producing a number of phage mutants within different bacterial host strains in an attempt to produce diversity by phage training [222, 223]. Performing these experiments in batches has multiple benefits including the efficient use of a standardised automated pipeline to screen phages alongside their hosts and in turn informing the use of specific clinical isolates. If clinical isolates can be identified as frequently producing safe preparations of phages irrespective of the phage isolated, future isolation protocols may be used more effectively by proactively defining appropriate isolation hosts. Using this study as an example, the bacterial isolate SA19 was utilised to isolate phages P1 and P3, both of which are genomically suitable for phage therapy however indications of contamination were found (Reads mapping to host were >5%) and upon inspection of the assembled unmapped reads confirmation of prophage contamination was determined based on the presence of integrase and Pantone-Valentine Leukocidin CDS belonging to a prophage within the host genome.

In conclusion this chapter has demonstrated that, whilst sparse within the environment, phages with the appropriate traits for therapy may be identified from environmental and clinical sources using a panel of clinically relevant *S. aureus* bacteria. Phages Koomba kaat 1 and Biyabeda mokiny 1 were identified as genomically appropriate phages for phage therapy within this chapter and samples produced using their initial host propagating strains were not seen to contain any virulence factors or contamination of any kind. These data support the decision to perform further, in depth, characterisations for efficacy against *S. aureus* from the respiratory context in Chapter 4. Based on the data shown in this chapter, and the closest references obtained for these phage candidates, there is good reason to believe that these phages are broad acting, polyvalent phages [212, 217] with potential for wide ranges of activity *in vitro*. Therefore, the findings shown within this chapter lend credence towards characterising these phages further in terms of their lytic capabilities and binding capacity.

Chapter 4: Characterising Koomba kaat 1 and Biyabeda mokiny 1 phages for respiratory implementation against *Staphylococcus aureus* from cystic fibrosis.

4.1. Introduction:

From the previous chapter, two phages, Koomba kaat 1 and Biyabeda mokiny 1, were isolated from wastewater and identified as lytic phages belonging to the *Herelleviridae* family (Genera: *Silviavirus* and *Kayvirus* respectively). They were genomically screened for safety when grown using their initial isolation hosts and determined to be homogenous populations of phage. However, lytic phages are diverse, and exhibit variety across multiple parameters including length of infection cycle, stability characteristics, host range activity, and biofilm targeting capacity [116, 120, 219]. Metrics such as these are important to characterise prior to use as they impact the implementation of the phage itself. For example, phages with a broader host range against a given bacterial species, such as *S. aureus*, are typically desirable for their ability to be utilised in a presumptive manner [224]. Yet this breadth of activity comes at a trade-off, if a phage's spectrum is too wide, and the phage can infect multiple bacterial species, then the risk of off target effects increases [163]. Phage stability is also important to determine prior to use, from a practical perspective; if it is difficult to maintain a recoverable concentration of phages over time, the cost of maintenance increases. Phage stability in storage is dependent on numerous conditions and remains an important base characterisation to obtain [111]. In addition, if phages exhibit sensitivity towards chemically induced stress such as acidic/basic conditions then they may be liable to damage or destruction in the process of purification rendering them ineffective when applied. Further, ability to survive aerosolised delivery via nebulisation is a significant feature as it enables the precise deposition of phages directly to the site of respiratory infection [95, 118, 142]. Localised administration benefits include increased effective titre and minimising systemic side effects [225].

With this in mind, this chapter aims to provide a comprehensive characterisation for both Koomba kaat 1 and Biyabeda mokiny 1 and to provide evidence for their suitability in respiratory applications. Specifically, it tested the hypothesis that the previously isolated phages, Koomba kaat 1 and Biyabeda mokiny 1, would be effective against a range of MSSA and MRSA isolates from various clinical sources. To achieve this, the first aim was to assess their stability characteristics to ensure the phages could be stored, purified, and aerosolised without degradation. The second aim was to characterise their efficacy against MRSA clinical isolates with a particular focus on biofilms. Finally, the third aim was to use a combination of colinear comparisons and machine learning algorithms to predict the identity and function of phage receptor binding proteins within the genomes of both phages and compare these traits with closely related phages targeting *Staphylococcus* species.

4.2. Materials and methods:

4.2.1. Bacterial isolates and phage propagation

Growth medium was prepared according to manufacturer instructions and bacteria isolates, unless specified as a public strain (American Type Culture Collection), were clinical isolates from a range of clinical sources (Refer to section 2.1). Both Biyabeda-mokiny 1 and Koomba-kaat 1 were isolated and propagated using their host clinical MRSA isolates (SA01 and SA09 respectively) (Refer to section 2.4.12). Bacteria were grown using Tryptic Soy (TS) broth (BD Difco™) from a single colony and incubated overnight (~16 hours) at 37°C with orbital shaking at 120 rpm. Frozen bacterial stocks were stored at -80°C in TS broth supplemented with glycerol to a final concentration of 25% (Refer to section 2.4.1).

4.2.2. High Pressure Liquid Chromatography

Purifications were performed using phage lysate filtered through 0.22 µm filters to remove bacterial debris prior to HPLC purification. Filtered phage lysates were then passed through a HiTrap BIA Monolithic Column (BIA Separations, Ajdovščina, Slovenia) using the ÄKTA M2 pure™ HPLC platform (Cytiva Life Sciences™, Marlborough, MA, USA) (refer to section

2.4.25). After each use, anion exchange columns were thoroughly cleaned and stored in 20% (v/v) ethanol at 4°C until further usage (Refer to section 2.4.26).

4.2.3. Stability assessments

4.2.3.1. *Long term storage*

To determine stability in storage, phages were stored for up to one year in SM-buffer at room temperature (RT), 4°C, -20°C, and -80°C. Tubes containing phage from the same sample were stored in separate tubes to ensure a single freeze-thaw cycle per measurement. Phages in storage were enumerated via serial dilution, spot plating, and plaque counting on their host bacterial strain at the storage timepoints of 1 week, 1 month, 3 months, 6 months, and 1 year, for comparison to their starting concentrations. Three replicate tubes were used for each phage at each timepoint, and all tubes were placed at RT one hour prior to performing titrations to enable aliquots to thaw (if frozen).

4.2.3.2. *High temperature stability*

Stability at high temperatures was determined by incubating phage 1 mL phage lysate aliquots in Eppendorf tubes for 1 hour at 30°C, 40°C, 50°C, 60°C, 70°C, and 80°C using a Ratek 1 Block Digital Dry Block Heater (Ratek Instruments Pty Ltd, Boronia, VIC, Australia). Phages were standardised to a concentration of 3-5 x 10⁹ PFU/mL prior to heat exposure and titrated immediately afterwards.

4.2.3.3. *Acid-base stability*

Effect of pH on phage stability was determined by using 1M HCl and 1M NaOH to adjust the pH of the storage media (SM buffer) to pH 3, 4, 7 or 9. Phages were then added to a starting concentration of 1-3 x 10⁹ PFU/mL and incubated for 24 hours at 37°C. All stability assessments were independently replicated three times per group and phage enumeration performed using titrations described in section 2.4.13.

4.2.3.4. *Aerosol stability*

To determine the aerosol stability of phage via nebulisation; we used the standard VMD Nebuliser Unit with Filler cap (Aerogen Ltd, Dangen, Galway, Ireland) and the Aeroneb Lab control module (Kent Scientific, Torrington, CT 06790, United States). Briefly, 2 mL of HPLC purified phage lysate (Refer to section 2.4.25), diluted to a starting concentration of 1×10^9 PFU/mL, was aerosolised into a 25 mL collection tube and allowed to settle for 10 minutes. The remaining suspensions were then collected to determine volume, and phage concentration determined via titration.

4.2.4. Lytic activity assessment

4.2.4.1. *Host-range and specificity*

Host range assays were performed by spot plating $10\mu\text{L}$ of $1 \times 10^{8-9}$ phage lysate onto host-overlay agar plates inoculated with $100\mu\text{L}$ of bacterial overnight cultures. In total, 138 strains of clinical *S. aureus* were assayed from various sites including respiratory ($n = 24$), blood ($n = 90$), tissue non-respiratory ($n = 12$), and a combination of wound sites ($n = 12$). Additional species of bacteria were used to determine if either phage could infect multiple species; these included *Pseudomonas aeruginosa* (*P. aeruginosa*) ($n=30$) clinical isolates, Group A Streptococci (GAS) ($n=8$), and Group B Streptococci (GBS) ($n=13$) clinical isolates. For the *P. aeruginosa* isolates, the culturing medium used was Luria Bertani (LB) broth and agar was made to manufacturers specifications (BD Difco™). Heart-infusion broth and agar (BD Difco™) were used for GAS & GBS and again prepared to manufacturer's instructions. Each of these experiments were repeated three times independently to ensure reproducibility.

4.2.4.2. *Dosage curves*

To determine dose dependant activity and phage infection kinetics, bacterial cultures were infected with multiplicities of infection (MOIs) of 0.1, 0.5, and 1.0. Bacterial growth was quantified using optical density measurements using a CLARIOstar Plus Plate Reader (BMG

LabTech, Ortenberg, Germany), taken at 600 nm (OD_{600nm}). Lytic activities of each phage were measured against their host bacterial isolate. Measurements were taken every 30 minutes for 6 hours post-infection.

4.2.4.3. *Efficiency of plating*

For plating efficiency (EOP) assays, phages were diluted down to 1×10^{-9} PFU/mL for titration against the host propagation strain and the target bacterial isolate. The calculation of EOP was performed by dividing the mean plaque-forming units (PFUs) observed against the target bacterial strain by the mean PFUs recorded against the host bacterial strain. This was conducted in triplicate for each EOP assay.

4.2.4.4. *Biofilm disruption*

Methods to assess biofilm formation were adapted from a previously described, crystal violet based 96-well microtitre plate assay [226]. For work performed in this chapter, five MRSA isolates from CF airways (SA04, SA05, SA07, SA08, SA09) and a laboratory strain of *S. aureus* (ATCC 6538) were chosen for biofilm production capacity and subsequent susceptibility to phage. Briefly, wells of a flat bottomed 96-well plate were inoculated with 200 μ L bacterial overnight cultures diluted in TSB to an OD_{600nm} of 0.05. For each bacterial isolate, six replicate wells were conducted. Once loaded, plates were transferred to an incubator for 24 hour static incubation at 37°C to enable biofilm growth. After incubation, the inoculation medium was removed, and excess bacterial planktonic cells were gently removed from the biofilm via washing wells 3 times with 200 μ L of phosphate buffered saline (PBS). Remaining biofilm bacteria that had adhered to the wells were stained using 125 μ L of 0.1% crystal violet v/v (CV) solution for 10 minutes at RT and subsequently dried for 1 hour. Washing was then repeated with 200 μ L of PBS, performed 3 times to remove excess CV. Stained biofilms were then solubilised in 125 μ L of 30% (v/v) acetic acid and read at OD_{550nm} using the BioTek™ Synergy™ Mx Multi Detection Top Monochromator Based Microplate Reader with Gen5 Software (Thermo Fisher Scientific, Waltham, MA, USA)

4.2.4.5. *Biofilm infection*

Methods to assess biofilm penetration and infection were adapted from a previously described, biofilm growth tube adherence assay [226]. Briefly, 1.5 mL tubes were inoculated with 1 mL of bacterial overnight culture diluted in TSB to an OD_{600nm} of 0.05. For each bacterial isolate, four replicate tubes were used. Once loaded, plates were transferred to an incubator for 24 hour static incubation at 37°C to enable biofilm growth. After incubation, the inoculation medium was removed, and excess bacterial planktonic cells gently removed from the biofilm via washing the wells 3 times with 1.2 mL of phosphate PBS. Phages suspended in 1 mL of PBS at a concentration of 1×10^9 PFU/mL were then added to the tubes and left in static incubation at 37°C for 6 hours. Post exposure, free phage were removed by washing 3 times with 1.2 mL of phosphate buffered saline, as above. Following this, 1 mL of sterile PBS was added to each tube and sonicated at 20-40 hz for 15 minutes to dislodge biofilms. Finally, suspended biofilms were serially diluted from 10^{-1} to 10^{-9} and plated to determine CFU counts.

4.2.5. Comparative genomics analysis

4.2.5.1. *Phylogenetic UPGMA trees*

Phylogenetic alignment of all phage sequences listed within the GenBank database were obtained using Inphared [191] and subset by the host bacteria ‘Staphylococcus’. Alignments were made using mafft (v7.520) and a UPGMA tree drawn using Biopython modules [227]. To compare the genomic synteny and arrangement between phage genomes, the closest phages used for comparisons and phylogenetic inference were identified using a BLAST (v2.5.0) [192] search against all phage genomes (n=20185) [191] within the Inphared database.

4.2.5.2. *Phylogenetic network*

Phylogenetic clustering was performed using vConTACT2 (v0.11.3) [216] to produce protein clusters in an ‘all vs all’ fashion. Network analyses were then visualised using Cytoscape (v3.9.1) [228] and coloured using the lowest genomic taxon assigned within the Inphared database (1st May access).

4.2.5.3. *Receptor Binding Proteins*

Phage receptor binding proteins (RBPs) were putatively identified within both phage genomes using a combination of methods, the first was prediction using a previously published machine learning pipeline: protein CDS were taken directly from Prokka (v1.14.6) outputs produced during the annotation process. Briefly, protein sequences were transformed into numerical vectors using the ProtTransBertBFDEmbedder module in python, which uses an embedding tool designed to capture sequence features using the ProtTrans-BFD language model [229]. A pre-trained XGBoost classifier model, previously trained and used by Boeckaerts et al (2022) [230] (Github: [PhageRBPdetection](#)) using known phage RBPs, was used to generate predictions for each phage protein analysed. Once these proteins were identified, they were manually curated using the HHpred webserver for homologue detection [231] and compared with closely related genomes that have empirically determined RBPs via colinear alignment. The second method involved comparing known *Staphylococcus* phages as a reference and looking for similarity within annotations and synteny. For comparisons, *Staphylococcus* infecting phages with previously identified and characterised RBPs were included within the analysis, these phages were *Staphylococcus* phages: SA012 (Accession: AB903967), MR003 (Accession: AP019522), and SLT (Accession: AB045978) [212, 232, 233]. These genomes were extracted from the Inphared database (accessed 1st May 2023) and annotated using Prokka (v1.14.6) in combination with the PHROGs database [194]. All genomes were reordered based on the small terminase subunit for colinear comparisons (refer to section 4.2.5.4).

4.2.5.4. *Colinear comparisons*

To compare the CDS arrangement between phage genomes, genomes were first extracted from the Inphared database (Accessed 1st May 2023) [191]. Alignments were produced by annotating genomes using Prokka (v1.14.6) [193] in combination with the PHROGs database [194] and reordering phages based on the small terminase subunits. CDS similarities were calculated using Mmseqs2 (v12-113e3+ds-3+b1) [234] and visualised using pyGenomeViz (v0.4.3) [235].

4.2.6. Statistical analysis

Statistical analyses were conducted using GraphPad Prism v8.4.3 (GraphPad Software, La Jolla, CA). Comparisons containing mixed model analyses were performed using 2-way ANOVAs. Plates that did not yield any viable bacterial counts were reported as zero. P-values less than 0.05 were considered significant for all tests used unless alpha has been specified otherwise. For dosage curve analysis, area under the curve (AUC) analyses were performed using GraphPad Prism v8.4.3 (GraphPad Software, La Jolla, CA).

4.3. Results

4.3.1. Storage

Phages Koomba kaat 1 and Biyabeda mokiny 1 were assessed for optimal storage temperatures over the course of 1 year (Figure 4.1). Results generated showed that the optimal preservation temperature was 4°C, followed by -80°C, and -20°C. After 1 year at room temperature, neither phage was recoverable and so room temperature storage concentrations were removed from further analysis. As a comparison, each storage temperature were compared to storage at 4°C. Results generated show that Koomba kaat 1 storage, across all timepoints, was significantly greater at 4°C in preserving effective titre in compared to RT (mean log reduction: 1.39×10^9 PFU/mL, $p < 0.001$), -20°C (mean log reduction: 1.13×10^9 PFU/mL, $p < 0.001$), and -80°C (mean log reduction: 5.9×10^8 PFU/mL, $p = 0.005$). Refrigerated storage at 4°C was also optimal for Biyabeda mokiny 1 across all timepoints. Storage at 4°C was significantly better at preserving effective titre compared to

RT (mean log reduction: 2.5×10^8 PFU/mL, $p < 0.001$), -20°C (mean log reduction: 2.7×10^8 PFU/mL, $p < 0.001$), and -80°C (mean log reduction: 1.4×10^8 PFU/mL, $p < 0.001$).

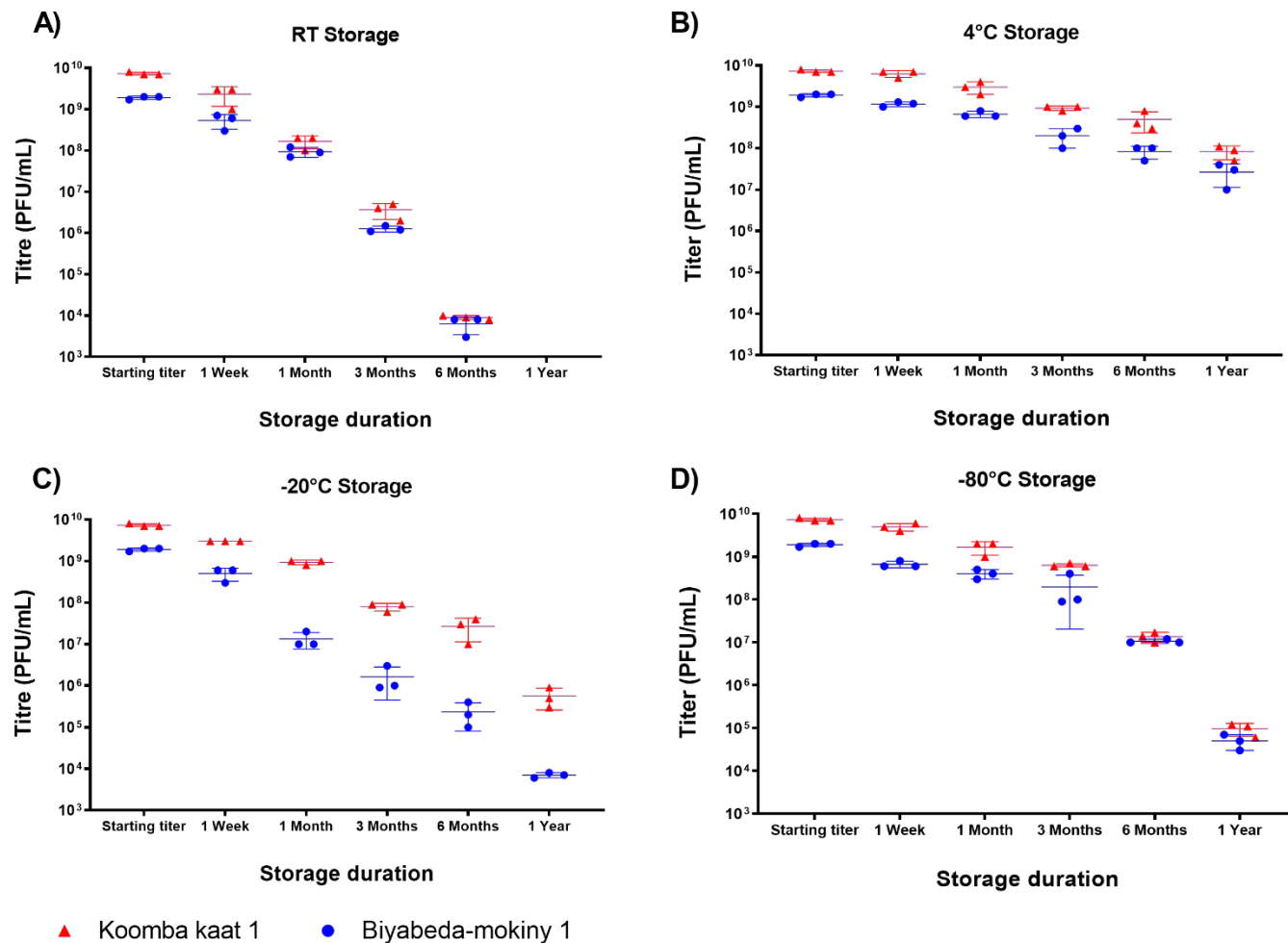


Figure 4.1: Storage profiles for Koomba kaat 1 (blue) and Biyabeda-mokiny 1 (red) were generated across 1 year. Phages were suspended in SM buffer and enumerated using PFUs / mL at each time point. A storage temperature of 4°C (Panel B) was significantly better at preserving phage activity for both Koomba kaat 1 and Biyabeda mokiny 1 than room temperature (RT) (Panel A), -20°C (Panel C), or -80°C (Panel D). Data are presented as mean \pm SD.

4.3.2. High temperature

To assess the thermotolerance of Koomba kaat 1 and Biyabeda mokiny 1, separate aliquots were subject to incubation for one hour at 30°C, 40°C, 50°C, 60°C, 70°C, and 80°C (Figure 4.2, panel A). Results generated found that both phages had similar tolerance profiles for high temperatures; phages were recoverable between 30°C and 70°C, although no phages were recoverable at 80°C, and as a result this temperature was removed from further analyses. The remaining temperatures were compared to the starting stock concentration (stored at 4°C) for statistical analyses. Biyabeda mokiny 1 was significantly degraded at 30°C ($p=0.033$, mean reduction: 2.3×10^9 PFU/mL), 40°C ($p=0.033$, mean reduction: 2.3×10^9 PFU/mL), 60°C ($p=0.011$, mean reduction: 2.7×10^9 PFU/mL), and 70°C ($p=0.001$, mean reduction: 3.4×10^9 PFU/mL). Koomba kaat 1 was significantly degraded at 60°C ($p=0.007$, mean reduction: 2.8×10^9 PFU/mL) and 70°C ($p=0.001$, mean reduction: 3.3×10^9 PFU/mL).

4.3.3. pH

Koomba kaat 1 and Biyabeda mokiny 1 were assessed for acid-base stability over the course of 1 hour (Figure 4.2, panel B). The various acid-base buffer strengths were compared to the control pH of 7 and results generated illustrated that both phages retained greatest viability at pH 7 (Figure 4.2). For Biyabeda mokiny 1, stability at pH 7 was significantly greater than pH 3 ($p<0.0001$, mean log difference: 1.9×10^9 PFU/mL), pH 5 ($p<0.0001$, mean log difference: 1×10^9 PFU/mL), and pH 9 ($p<0.0001$, mean log difference: 1.4×10^9 PFU/mL). For Koomba kaat 1, stability at pH 7 was significantly greater than pH 3 ($p<0.0001$, mean log difference: 1.2×10^9 PFU/mL), pH 5 ($p<0.0001$, mean log difference: 3.7×10^8 PFU/mL), and pH 9 ($p<0.0001$, mean log difference: 3.7×10^8 PFU/mL).

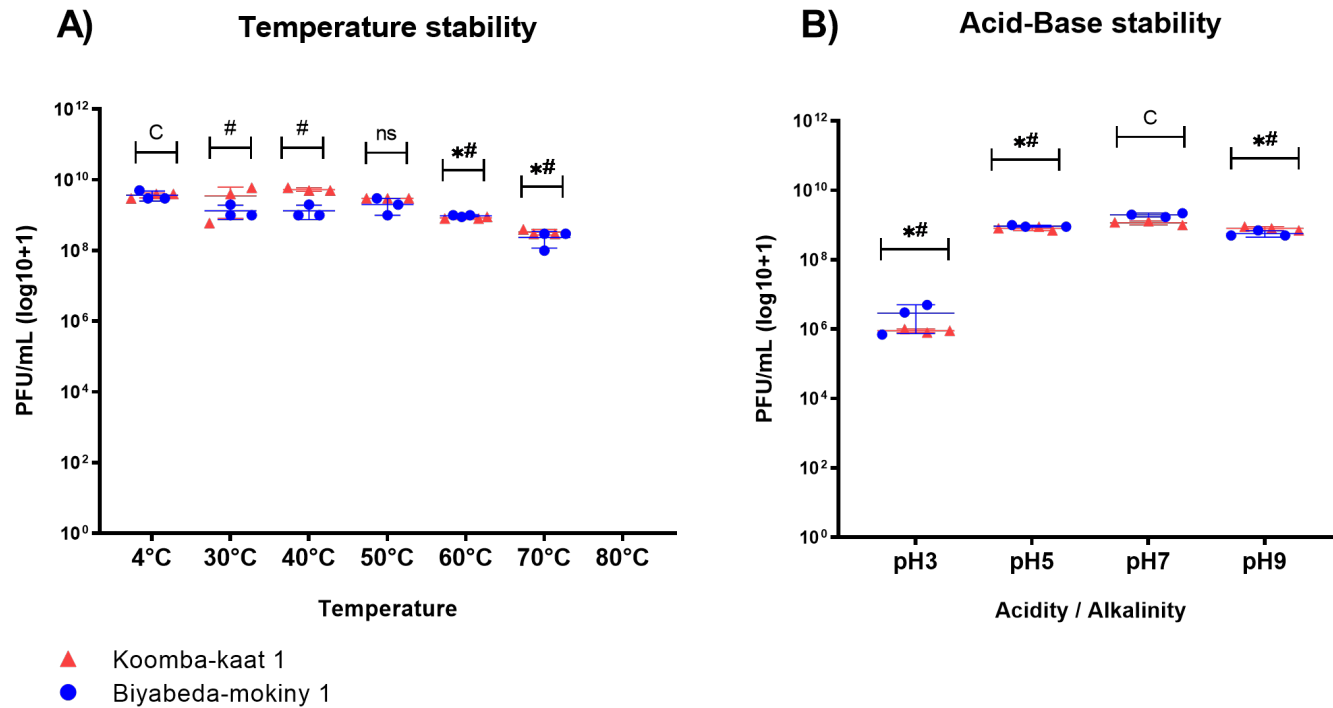


Figure 4.2: Stability profiles for Koomba kaat 1 (blue) and Biyabeda-mokiny 1 (red) were generated for: **(A)** high temperatures for 1 hour at 30-80°C and **(B)** a range of pH for 24 hours. The results show that phages are most stable at 4°C. Data also shows that the optimal pH is 7 for both phages. Data are presented as mean \pm SD. Significant differences for Koomba kaat 1 are denoted using “*” whereas significant differences for Biyabeda mokiny 1 are denoted using “#” when compared to the control group (marked with a “C” on both panels).

4.3.4. Nebulisation

Phages Koomba kaat 1 and Biyabeda mokiny 1 were assessed for their ability to be aerosolised without damage. The data generated show that both phages were recoverable and maintained their activity at various concentrations post-nebulisation (Table 4.1). There were no significant differences between Koomba kaat 1 and Biyabeda mokiny 1 aerosol stability ($p=0.138$) and no significant differences between the percentage loss between a high (1×10^9 PFU/mL) or low (1×10^6 PFU/mL) starting titre ($p=0.407$).

Table 4.1: Aerosol stability characteristics for Koomba kaat 1 and Biyabeda mokiny 1. Data suggests there are no significant drop in concentration for either phage at concentrations tested. Values shown are mean average values \pm SD across 6 replicate values.

Phage	Starting concentration (PFU/mL)	Return concentration (PFU/mL)	Return volume (μ L)	Percentage concentration remaining (%)
Koomba kaat 1	1×10^9	$9.7 \times 10^8 (\pm 7.6 \times 10^7)$	1783 (± 29)	96.7
Koomba kaat 1	1×10^6	$9.8 \times 10^5 (\pm 3.8 \times 10^5)$	1817 (± 29)	98.3
Biyabeda mokiny 1	1×10^9	$8.2 \times 10^8 (\pm 1 \times 10^8)$	1850 (± 50)	81.7
Biyabeda mokiny 1	1×10^6	$9.3 \times 10^5 (\pm 3.3 \times 10^5)$	1808 (± 14)	93.3

4.3.5. Lytic activity assessments

4.3.5.1. Spectrum of activity

In the host range screen against *S. aureus* isolates, Koomba kaat 1 was able to successfully infect 83% (n = 104/126) clinical strains and Biyabeda mokiny 1 was able to successfully infect 37% (n = 47/126) via host range assay. Against these strains, Koomba kaat 1 could infect a significantly broader range of *S. aureus* clinical isolates than Biyabeda mokiny 1 (p=0.028). When the isolates were subset based upon their clinical isolation sites, Koomba kaat 1 had greater activity from each site apart from the non-respiratory tissue *S. aureus* strains (Figure 4.3). Against a panel of other *Staphylococci* pathogens including *S. epidermidis* (n = 2), *S. saprophyticus* (n = 2), and *S. xylosus* (n = 1), Koomba kaat 1 could not infect any of these isolates. In contrast, Biyabeda mokiny 1 was able to infect the *S. xylosus* isolate and a single *S. epidermidis* isolate successfully and the remaining bacterial isolates were considered partially susceptible to Biyabeda mokiny 1. Despite this, neither phage could infect bacteria outside the *Staphylococcus* genus, namely *P. aeruginosa* (n=30), *Burkholderia cepacia* complex (n = 30), Group A *Streptococci* (n = 6), and Group B *Streptococci* (n = 6).

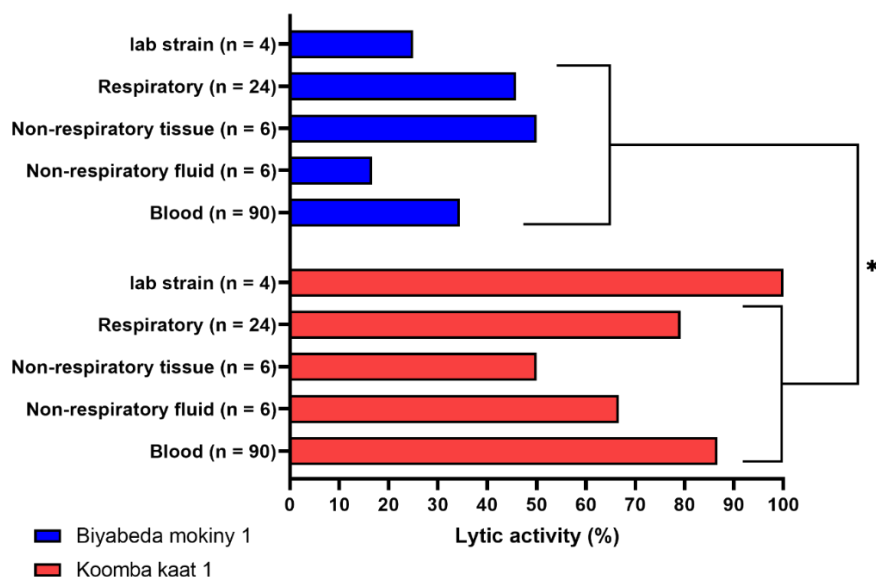


Figure 4.3: Host range activity against *S. aureus* collected from various different clinical sites. Koomba kaat 1 could infect a significantly broader range of *S. aureus* clinical isolates than Biyabeda mokiny 1 (p=0.028). Data was calculated from host range scores from three replicate values, partially susceptible bacteria were counted as resistant.

4.3.5.2. *Dosage curves*

When phages were assessed for dose dependent activity against their host bacterial strains, both phages were significantly effective at reducing overall bacterial concentrations at all infective doses (MOI 0.1, MOI 0.5, and MOI 1.0) over the course of six hours ($p < 0.001$ in all cases, Figure 4.4). For Koomba kaat 1, the differences between each dose were also significant ($p < 0.001$ in all instances) when compared to each other. This indicates that there was a strong dose dependent association between the MOIs tested for this phage. For Biyabeda mokiny 1, there was a significant difference between an MOI of 1.0 and 0.1 (AUC: 43.39, $p < 0.001$) however the difference between MOI 1.0 and 0.5 was not significant (AUC: 5.68, $p = 0.251$).

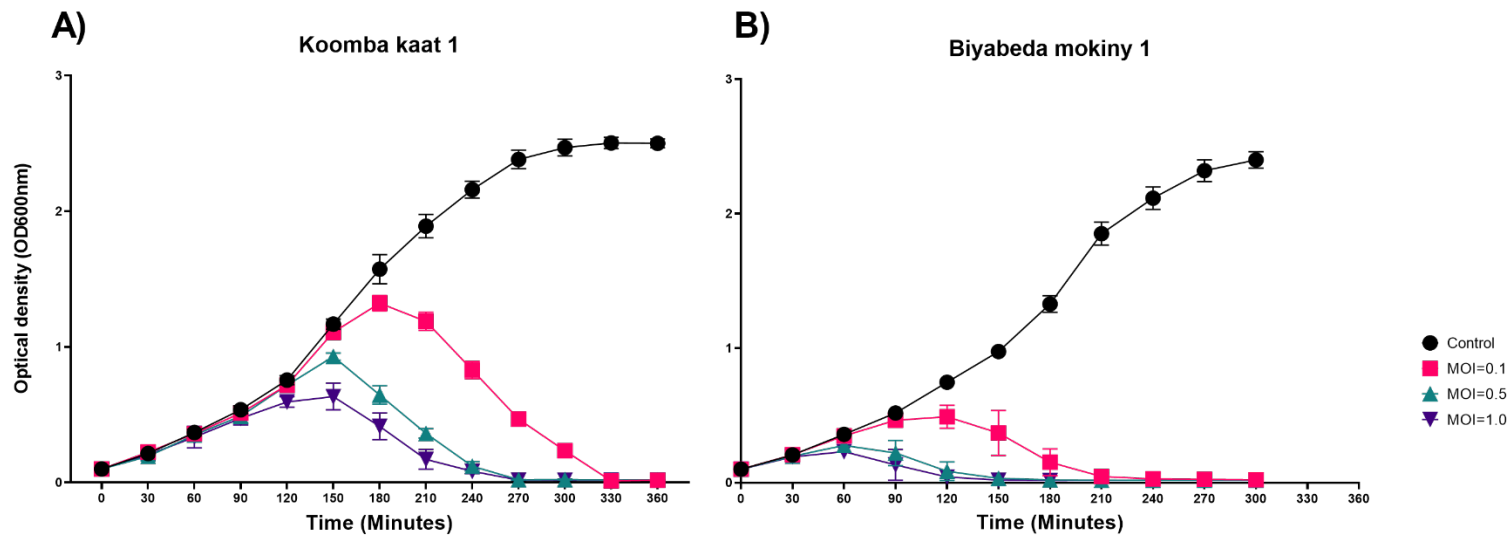


Figure 4.4: Dosage curves for Koomba kaat 1 and Biyabeda mokiny 1 against their host bacterial isolates SA09 and SA01 at MOIs of 0.1, 0.5, and 1.0. **(A)** Koomba kaat 1 phages applied to host bacterial strain SA09 at all MOIs caused a significant reduction of bacterial density (MOI 0.1: AUC = 309, MOI: 0.5 AUC = 402, MOI: 1.0 AUC = 430) when compared to controls ($p < 0.001$ in all cases). **(B)** Biyabeda mokiny 1 phages applied to host bacterial strain SA01 at all MOIs used caused a significant reduction of bacterial density (MOI 0.1 AUC = 284.5, MOI 0.5 AUC = 322.2, MOI 1.0 AUC = 327.9) when compared to controls ($p < 0.001$ in all cases). Data are presented as mean \pm SD, (n=3).

4.3.6. Antibiofilm activity

4.3.6.1. *Biofilm disruption*

Biofilm disruption results (Figure 4.5A) indicated that overall, Koomba kaat 1 was significantly better at disrupting the biofilms produced by clinical CF-MRSA strains ($n = 5$) when compared to Biyabeda mokiny 1 ($p < 0.0001$, mean difference = 25.64 %). The anti-biofilm activity of Koomba kaat 1 was not 100% effective across the selected CF-MRSA isolates; when assessed individually Koomba kaat 1 was able to significantly reduce biofilms produced from ATCC-6538 ($p < 0.001$), MRSA-1 ($p < 0.001$), MRSA-2 ($p = 0.004$), MRSA-3 ($p = 0.004$), and MRSA-5 ($p = 0.001$), but not MRSA-4 ($p = 0.111$). Biofilms infected by Biyabeda mokiny 1 were observed to be visibly reduced, however only MRSA-1 biofilms were significantly disrupted ($p = 0.003$). Also noted was a significant increase in the production of ATCC-6538 biofilm when infected with Biyabeda mokiny 1 ($p = 0.002$).

4.3.6.2. *Biofilm infection*

When assessing the infection of the bacteria within the biofilms, Koomba kaat 1 could infect and significantly reduce the viable bacterial load of biofilms produced by ATCC-6538, MRSA-1 (mean reduction: 1.5×10^7 CFU/mL), MRSA-2 (mean reduction: 1.6×10^7 CFU/mL), MRSA-3 (mean reduction: 6.4×10^6 CFU/mL), and MRSA-5 (mean reduction: 6.9×10^6 CFU/mL) (all p values < 0.001 , Figure 4.5A), but again did not impact MRSA-4 (mean reduction: 4.3×10^5 CFU/mL) biofilms ($p = 0.933$, Figure 4.5A). For Biyabeda mokiny 1, viable bacteria were also significantly reduced in biofilms produced by MRSA-1 (mean reduction: 1.5×10^7 CFU/mL, $p < 0.001$), MRSA-2 (mean reduction: 2.5×10^6 CFU/mL, $p = 0.008$, Figure 4.5B), and MRSA-5 (mean reduction: 2.3×10^6 CFU/mL, $p = 0.014$, Figure 4.5B). There was a significant increase in the viable bacterial growth of ATCC-6538 when infected with Biyabeda mokiny 1 (mean increase: 5.8×10^6 CFU/mL, $p < 0.001$,) (Figure 4.5B).

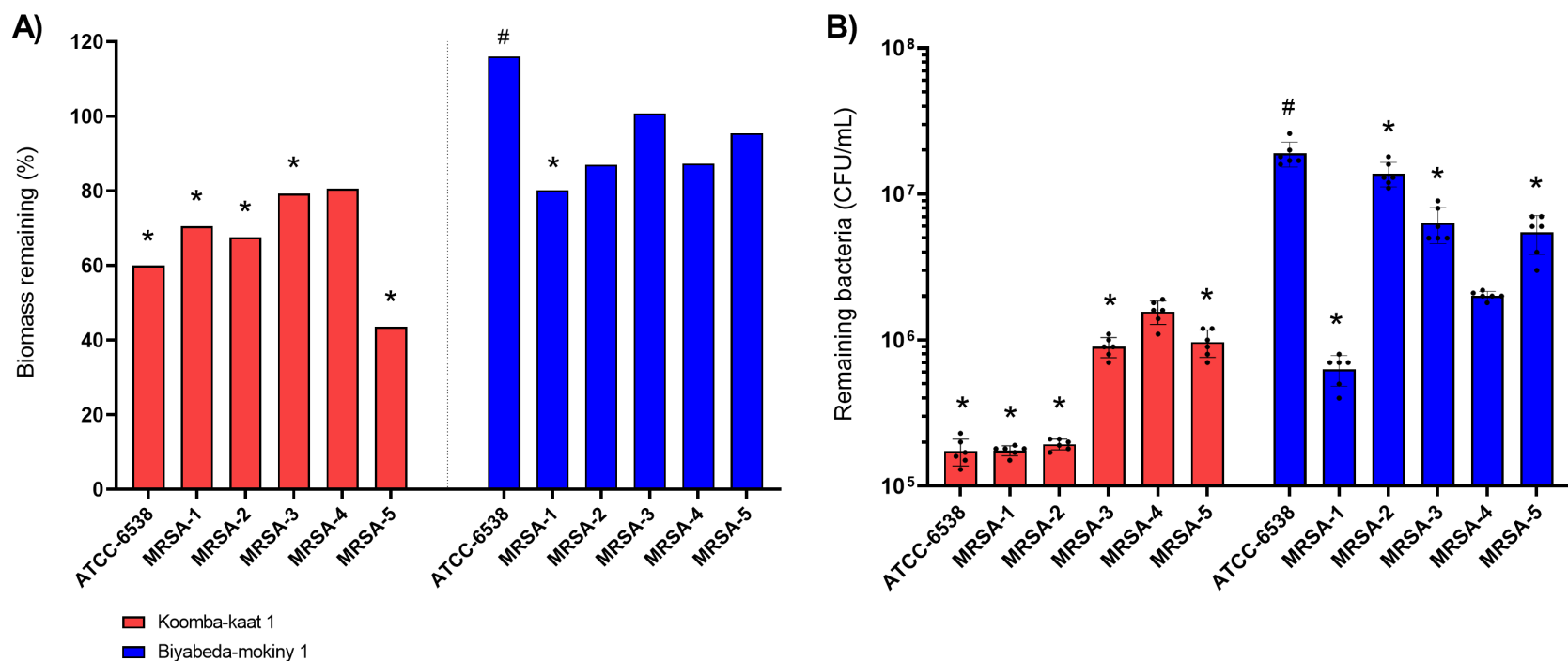


Figure 4.5: Anti-biofilm activity: A) Koomba kaat 1 was able to significantly reduce biofilm mass (%) produced from ATCC-6538 ($p < 0.001$), MRSA-1 ($p < 0.001$), MRSA-2 ($p = 0.004$), MRSA-3 ($p = 0.004$), and MRSA-5 ($p = 0.006$) however was not able to significantly disrupt biofilm produced by MRSA-4 ($p = 0.111$). Biyabeda mokiny 1 could only reduce MRSA-1 biofilms significantly ($p = 0.003$). Data in panel A are presented as mean percentage reduction across 4 technical replicates. **B)** Koomba kaat 1 was able to infect and significantly reduce the viable bacterial load of biofilms produced by ATCC-6538, MRSA-1, MRSA-2, MRSA-3, and MRSA-5 (all p values < 0.001). Viable bacteria were also significantly reduced in biofilms produced by MRSA-1 ($p < 0.001$), MRSA-2 ($p = 0.008$), and MRSA-5 ($p = 0.014$) when infected with Biyabeda mokiny 1. There was a significant increase in the viable bacterial growth of ATCC-6538 when infected with Biyabeda mokiny 1 ($p < 0.001$).

4.3.7. Comparative genomics analyses

4.3.7.1. Phylogenetic identification of closest relatives

When analysed using vConTACT 2 (v0.11.3) in conjunction with phage genomes from the Inphared database (accessed 1st May 2023), Koomba kaat 1 and Biyabeda mokiny 1 clustered into known genera belonging to the *Herelleviridae* family (Figure 4.6). Koomba kaat 1 significantly clustered alongside 32 *Silviaviruses* and Biyabeda mokiny 1 clustered alongside 3 *Kayviruses* (Table 4.2). The Kayvirus genus is diverse and splits into 18 different viral clusters and the Silviavirus splits into 2, the smaller of which contains a single genome as an outlier (VC_159_1). Compared to the genomes of their predicted genera using a 1 standard deviation of mean average as threshold for outliers, Koomba kaat 1 and Biyabeda mokiny 1 were normal in terms of genome length, GC%, coding density, and number of CDS.

Table 4.2: Phylogenetics analysis data from vConTACT2 for phages Koomba kaat 1 and Biyabeda mokiny 1. The topology confidence score (range: 0-1) aggregates information about the networks topological properties and infers the strength of links within the viral cluster. The genus confidence score (range:0-1) estimates the likelihood of viral clusters to be equivalent to a single genus (assigned by the ICTV). The adjusted p value (range: 0-1) estimates the significance of two phage sequences sharing an observed number of proteins.

Genome	Viral cluster			Quality	Topology confidence	Genus confidence	Adjusted P-value
	Name	Size (n)	Average distance				
Koomba kaat 1	VC_159_0	32	5.92	0.9	0.9	1	1
Biyabeda mokiny 1	VC_154_16	3	7.39	0.012	0.0119	1	0.996

4.3.7.2. *Phylogenetic UPGMA tree alignment*

Koomba-kaat 1 and Biyabeda-mokiny 1 (positions indicated with red stars; Figure 4.7) both cluster alongside *Silviavirus* and *Kayvirus* genera when aligned using the UPGMA method. Amongst all genomes surrounding both phages, those belonging to *Silviavirus* and *Kayvirus* were absent of integrase genes and of similar genome sizes (~130,000 to 150,000 bp). Koomba kaat 1 and Biyabeda mokiny 1 are denoted by red stars on the outside of Figure 4.7.

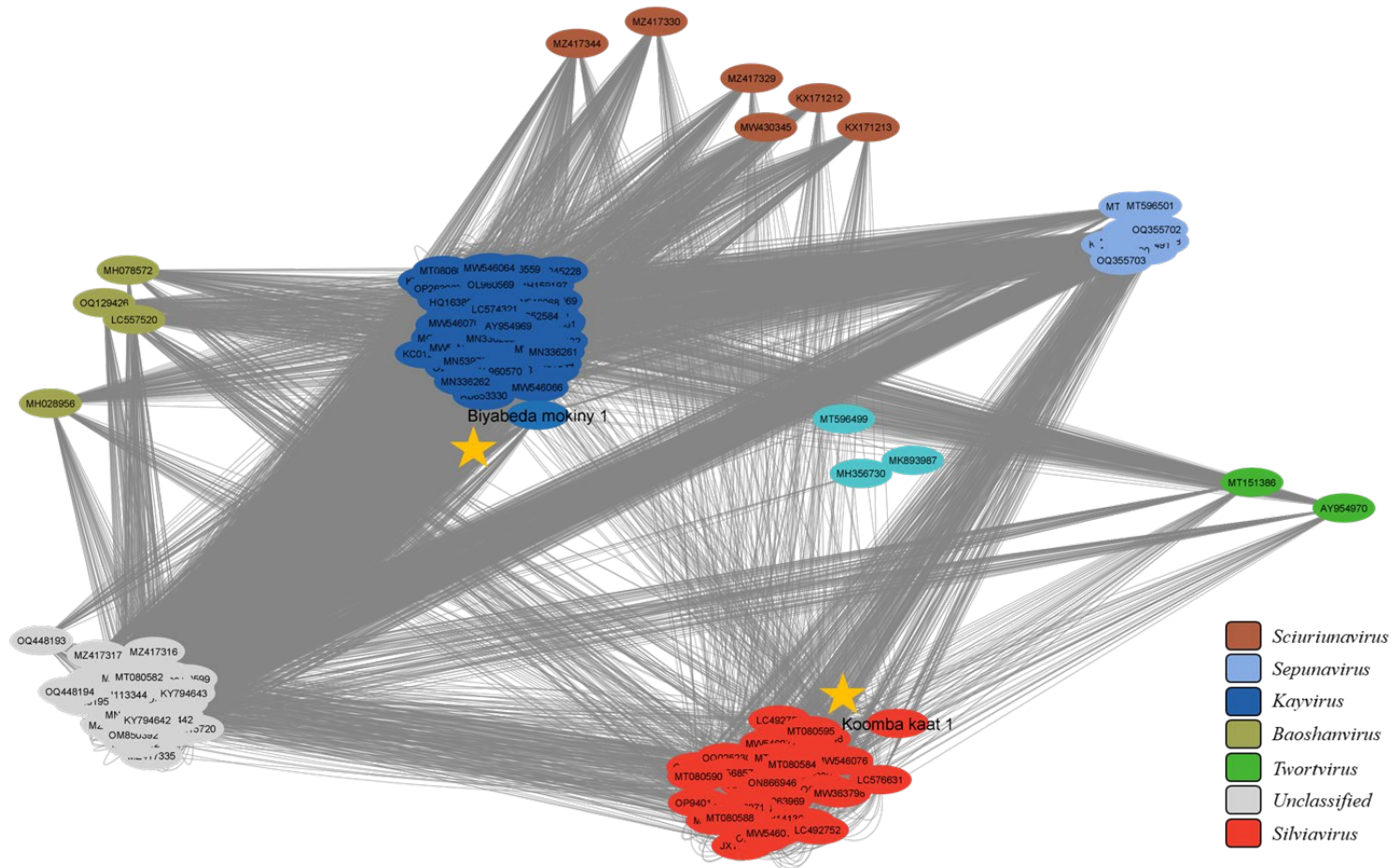


Figure 4.6: Phylogenetic vConTACT 2 (v0.11.3) network graph with taxonomic annotations for 6 genera and the unclassified phage genomes (light grey). Koomba kaat 1 clustered significantly alongside the *Silviavirus* genomes in red ($p=1$) and Biyabeda mokiny 1 clustered significantly alongside the *Kayvirus* genomes in blue ($p=0.996$). Cytoscape (v3.9.1) was used to visualise the network graph. Phages Koomba kaat 1 and Biyabeda mokiny 1 are marked with orange stars for identification.

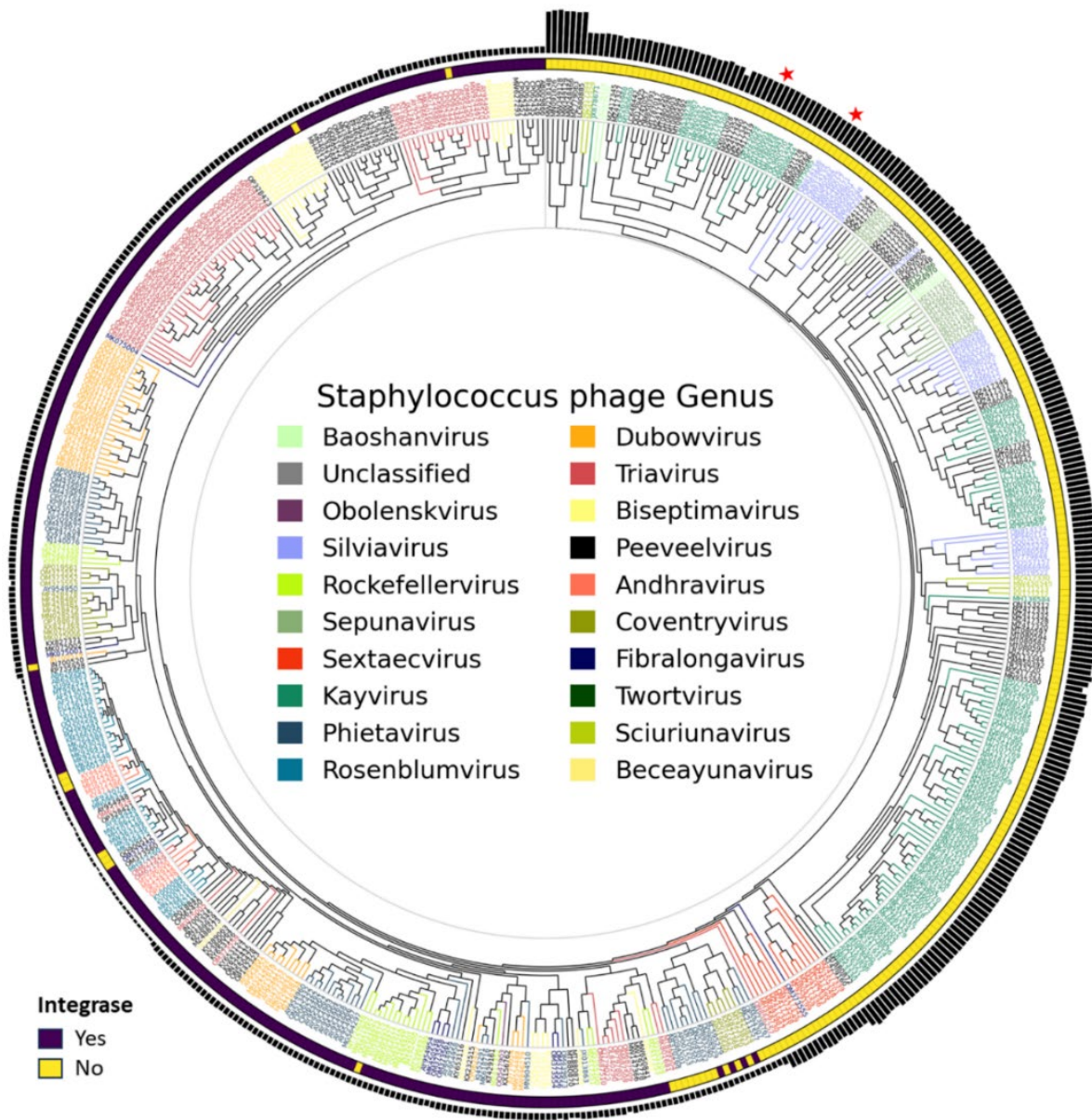


Figure 4.7: Panel (A): Phylogenetic tree produced using Unweighted Pair Group Method with Arithmetic Mean (UPGMA). This analysis includes all *Staphylococcus* phages ($n=574$) within the Inphared database (accessed 1st May 2023). Koomba-kaat 1 and Biyabeda-mokiny 1 (positions indicated with red stars) both cluster alongside *Silviavirus* and *Kayvirus* genera. The presence of integrases was determined via annotation using the PHROGs database; all phages belonging to *Kayvirus* and *Silviavirus* were absent of integrase genes. Genome size is on the outermost ring as a relative metric (Smallest=10440bp, Largest =274478 bp).

4.3.7.3. Colinear assessment

The top 5 closest hits were extracted from the Inphared database (accessed 1st May 2023) using BLASTn (v2.5.0) for Koomba kaat 1 and Biyabeda mokiny 1. These were ordered and annotated to observe genomic synteny between phages. The overall similarity between the CDS of both phages match highly with their closest relatives (Table 4.3). The average CDS protein identity score between Koomba kaat 1 and its closest alignment (KP881332) was 94.94% (Figure 4.8) and the score between Biyabeda mokiny 1 and its closest alignment (MN045228) was 96.22% (Figure 4.9).

Table 4.3: Closest relative genome statistics for Koomba kaat 1 and Biyabeda mokiny 1, the Genome Accession numbers identified are from the GenBank database, the genomes were extracted from the Inphared database (Accessed 1st May 2023).

Reference genome	Genome Accession	Description	Genome length (bp)	GC%
Biyabeda mokiny 1	JX878671	Staphylococcus phage JD007	141836	30.371
	AP018375	Staphylococcus phage phiSA039	141038	30.378
	MH107769	Staphylococcus phage vB_SauM_0414_108	151627	30.388
	MN045228	Staphylococcus phage Maine	141712	30.409
	MT554104	Staphylococcus phage ESa1	153106	30.315
Koomba kaat 1	ON814135	Staphylococcus phage vB_SauM-V1SA20	136866	30.019
	ON814136	Staphylococcus phage vB_SauM-V1SA22	133701	29.915

	KP881332	Staphylococcus phage Stau2	133798	29.974
	OQ025230	Staphylococcus phage SAP6	144705	29.715
	OQ025229	Staphylococcus phage StAP1	144705	29.716

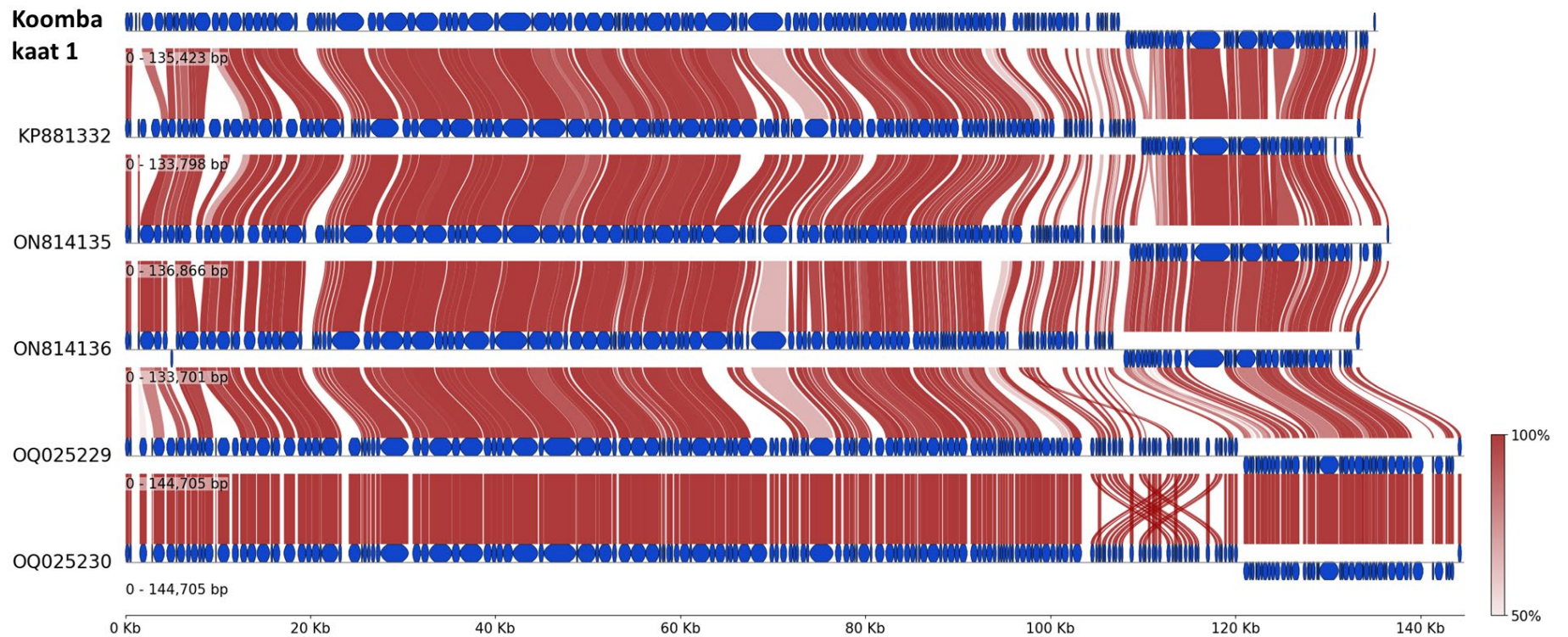


Figure 4.8: Genome alignment alongside closest relatives identified using BLASTn (v2.5.0). Genomes shown display CDS in blue and connections in red. The opacity of the links represent protein similarity calculated using MMseqs2 (v12-113e3+ds-3+b1) [234] and visualised using pyGenomeViz (v0.4.3) [235]. Genomes shown display an overall, highly similar arrangement and identity between 0 and 100 kb and on the reverse strand between 110 to 130 kb for Koomba kaat 1, KP881332, ON813135 and ON813136 and 120 to 140 kb for genomes OQ025229 and OQ025230. The average similarity of all protein CDS alignments between Koomba kaat 1 and its closest alignment (KP881332) was 94.94%.

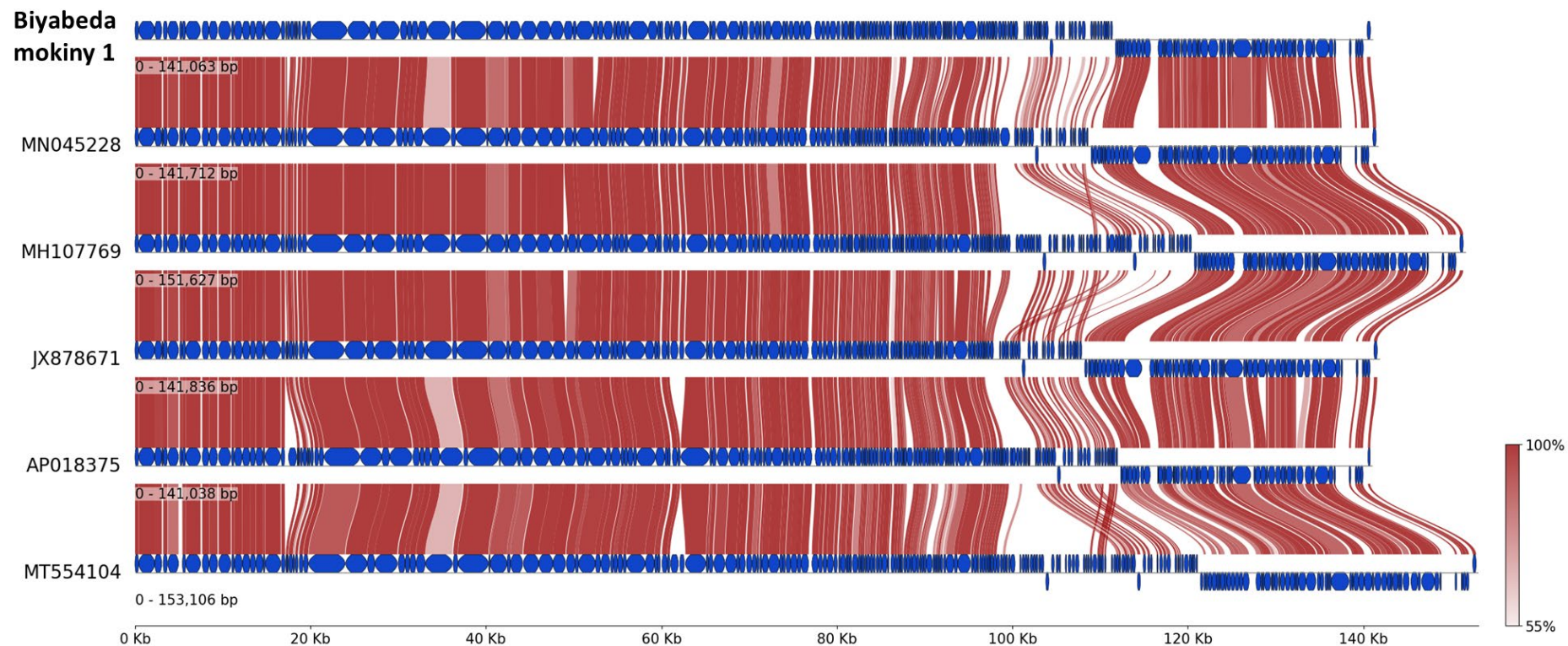


Figure 4.9: Genome alignment alongside closest relatives identified using BLASTn (v2.5.0). Genomes shown display CDS in blue and connections in red. The opacity of the links represent protein similarity calculated using MMseqs2 (v12-113e3+ds-3+b1) [234] and visualised using pyGenomeViz (v0.4.3) [235]. Genomes shown display a highly similar genomic arrangement and high identity scores through regions 0-100 kb and across the reverse strand at the end of the genomes between 120 kb and 140kb. The average similarity of all protein CDS alignments between Biyabeda mokiny 1 and its closest alignment (MN045228) was 96.22%.

4.3.8. Identification of receptor binding proteins

Phage receptor binding proteins (RBPs) were identified within both phage genomes using the previously published machine learning pipeline (Github: [PhageRBPdetection](#)) [230] (refer to section 4.3.9). These data were further corroborated using comparisons to known *Staphylococcus* phages as a reference (refer to section 4.3.10). Overall, phages Koomba kaat 1 and Biyabeda mokiny 1 were determined to be polyvalent phages with 2 predicted RBPs. These RBPs match with known genomes of *Staphylococcus* phages belonging to the same genus. Annotation data revealed that these RBPs share functional HMM profiles within the PHROGs database when annotated (Figure 4.10).

4.3.9. Machine learning RBP detection

Both Koomba kaat 1 and Biyabeda mokiny 1, only had a single CDS score above the default 0.5 required to classify as an RBP detection. The CDS were different between the two phages. The prediction for Koomba kaat 1 (score = 0.968) was a hypothetical protein (ORF 158) product, 3219 bp in length belonging to a category of unknown function within the PHROGs database. For Biyabeda mokiny 1, the prediction (score = 0.998) was for a tail fibre protein (ORF 42), 1377 bp in length.

4.3.10. Comparison and alignment to phages with known RBPs

Phages Koomba kaat 1 and Biyabeda mokiny 1 had similar genomic structures with SA012 and MR003 (Figure 4.10). The primary receptor binding proteins of SA012 and MR003 were found to be in the same regions as orthologous proteins identified within Koomba kaat 1 (ORF 46 and 48) and Biyabeda mokiny 1 (ORF 40 and 42) (Figure 4.10). Orthologous pairs of CDS between Biyabeda mokiny 1 and SA012 were high, (phrog_2665 similarity = 87.3%, phrog_2691 similarity = 91.3%) whereas comparison to MR003 were both low (<60%). Orthologous pairs of CDS between Koomba kaat 1 and MR003 were high (phrog_2665 similarity = 91%, phrog_2691 similarity = 99.3%) whereas comparison to SA012 were low (<60%).

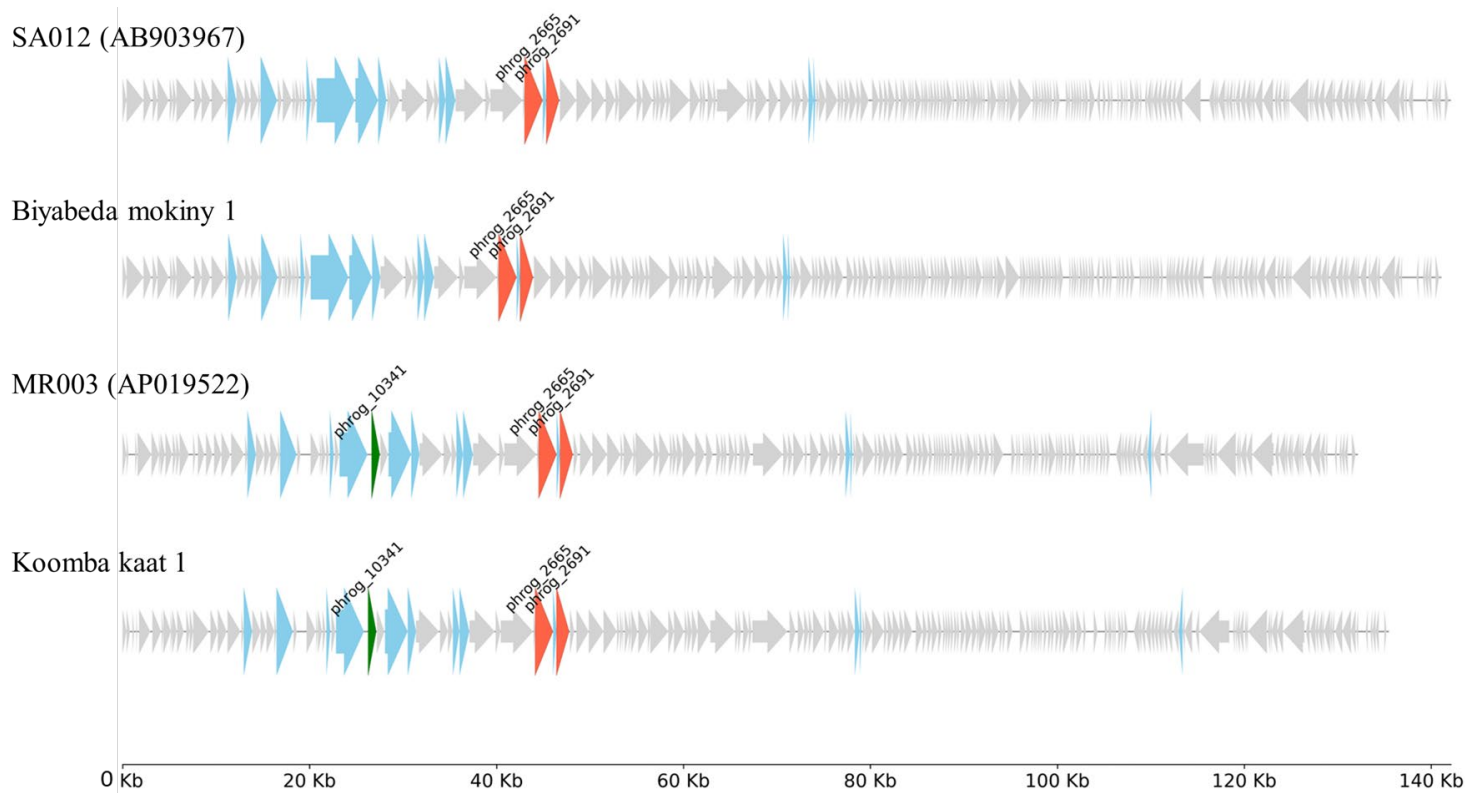


Figure 4.10: Colinear alignment of Koomba kaat 1 and Biyabeda mokiny 1 alongside SA012 and MR003 phages, all tail fibre proteins are coloured in blue to show co localisation of tail components alongside putative RBPs. Orthologous pairs of CDS between Biyabeda mokiny 1 and SA012 were high, (phrog_2665 similarity = 87.3%, phrog_2691 similarity = 91.3%) whereas comparison to MR003 were both low (<60%). Orthologous pairs of CDS between Koomba kaat 1 and MR003 were high (phrog_2665 similarity = 91%, phrog_2691 similarity = 99.3%) whereas comparison to SA012 were low (<60%). The presence of an N-acetyl glucosamidase is seen in green (phrog_10341) and present in Koomba kaat 1 and MR003 genomes (Similarity = 97.2%). All comparison scores were calculated using BLASTp (v2.5.0).

4.4. Discussion

The characterisation of *Staphylococcus* phages (and many others) remains a difficult task for many reasons. As a parasitic viral entity, phages are diverse, prone to changing due to random mutations, and contain large numbers of ‘hypothetical’ proteins. Furthermore, their predominant utility, their bactericidal activity, is impacted by epigenetic modifications conferred by their propagation host and may require new sequencing data when the host bacterial isolate changes [219, 236]. This may cause discrepancies across multiple studies that utilise the same phage grown in separate propagation hosts, or in cases where phages have been shared within groups with access to different bacterial repositories. In addition, this increases the cost and preparation time for phages that may require renewed characterisation in situations where prophage contamination has occurred due to the host bacterial isolate [237]. In the previous chapter, it was shown that phages Koomba kaat 1 and Biyabeda mokiny 1 were lytic phages that could be propagated within their host bacterial strains without inducing prophage contamination. However, for successful therapeutic intervention, phages must be able to reach the site of infection without significant loss of activity and they must be able to successfully infect the target bacteria at the site of infection [158, 224, 238]. To ensure downstream processes, such as phage sample purification and delivery will not interfere with phage activity, several stability characterisations are required. In addition, to ensure that these phages will be efficacious once delivered, lytic assays are performed throughout the characterisation process to confirm retention of activity. In this chapter, the resilience of phages Koomba kaat 1 and Biyabeda mokiny 1 were assessed; it was found that both phages could be reliably recovered from storage, propagated, and aerosolised without significant reductions in phage activity. When phages were assayed against MRSA and MSSA from various clinical sources (respiratory, non-respiratory tissue, non-respiratory fluid, and blood cultures), wide ranges of activity were seen which further corroborates previous data generated for *Kayviruses* and *Silviaviruses* targeting *Staphylococcus* species [112, 212, 217, 239]. Furthermore, the antibiofilm activity of these phages were demonstrated against MRSA specifically from the airways of persons with CF. This chapter demonstrates the utility of these phages to significantly reduce the bacterial load in addition to reducing the physical biomass of biofilms produced by these bacterial strains. An in-depth look at the genomes of Koomba kaat 1 and Biyabeda mokiny 1 revealed clustering alongside multiple phages previously characterised for therapeutic applications

Page | 119

[212, 214, 215, 217, 240, 241]. Leveraging this information, multiple receptor binding proteins belonging to both phages were identified and these phages were determined to be polyvalent [242].

The physiochemical stability profiles of Koomba kaat 1 and Biyabeda mokiny 1 show that phages were inactivated at temperatures above 70°C (Figure 4.2A). This is consistent with previous data demonstrating the stability of *Staphylococcus* phages at high temperatures (60-70°C) [141, 209]. For pH stability, a previously characterised *Staphylococcus* phage was found to be stable across a pH range of 4-9 [243]. This was consistent with the findings in this study, as both Koomba kaat 1 and Biyabeda mokiny 1 were stable at pH 5, 7, and 9 (Figure 4.2B) with less than 1 log reduction between these conditions. Stability at different acid-base concentrations will affect the overall outcome of different purification methods and the yield of phages returned; this is because many methods of purification involve organic solvents or ion-exchange chromatography that may inactivate phages [244]. Furthermore, phage resistance to external factors such as temperature and acidic or basic environments is multifactorial in that the variation of one factor will influence sensitivity to the others [244, 245]. Whilst combinations of all possible solutions would not be feasible, understanding the influences of a standard range of factors may lead to greater insights towards the improvements of preservation techniques for phages that do not retain activity well in storage [244, 245].

The resilience of phages via nebulisation is related to numerous factors including pre-aerosolisation media and ambient conditions such as humidity [246, 247]. In regards to inherent characteristics the tail morphology, in particular the tail length, is known to effect the aerosol stability characteristics of phage as previous data have shown that the short ‘stubby’ tailed Podoviruses are less prone to damage than Siphoviruses and Myoviruses when nebulised [98]. Both Koomba kaat 1 and Biyabeda mokiny 1 have Myovirus morphotypes (Figure 3.3A & C) with an icosahedral head and long contractile tails of different sizes (Table 3.8) as discovered in the previous chapter. Compared with known literature, Koomba kaat 1 has a shorter tail length than previously published *Silviaviruses*

[212, 217] and Biyabeda mokiny 1 has a longer tail than some *Kayviruses* with length determined via TEM [248, 249] however within the literature this can vary (Between 122 and 280nm for phage K), possibly due to the contractile nature of Myoviridae phage tails.

The stability of both phages when aerosolised was high, approximately 3% reduction in viable titre for Koomba kaat 1 and 12.5% reduction in viable titre for Biyabeda mokiny 1. When compared to previous literature regarding mesh-type nebulisation; the effects of nebulisation on a *P. aeruginosa* infecting phage (PEV44) reported a 50-60% increase in 'broken' phage particles [116]. Whilst there are no studies looking at the effects of nebulising *Staphylococcus* phages specifically *in vitro*, phages have been nebulised previously with successful treatment of MRSA infections in rats [136]. In more *in vivo* studies, it has been shown within macaque monkeys [250] that nebuliser type (mesh, jet, ultrasonic) has no effect on phage viability and that large amounts of phage can be delivered using nebulisation [251]. Overall, there were no significant drops in concentration during nebulisation for either phage within this study and based on previous use cases of *Staphylococcus* phages *in vivo* there is a good chance aerosol viability will remain high *in vivo* [136].

Next, the lytic efficiency of both phages was determined against a range of *S. aureus* bacteria. Koomba kaat 1 demonstrated a much broader range of activity against *S. aureus* than Biyabeda mokiny 1, yet unlike Biyabeda mokiny 1, Koomba kaat 1 was not able to infect any other *Staphylococcal* species. Unfortunately, the low number of non-aureus *Staphylococci* within this bacterial repository (n = 5) prevented further work to truly understand the range diversity. However, it could be possible for the ability of Biyabeda mokiny 1 to infect *S. xylosus* to be leveraged as a non-pathogenic propagation host in manufacturing. This alternative approach has been reported using a food-grade *S. xylosus* strain previously in the literature and a key benefit is that this method overcomes concerns around large scale propagation (required for clinical translation of any phage) of a human pathogenic bacterium [209]. Outside of the *Staphylococcus* genus, neither phage was able to infect any of the other bacterial species assayed. Collectively these data are supported by

what is commonly seen in the literature for *Staphylococcus* infecting *Kayvirus* and *Silviavirus* phages [112, 212, 214, 217, 240].

Despite host range activity differences, analyses revealed that Koomba kaat 1 and Biyabeda mokiny 1 are likely to share similar receptor binding proteins (Figure 4.10). Results generated showed that both phages are polyvalent and have at least two RBPs, with predictions that they likely share the same receptors of phage SA012 (Figure 4.10, phrog: 2665, 2691), receptors shown to bind to the Wall Teichoic Acids (WTAs) backbone or N-acetylglucosamine (α -GlcNAc) residues on the WTA. These receptors were previously described for phage SA012 [232] and a similar process of genome comparison were produced for phage MR003 [212] whose genome also contained an N-acetylglucoamidase motif (Figure 4.10, phrog_10431) within a similar region that the authors speculate to be responsible for this *Silviaviruses* broad range of activity. In this analyses these factors were identified independently (RBPs, endolysin motifs) and labelled according to their functional assignments from the PHROGs database [194] (Figure 4.10). When the phage genomes are ordered and visualised alongside each other (Figure 4.10) to observe the co-localisation of homologues, in addition to BLASTp similarity, the genomic arrangement of Biyabeda mokiny 1 is more similar to SA012 and Koomba kaat 1 is more similar to MR003, supporting this phylogenetic analysis. Whilst phage activity does depend on ability for phages to recognise and bind to their target bacterium, the infection process can be resisted by bacteria across all steps of the phage lifecycle [219, 236]. In addition to RBPs it has been shown that the endolysin encoded by the phage, and endolysin type, may contribute to the phage lytic efficiency against the host bacteria and could potentially impact the phages range of activity [218].

Concern around bacterial resistance to phages is a widely discussed topic, with numerous manuscripts reporting host-pathogen interactions between bacteria and their phages [252-259]. The consensus seems to be that whilst phage usage does lead to resistance *in vitro*, these effects have fitness costs associated with them such as increased susceptibility to antibiotics and/or host immune factors [259], which may prevent their translation into *in vivo*

or clinical studies. General understanding of these interactions is developing at a rapid rate, and recent data have shown a hierarchical nature of resistance in certain bacterial species [219], or modular cross resistance reported in others [260]. Whilst more data are required to determine the complexity and reach of these effects, and whether they are relevant *in vivo*, it is clear that these interactions are not only phage-host specific, but also specific to their host microenvironment where the immune system may play a role for, or against, the introduction of phage [259, 261, 262]. With this in mind, future work that may make use of the data within this study may include the acquisition of bacterial genome sequencing data to accompany the lytic profiles generated for Koomba kaat 1 and Biyabeda mokiny 1. Access to this information may enable an investigation into the mechanisms by which non-susceptible bacterial isolates resist phage infection [219, 236]. The benefits of such an analysis may include the production of predictive tools that utilise the bacterial genome to select phages based on known resistance mechanisms encoded within. Similar computational tools have been attempted with various degrees of success but still cannot predict activity with strain level specificity [263-265]. Another advantage of sequencing the bacterial isolates is the standardisation of information since currently, host range bacterial panels have not been standardised for *S. aureus*. Attempts have been made for other bacterial genera [266] but not widely adopted, further, the use of laboratory strains may not accurately represent the bacteria causing infections today. By treating WGS of bacterial isolates as a crucial aspect of host range and lytic efficiency data, analyses that compare ranges of activity across the wider literature may be a possible future.

Nevertheless, information from the broader scientific community may be leveraged for phages Koomba kaat 1 and Biyabeda mokiny 1. In this analysis, 574 *Staphylococcus* infecting phage genomes were identified within the 1st May 2023 Inphared database update [191]; the majority of which were not assigned into families and are left as ‘Unclassified’ since the abolishment of numerous widespread phage families in the latest International Committee on Taxonomy of Viruses (ICTV) update [200]. The most significant of these changes were the removal of the order *Caudovirales* and the morphologically based families *Myoviridae*, *Podoviridae*, and *Siphoviridae* [200]. Despite this, access to characterisation manuscripts concerning the closest relatives were available for most relative genomes

identified (Table 4.3) [157, 214, 239, 240, 267-269]. In the absence of these families, which have previously been used to infer broad characterisations such as lifecycle [172, 214, 270, 271], this study utilised the presence of multiple lysogeny associated genes and the BACPHLIP machine learning pipeline to inform lifecycle groups [272]. This approach enabled us to classify the phages into distinct lifecycle categories, based on genetic signatures associated with lysogeny. The utilisation of machine learning algorithms like BACPHLIP offers a means to predict lifecycle beyond the scope of 'known' lysogenic factors to determine lifecycle. In addition, the use of vConTACT2 [216] clusters phages in a 'blind' manner, without bias based on known or 'officially classified' genera. This approach also offers a less biased approach; grouping phages based on genetic similarities rather than predefined taxonomies enables the identification of viral clusters that may not conform to traditional taxonomic boundaries. By performing these analyses, Koomba kaat 1 and Biyabeda mokiny 1 are accurately placed within the wider phage genomic landscape. Within these analyses (Figures 4.6 and 4.7) both genomes are clustered alongside genomes that have been assessed for therapeutic use independently [157, 214, 239, 240, 267-269] and do not have any aberrant genomic qualities or rearrangements (Figures 4.8 and 4.9).

Overall, this chapter has demonstrated that Koomba kaat 1 and Biyabeda mokiny 1 are able to meet the temperature and pH requirements of typical phage manufacturing, can withstand the effects of mesh nebulisation, and have an ability to infect and disrupt biofilms produced by MRSA from CF airways (Figure 4.5). Koomba kaat 1 has a broader range of activity against MRSA biofilms within this study, this agrees somewhat with previous literature reporting the ability for *Silviaviruses* to prevent regrowth from biofilm however comparisons are difficult as the authors did not quantify biofilm CFU within the study [273]. Biyabeda mokiny 1 was also able to infect biofilms and effectively reduce biofilm CFU counts but had less of an ability to disrupt the biofilms biomass (Figure 4.5, panel A and B). Despite this, activity has already been reported for *Kayviruses* [222, 248] including the well-studied Phage K representative of this Genus. Irrespective of lytic efficiency against particular bacterial isolates, therapeutic agents require stringent safety assessments and purifications prior to their use in clinic [274]. Whilst the previous chapter demonstrated that Koomba kaat 1 and Biyabeda mokiny 1 are genomically safe in terms of generalised transduction, lifecycle, and

virulence factors, this chapter has demonstrated that these phages are stable and efficacious against numerous *S. aureus* bacterial pathogens.

In summary, the data provided here provides strong evidence that these phages may be used to great effect in targeting *S. aureus* from a range of clinical sources. However lytic capabilities are not the only concerns for therapeutic agents and the intrinsic safety characteristics of both phages to the recipient host are yet to be determined. This is especially true given the respiratory context of persons with CF, as the burden of inflammation, in response to pulmonary infection, is a particular concern. As such, the next steps for these phages are to validate the safety of Koomba kaat 1 and Biyabeda mokiny 1 using appropriate *in vitro* and *in vivo* models of the airways.

Chapter 5: Preclinical safety assessment of Koomba kaat 1 and Biyabeda mokiny 1 phages

5.1.Introduction:

The resurgence of phage therapy is due to the expanding rates of antibiotic resistance prompting demand for alternative treatments [14, 23]. Naturally, the resurgence is seeing an increasing number of phage candidates being characterised for their therapeutic abilities [212-215, 240, 275-278]. However, despite the growing need for innovative antimicrobial solutions, the need for pharmaceutical grade manufacturing methods to ensure high quality standards and minimise batch variability are required [279, 280]. There are now multiple studies that indicate phages are safe when purified of potentially harmful contaminants [148, 277, 278, 281-284]. However, whilst current data have provided a foundation for phage therapy, the adverse effects that have been noted in human trials of phage cannot be overlooked. In a 2021 clinical trial (ClinicalTrials.gov registered: NCT03140085), rapid fever development ($>38.0^{\circ}\text{C}$) occurred in one of the nine patients after three days of treatment with a phage cocktail [285]. Several case studies have also demonstrated some adverse activity of phages [165, 241, 286], including withdrawal due to anaphylaxis concerns [286]. In a systematic review of safety and toxicity data for phages within both animal and clinical studies [164], it was found that, of the twenty animal studies that met selection criteria, only four were focussed on safety [139, 256, 287, 288]. In addition, the variety of endpoints across these four studies did not match, making larger scale comparisons difficult. This lack of standardisation has also been noted in several broader reviews of phage therapy [164, 289].

For treatments utilising *Staphylococcus* phages specifically, there has been a single adverse event reported in humans, and this was relatively minor [165]. In a case study concerning a 72-year-old patient with a prosthetic joint infection, a single *Staphylococcus* phage (SaGR51 ϕ 1) was used and after three intravenous doses were given, the recipient developed an increase in liver enzymes (aspartate aminotransferase and alanine aminotransferase) and phage treatment was discontinued [165]. Although the effect on the liver (transaminitis) was

reversible and the patient stabilised after discontinuation, the authors postulated that the cause was due to dysregulated cytokine responses from liver macrophages. As such, further studies are required to clarify the safety of MRSA phages. These studies, in combination with a lack of pulmonary specific endpoints, highlight the need for safety studies concerning the application of phage directly into the airways. Specifically, most animal studies published to date have administered a single dose of phages at a single timepoint to target acute infections [148, 256, 290, 291]. In humans, this is unlikely to be the case, as many antibiotic resistant infections are chronic in nature, and typically require long treatment periods with multiple doses to eradicate the infection [42, 292]. This is especially pertinent for individuals suffering from CF, where persistent lung infections with *S. aureus* cause increased inflammation and subsequent lung function decline [46, 293].

In the previous chapter, work performed identified the therapeutic potential of 2 phages of interest, Koomba-kaat 1 and Biyabeda-mokiny 1. Knowing that these phages are specific for respiratory derived *S. aureus* clinical isolates, this chapter sought to determine the intrinsic safety characteristics of these phages in the absence of confounding factors such as an active infection or additive substances. Specifically, the hypothesis being tested was that once adequately purified, high concentrations of phages Koomba kaat 1 and Biyabeda mokiny 1 would not induce any cytotoxic effects or pathology either *in vitro* or *in vivo*. The first aim was to characterise the safety of these phages when administered onto a 3-dimensional primary airway epithelial cell model. Following this, the next aim was to assess the two phages for pulmonary safety in an animal model, using a combination of physiological and inflammatory endpoints. Results from this chapter comprehensively demonstrate the safety of Koomba kaat 1 and Biyabeda mokiny 1.

5.2. Materials and methods:

5.2.1. Bacterial isolates and phage propagation

Growth medium was prepared according to manufacturer instructions and bacteria isolates, unless specified as a public strain (American Type Culture Collection), were clinical MRSA

isolates derived from the respiratory tract (courtesy of Professor Scott Bell). Both Biyabedamokiny 1 and Koomba-kaat 1 were isolated and propagated using their host clinical isolates (SA01 and SA09 respectively) (Refer to section 2.4.12). Bacteria were grown using Tryptic Soy (TS) broth (BD Difco™) from a single colony and incubated overnight (~16 hours) at 37°C with orbital shaking at 120 rpm. Frozen bacterial stocks were stored at -80°C in TS broth supplemented with glycerol to a final concentration of 25% (Refer to section 2.4.1).

5.2.2. High Pressure Liquid Chromatography

Phage purifications for all experiments originate from a single batch of filter-sterilised, high titre phage preparation. Purifications were performed using phage lysate filtered through 0.22 µm filters to remove bacterial debris prior to HPLC purification. Filtered phage lysates were then passed through a HiTrap BIA Monolithic Column (BIA Separations, Ajdovščina, Slovenia) using the ÄKTA M2 pure™ HPLC platform (Cytiva Life Sciences, Marlborough, MA, USA) (refer to section 2.4.25). After each use, anion exchange columns were thoroughly cleaned and stored in 20% (v/v) ethanol at 4°C until further usage (Refer to section 2.4.26).

5.2.3. Preparation of *S. aureus* for primary airway epithelial cell exposure

Heat killed *S. aureus* was used as a reference for epithelial inflammation induced by local bacterial death. To produce solutions of heat killed bacteria, a single colony of *S. aureus* was used to inoculate 5 mL of TS-broth media and grown at 37°C to an optical density measured at 600nm (OD_{600nm}) of 1.0 (approximately 1×10^9 CFU/mL). To wash cells and remove media components, 1 mL of bacterial culture was initially centrifuged at 3220 g for 5 minutes at RT to pellet the bacterial cells, supernatant removed, and the pellet resuspended in 1mL of sterile PBS. This was repeated 3 times. For heat inactivation, bacterial aliquots were heated at 80°C for 60 minutes in 1.5 mL tubes. To ensure no remaining bacterial viability, 10 µL was spotted onto TS agar and incubated at 37°C overnight and inspected for growth 16-24 hours post-incubation. In addition, a sterile loop was used to transfer some inoculum from

the heat inactivated sample to 5 mL of fresh TS broth which was incubated at 37°C overnight in an orbital shaker at 120 rpm and also inspected for growth 16-24 hours post-inoculation. Heat inactivated bacterial aliquots were then stored at 4°C prior to usage.

5.2.4. Enterotoxin screen

The common *S. aureus* enterotoxins A, B, C, D, and E were screened in phage preparations using the RIDASCREEN® enzyme immunoassay kit (R-Biopharm, Bergstraße 17 64297 Darmstadt, Germany) as per the manufacturer's instructions. The limit of detection for this kit is 0.25 ng toxin per mL of sample and if obtained absorbance values were below the mean value calculated for negative controls, the sample was considered negative. This was performed in duplicate for each enterotoxin independently.

5.2.5. WAERP Participant demographics

Primary airway epithelial cells (AECs) were derived from children recruited into the Western Australian Epithelial Research Program (WAERP), when they attended St. John of God Hospital (Subiaco, WA, Australia) for non-respiratory elective surgery. Recruited participants had no history of respiratory disease at the time of sample collection nor a history of atopy. Furthermore, participants were confirmed to be free from respiratory symptoms and bacterial or viral chest infections using ISAAC and American Thoracic Society (ATS) respiratory questionnaires [294]. Written consent was provided by parents for their children's participation into WAERP program. WAERP numbers and participant gender can be found in (Appendix H).

5.2.6. Primary airway epithelial cell collection

Primary AECs were collected using interdental brushes (Esro AG, Kilchberg, Switzerland) to gently sample the nasal turbinate whilst the child was under anaesthesia. The brush, along with the collected cells were immediately stored in sterile collection media (RPMI-1640 with

20% HI-FCS v/v). This process was repeated for both nostrils. The collection tubes were then put on ice and transported to the Telethon Kids Institute laboratories for cell processing.

5.2.7. Primary airway epithelial cell processing

On arrival, brushes were gently vortexed to dislodge cells from the brushes and the supernatant containing cells collected. To dissociate the epithelial cell clumps further, the cell suspension underwent gentle passage through a 25 G needle, followed by a 27 G needle with a ½-inch length. This process was repeated three times per needle. To assess total cell count and viability, a haemocytometer was used (Refer to section 2.4.20). Following this, cells were either processed for liquid nitrogen storage (refer to section 2.4.21) or recovered for co-culturing at a density of 5,000 cells per cm² alongside 5,000 cells per cm² γ -irradiated NIH-3T3 fibroblasts in flasks that were precoated with fibronectin buffer the day prior (Refer to section 2.4.22). Cell cultures were incubated in a Heracell™ VIOS 160i incubator at 37°C, 5% CO₂, and 95% air. When confluent, cells were cryopreserved at in liquid nitrogen (refer to section 2.4.21)

5.2.8. Primary airway epithelial cell co-culture

Primary AECs were recovered by rapid thawing from liquid nitrogen storage (Refer to section 2.4.22) and seeded into a fibronectin-coated tissue culture flasks at a density of 5,000 cells per cm² and co-cultured with 5,000 cells per cm² γ -irradiated NIH-3T3 fibroblasts. These cell cultures were incubated in a Heracell™ VIOS 160i incubator at 37°C, 5% CO₂, and 95% air. Regular mycoplasma testing was carried out to ensure mycoplasma free cultures were used for this study as described in section 2.4.23. Once at ~80% cell confluency, cultures were subcultured using a commercial subculture reagent pack (LONZA™) (refer to section 2.3.9). First, the cell monolayer was rinsed with HEPES buffered saline solution to clean any dead cells or debris from the surface. Subsequently, cells were incubated in 1% (v/v) trypsin-EDTA solution for 7 minutes at 37°C. To neutralise the trypsin, an equivalent amount of trypsin neutralising solution was added to the flask. The remaining cell suspension was then collected and centrifuged at 500 x g for 7 minutes in a centrifuge precooled to 4°C.

The supernatant was discarded and the cell pellet resuspended in CCM. Cells were then seeded into a fibronectin-coated tissue culture flasks, at a density of 5,000 cells per cm² and co-cultured with 5,000 cells per cm² γ -irradiated NIH-3T3 fibroblasts. These cell cultures were maintained in a Heracell™ VIOS 160i incubator at 37°C, 5% CO₂, and 95% air.

5.2.9. Primary airway epithelial growth at the air liquid interface

Primary AECs that had been co-cultured within flasks (Refer to section 5.2.8) to a maximum passage number of p3 were used for growth at the air liquid interface (ALI) [21]. Once monolayer cell cultures reached approximately 80% confluency, cells were lifted from their monolayer using trypsin and enumerated using a haemocytometer and trypan blue solution (Refer to section 2.4.20). Cells were then used to seed 24-well Corning CoStar Transwell® plates with permeable inserts (6.5mm in diameter) that have a 0.4 μ m polyester membrane. Each insert was coated with Type 1 rat tail collagen the night before (Roche, Castle Hill, NSW, Australia) and seeded with 150,000 cells/cm². Both the apical (200 μ L) and basolateral (500 μ L) compartments of the transwell insert were filled with PneumaCult™-Ex Plus media for expansion for the next 5-7 days, at which time the cells reach 100% confluency. During this 'pre-airlift' period, media were replaced every day. Then, media was removed from both compartments and PneumaCult-ALI added solely to the basolateral compartment.

5.2.10. Primary airway epithelial cell exposures

Prior to exposure to phages, all media in the basolateral compartment was replaced with PneumaCult-ALI without pen/strep or hydrocortisone for 24 hours. Samples of Koomba kaat 1 and Biyabeda mokiny 1 were purified using HPLC and their bacterial hosts, SA01 and SA09, were used to prepare heat killed *S. aureus* aliquots for cell exposures. Cell exposures had four experimental conditions and a control group: #1 Sterile PBS (control), #2 Koomba kaat 1 diluted in PBS to a concentration of 1 x 10⁸ PFU/mL, #3 Biyabeda mokiny 1 diluted in PBS to a concentration of 1 x 10⁸ PFU/mL, #4 Heat-inactivated SA01 (1 x 10⁸ CFU/mL), #5 Heat-inactivated SA09 (1 x 10⁸ CFU/mL). Each treatment was applied directly onto the apical surface of transwell inserts in volumes of 10 μ L per insert and incubated for 24 hours.

Post-exposure, 100 μ L of PBS was added to the apical surface of each insert and incubated for 5 minutes at 37°C. This was collected and spun at 700 x g for 5 minutes at RT to pellet any cells removed from the surface. Cell free supernatant was collected and stored at -80°C for downstream analysis. Protein was extracted from samples using 350 μ L of cell extraction buffer (Refer to section 2.3.25) and stored at -80°C for downstream analysis. Inserts required for histological analysis were fixed by filling the apical (200 μ L) and basal (500 μ L) compartments with 10% neutral buffered formalin (10% NBF) for 60 minutes at RT. The 10% NBF was then replaced with sterile PBS and stored at 4°C for downstream analysis.

5.2.11. Primary airway epithelial cell staining and histology

Cell sections of AEC air liquid interface cultures were used to confirm pseudo stratification by visualising multiple cell layers and types. Inserts fixed with NBF were embedded in paraffin and sliced to generate 5 μ m sections, that were then fixed onto Superfrost plus slides (Waldemar Knittel Glasbearbeitungs GmbH, Braunschweig, Germany). Slides were air-dried and incubated at 60°C for 30 minutes before deparaffinisation in an autostainer (Leica autostainer XL, Leica, Mt Waverley, VIC, Australia). Following this, two rounds of xylene treatments for 2 minutes each were performed, succeeded by rehydration through a series of decreasing ethanol concentrations (100%, 95%, 70%, and 40%; all v/v). Staining was then performed using Gill's Hematoxylin II stain for 5 minutes. Washing was performed with two 5-minute rinses in tap water. Next, a 2% (v/v) acetic acid/ddH₂O treatment for 10 seconds was carried out, followed by a 45-second bluing step. Slides were rinsed under tap water and subjected to dehydration through increasing ethanol concentrations (40% and 70%; both v/v). A 5-minute incubation in alcoholic eosin was followed by further dehydration in 95% and 100% ethanol. Finally, two rounds of xylene treatment were done before applying Permount (Thermo Fisher) and placing a coverslip over the sections. Cell sections were also stained with Alcian blue to confirm the presence of mucus. For Alcian blue staining, ALI inserts previously fixed with 10% (v/v) NBF were processed as above for embedding. Alcian blue 8GX in 3% acetic acid was added to the slide-mounted section for 60 minutes, followed by a 1-minute rinse with water. Subsequently, nuclear fast red staining was conducted for 5 minutes, and then washed three times with tap water. After dehydrating with 70% (v/v) ethanol, a coverslip was applied using Permount (Thermo Fisher).

5.2.12. Quantification of Alcian Blue Stain

Quantification of Alcian blue staining in histological sections was performed using open source software developed by Mr Alphons Gwatimba and Dr Yuliya Karpievitch [295]. Briefly, the software quantifies the Alcian blue stain's presence within the epithelium's histological sections as a percentage of pixels corresponding to tissue in each blue slide image. The software employed set pixel values to distinguish between tissue and non-tissue areas, using contour detection to identify regions of interest. Specifically, pixels within defined RGB ranges were marked as Alcian blue stain irrespective of intensity of staining. The calculation for quantification involved determining the ratio of 'Alcian blue stain' pixels to 'tissue' pixels. Data were then used to calculate the amount of Alcian blue stain as a percentage of the total tissue area.

5.2.13. Transepithelial Electrical Resistance

Barrier integrity of AEC ALI cultures was monitored on a representative subset of transwell inserts from each patient ID, both pre- and post-exposure, by assessing TEER (described in section 2.2.23) measured with an EVOM2 volt-ohmmeter (World Precision Instruments, Sarasota, Florida, USA). Electrodes were first sterilised using 70% (v/v) ethanol for 5 minutes and air dried within a biosafety cabinet. Then, both the apical (500 μ L) and basolateral (500 μ L) media compartments of the inserts were replaced with PBS. For each insert, three measurements were taken, and these measurements were subsequently averaged to yield a representative TEER value.

5.2.14. Cell viability (LDH assay)

Cytotoxicity was measured with the CytoTox 96® Non-Radioactive Cytotoxicity Assay kit from Promega Corporation (Madison, WI, USA) according to the manufacturer's instructions. This assay uses levels of lactate dehydrogenase (LDH) release as a proxy for compromised membranes by cell death [296]. Apical and basolateral cell free supernatants

were assayed. For a positive control heat killed bacteria were utilised and baseline measurements were taken using PBS controls.

5.2.15. IL-8 ELISA

Interleukin 8 (IL-8) levels were determined using previously established protocols [297] via enzyme linked immunosorbency assays (ELISA) (Biosciences, San Diego, CA, USA) (refer to 2.4.26). The amount of IL-8 released was measured from the apical and basal compartments and normalised to PBS exposure. Sensitivity for this assay ranged between 3.125 pg/mL to 200 pg/mL. Data were normalised to the total amount of protein produced with whole protein levels using commercially available BCA Protein Assay Kits (Refer to section 2.4.24).

5.2.16. Mouse exposure model

All procedures were approved by the Telethon Kids Institute Animal Ethics Committee (#P2267). Thirty-six adult (~8 weeks of age) C57BL/6J mice (18 males and 18 females) were obtained from the Animal Resources Centre (Murdoch, WA, Australia) and group-housed according to sex (3 per cage) within individually ventilated cages (Tecniplast, Buguggiate, Italy). Mice were provided with *ad libitum* access to chow (Rat and Mouse Cubes, Specialty Feeds, Glen Forrest, Australia) and water. For phage administration, mice were anaesthetised with isoflurane and then intranasally inoculated with 10^9 PFU/mL of bacteriophage suspended in 50 μ L of PBS. Control mice received 50 μ L of PBS. Mice were inoculated twice daily for 14 days, with at least 6 hours in-between treatments. There were 6 males and 6 females per treatment, and three treatment groups: Koomba kaat 1, Biyabeda mokiny 1, and control (PBS). Mice were weighed and assessed for changes in behaviour/wellbeing via standard institutional clinical scoring daily. Clinical scoring metrics included: behaviour, activity level, body posture, breathing, and coat quality. Cage average water and chow consumption were recorded every 5 days from day 1 of treatment.

5.2.17. *In vivo* sample collection and analysis

Approximately 20 hours after their final inoculation, mice were terminally anaesthetised with an inter-peritoneal injection of ketamine (40 mg/mL; Troy Laboratories, New South Wales, Australia) and xylazine (2 mg/mL; Troy Laboratories, New South Wales, Australia) in saline at a dose of 0.1 mL/10 g body weight. When a surgical level of anaesthesia was obtained, they were then tracheostomised with a 1 cm long polyethylene cannula (internal diameter 0.086cm), secured with surgical silk and mechanically ventilated at ~300 breaths/min with a tidal volume of 8 mL/kg and 2 cmH₂O of positive-end expiratory pressure (HSE Harvard Minivent; Hugo Sachs Harvard Elektronik, March-Hugstetten, Germany). While being ventilated, the chest wall was opened, the heart visualised, and blood obtained from the left ventricle via cardiac puncture. A subsample of whole blood was immediately taken for analysis of blood gases, haematology, and chemistry: sodium, potassium, ionised calcium, glucose, haematocrit, haemoglobin, pH, partial pressure of carbon dioxide (*PCO*₂), partial pressure of oxygen (*PO*₂), total carbon dioxide (*TCO*₂), bicarbonate (*HCO*₃), base excess and oxygen saturation (*sO*₂) using the iStat Alinty (Abbott laboratories, Chicago, IL, USA). Remaining blood was centrifuged at 6,500 x g for 10 minutes and serum frozen at -80°C for potential downstream analyses. After cardiac puncture, mice were removed from the ventilator and bronchoalveolar lavage fluid (BALf) was collected by washing the lungs with 0.5 mL of chilled saline three times via tracheal cannula. A gross necropsy was then performed which involved visual examination of external anatomy and key organs (lungs, gastrointestinal tract, liver, spleen, kidneys, reproductive organs) followed by removal and weighing of the liver, spleen, and kidneys.

BALf was analysed via a slight modification of a process previously described [298]. Briefly, BALf samples were centrifuged once at 400 x g for 5 minutes to pellet the cells. Supernatant was removed and centrifuged a second time at 6,500 x g for 10 minutes to pellet any bacteria or cell debris. This second supernatant and pellet were stored at -80°C for potential downstream analyses. The initial cell pellet was resuspended in 100 µL PBS and a 10 µL aliquot was stained with trypan blue for live/dead cell counts using a haemocytometer. Remaining cells were used to generate cytopins, that were stained with Rapid Stain (Amber Scientific, Traralgon, Vic, Australia) and 300 cells counted to determine the proportion of

cell types within the lungs. BALf supernatant was also analysed for mediator levels using the Bio-Plex Pro Mouse Cytokine 23-Plex assay (Bio-Rad, South Granville NSW Australia) and accompanying software; Bio-Plex Manager (v6.11). Whole protein was also analysed in BALf using the Pierce™ BCA protein assay kit (ThermoFisher Scientific) in the same manner as described above for the AEC supernatants (Refer to section 2.4.24).

5.2.18. Statistical analyses

Differential cell counts, blood gases/chemistry, whole protein quantitation, and organ weight data for the spleen, liver, and kidneys were assessed using two-way ANOVA with sex and treatment as factors. Data were transformed where required to satisfy the assumptions of normality and homogeneity of variance. Protein data were filtered for outliers that were 2x standard deviations away from the group mean. Statistical tests were run using Jamovi [299] version 2.3 (2022 release) and R statistical programming [300]. Bioplex raw data were filtered to remove individual mediators where every value fell below the detection limit and remaining data were processed by removing outliers that lay 2x standard deviations outside of the group mean. Remaining data points that fell below the detection range were changed to half of the lowest standard to enable subsequent statistical analysis as previously described [298]. To assess differences between males, females, phage treatments, and controls a Generalised Linear Model (GLM) approach was used, to perform this, the Python module SciPy v1.11.0 [301] was implemented.

5.3.Results:

5.3.1. Phages Koomba kaat 1 and Biyabeda mokiny 1 phages were successfully purified using HPLC.

Both the phages Koomba kaat 1 and Biyabeda mokiny 1 were able to be purified via HPLC. The UV280 nm peaks were used to determine the optimal fraction collections. All fractions chosen contained more than 1×10^9 PFU/mL and did not need further concentration prior to use within either safety models (*in vitro* and *in vivo*). Furthermore, every collected fraction of Koomba kaat 1 (n=3) or Biyabeda mokiny 1 (n=3) tested negative for the presence of *Staphylococcal* enterotoxins A, B, C, D and E when assessed using the RIDASCREEN assay.

5.3.2. Primary airway epithelial cell integrity is not adversely affected by Koomba kaat 1 or Biyabeda mokiny 1 phages.

Results indicated that primary cultures were successfully grown into morphologically intact layers at the ALI. Average TEER of inserts prior to exposure were $740 \pm 111 \Omega/\text{cm}^2$. Barrier integrity was not adversely affected by 24 hours exposure to phages (Koomba kaat 1: $519 \pm 353 \Omega/\text{cm}^2$; Biyabeda mokiny 1: $384 \pm 402 \Omega/\text{cm}^2$) or heat inactivated bacteria (heat killed SA1: $352 \pm 421 \Omega/\text{cm}^2$; heat killed SA9; and $546 \pm 394 \Omega/\text{cm}^2$), as changes in TEER were similar to the mock challenge ($409 \pm 385 \Omega/\text{cm}^2$). Overall, there were no significant differences in TEER over the course of 24h ($p=0.751$) (Figure 5.1). In terms of cellular architecture, exposure to Koomba kaat 1, Biyabeda mokiny 1, SA01, or SA09 did not induce any gross visible changes (Figure 5.3, panels A-E) when compared to the PBS control.

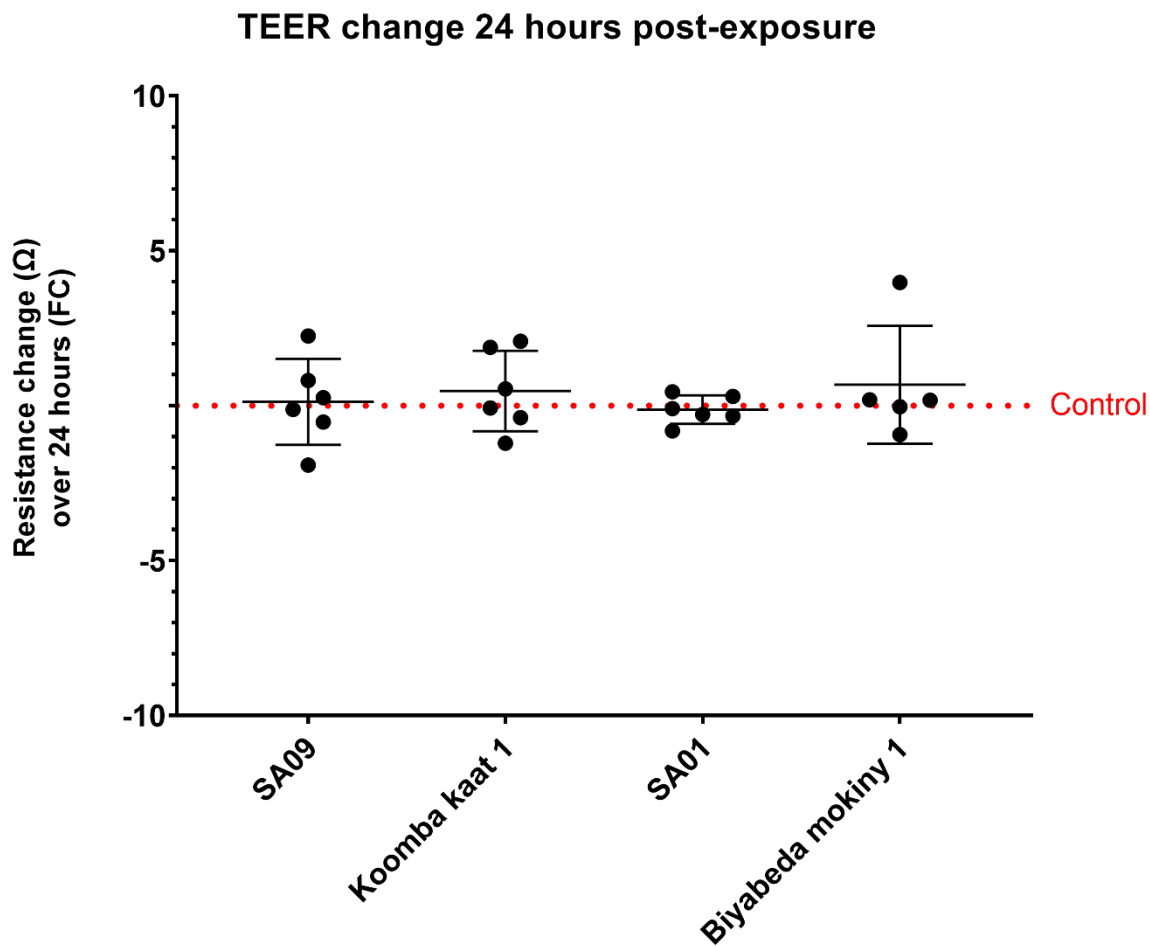


Figure 5.1: Barrier integrity assessments 24 hours post-exposure. Resistance measurements were calculated immediately prior to and 24 hours post-exposure to phages Koomba kaat 1, Biyabeda mokiny 1, *S. aureus* bacterial strains: SA01 and SA09, and PBS controls. All data are reported as fold change respective to the experimental control group (dotted line). There were no significant differences found in TEER across any experimental groups ($p=0.751$). Data are presented as mean values (\pm SD, $n=6$ across all groups apart from Biyabeda mokiny 1 group where 1 value was removed as an outlier).

5.3. Primary airway epithelial cell mucus production is not influenced by Koomba kaat 1 or Biyabeda mokiny 1 phages.

To measure the effects of phages on mucus production, Alcian blue staining was performed and an image analysis tool (5.2.12) used to quantify the percentage of Alcian blue staining across the pAEC inserts (Visualised in Figure 5.4). There were no differences in mucus production (stained pixels to tissue area pixels ratio) across all treatment groups: Koomba kaat 1: 0.043 ± 0.025 , SA09: 0.097 ± 0.073 , Biyabeda mokiny 1: 0.088 ± 0.087 , SA01: 0.106 ± 0.070 , PBS control: 0.092 ± 0.062 ($p=0.535$; Figure 5.2).

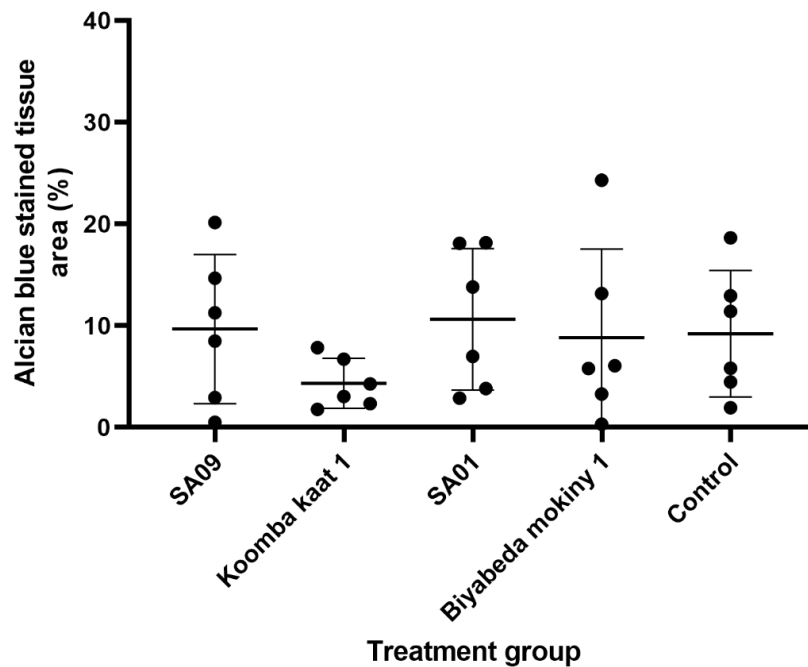


Figure 5.2: Assessment of mucus production via Alcian blue staining 24 hours post-exposure. Sections were stained and processed using software developed in-house [295]. There were no significant differences in the amount of mucus produced across each treatment group after 24 hours ($p=0.535$). Data were normalised against the total count of 'tissue' pixels and the percentage of Alcian blue staining was quantified as a percentage value. Data are presented as mean values (\pm SD, $n=6$).

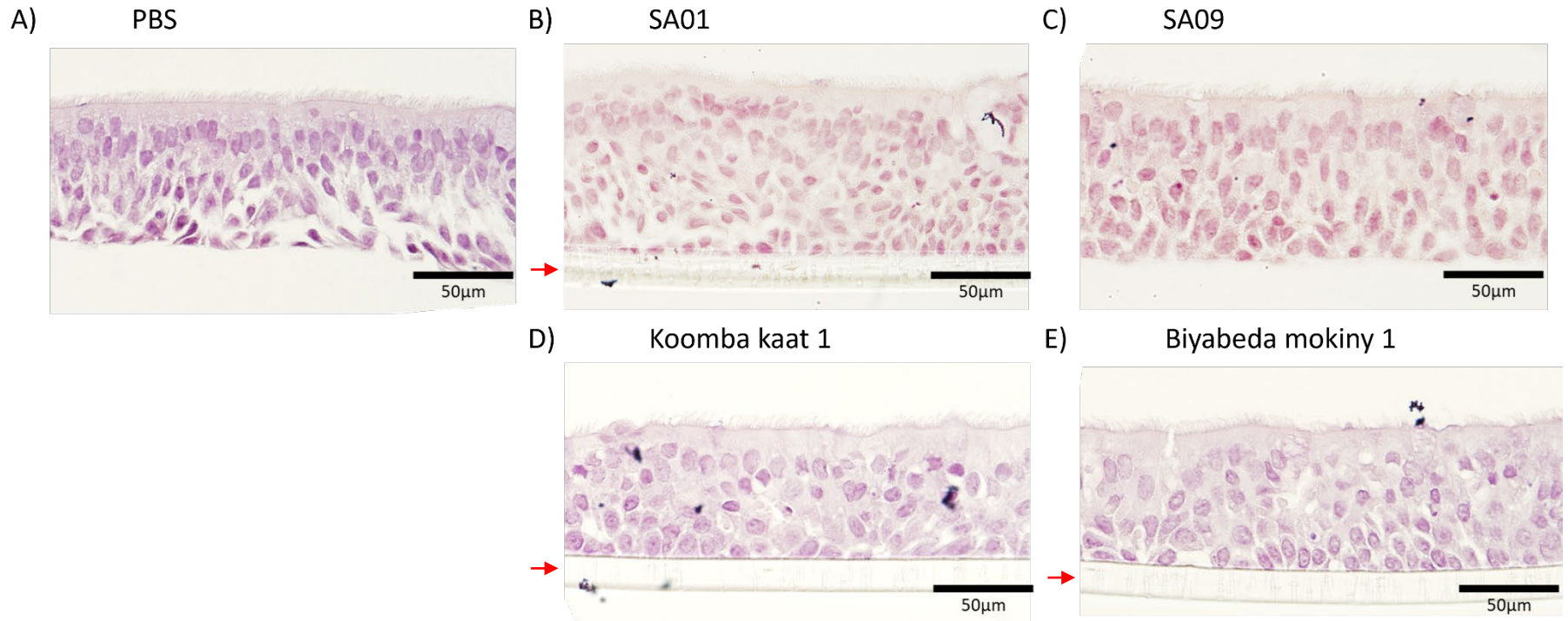


Figure 5.3: Haematoxylin and eosin-stained primary AECs collected from children and cultured at the air liquid interface as described in section 5.2.15. There were no visible differences in the AEC structures formed between groups B to E when compared to the untreated (PBS) controls (A). In each group intact AECs can be seen in a multi-layered formation with a ciliated top layer 24h post-infection. The images shown are representative (taken at 40X magnification) of 1 biological replicate of 6 performed, and reflect the observations seen across each treatment group. Red arrows indicate the presence of the cell culture mebrane (if present).

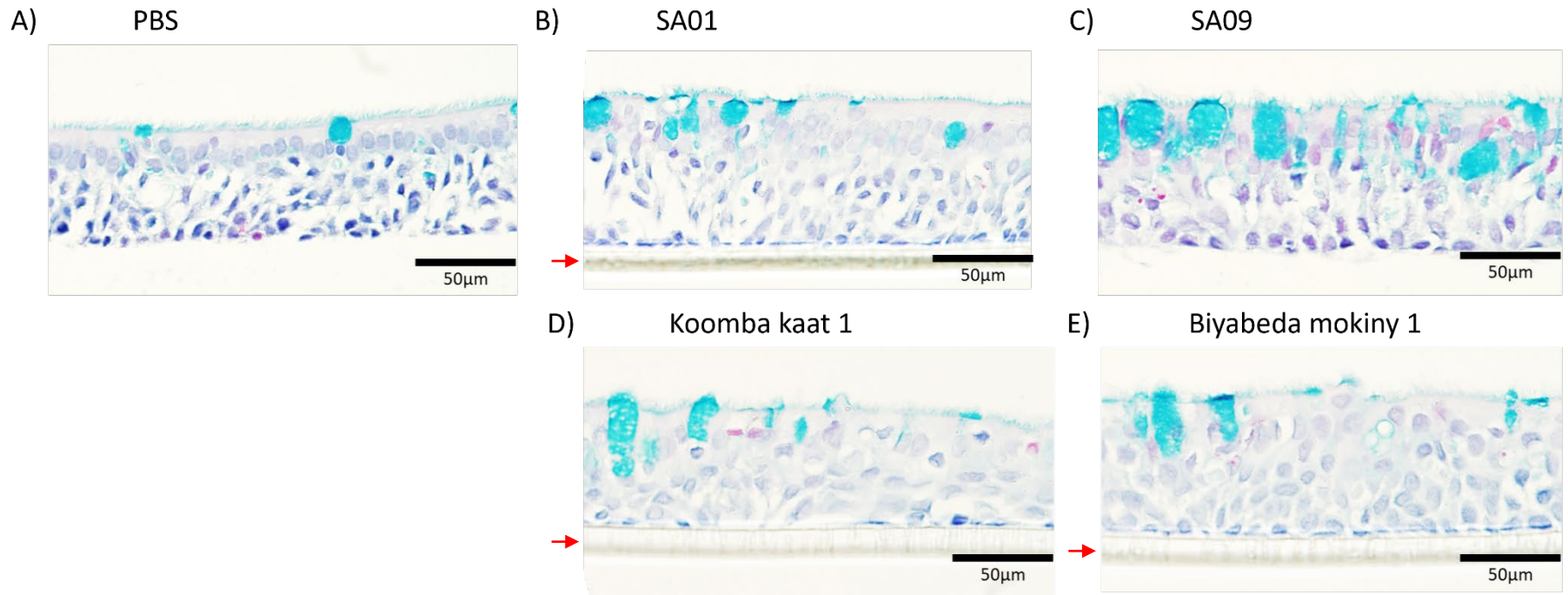


Figure 5.4: Alcian blue stained primary AECs collected from children and cultured at the air liquid interface as described in section 5.2.15. Primary AECs were grown for 28 days to promote pseudo stratification into multiple cell types and layers. Inserts were fixed from each experimental group (A to E) using 10% NBF and embedded them in paraffin prior to sectioning. When quantified, there were no differences in mucus secretion between the experimental groups (B to E) and our untreated PBS controls (A) (Figure 5.3). The images shown are representative (taken at 40X magnification) of 1 biological replicate of 6 performed, and reflect the observations seen across each treatment group. Red arrows indicate the presence of the cell culture mebrane (if present).

5.4. Phages Koomba kaat 1 and Biyabeda mokiny 1 are nontoxic and noninflammatory towards airway epithelial cells *in vitro*.

There were some significant effects of treatment on LDH release in both apical and basal compartments. Koomba kaat 1 induced more basolateral LDH release than Biyabeda mokiny 1 ($p=0.041$), as did its host *S. aureus* SA09 ($p=0.017$; both Figure 5.5A). On the apical surface, *S. aureus* SA09 induced more LDH release than Biyabeda mokiny 1 ($p=0.016$; Figure 5.5B). Both phages resulted in the induction of apical IL-8 release that was slightly higher than their bacterial hosts. However, the overall IL-8 results were largely similar between all conditions with no significant differences across the mean values of all groups ($p=0.068$). When compared individually, the mean difference (fold change relative to control) in the Koomba kaat 1 group (1.21x), was significantly higher than its heat killed host (SA09: 0.69x; $p=0.047$; Figure 5.6).

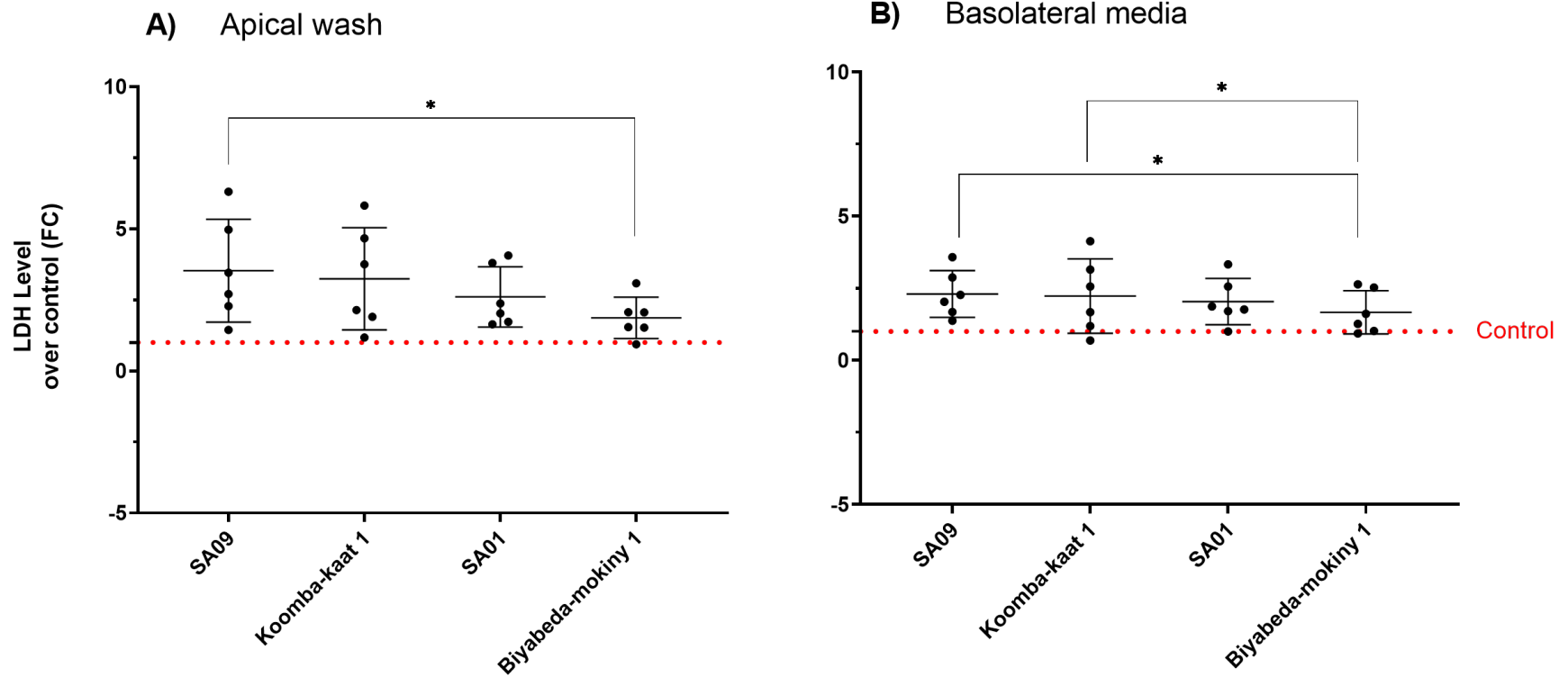


Figure 5.5: Quantification of LDH from the apical washings (A) and basolateral media (B) compartments of the primary AEC air-liquid interface cultures, 24 hours post-exposure to phages Koomba kaat 1, Biyabeda mokiny 1, and *S. aureus* bacterial strains: SA01 and SA09. All data are reported as fold change respective to the experimental control group (PBS). Data are presented as mean fold change with standard deviation. Bars that connect groups indicate significant differences.

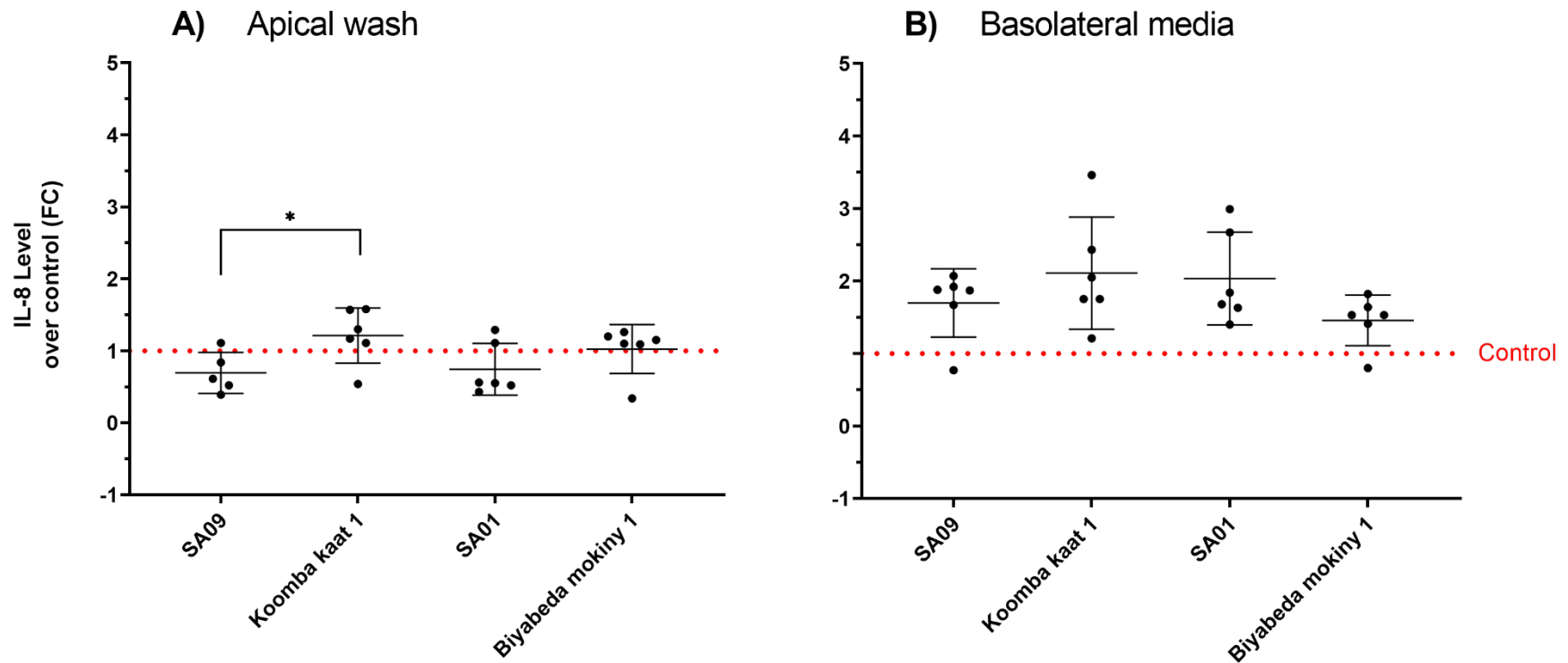


Figure 5.6: Quantification of IL-8 in the apical washings (A) and basolateral media (B) compartments of the primary AEC air-liquid interface cultures, 24 hours post-exposure to phages: Koomba kaat 1, Biyabeda mokiny 1, and *S. aureus* bacterial strains: SA01 and SA09. There was a significant increase in IL-8 in Koomba kaat 1 exposed inserts ($p=0.047$) when compared to its host bacteria SA09. All data are reported as fold change respective to the experimental control group (PBS; dashed line). Data shown are mean value bars with standard deviation. Data have been normalised using whole protein levels determined via BCA assay. Bars that connect groups indicate significant differences.

5.4.2. Airway implementation of Koomba kaat 1 and Biyabeda mokiny 1 does not induce pathology in a respiratory mouse model.

Phages were successfully administered intranasally to mice twice daily for the duration of the treatment period (14 days) and no adverse events in the mice were observed. Overall there were no detectable changes in the clinical score throughout and mice subjected to either phage were indistinguishable from controls in all clinical parameters (refer to section 5.2.17). Phages Koomba kaat 1 and Biyabeda mokiny 1 did not have a significant effect on body weight from the beginning to end of the treatment period for either males ($p=0.456$) or females ($p=0.535$; Figure 5.7). Supporting this, food and water consumption (Table 5.1) was not impacted. Males treated with Koomba kaat 1 (Food: 2.7 ± 0.11 g/mouse/day, Water: 2.4 ± 0.11 mL/mouse/day), Biyabeda mokiny 1 (Food: 3.3 ± 0.73 g/mouse/day, Water: 2.7 ± 0.50 mL/mouse/day) were similar to controls (Food: 3.4 ± 0.63 g/mouse/day, Water: 3.3 ± 0.84 mL/mouse/day). This finding was the same for females treated with Koomba kaat 1 (Food: 3.1 ± 1.08 g/mouse/day, Water: 2.8 ± 0.52 mL/mouse/day), Biyabeda mokiny 1 (Food: 2.7 ± 0.52 g/mouse/day, Water: 2.7 ± 0.53 mL/mouse/day) and controls (Food: 2.7 ± 0.87 g/mouse/day, Water: 2.4 ± 0.23 mL/mouse/day) throughout the duration of the study ($p > 0.05$ in all cases).

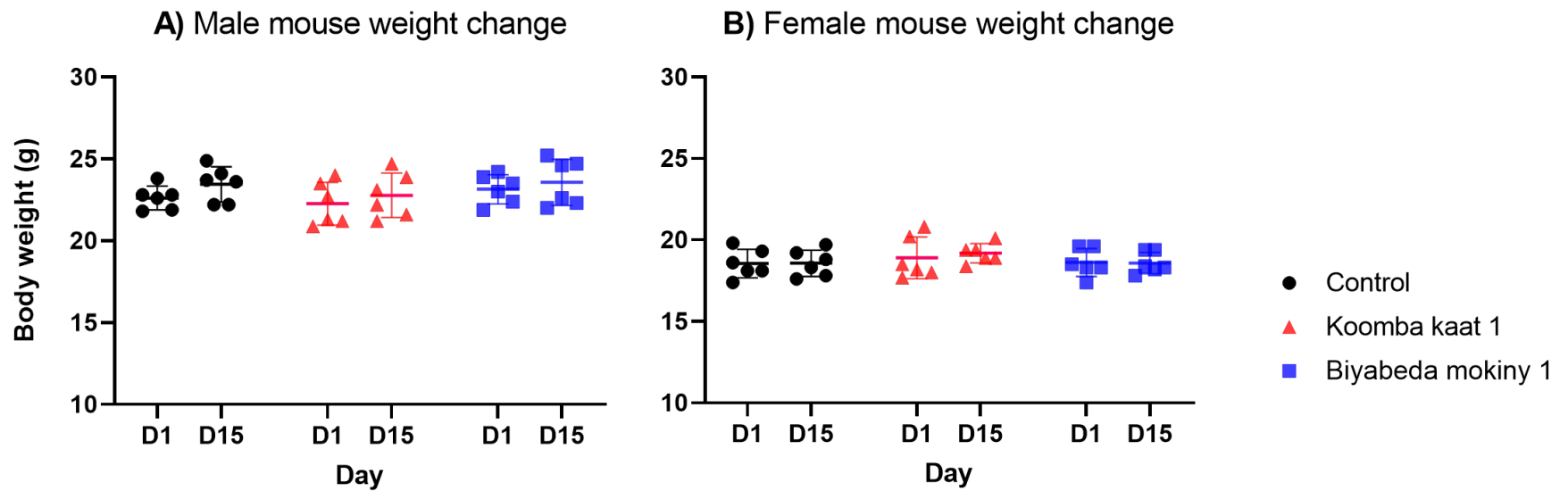


Figure 5.7: Weight change between the first (D1) and last (D15) day of the mouse animal phage exposure period for controls, Koomba kaat 1 exposed mice, and Biyabeda mokiny 1 exposed mice. Neither male (panel A) or female (panel B) weight changed significantly between D1 and D15 for any treatment. . Data are presented as individual mice with mean (\pm SD).

Table 5.1: Total average water and food consumption per day (mL/mouse per day and grams/mouse per day). Data have been calculated using three food and water measurements and are presented as the mean (\pm SD).

Sex	Treatment	Water intake (mL/mouse/day)	Difference to control (%)	Food intake (g/mouse/day)	Difference to control (%)
Male (n=6)	Control (PBS)	3.3 \pm 0.84	--	3.4 \pm 0.63	--
Male (n=6)	Koomba kaat 1	2.4 \pm 0.11	-28%	2.7 \pm 0.11	-18%
Male (n=6)	Biyabeda mokiny 1	2.7 \pm 0.50	-17%	3.3 \pm 0.73	-2%
Female (n=6)	Control (PBS)	2.4 \pm 0.23	--	2.7 \pm 0.87	--
Female (n=6)	Koomba kaat 1	2.8 \pm 0.52	+19%	3.1 \pm 1.08	+17%
Female (n=6)	Biyabeda mokiny 1	2.7 \pm 0.53	+12%	2.7 \pm 0.52	+2%

On examination of the external anatomy, nothing overtly abnormal was identified suggesting no effects of phage on mouse well-being. Examination of the internal anatomy supported these findings, as there were no abnormalities in the lungs, liver, kidneys, adrenals, spleen, testis/ovaries, heart, stomach, or bladder observed. Amongst these: the liver, spleen, and both kidneys were carefully excised and weighed (Table 5.2) and analyses found no effect of phage on liver ($p=0.969$), spleen ($p=0.561$), left kidney ($p=0.372$), or right kidney ($p=0.415$) weights. However, males did have larger livers (average weight = 1.11 ± 0.1 g for males, average weight = 0.83 ± 0.09 g for females) and kidneys compared to females (average weight = 0.15 ± 0.01 g for males, average weight = 0.12 ± 0.02 g for females) ($p < 0.001$ in both cases).

Table 5.2: Organ weights for the liver, spleen, and both kidneys. Each treatment group comprised of 12 mice in total (6 males and 6 females). Data are presented as mean values (\pm SD).

Sex	Treatment	Liver weight (g)	Spleen (g)	Left kidney (g)	Right kidney (g)
Male (n=6)	Control (PBS)	1.14 \pm 0.05	0.07 \pm 0.02	0.15 \pm 0.01	0.15 \pm 0.01
Male (n=6)	Koomba kaat 1	1.13 \pm 0.09	0.07 \pm 0.01	0.15 \pm 0.01	0.15 \pm 0.01
Male (n=6)	Biyabeda mokiny 1	1.05 \pm 0.13	0.07 \pm 0.01	0.16 \pm 0.01	0.16 \pm 0.02
Female (n=6)	Control (PBS)	0.80 \pm 0.07	0.06 \pm 0.01	0.12 \pm 0.00	0.12 \pm 0.01
Female (n=6)	Koomba kaat 1	0.82 \pm 0.08	0.07 \pm 0.01	0.12 \pm 0.01	0.13 \pm 0.02
Female (n=6)	Biyabeda mokiny 1	0.88 \pm 0.14	0.07 \pm 0.01	0.12 \pm 0.02	0.13 \pm 0.03

Blood glucose levels were significantly higher in male controls compared with males exposed to Biyabeda mokiny 1 (Controls: 22.37 ± 2.13 mmol/L, Koomba kaat 1: 20.20 ± 1.16 mmol/L, Biyabeda mokiny 1: 17.98 ± 2.33 mmol/L, $p=0.038$). Apart from this, there were no significant effects of phage treatment on any haematological, blood gas, or blood chemistry parameter when compared to same-sex controls (Table 5.3). Interestingly, there was a significant difference between male and female mice for base excess (BE) (Controls: -6.17 ± 2.64 mmol/L, Koomba kaat 1: -7.33 ± 3.20 mmol/L, Biyabeda mokiny 1: -5.50 ± 2.07 mmol/L, $p=0.011$), whereby female mice had significantly higher BE than males.

Table 5.3: Haematology, blood gas and blood chemistry parameters across experimental groups and controls separated by sex. The only significant effects seen were higher BE in females (when compared to males) and lower blood glucose in males treated with Biyabeda mokiny 1 (when compared to sex matched controls). Data shown are mean (\pm SD) values (n=6 per treatment group).

Parameters	PBS control (Males)	Koomba kaat 1 (Males)	Biyabeda mokiny 1 (Males)	PBS control (Females)	Koomba kaat 1 (Females)	Biyabeda mokiny 1 (Females)
Na (mmol/L)	144.67 (\pm 2.34)	146.00 (\pm 3.35)	147.00 (\pm 1.90)	146.33 (\pm 1.63)	148.00 (\pm 1.00)	146.67 (\pm 2.42)
K (mmol/L)	4.05 (\pm 1.34)	3.47 (\pm 0.73)	3.80 (\pm 0.52)	3.78 (\pm 0.29)	3.84 (\pm 1.06)	3.60 (\pm 0.71)
iCa (mmol/L)	1.08 (\pm 0.08)	0.97 (\pm 0.13)	1.01 (\pm 0.08)	0.99 (\pm 0.06)	0.97 (\pm 0.20)	0.94 (\pm 0.13)
Glucose (mmol/L)	22.37 (\pm 2.13)	20.20 (\pm 1.16)	17.98 (\pm 2.33) *	20.52 (\pm 2.74)	18.45 (\pm 1.89)	21.97 (\pm 3.02)
Hct (%PCV)	38.67 (\pm 2.73)	40.00 (\pm 2.10)	37.17 (\pm 3.43)	38.17 (\pm 1.72)	38.00 (\pm 1.87)	38.50 (\pm 1.38)
Hb (g/L)	131.50 (\pm 9.22)	136.17 (\pm 7.25)	126.50 (\pm 11.81)	129.83 (\pm 6.18)	129.00 (\pm 6.28)	131.00 (\pm 4.94)
pH	7.36 (\pm 0.06)	7.39 (\pm 0.15)	7.36 (\pm 0.04)	7.32 (\pm 0.06)	7.35 (\pm 0.03)	7.42 (\pm 0.10)
PCO ₂ (kPa)	4.68 (\pm 0.86)	4.16 (\pm 1.62)	4.73 (\pm 0.86)	4.52 (\pm 1.04)	4.73 (\pm 1.43)	3.57 (\pm 0.87)
PO ₂ (kPa)	5.02 (\pm 1.70)	6.35 (\pm 2.65)	5.38 (\pm 1.46)	5.82 (\pm 1.40)	5.88 (\pm 1.41)	6.52 (\pm 4.32)
HCO ₃ (mmol/L)	19.52 (\pm 2.45)	17.70 (\pm 3.07)	19.98 (\pm 2.45)	17.53 (\pm 3.39)	17.48 (\pm 2.94)	16.72 (\pm 1.42)

BE (mmol/L)	-6.17 (± 2.64)	-7.33 (± 3.20)	-5.50 (± 2.07)	-8.50 (± 3.73)	-8.20 (± 3.03)	-7.83 (± 0.75)
sO ₂ (%)	65.33 (± 24.24)	74.17 (± 22.17)	70.50 (± 14.64)	72.83 (± 12.81)	72.80 (± 16.38)	73.50 (± 13.26)
TCO ₂ (mmol/L)	20.50 (± 2.51)	18.67 (± 3.39)	21.00 (± 2.83)	18.67 (± 3.50)	18.20 (± 3.11)	17.33 (± 1.37)

Significant difference indicated with a “*” are between that cells treatment group and sex-matched controls (p< 0.05).

An assessment of the cellular inflammation within BALf revealed no significant effects of either phage on the number of total cells (Controls: $30,097 \pm 11,030$ cells/mL, Koomba kaat 1: $25,199 \pm 10,186$ cells/mL, Biyabeda mokiny 1: $29,909 \pm 9,093$ cells/mL, $p=0.473$), macrophages (Controls: $29,371 \pm 10,905$ cells/mL, Koomba kaat 1: $24,795 \pm 9,871$ cells/mL, Biyabeda mokiny 1: $29,144 \pm 8,636$ cells/mL, $p=0.520$) or neutrophils (Controls: 727 ± 646 cells/mL, Koomba kaat 1: 403 ± 403 cells/mL, Biyabeda mokiny 1: 765 ± 981 cells/mL, $p=0.146$) in the BALf of mice (Figure 5.8). There were no significant effects of either phage on the amount of protein detected within the BALf samples of male mice (Controls: 299 ± 59 $\mu\text{g/mL}$, Koomba kaat 1: 317 ± 38 $\mu\text{g/mL}$, Biyabeda mokiny 1: 251 ± 38 $\mu\text{g/mL}$, $p=0.072$) or female mice (Controls: 313 ± 47 $\mu\text{g/mL}$, Koomba kaat 1: 346 ± 89 $\mu\text{g/mL}$, Biyabeda mokiny 1: 243 ± 38 $\mu\text{g/mL}$, $p=0.070$) (Figure 5.9).

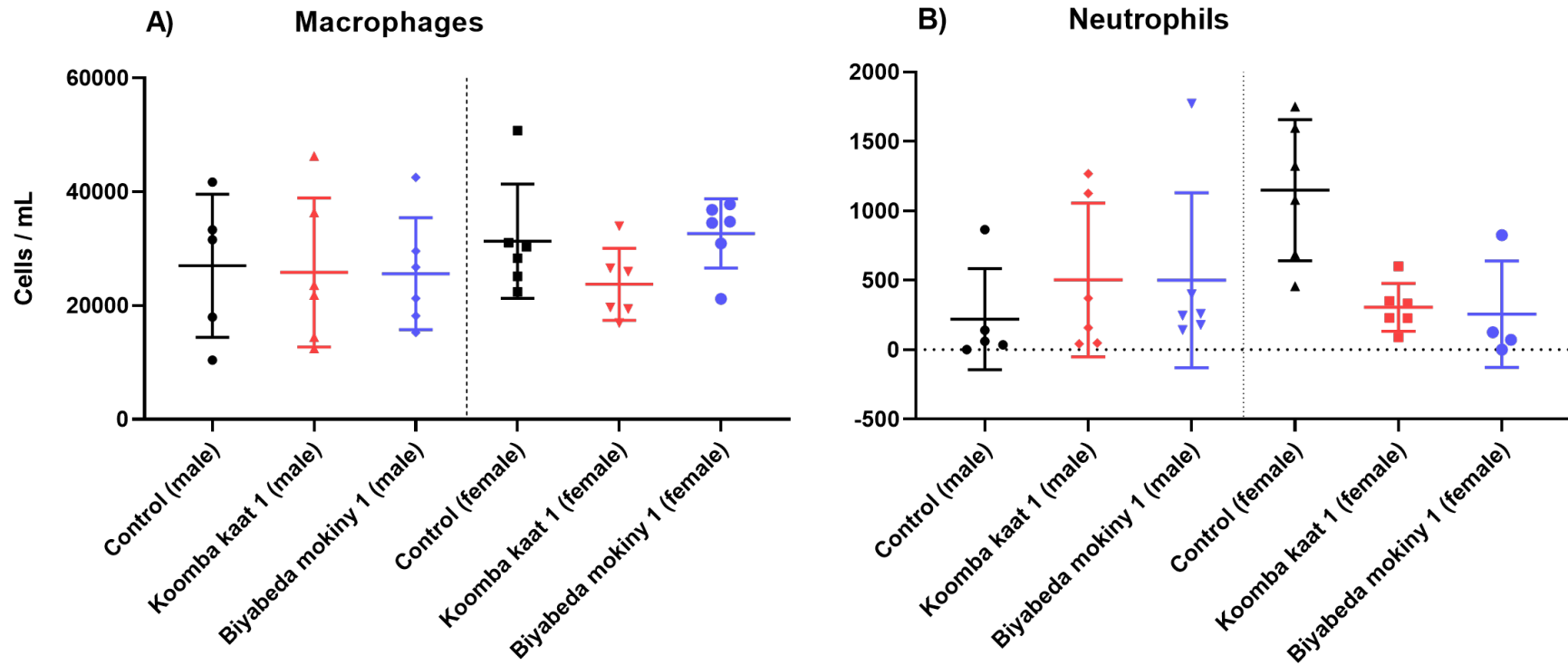


Figure 5.8: Differential cell counts obtained from stained cytospin samples of BALF collected from mice. There were no significant differences in cell counts for macrophages or neutrophils amongst our phage treated groups when compared to experimental controls of the same sex. Data are presented as individual mice with mean (\pm SD). Eosinophils and lymphocytes were counted but none were present within the first 300 cells counted. Note different scales.

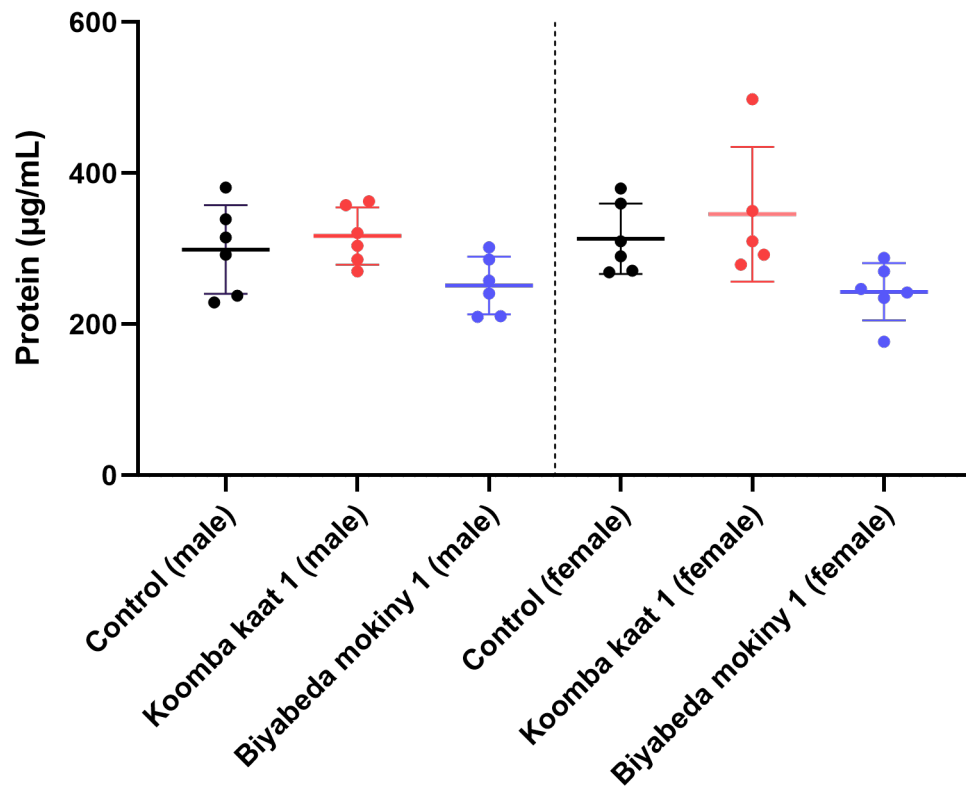


Figure 5.9: Quantification of total protein from mouse BALF. All data are reported as mean (\pm SD). There were no significant differences in protein concentrations in male or female mice exposed to Koomba kaat 1 or Biyabeda mokiny 1 compared with sex-matched controls. Data are presented as individual mice with mean values (\pm SD).

Out of the potential 23 mediators assessed, 18 had measurements that were above the limit of detection, but Interleukin-1 beta (IL-1 β), Interleukin-3 (IL-3), Interleukin-9 (IL-9), Granulocyte-Macrophage Colony-Stimulating Factor (GM-CSF or GM-GCF), and Monocyte Chemoattractant Protein-1 (MCP-1) were all removed from analyses due to being below the detection limit. There was no significant effect of sex or treatment for Interleukin-1 alpha (IL-1 α), Interleukin-2 (IL-2), Interleukin-4 (IL-4), Interleukin-5 (IL-5), Interleukin-6 (IL-6), Eotaxin, Granulocyte-Colony Stimulating Factor (GCSF), Keratinocyte Chemoattractant (KC), Macrophage Inflammatory Protein-1 alpha (MIP1 α), Macrophage Inflammatory Protein-1 beta (MIP1 β), Regulated on Activation, Normal T Expressed and Secreted (RANTES), and Tumour Necrosis Factor alpha (TNF α) (Table 5.4). There were

borderline differences between males and females for IL-5 ($p=0.050$) as well as IL-12(p70) ($p=0.050$). Within an analysis of the remaining six mediators: Interleukin-10 (IL-10), Interleukin-13 (IL-13), Interleukin-12 subunit p40 (IL-12(p40)), Interleukin-12 subunit p70 (IL-12(p70)), Interleukin-17 (IL-17), and Interferon-gamma (IFN γ), there were no significant differences found for IL-10, IL-13, and IL12(p70). However, there were significant decreases in the amount of IL-17 ($p=0.017$), and IFN γ ($p=0.008$) in both male mice treated with Koomba kaat 1 (IL-17: 0.67 ± 0.13 pg/mL, IFN γ : 0.40 ± 0.16 pg/mL) when compared to male controls (IL-17: 0.75 ± 0.26 pg/mL, IFN γ : 0.86 ± 0.46 pg/mL) and female mice treated with Koomba kaat 1 (IL-17: 0.52 ± 0.24 pg/mL, IFN γ : 0.58 ± 0.39 pg/mL) compared to female controls (IL-17: 0.83 ± 0.11 pg/mL, IFN γ : 0.92 ± 0.30 pg/mL). There was also a significant increase in the amount of IL-12(p40) ($p=0.016$) in Koomba kaat 1 treated male mice (148.93 ± 58.33 pg/mL) when compared to male controls (74.89 ± 24.12 pg/mL).

Table 5.4: Bronchoalveolar lavage mediators across experimental groups and controls separated by sex. Overall, the only significant effects seen were with respect to IL-12(p40), IL-17, and IFN- γ for mice treated with Koomba kaat 1. Data shown are mean (\pm SD) mediator levels in BALf from male and female mice exposed to phages Koomba kaat 1, Biyabeda mokiny 1 phages, or controls (n=6 per treatment group).

Parameters (pg/mL)	PBS control (Males)	Koomba kaat 1 (Males)	Biyabeda mokiny 1 (Males)	PBS control (Females)	Koomba kaat 1 (Females)	Biyabeda mokiny 1 (Females)
IL-1 α	1.03 (\pm 0.26)	0.76 (\pm 0.21)	1.10 (\pm 0.22)	0.94 (\pm 0.20)	0.87 (\pm 0.31)	1.03 (\pm 0.32)
IL-2	0.63 (\pm 0.00)	0.63 (\pm 0.00)	0.63 (\pm 0.00)	0.63 (\pm 0.00)	0.75 (\pm 0.29)	1.08 (\pm 0.70)
IL-4	0.17 (\pm 0.00)	0.26 (\pm 0.22)	0.27 (\pm 0.24)	0.17 (\pm 0.00)	0.17 (\pm 0.00)	0.30 (\pm 0.23)
IL-5	0.46 (\pm 0.00)	1.39 (\pm 1.66)	1.21 (\pm 1.83)	0.46 (\pm 0.00)	1.29 (\pm 0.95)	2.63 (\pm 2.83)
IL-6	0.18 (\pm 0.00)	0.18 (\pm 0.00)	0.24 (\pm 0.16)	0.22 (\pm 0.12)	0.54 (\pm 0.64)	0.28 (\pm 0.26)
IL-10	1.73 (\pm 0.00)	2.25 (\pm 1.28)	1.73 (\pm 0.00)	1.73 (\pm 0.00)	1.73 (\pm 0.00)	1.73 (\pm 0.00)
IL-12(p40)	74.89 (\pm 24.12)	148.93 (\pm 58.33) *	76.77 (\pm 13.47)	96.75 (\pm 52.62)	88.63 (\pm 22.36)	100.22 (\pm 42.75)
IL-12(p70)	4.39 (\pm 2.11)	3.11 (\pm 1.31)	5.04 (\pm 1.36)	4.63 (\pm 1.53)	3.24 (\pm 2.18)	4.25 (\pm 1.06)
IL-13	7.39 (\pm 0.00)	7.39 (\pm 0.00)	8.97 (\pm 3.87)	7.39 (\pm 0.00)	7.39 (\pm 0.00)	8.69 (\pm 3.19)
IL-17	0.75 (\pm 0.26)	0.67 (\pm 0.13) *	0.84 (\pm 0.26)	0.83 (\pm 0.11)	0.52 (\pm 0.24) *	0.94 (\pm 0.33)

Eotaxin	4.62 (± 1.49)	3.00 (± 0.97)	3.23 (± 1.10)	4.42 (± 2.79)	9.91 (± 12.74)	4.35 (± 2.06)
G-CSF	3.74 (± 1.69)	3.56 (± 1.25)	3.57 (± 1.27)	3.05 (± 0.00)	7.23 (± 5.53)	4.24 (± 2.91)
IFN- γ	0.86 (± 0.46)	0.40 (± 0.16) *	1.09 (± 0.21)	0.92 (± 0.30)	0.58 (± 0.39) *	0.85 (± 0.37)
KC	4.00 (± 1.31)	4.33 (± 1.18)	4.68 (± 2.41)	3.52 (± 1.18)	6.47 (± 4.48)	4.12 (± 1.51)
MIP-1 α	0.31 (± 0.18)	0.54 (± 0.41)	0.40 (± 0.24)	0.41 (± 0.27)	0.63 (± 0.38)	0.59 (± 0.42)
MIP-1 β	2.09 (± 0.00)	2.78 (± 1.71)	4.27 (± 5.36)	2.96 (± 2.15)	8.65 (± 10.91)	5.65 (± 6.08)
RANTES	4.16 (± 1.54)	2.95 (± 1.38)	3.98 (± 0.82)	3.79 (± 0.51)	3.87 (± 0.52)	4.18 (± 2.01)
TNF- α	3.09 (± 1.52)	2.13 (± 0.92)	2.34 (± 1.43)	3.01 (± 1.38)	3.21 (± 2.37)	4.54 (± 2.48)

Significant difference indicated with a “*” are between that cells treatment group and sex-matched controls (p< 0.05)

5.4 Discussion

This chapter aimed to comprehensively assess the potential risks associated with the direct airway administration of two novel characterised phages Koomba kaat 1 and Biyabeda mokiny 1. Respiratory safety endpoints were the focus of this chapter as it is a key gap within phage literature and the effects of phage were assessed using both *in vitro* and *in vivo* studies to investigate safety across different biological contexts. Outcomes demonstrated that when Koomba kaat 1 and Biyabeda mokiny 1 were grown to high concentrations and purified via HPLC, they were safe to administer directly to the airways. This was evident first in the *in vitro* application directly onto primary airway cultures at high concentrations, where no effects were seen on barrier integrity, mucus production, toxicity, or inflammation. In the *in vivo* model, phage administered to mice intranasally at clinically relevant concentrations were shown to be well tolerated. This was indicated by general well-being of the animals with no adverse events throughout the treatment period. Physiological data supported this, as there were no significant effects of phage treatment across any of the outcomes assessed post-euthanasia. These outcomes included assessment of blood gasses and chemistry in addition to respiratory specific parameters such as total and differential cellular inflammation, BALf protein level, providing a rigorous and thorough test of the hypothesis that Koomba kaat 1 and Biyabeda mokiny 1 would not induce any cytotoxic effects or pathology.

Neither phage was cytotoxic when compared to their isolation host *in vitro*, and there were no signs that Koomba kaat 1 or Biyabeda mokiny 1 were able to induce significant amounts of inflammation or protein production when applied to human airway epithelial cells. *In vitro* data demonstrated that phages did not affect cellular integrity or morphology, nor were they cytotoxic when applied to the apical surface. In terms of inflammation, inferred from cytokine production, it was seen that IL-8 production was significantly increased across Koomba kaat 1 treated ALI inserts compared to heat-killed SA09, its host propagation bacteria (MRSA). Despite this result, it was found that the fold change relative to controls for SA09 was 0.69, indicating an anti-inflammatory effect compared to controls. Whilst there are data to suggest that *Staphylococcus* phages effect the release of IL-8 indirectly through nuclear factor κ B (NF- κ B) induction [302]. This does not explain the effects of IL-8 production in our pAEC model as the results suggest an anti-inflammatory effect of *Kayvirus* (vB_SauM_JS25) when investigated using

primary bovine mammary alveolar cells [302]. However, when assessed for significance compared to PBS treated controls, there was no significance found amongst any of the groups. This, in addition to the barrier integrity and cytotoxicity findings suggest that, whilst Koomba kaat 1 phages may elicit more of an immune response than to its host SA09, it is not intrinsically inflammatory. Existing data of live *S. aureus* infections *in vitro* have been established as both toxic and hyperinflammatory and may provide a more accurate comparison in regard to an infection scenario [303-307]. A previous study looking at *S. aureus* colonisation using Calu-3 cells (epithelial cell line) cultured at the ALI demonstrated that, without intervention, *S. aureus* cultures are toxic towards (measured via LDH assay) and result in cell death [303]. Interestingly, *S. aureus* strains lacking alpha-toxin are able to persist on epithelial cells for longer than their WT counterparts, and this study also demonstrated that alpha-toxin is the primary driver of cellular toxicity and airway damage [303]. However, *S. aureus* is a diverse pathogen capable of immunomodulatory activity and, conversely, it has also been shown that *S. aureus* can inhibit the production of IL-8 in some scenarios especially relevant to individuals with CF, such as co colonisation with *P. aeruginosa* [308]. In one study, it was shown that bacteria free filtrates from *S. aureus* had a potent anti-inflammatory effect on the immortalised epithelial cell line (Beas-2B) by dampening the TLR1/TLR2 mediated activation of IL-8 and NF- κ B [308].

Whilst past studies have conducted *in vitro* investigations into any possible interactions between phages and mammalian cells, many studies utilised cell lines that were cultured as a monolayer, which do not accurately reflect the polarised epithelial cell layer of the lung tissue [94, 309]. The airway is comprised of numerous cell types and, upon polarisation, will differentially express cytokines onto the apical or basolateral surfaces [310]. Previous data have shown that primary airway cultures grown at ALI have a transcriptional profile most similar to *in vivo* derived airway epithelia when compared to submerged cultures and a commonly used cell line (Calu-3), also grown at ALI [311]. As such, the utility of prior work using monolayer cell line models to assess the inflammatory responses of phages exposed to the luminal side may be limited in this regard [310]. Irrespective of model limitations, it can be said that phages able to infect numerous MDR pathogens have been investigated *in vitro* for safety using cell lines [148, 312-314]. Such studies suggest that phage morphology may influence cytokine induction, as seen in *Escherichia* phages applied to a human cell line (HT-39) in the absence of a bacterial host,

Page | 160

although the differences were not significant compared to bacterial controls [314]. Another study using the same cell line (HT-39) suggested *Clostridium* phage phiCDHS1 was toxic to monolayers due to increased LDH release [312]. Specific to airway cells, the A549 human lung epithelial cell line was not affected by *Acinetobacter* phage phikm18p even at high concentrations (1×10^9 PFU/mL), with various phage MOIs able to protect cells against *Acinetobacter baumannii* infection [313]. Unlike the LDH assay of the previous studies, the *Acinetobacter* phage phikm18p study performed live cell counts of the A549 cells to determine toxicity. Another study was CF-centric and used a CF bronchial epithelial cell line (CFBE41o-) to demonstrate strong antibiofilm activity of two *Pseudomonas* infecting phages without harming the human cells [148]. These data, in corroboration with results presented in this chapter, suggest that any increases in inflammatory cytokine production with phage treatment *in vitro* are likely a result of phage-mediated bacterial lysis rather than the innate inflammatory characteristics of the phages [274, 279, 280].

In the context of the respiratory system, mucosal protection is necessary to manage the influx of inhaled substances, including particulate matter and pathogens, coming into the lungs [315, 316]. However, excessive mucus production is especially concerning for individuals with CF, where hypersecretion of thick, sticky mucus becomes difficult to clear from the lungs and impedes the ability to effectively clear pathogens [33, 317, 318]. Culturing cells at ALI also enables the growth of goblet cells, and subsequently the production and secretion of mucus onto the cell surface. This enabled a comparison of mucus production across treatment groups, and while only CFTR wildtype cells were used, this study clearly demonstrated that neither phage induced significant changes in the production of mucus when compared to controls *in vitro*. Whilst effects of phage on mucus production and the underlying mechanisms involved have not been studied in depth, there is a growing body of knowledge surrounding the interactions between phages and mucoid surfaces [127, 319, 320]. Current data have revealed a synergistic relationship between phages and mucus whereby phages aid in the bacterial defence of mucosal surfaces [319]. The potential of phages to adapt to the mucosal environment has been made apparent within the literature, as previous data have characterised adaptations that specifically alter the Ig-like domain within the capsid protein Hoc [127] to provide a fitness advantage. These Ig-like domains are widespread amongst phage structural proteins and are thought to play a role in helping to maintain cell surface proximity

Page | 161

through weak non-specific interactions with carbohydrates on the cell surface until irreversible receptor binding and phage attachment can occur [321].

Following the *in vitro* safety study, *in vivo* assessments were then conducted to investigate the effects of phage towards an intact biological system. In addition to the biological samples and clinical scoring / behavioural characteristics; the study was designed to follow a clinically relevant dosing regimen based on a previous clinical study using *Staphylococcus* phages in humans [93]. Result generated showed no effect of either phage treatment on clinical score or overt signs of health/wellbeing when compared to controls. Mice also had consistent body weights throughout the phage exposure period, with no significant weight variations noted between the start and conclusion of the treatment period for either phage groups or controls. This indicates that repeated doses of phage were well tolerated throughout the dosing schedule utilised. In terms of food and water consumption, there were no significant differences between phage treated mice and controls indicating no effects of phage on appetite and further reinforcing our assessment that phages have no effect on mouse wellbeing. Necropsy examination post-euthanasia did not reveal any macroscopic abnormalities or internal organ irregularities of the heart, lungs, adrenals, liver, spleen, or kidneys. There was also no effect of phage treatment on the weights of the liver, spleen, or kidneys. For *Staphylococcus* phages there have been no previous *in vivo* safety assessments that have reported the aforementioned outcomes. However, a comparison may be drawn from a separate study investigating the effects of phage therapy for *Salmonella* Pullorum infections in chicks [322]. In this study, the *Salmonella* phage CKT1 alone (no infection scenario) did not induce any significant differences in overall bodyweight or the organ/bodyweight ratios for the liver or spleen when phages were orally administered in a volume of 0.5 mL (Suspended in SM buffer: 10^7 PFU/mL) when compared to controls [322].

Assessment of the physiological effects induced by phage exposure involved analysing haematology, blood gases and chemistry, pulmonary cellular inflammation, and mediators in bronchoalveolar lavage fluid. No effect of phage treatment was seen for the majority of the blood gas and chemistry parameters including Na, K, iCa, Hct, Hb, pH, PCO_2 , PO_2 , HCO_3 , sO_2 or TCO_2 . To the best of our knowledge, these parameters have not been

assessed in an *in vivo* phage exposure model previously, however they provide valuable information as to the general wellbeing of the experimental animals, and also insight into the proper functioning of the respiratory and cardiovascular systems. The fact that no effects of phage treatment were seen in these parameters provides more evidence of their safety in mice when treated over 14 days. A statistically significant decrease in blood glucose concentration was observed in Biyabeda mokiny 1-treated males compared to male controls, however, this difference (4.39 mmol/L) is unlikely to have physiological relevance due to the inherent variability in this metric [323] without the use of fasting techniques to improve concordance with averaged daily blood glucose measurements. Significant differences were also noted in the Base Excess and TCO₂ measurements between males and females. This has not been reported in the literature previously for mice, however differences in acid-base balance in humans have been reported in relation to inflammatory status within infection scenarios [324]. The differences seen between sexes are consistent with observations of BE and TCO₂ differences seen in healthy ostriches where significant differences can also be found in HCO₃ [325]. Regardless, these sex differences do not detract from the main finding of no effect of phage on the majority of haematology, blood gases and chemistry parameters.

There was no effect of phage treatment on the total number or types of cells including macrophages, neutrophils, and eosinophils (of which none were found) in the BALf of mice when compared to controls (Figure 5.8). This indicates that phages did not induce cellular inflammation at the site of exposure. Cellular inflammation (differential cell counts) data within animal studies are commonly reported in relation to a wide variety of inhaled insults including exhaust fumes and silica dust [298, 326] and respiratory infections from viruses such as SARS-CoV-2 (inactivated) [327] and Influenza A viral infection [328]. However, cell counts have not been performed in any mouse studies utilising *Staphylococcus* phages to date [105, 136, 137, 241, 282]. For the study of phages active against a highly relevant CF pathogen; this is an overlooked feature of phage safety, as macrophages recruited into the lungs drive pulmonary neutrophilic inflammation and irreversible airway damage [329]. Within the wider phage literature, there have been pulmonary focussed animal models conducted for phages active against *P. aeruginosa* [148, 277, 278, 281, 291, 330]. In one of these studies, differential cell counts were determined from BALf 48 hours post exposure to phage; their data indicated that phages

significantly reduced the number of neutrophils and macrophages in a *P. aeruginosa* acute infection model [281], however there were no 'phage only' controls in this study.

As previously mentioned, a primary concern in CF healthcare is pulmonary inflammation, as cycles of infection and ensuing inflammation cause damage and lung function decline [153, 331]. Some of the predominant cytokines involved in this process (particularly neutrophil recruitment and activation within the airways) are IL-8 (mouse equivalent KC), TNF α , and IL-1 α . Within this study, levels of IL-1 α in BALf were below the detection limit of the kit used and there were also no significant differences between the amount of KC and TNF α between phage groups and controls. For the majority (12/18) of the cytokine mediators assessed from BALf, there were very few statistically significant effects of phage treatment (Table 5.4), and where significant differences were seen, the biological significance is likely low, as described below. Pertaining to *Staphylococcus* phages, administration of intravenous phage to rats has been reported to induce production of IL-1 β but when delivered via nebulisation, at a concentration of 2×10^{10} PFU/mL in 2mL, IL-1 β production was significantly less [136]. Within this study, there were no significant differences in IL-1 β as the values were below the detection limit of the kit used indicating no production of IL-1 β within this study. This is a clear benefit towards the use of aerosolisation as a delivery method for phages, as previous data have demonstrated that *Staphylococcus* phages retain their activity *in vivo* and have uniform distribution within the lungs [136, 137]. Furthermore, *Staphylococcus* phages delivered in this manner have been shown to be equally effective in preventing fatal MRSA pneumonia when used alone versus in combination with daptomycin within a rat model of infection [137]. This has also been demonstrated within a porcine model of *P. aeruginosa* infection that demonstrated nebulised anti-pseudomonas phages were fast and effective at reducing bacterial burden when administered via nebulisation [251]. However, a limitation concerning many of these studies are that the models utilised have a high bacterial inoculum and are not representative of chronic infections that have been established but not repeated [146, 330].

In this study, Koomba kaat 1 phage exposure elicited a significant increase in IL-12(p40) in male mice. IL-12(p40) is a known chemoattractant for macrophages and bacterially

stimulated dendritic cells [332]. Amounts of IL-12(p40) measured in our study may be biologically relevant, with Koomba kaat 1 treated males having almost double (148.93 ± 58.33 pg/mL) the level of male controls (74.89 ± 24.12 pg/mL). In a previous study looking at the production of IL-12(p40) in the BALf of C57BL/6 mice, various silica insults elicited inflammatory responses of ~ 100 pg/mL [326]. However, within this study, there were no significant increases in the macrophage counts derived from the BALf of mice exposed to Koomba kaat 1. Therefore, the increase may have had different effects on different cell types, such as dendritic cells which were not counted, or the timepoint used may not have been able to capture the downstream effect of increased IL-12(p40) production. There was also a significant decrease in cytokine IL-17 production in our Koomba kaat 1 exposed mice however this decrease was less pronounced (< 1 pg/mL) and is lower than previous reports of IL-17 within the BALf of C57BL/6 wild-type mice treated with saline via intrathecal administration (5.4 ± 0.4 pg/mL). Therefore, this is unlikely to be a biologically relevant finding. Similar to this, Koomba kaat 1 significantly reduced levels of IFN- γ in the BALf when compared to controls, whilst this amount was also likely biologically insignificant (< 1 pg/mL), IFN- γ plays an important role in the modulation of allergic inflammatory states of the airway epithelium [333]. Quantification of IL-17 has been reported within allergy studies involving mice previously, but the induction of this cytokine was not reported to be increased in BALf [334].

In hindsight, a single timepoint measurement may have meant that mediators with shorter half-lives may have been missed with this study design. Previous studies have reported that immune mediators may be depleted where a prior adverse insult / exposure to the lungs has occurred, and thus may require prolonged recovery periods (> 24 hours) [335]. Our analysis of total protein content in BALf corroborates the current safety observations made within this chapter. Total protein abundance serves as an indicator of increased lung permeability and epithelial damage [335, 336]. This study reported no statistically significant changes in BALf protein levels between the phage treatment groups and controls.

Whilst the rodent models to date produce a foundation for understanding the safety and efficacy of *Staphylococcus* phages, many of these are siloed experiments with vastly

different treatment periods, doses, and endpoint measurements [136, 137, 241]. This is advantageous in its ability to capture a broad range of scenarios in which phage therapy may be used and reflects the current state of clinical phage usage on an 'ad hoc' basis through special access schemes and usage on compassionate grounds. Unfortunately, the limitations of this are that cross study comparisons are difficult to perform, and statements concerning the exact cause of differences between the immunogenic or cytotoxic profiles of individual phages between these studies are only conjectural. The majority of studies discussed here agree that phage therapy for *S. aureus* is safe and well tolerated when applied alone or within infection scenarios [105, 136, 137, 241, 282].

These are encouraging insights, and the continued exploration of phage safety may soon push phage therapy into standard clinical care. However, the design of future safety studies should be informed by the current base of literature surrounding phage safety. Based on the increasing number of phages being isolated for therapeutic use, it would soon become inefficient to perform *in vivo* safety studies for every newly isolated phage. There are a few potential solutions for this. Phages are broadly grouped in numerous ways and representatives could be chosen and studied to infer safety. However, a problem with this is that phages have a pervasively mosaic genome [272, 337], and our current methods of phylogenetic classification are based on monophyletic evolution whereas phages are likely to arise from polyphyly [338]. This means that phages belonging to similar phylogenetic clades may have vastly different attributes pertaining to a single protein which, if structural, may have greater implications on host-cell interactions than inference from its overall genome may suggest. A suggestion here would be to delineate characterisations of phage safety into two separate designs: intrinsic phage safety (or phage structural immunogenicity) and phage-bacterial safety (the study of whether products arising from phage-bacterial interactions are safe). By doing this, immunogenicity studies could group phages based on structural compositions and similarity, this way newly isolated phages with known structural attributes may infer safety from these sources [314]. Safety in the context of an active infection is typically performed through infection studies mentioned previously [241, 339]. However, these interactions are even more complex than phage alone, as each phage-bacterial interaction may have its own unique signature. To account for this, high throughput *in vitro* infection assays could be designed to cover a large number of unique interactions, and the ability

of this study to produce clinically relevant data could then be assessed using a subset of *in vivo* infection models to assess the translatability of *in vitro* findings.

This chapter's findings underscore the significance of employing different preclinical models that can recapitulate relevant features of the target environment. Using a differentiated airway culture model enabled the growth of multiple cell types and the production of mucus, an increasingly realised factor in the tripartite activity of phage, bacteria, and host [127, 319]. Novel insights towards the effect of phages on mucus production using this model have been generated for *Staphylococcus* infecting phages, and further safety validations for the pulmonary application of these phages can be seen using differentiated airway cultures. In addition to cell culture, the rodent safety model performed provides safety confirmations towards the inherent characteristics of *Staphylococcus* infecting phages when applied directly to the airways. Using this model, respiratory outcomes were prioritised based on the intended use case for Koomba kaat 1 and Biyabeda mokiny 1 against MRSA able to cause pulmonary infection.

Chapter 6: General discussion

Despite mainstream implementation in certain countries [340-342], the use of phages still remains restricted to compassionate use cases and a limited number of clinical trials [91-93, 166, 285]. Even though there have been improvements in their preparation [274], their unique attributes, such as genetic composition and production using bacteria, necessitate individualised safety examinations prior to use [157]. Studies of phages that target pulmonary infections are also very limited, and few have comprehensively evaluated the inflammatory effects of aerosolised phages [164]. This is especially true for *Staphylococcus* phages, where the primary delivery methods of many *in vivo* studies to date do not result in the application of phages directly into the lungs [125, 261, 343, 344]. The work reported in this project sought to provide insights into the feasibility of isolating and characterising phages able to infect *S. aureus* bacteria within the pulmonary context. Specifically, this thesis investigated the hypotheses that phages isolated from the environment may demonstrate an ability to infect and kill antibiotic resistant *S. aureus* bacteria from the airways including MRSA and that these will be non-toxic and non-inflammatory when applied to *in vitro* and *in vivo* models of the airways.

6.1. Thesis summary:

Chapter 3 established and modified several isolation protocols and identified challenges including isolating lytic phages active against *Staphylococcus aureus* from wastewater, a finding similarly identified by others [1]. The same work also attempted to isolate phage from breastmilk samples that had tested positive for the presence of *Staphylococcus* species via 16s sequencing. Despite the low hit rate in both sources, lytic phages active against a panel of respiratory *S. aureus* isolates were successfully obtained. Sequencing of bacterial host isolates enabled assessment of prophage contamination as well as transduction events, that then identified phage-host pairings, namely P7 (renamed: Koomba kaat 1) with *S. aureus* SA09 and BMP1 (renamed: Biyabeda mokiny 1) with *S. aureus* SA01 for follow-up studies. Chapter 4 explored the potential of these two phages for application in respiratory disease. Koomba kaat 1 and Biyabeda mokiny 1 exhibited different host range profiles, with Koomba kaat 1 possessing a much broader host range than Biyabeda mokiny 1. Interestingly, while Biyabeda mokiny 1 displayed a narrower

host range in *S. aureus*, it could also infect other *Staphylococcus* species such as *S. epidermidis* and *S. xylosus*. Since biofilm is a key bacterial defence characteristic in respiratory infection, activity of the two phages against five biofilm forming MRSA respiratory isolates derived from CF airways was also performed. Both phages were to disrupt and infect biofilms, although this capability differed between MRSA isolates. In addition, both phages were viably stable when aerosolised via a vibrating mesh nebuliser. The combined data from Chapter 3 and 4 strongly indicated both phages were candidates for translating into a respiratory treatment. Chapter 5 assessed pulmonary phage safety and demonstrated that neither Koomba kaat 1 nor Biyabeda mokiny 1 were intrinsically cytotoxic or inflammatory. This was the case when applied to primary derived human cells in a preclinical 3-dimensional model of the airway and as well when administered to the lungs of mice *in vivo*, where a host of physiological and respiratory inflammatory outcomes were not significantly affected. Collectively, this thesis is a comprehensive body of work that provides new knowledge and protocols for the field across the isolation, characterisation, and application of phage for *S. aureus*. Specifically, it illustrates the potential of two phages active against *S. aureus*, however, several key considerations relevant to the generation of a *Staphylococcus* phage library were raised and will now be discussed in the context of the wider phage literature.

6.1.1. Genomics: whole genome sequencing

Once a phage sample is isolated, characterising the genomes within follows a series of steps: DNA extraction and sequencing to produce raw reads, assembly to produce contigs (DNA segments), and analysis of these contigs (putative phage genomes) to assess genetic composition [157]. Each of these steps is complex, loosely controlled, and has the potential to introduce bias or error based on the processes used [157, 190]. At this point, it can be easier to delineate the characterisations into categories for better understanding including assessments of contamination (phage, host, or unknown DNA), transduction, population diversity (or genomic flexibility), and genome completeness (coverage, sequencing depth) [157, 190]. These traits apply to most, if not all, dsDNA phages irrespective of their origin or attributes [159]. These processes were performed and discussed in detail within Chapter 3 and paralleled work by Strancar et al (2023) [195] who demonstrated the importance of selecting appropriate hosts for *Staphylococcus* phages at an early stage of phage research. It is worth noting that without the host bacterial

Page | 169

genome, it is possible to determine the amount of DNA that does not map to the phage genome but impossible to determine how much of the DNA that isn't sequenced from the phage genome belongs to the host bacterial genome. This makes it impossible to search for signs of generalised transduction from the bacterial genome without using a reference genome from public data sources [161]. Overall, the potential effect of the host on the final phage preparation and its genomic constituents (such as potential transducing genes) or physical attributes (potential prophage contaminants) is such that phages characterised for therapeutic potential should be reported alongside the host bacterial genome.

Although the ability to discern minute differences between phages using traditional methods is a challenging process it has now become highly feasible using WGS data [1, 161]. Production of open source phage genomics tools (packages/pipelines), able to process WGS data (assembly of reads) and nucleotide sequencing data (analysis of contigs), has democratised complex analytical tasks that previously required extensive amounts of expertise. For these reasons this should be standard practice in phage characterisation when therapeutic application remains the end goal. Specifically, in the pursuit of therapeutic phages, genome analysis tools (such as VIRIDIC and vConTACT2 [216, 345]) have played a pivotal role in facilitating more sensitive analyses, enabling the nuanced assessment of phage identity. The use of such tools was beneficial in this thesis, where numerous phage samples were identified as multiple instances of the same phage. In addition to producing detailed characterisations, the precision afforded by WGS data prevented potential mischaracterisations at this stage and averted time consuming and costly redundant downstream purification and analysis.

6.1.2. Phage purification and storage for therapeutic testing

From a macromolecular perspective, phage are protein packages of genetic material released upon bacterial cell lysis and because of this, extensive purifications are required before they can be considered safe for use within humans [274]. The most basic and often first performed form of purification is filtration that removes any bacterial cells from the crude lysate. This leaves a number of products, such as cellular debris, that require

purification from the sample prior to use within models of phage safety [274]. Sample purity is a major concern due to the presence of endotoxin, the Lipid A component of lipopolysaccharides within Gram-negative cell membranes, found within phage samples [274]. The presence of LPS is known to induce inflammatory effects that, if severe enough, may result in death [346]. Currently, purification methods for phages are not standardised, and there is no 'gold standard' that has been established for the purification of phages for therapeutic applications (Methods reviewed: [274]). Irrespective of this, the International Council for Harmonisation (ICH) provides the technical requirements for pharmaceutical products, namely <5 endotoxin units per kilogram of bodyweight per hour for intravenous administration [274]; however, there are no specified values for direct application of phages into the lungs. Phages intended for therapeutic use against resistant bacterial pathogens are usually purified to these guidelines using a variety of methods, commonly involving filtration and resuspension using diluents such as saline, followed by additional purifications or dilutions if required [91, 165, 347, 348].

Whilst endotoxin is a prime concern for Gram-negative bacteria, Gram-positive bacteria may still release potentially harmful byproducts, such as bacterial toxins, into the phage lysate [274, 349]. Concerns pertaining to *Staphylococcus* specifically include the production of enterotoxins, alpha haemolysin, and lipoteichoic acids that constitute a large portion of Gram-positive cell walls [289]. Few studies report enterotoxin content within phage samples [350], however staphylococcal enterotoxin A is known to induce inflammatory cytokine responses and toxic shock within *in vivo* models via the Myeloid differentiation primary-response protein 88 mediator [351]. Another concern is the presence of enterotoxin B, which is a potent superantigen that is potentially lethal at low doses (LD₅₀: 20µg/kg, ED₅₀: 400 ng/kg) [352]. Specifically for *Staphylococcus* species, there is no standard panel of toxins that are tested for, and whilst some are assayed [104, 105, 350], these tend not to be reported [141, 283, 343]. Whilst there is no strict limit set for the presence of enterotoxins within medicinal products, reducing enterotoxin levels as much as possible would be ideal practice and here the use of anion exchange chromatography to reduce the amount of enterotoxins within phage samples is suited [274]. It is also rare that the DNA-free status of phage preparations are reported despite the importance of transformation events occurring that may spread resistance [166]. Nevertheless, data from numerous studies involving purified phages suggest that most modern purification methods used to date, standardised or not, are able to produce reliably

Page | 171

toxin free samples for experimentation [91, 165, 347, 348]. Overall, the need for a benchmark toxin panel regulated by international bodies is essential to drive the standardised production of phage preparations. This requirement ensures that quality standards are met, regardless of the purification methods used for phage preparation.

6.1.3. Therapeutic phages: safety

The next consideration for clinical translation of phage is their safety. Today, phage research is on the cusp of clinical implementation on a broader scale, with multiple case studies and several clinical trials [91-93, 166] demonstrating their safety in humans. Whilst these cases provide a strong foundation for phage research, standard clinical care requires strict rules and regulation [100]. Currently, there are multiple attributes pertaining to both the phage samples (purification standards [274]) and the accompanying phage data (contamination status, lifecycle, taxonomy [157, 353]) that have no overarching regulation. This is due to reasons that have led to the widespread belief within academic literature that more robust data are required to translate phages into clinic [94, 100, 101, 354-360]. While in some cases this is true, there are also missing, or unreported attributes including host propagating bacterial genome, prophage contamination analysis, and microdiversity within the sample, which if left unreported, limit the use of downstream safety and efficacy data [164, 195, 361]. Based on current literature, *Staphylococcus* phages with a myovirus (which Koomba kaat 1 and Biyabeda mokiny 1 belong) [99, 207, 362] and a podovirus morphotype have been reported to be safe [141, 363]. Siphoviruses of *Staphylococcus* are typically lysogenic [205, 210], and are understudied within the context of therapeutic safety. In addition to this, many *Staphylococcus* Siphoviruses are known to carry toxins [210, 364]. Several phages were identified and excluded from further analysis in Chapter 3 due to the presence of Panton-Valentine Leukocidin within annotation data (Section 3.3.8).

Beyond toxins which can be identified with genomics, the morphology of the phage virion may also impact host physiological response. Variance in safety outcomes has been associated with the structural morphology for *Escherichia* phages [314], but direct comparisons of this type have not been performed for *Staphylococcus* phages. An analysis of this kind may be useful to infer the intrinsic safety for *Staphylococcus* phages;

however, morphotype may not be the most sensitive or appropriate method of clustering phages. Leveraging the sensitivity of WGS data, clustering phages using the structural proteins on the phage surface may enable a more precise grouping based on aspects relevant to the interactions that confer phage safety. In addition to sequencing-based techniques, the use of *ab initio* protein folding of unknown structures may provide greater resolution in assessing the structural similarities and differences between surface features [365]. This may be more suited to *Staphylococcus* phages, where much of the genetic diversity lies within a single Genus (*Kayvirus*), which have been shown to have considerable variation in their size despite all belonging to the myovirus morphotype. The remaining characteristics that are unique to each phage, regardless of their structural components, comprise the products (proteins, tRNAs) that may be transcribed from the phage genome upon bacterial infection. These include products that are required for host takeover and replication, and their transcription may change depending on unique bacterial-phage interactions. This is especially pertinent for *Staphylococcus* phages, as it was the genomic diversity between Koomba kaat 1 and Biyabeda mokiny 1, that resulted in functional differences such as their lytic activity [219], despite having similar structural components, RBPs, and safety profiles when applied alone. By performing studies that investigate the link between structural surface features and safety data, the intrinsic safety of phages may be more accurately inferred from phage literature.

6.1.4. Data: storage and manipulation

Moving towards consistent WGS based assessments in phage discovery and characterisation is not without logistical challenges. With the intrinsic flexibility phage characteristics have, and the number of tools required to characterise them, a large amount of complex data is required to maintain data accuracy. As mentioned previously, understanding of what exactly a phage sample entails and how resulting data should be structured is still being developed [191, 366, 367]. As a result, multiple tools have been developed in efforts to structure the increasing amount of data. One example is ‘Phamerator’ which has been used to create and manage custom databases tailored to bacterial hosts by students and staff within the Science Education Alliance—Phage Hunters Advancing Genomics and Evolutionary Science (SEA-PHAGES) program [367]. This is an on-going process, and numerous packages / application programming interfaces (API) have been designed to aid researchers in interacting with large genomics datasets

[192]. This is the only example of an API specifically built to interact with a phage specific SQL database is *pdm_utils*, which provides the user with a set of tools to quickly import and analyse (completeness verification, annotation, comparison) phage genomes within a compatible database [366]. Another tool developed for phage researchers is the INPHARED database, specifically curated for erroneous genomes and tailored to make public phage data accessible [191]. In addition to providing a curated dataset online, users may use the program itself to provide local downloads of publicly accessible genomes [191]. In summary, the use of these tools enables complex data to be imported, stored, and analysed in an efficient manner. This provides a large benefit to phage researchers by enabling the ability to distribute and update large bodies of information within the community.

6.2. Phages for *Staphylococcus* species:

Ideally, a diverse phage library should provide potentially many therapeutic options, yet some phage types are rarer than others including podoviruses (small, tailed phages, <30kb genome size) and jumbo phages (myoviruses, >200kb genome size) [368, 369]. As mentioned, isolation of phages active against *S. aureus* is rather challenging and further research is critical to expand upon the limited repositories currently available (excluding metagenomic study data), which is currently around 574 *Staphylococcus* phages within the Inphared database (1st May 2023 access) [191]. Despite the low abundance within some geographic regions [1], phages active against *S. aureus* have been discovered within a variety of sources including wastewater from farms, soil/goat faeces, sewage effluents, human milk, and raw fish rinse [141, 172, 174, 213, 370-372]. Farmyard sources such as slurry (farmyard ‘run off’ fluid) or cow milk from cows with mastitis infections, of which the cause is likely to be *S. aureus*, might be more reliable alternatives as several *Staphylococcus* phages have already been isolated from these sources [99, 172]. Investigation of *S. aureus* phage prevalence in wastewater within this thesis found that most were likely to have a lysogenic lifecycle, containing CDS associated with lysogeny such as integrase. Attempts to increase the isolation rate of lytic bacteriophages appropriate for phage therapy extended the search to a second source, clinical breastmilk samples, from which a single *Kayvirus* (Biyabeda mokiny 1) was obtained.

What is evident from this thesis and published works is that the idea of *ad hoc* isolation of phages from the environment to treat a *S. aureus* bacterium for which there are no effective phages already, is difficult and lengthy. Thus, it is critical for phage clinics to curate a well characterised phage library with a wide range of activity to ensure optimal coverage of *S. aureus* bacteria to avoid the need for ‘*ad hoc*’ isolation. Fortunately, lytic phages active against *S. aureus* are typically polyvalent myoviruses capable of infecting a wide range of isolates [112, 212, 240] and thus the diversity required within a library may be smaller [212, 217, 240]. Regardless, if phages appropriate for therapy are even a fraction of the estimated number of phage virions within the biosphere (1×10^{31} [360]) then the high throughput characterisation of new phages should remain a priority. Collectively, while isolation of new phages may provide a source in an *ad hoc* manner, technological advances within the field have opened new solutions of phage training and genetic modification of phage.

6.2.1. Phage training

Phage training is a process whereby continuous subculturing techniques are used to ‘train’ phages against a particular pathogen to increase lytic efficiency [373]. This method generally involves subculturing phages with bacteria and reisolating the phage progeny that may have adapted to the target host. This has already been used to generate phages with modified lytic efficiency against MRSA strains [374] and produce effective phages for biofilm removal [222, 223]. In addition, recent data suggest that pre-training a phage against a target bacterium prior to exposure may improve the phage's ability to counter resistance development in the bacteria [373]. A primary limitation of this approach lies in the fact that phage training seems only able to improve lytic activity that already exists [373]. In addition, it remains a non-targeted approach whereby lytic efficiency of phage may be improved without a clear comprehension of how this occurs. To streamline phage training and reduce the associated laboratory expense, it may be prudent to determine the parameters that influence phage activity completely to identify phages with greater training potential prior to the training itself [242]. One of these may be the phage epigenomic landscape, the diversity of which originates from a combination of host and phage encoded methyltransferases. These modifications are primarily generated by enzymatic alterations of the deoxynucleotide monophosphates that contribute to

deoxynucleotide triphosphate (dNTP) pools utilised during the lytic phase to produce phage DNA [375]. These genetic adaptations serve various purposes, with a prominent one being the evasion of host defence mechanisms. In order to improve the reliability of data generated *in vitro*, these epigenetic modifications need to be captured within phage characterisations; in absence of this, host bacteria that phages are propagated in prior to phage lytic assays should be reported [219, 376]. Currently, these nucleotide modification patterns are mostly uncaptured within public repositories, partly due to the popularity of the Illumina short read sequencing platform [377]. Characterising these methylation patterns may be pivotal in correctly interpreting phage-bacterial interactions and the reasons for host range variability amongst genetically similar phages [219, 236].

6.2.2. Genetically modified phages

In several reports, it has been shown that *S. aureus* strains frequently carry multiple prophages that, unlike obligately lytic phages, are able to integrate into the host bacterial genome [210, 211, 378]. Yet these prophages themselves have been shown to carry virulence factors [210] and interfere with the actions of lytic phages via superinfection immunity and phage piracy [379]. The capability of phages to induce the endogenous production and release of prophages from their target bacterium may also result in the transduction of host DNA between bacteria via the packaging of prophage induced chromosomal islands, a known form of genetic transfer between *S. aureus* isolates [185, 379]. In addition to chromosomally encoded prophages, which are detectable via WGS methodologies [380], there are also episomal prophages that contribute to the genomic landscape of *S. aureus* bacteria [381]. In review of the isolate phage data within this thesis, it was found that 48% of phages active against *Staphylococcus* ($n=278/574$) within the Inphared database (1st May 2023 access [191]) contained integrase genes. These phages were predominantly Siphoviruses and represented 10 different genera of phages currently deemed inappropriate for phage therapy.

The ability to tap into these phages for use may lie in the careful application of phage genome engineering, where prior work has shown that targeted removal of integrases may

be used to engineer lytic phages for therapeutic usage [382]. In addition, phage engineering efforts have enabled researchers to adapt the host range of phages by modifying the receptor binding proteins (RBPs) of lytic phages [383, 384]. The ability to conduct these manipulations is not without challenges, yet fortunately, due to stable prophage integration, the engineering of prophage genomes is possible using well-established bacterial genome engineering techniques [360, 383]. The engineering of lytic phage genomes typically larger than 20kb in size requires the use of techniques such as homologous recombination with an engineered plasmid containing the alternative RBP [383, 385]. This process is costly and subject to low recombination frequencies, and, for *Staphylococcus* and other Gram positive infecting phages, the large size of lytic phage genomes and thick cell walls prevent the uptake of synthetic phage DNA fragments [383]. In response, numerous ‘boot up’ methods have been described to circumvent the issue; specifically, for *S. aureus* phages a non-electroporation *Staphylococcus* transformation method termed “NEST” has been developed successfully [385, 386]. This system avoids a common bottleneck in difficult to transform bacteria such as *S. aureus* and *E. faecalis* by utilising enzymatic treatments with lysozyme and ampicillin to transform phage DNA into *S. aureus* [386]. The NEST system has demonstrated that purified gDNA from a large phage genome (Myophage K, 148 kb) can be transformed into ‘NEST competent’ *S. aureus* cells to produce phage virions (plaques) over the course of 4 days [386]. Practically, the production of diverse cocktails against a clonal complex pathogen for which there are a number of natural, polyvalent (multiple RBPs) phages readily available may be necessary for empiric phage usage [124, 383]. Engineering phages with custom genomic traits is a potential avenue to generate new phages that surpass the existing natural phage diversity that results from natural selection pressures within the environment.

6.3. How can bottlenecks in phage characterisation be addressed?

Regardless of how the diversity of phages fit for therapy is acquired, whether by isolation, training or genetic modification, the phage genomic landscape is growing larger with no signs of slowing down. In response to the rapid increases in sequencing data being generated, numerous high throughput methods have been developed to rapidly process phage genomes [189, 193, 387] in a reproducible manner. These methods are predominantly automated pipelines that enable batch processing of large data sets in a

single continuous run without the need for manual supervision. Automated pipelines for the assembly, screening, and annotation were performed within Chapter 3 of this thesis and are a simple means of stitching together complex, previously time-consuming workflows [161]. However, the question remains of whether more data may be inferred from *in silico* analyses alone.

6.3.1. High throughput study design

As the abundance of phage genomes and the analysis tools required to analyse these datasets increases; new challenges have been presented [159, 160]. Whilst open-access repositories like the National Center for Biotechnology Information (NCBI) and the European Nucleotide Archive (ENA) have played a crucial role in centralising and disseminating large sequencing datasets, the vast number of different open-source software options available to perform various tasks such as assembling and analysing phage sequences poses several challenges. Different tools are being developed frequently and often produce varying results in various formats [377]. Thus, the selection of the most suitable tool for a specific research question can be difficult and requires researchers to become familiar with numerous options at their disposal [377]. As such, reporting of phage genomes within the literature remains obscure due to the large number of highly specific and often complex methods being performed with no ‘official’ guidance [157, 191]. To address the issues surrounding variability within these analyses, a consensus-based approach has been adopted by some research groups [157] which involves comparing the outcomes of multiple tools or methods and deriving conclusions based on a collective agreement between them. This has resulted in published assembly and annotation guides [159-161]. Collectively, bioinformatic pipelines are being used to assemble and analyse genomes at rate incommensurate with the ability to generate empirical data to accompany the phage genomics. *In silico* machine learning (ML) algorithms are ideal to help bridge the gap between the large amounts of genomics data and the smaller sets of empiric data, with the aim of allowing inferences to be drawn from data based on the analysis of patterns within known, partially known, or unknown data [388].

6.3.2. Predictive capacity: Machine learning

Open-access repositories have facilitated the centralisation and dissemination of sequencing data. In contrast to sequencing data, empirically generated lab characterisations present a distinct set of hurdles and are inherently resource intensive to perform as lab characterisations involve substantial infrastructure costs, delivery times, and the use of costly consumables, all dependent on the provision of specialist expertise in a range of fields [389, 390]. Despite these challenges, various strategies can be employed that navigate the difficulties in characterising large repositories of unknown / novel phages in a cost-effective manner using a subset of phages with known attributes. Here, ML methods can be well suited to extrapolating known genome-attribute relationships to the analysis of uncharacterised phage genomes. Already, numerous ML methods utilising different approaches have been specifically developed for use in phage research [216, 230, 391]. Supervised methods such as Bacphlip [391] utilise training data sets to make lifecycle predictions based on empirically generated data, whereas tools like VirFiner [392] have been used to identify viral sequences within metagenomic data sets. This thesis utilised vConTACT 2.0 [216], a ML based tool that utilises clustering algorithms to determine phage phylogenetic relationships in a manner independent of known classifications. Similar techniques were utilised to identify the RBPs of Koomba kaat 1 and Biyabeda mokiny 1 phages using a model pre-trained on a database of 887 RBP sequences [230]. Furthermore, a combination of ML approaches and annotation methods were used to determine the RBP of Koomba kaat 1 and Biyabeda mokiny 1 (Section 4.3.9). A previously described ML method was used to predict the RBPs amongst the many CDS annotated for both phages, then each prediction was compared to functional homologues identified within closely related phages with known RBPs to corroborate data generated [230]. This enabled the informed use of a ML pipeline to guide the manual curation of data and streamline phage characterisation.

Processes using ML have emerged quickly within phage research amongst the increase in genomics data. These methods are well placed to effectively bridge the gap between genomics data and empirical characterisations seen within the phage literature. By leveraging the known genome-attribute relationships, ML methods, like vConTACT and Bacphlip, enable the cost-effective analysis of uncharacterised phage genomes [216, 391]. This not only streamlines the resource-intensive process of lab characterisations but also

enhances our capacity to draw meaningful connections between the genomic information and empirical findings seen within the wider phage literature. Some of the key questions ML methods are currently being developed to answer are related to phage activity and answering the question of whether phage activity may be predicted *in silico*. This has been reported previously for *Klebsiella* phages, however, the widespread availability of such tools is not yet available [196, 393]. If tools such as these are going to become a reality, robust preclinical data is essential to comprehensively map the genomic attributes of phage samples to the data generated downstream that assess their safety and activity.

6.4. Preclinical models of phage activity

A recent review of preclinical measurements for phage characterisation [158] describes their virulence as a complex, variable, and dynamic phenomenon relying on both phage and host factors. Modelling the interactions between phage, bacteria, and eukaryotic host is complicated and reported to be a reason for the lack of correlations between *in vitro* and *in vivo* data [394]. However, the process of ‘stacking’ complexity within models paradoxically hinders the ability to accurately answer specific questions. In recognition of this inability of many models to capture the full spectrum of physiological responses generated within an infection scenario, a multi-model strategy is often applied [283, 395, 396]. In this thesis, a series of experiments was performed to generate a safety consensus for the two phages that passed the bioinformatics checkpoints. Specifically, in Chapter 5, purified phages were found to exhibit similar safety profiles in both *in vitro* and *in vivo* models. These models were able to assess the safety of the phage structural components in the absence of any products that may be transcribed by the phage or bacteria as part of the phage infection process.

Modelling the activity of each phage on an individual basis may be both time consuming and laborious, depending on the number of bacteriophages being characterised for therapy. The *in vitro* pAEC model enables a higher throughput method of assessing phage safety than *in vivo* models with the limitation of being unable to recapitulate a complete biological system with adaptive immune responses over time. An alternative study design may leverage this capacity, in a similar manner to host range assays, in a ‘one against many’ structure whereby a single phage is assayed against an array of bacteria that

represent the diversity that may be seen within clinic. Within such a study, phage infections within liquid culture may be used to produce the products that are released through phage-bacterial interactions into the resulting media. This can then be filtered and assessed for toxicity and inflammation on pAECs. This design approach could be used to eliminate potentially unsafe phage-bacterial interactions using high throughput screening. Furthermore, the use of commercially available reporter cells that fluoresce if particular inflammatory pathways are activated might be particularly suited if assessing safety in primary cell models [397, 398]. For example, the activation of particular inflammatory cytokines (IL-8, NF- κ B, KC) are a particular concern for individuals with CF, thus the use of these cell lines may also be used to screen safety for phages.

Within the context of CF, patients are often co-colonised with multiple pathogenic bacteria and, amongst those with a single *S. aureus* culture, the idea that a single founding colonising strain predominates has also been challenged [54, 63]. Thus, the current modelling strategies of phage activity against single *S. aureus* clinical isolates, whilst useful to verify the utility of a bacteriophage against MSSA or MRSA strains independently, may not reflect the resistance of bacterial communities that high resolution techniques have recently been able to capture [219, 236]. Whilst the immediate suggestion might be to generate polymicrobial infection models, stacking complexity may lead to increased uncertainty in accurately investigating causation. Prior to this, an investigation should be launched into whether polymicrobial activity does in fact impact phage activity. It is difficult to come to a general consensus from the wider literature as the only clinical cases reporting phage activity against polymicrobial bacteria report different findings [399, 400]. In one of these studies, the polymicrobial nature of a *S. aureus* diabetic foot ulcers did not seem to impact phage therapy, resolving in 4 of 5 patients who had polymicrobial infections [399]. In the other, adjunctive phage therapy for a polymicrobial infection of a pelvic bone allograft led to clinical improvement in the short term but did not prevent recurrence [400]. Whilst many reasons may be attributed to this, the authors suggest that incomplete coverage of the polymicrobial infection by phage therapy may have led to midterm failure [400].

6.4.1. Biofilms and Intracellular switches

Respiratory bacterial infections are often associated with biofilm formation and modelling this biofilm production accurately *in vitro* can be difficult [89, 101]. Biofilms are complex structures that enable populations of bacteria, or multiple species of bacteria, to resist antibiotics at concentrations that would otherwise eradicate their planktonic counterparts [401]. Some *Staphylococcus* phages have already shown promising results in removing biofilms [402, 403], however they have been associated with enhanced resistance to phage infection and some may contain phage inactivating enzymes [89, 401]. As this effect seems to be dependent on interactions between phage resistant aspects of the biofilm and biofilm dispersal mechanisms of the phage, it is important to incorporate appropriate penetration assays into the characterisation of newly isolated phage [94, 401]. Within this thesis, the capability of phage candidates to target and disrupt biofilms produced by MRSA isolates from CF airways were assessed in Chapter 4 using a crystal violet assay. Results generated showed that Koomba kaat 1 and Biyabeda mokiny 1 had differential and specific antibiofilm activities. However, whilst the crystal violet assay enables quantification of biofilm in a fast and high throughput manner, it doesn't capture biofilm composition and is a general measurement of abundance. Alternatives have made use of confocal or scanning electron microscopy techniques to characterise biofilms and the effects of biofilm disrupting particles [404, 405]. The importance of understanding the effects of phage on biofilm are especially pertinent for phage interactions with *S. aureus*, as the production of biofilm is a key virulence factor that protects against host immune factors and antibiotic treatments [406, 407]. Furthermore, the effects of biofilm production within the pulmonary context have been well established in CF and represent a barrier to effective clinical treatment [304, 408].

In addition to biofilms, *S. aureus* demonstrates its versatility through its capacity to become an intracellular pathogen and evade the effects of antimicrobial treatments [155]. Whilst the prevalence of this phenotype is presently unknown, the recurrence of MRSA infections are common despite prolonged antibiotic treatments [409]; one explanation for this is the existence of an intracellular reservoir of MRSA causing the infection. This capability enables *S. aureus* to temporarily enter a "persister" state associated with increased multi-drug resistance [155]. Several publications report the ability of phages to target *S. aureus* bacteria within an intracellular context *in vitro*, using mouse derived

macrophages and human derived osteoblasts to demonstrate phage activity [343, 410]. Within the mouse derived macrophage study, phage M^{Sa} was shown to efficiently kill intracellular bacteria within 24 and 42 hours [343]. Conversely, it was shown that phages may be internalised by human osteoblasts but were not active against *S. aureus* after 24 hours of treatment to high concentrations ($1 \times 10^{7-9}$ PFU/mL) of three phages (PP1493, PP1815, and PP1957) [410]. Until more studies investigating this activity are performed, it is difficult to generate a clear consensus of whether phages may be reliably used to target intracellular *S. aureus* alone. Interestingly, phage K has been investigated for its ability to target intracellular *S. aureus* within an invasive cancer cell model as an adjunct to different chemotherapies [411]. Within this report, the anticancer drug, doxorubicin, displayed synergism with phage K to prevent migration of *S. aureus* to the intracellular niche [411]. Since doxorubicin is toxic and may not be applicable beyond the cancer setting [412], identification and investigation of similar/parallel adjuvants that prevent the migration of *S. aureus* in combination with phages seems warranted.

6.4.2. How can challenges in modelling phage interactions be overcome?

To effectively model the interactions between phages, their bacterial hosts, and the immune system, the foundational aspects of phage activity must be defined clearly to remove as much subjective bias as possible. This entails establishing clear and comprehensive definitions of lytic activity. For example, one of the most widely utilised metrics to describe phage activity is the range of hosts it can infect [158, 168, 173, 219, 223, 224]. Whilst this may have been adequate for the characterisation of static products such as antibiotics or other chemical antimicrobial compounds, these measurements alone give the impression that phage activity is fixed [413]. Irrespective of this mutable characteristic there is still no clear standard, for any bacterial species, of the minimum number of strains required within a host range analysis to determine whether a phage's activity is “broad” [413]. Due to the highly specific nature of phage interactions, comprehensive bacterial characterisations are required for both the host propagation strain and the bacterial panel from which host range data are derived from to avoid biases in evaluating phage host ranges.

Once the parameters effecting the activity of phage are well established, the use of mathematical models in conjunction with preclinical models may help to generate empirically informed treatment doses in a phage specific manner. Mathematical models have been used previously with success in modelling the interactions between antibiotics, a target bacterium, and the eukaryotic host [414, 415]. For phages, considerations involved in defining model parameters are more difficult due to the phage's ability to replicate and change *in situ* and, to date, no large-scale models utilising genetic pathways and stoichiometric analyses (flux-based analyses) have been produced [394]. However, a number of groups have already defined mathematical parameters for self-replicating particles and kinetic models have been used to derive insights from empirical studies [238, 416] and *in vivo* models of pneumonia caused by *Pseudomonas aeruginosa* [417]. In practice, these studies help to provide credence towards strict definitions; for example the importance of using the terms active and passive therapy to distinguish the difference between phage therapy that requires the ongoing replication of phage at the site of infection (active) and phage therapy whose initial dose and (primary) infection is enough to reduce the bacterial population alone [238]. Collectively, these results demonstrate the increasing need to incorporate various mathematical modelling approaches to clarify the interactions between phages, bacteria, and host immune system.

In summary, the effective modelling of phages, bacterial hosts, and the immune system demands a clear definition of foundational aspects of phage activity to mitigate subjective bias. Whilst some challenges are likely to persist, such as the need for standardised criteria in determining the breadth of a phage's range of activity and the complexities in developing mathematical models for dynamic phage behaviour, these represent ongoing processes that may be improved as clinical data are generated. The current body of literature generated strongly suggests that phage therapy is poised for transition into clinical care.

6.5. Translation of phages into clinical care

Clinical trials are necessary to demonstrate that safety and efficacy data generated in a preclinical laboratory environment are translated reliably into clinical practice. However, the disparity between the amount of preclinical data and actively recruiting clinical trials

for phage therapy is vast. This may be explained, in part, by the difficulties of producing or obtaining phage preparations made according to GMP standards as labs must be outfitted correctly and have the necessary accreditations [280]. There has been no market authorisation or approval for phage products to treat human infections at the time of writing this thesis [105]. Recently however, there has been significant progress in the regulated implementation of personalised phage therapeutics [280, 341]. The magistral framework set in place by relevant health authorities has enabled the use of personalised phage preparations prepared by a pharmacist and responsible clinician [280]. Yet as reviewed elsewhere [280], this approach is tailored to treat individuals who have exhausted all other treatment options and has not yet extended into clinical trials [280]. Despite the progress in phage therapy research, there still remains a bias in published literature, with a discrepancy between the number of clinical trials that have taken place versus the number of clinical trials completed and subsequently published [94]. Greater data transparency is required to maximise the utility of time consuming and costly clinical trials regardless of their outcome [100].

Several clinical trials have reported on the safety and tolerability of phage preparations when administered intravenously or topically for otitis media, or wound site infections [93, 108, 109] and others have identified minor adverse events, aligning with observations *in vivo* [93, 101, 151]. Within the respiratory context, nebulised phages are being investigated in clinical trials for the treatment of *P. aeruginosa* infections (Trial registration numbers: NCT04684641, NCT04596319), however the results of these studies have not yet been published. For *S. aureus* infections specifically, the only clinical trial investigating the application of phages into the respiratory system has been on the phage cocktail AB-SA01 delivered via intranasal irrigation (Trial Registration <http://anzctr.org.au> identifier: ACTRN12616000002482) [418]. Regardless of delivery route, general safety parameters have been established by such trials, however the order of treatment, and the use of cocktails still require further preclinical data to support rational clinical trial design.

6.6. Phage resistance

Resistance to phages is undesirable yet unavoidable, and multiple phage resistance mechanisms have been described in *Staphylococci* [219, 236]. As with antibiotics, the emergence of bacterial resistance to phage is observable using standard culturing procedures in the lab [259, 419]. This has led to publications that discuss this area of concern [242, 257, 354, 420], one of which reviews resistance development across numerous animal models of infection and treatment with PT [421]. In recent years, novel resistance mechanisms have been described such as the bacteriophage exclusion (BREX) and defence island system associated with restriction-modification (DISARM) systems [219, 259]. These systems are known determinants of bacterial resistance that recognise methylation patterns to restrict or block phage DNA replication but does not cleave the target DNA like restriction-modification systems do [422, 423]. However, the emergence of resistance *in vitro* is not always reflected *in vivo*. This is thought to be because the more common mutations conferring resistance to the phage (the attachment interference resistance mechanism) are for the cell surface molecules that are also required for infectivity within the host [102, 236]. As mentioned previously, phage training is an option that may be useful in overcoming bacterial resistance by producing phage derivatives [222, 424]. Derivates of known phages active against *S. aureus* have been used to prevent biofilm formation of *S. aureus* and reduce the density of previously established biofilms *in vitro* [222].

Fortunately, findings from previous studies indicate that phage resistance has no attenuative effect on bacterial virulence, generally thought to be due to fitness costs imposed on bacteria with mutations or adaptive defence mechanisms such as CRISPR [259, 421]. Due to the personalised nature of phage preparations used in clinical trials thus far, their justification has taken this concern into account by quantifying the rate of resistance development; this was done to inform the clinical trial for AB-SA01 phage product [93, 105]. These findings do not necessarily mean that phage therapies will not face issues with resistance in the future; as short-term and long-term resistance to phages may use disparate mechanisms and bacterial isolates may enter a coevolution cycle in which both populations may expand in parallel [421]. To address this concern, proactive monitoring and characterisation of pathogenic bacteria and the antiviral mechanisms they

harbour is required to sustain the accuracy of identifying effective phage within a continuously evolving phage bank.

Some bacterial species will require more stringent characterisation than others, as the abundance of phage resistance mechanisms, and the amount of interference from prophage, is highly variable between isolates [219]. Prophages are phages that may not obligately follow the virulent cycle of replication and may integrate into their bacterial hosts genome [424]. It is generally recommended that production strains that are free from prophage be used to amplify phage products for therapeutic application, however these can be difficult to obtain [424]. In addition, basic characterisations such as host-range assays can become increasingly difficult to assess considering the hierarchical nature of resistance mechanisms found in some bacterial species [219]. To fully understand these complex reactions, more clinically relevant bacterial and phage isolates must be characterised regardless of their lifecycle and therapeutic potential. Further, the associations between prophages, resistance, and their propensity to contaminate therapeutic products have led researchers to realise the importance of readily available production strains for certain bacterial species and the characterisation of prophage within them [424].

In the context of phages active against *S. aureus* bacteria specifically, a series of investigations by Moller and colleagues [102, 219, 236] have generated valuable insights. Phage resistance in *S. aureus* is hierarchical, and the genes associated with resistance via phage adsorption (n = 87/331), biosynthesis interference (n = 235/331), and assembly stages (n = 8/331) of the infection cycle were analysed [219] across a total of 43,000 *S. aureus* bacterial genomes [236]. In addition, they elucidated the connections between phage resistance and genetic mobility across these isolates. By splitting the resistance genes (n = 331) into 'core' and 'non-core' within the *S. aureus* pangenome, the distribution of genes influencing phage resistance and their method of acquisition were studied and the authors reported that genes associated with adsorption resistance were the most conserved (51/63 core genes present in 34400/43000 genomes) [236]. They also noted that models of phage resistance thus far did not predict the experimentally determined phage resistance or horizontal gene transfer; possibly due to the inability to

recapitulate an environmental factor or pressures leading to phage resistance [102]. Research elucidating these factors may be pivotal in the final steps towards the provision of a precision *S. aureus* phage pipeline in future. Overall, whilst the emergence of bacterial resistance to phages, akin to antibiotics, is a concern, ongoing research is actively uncovering novel resistance mechanisms and refining phage therapy strategies to overcome these potential scenarios. Despite the concerns of resistance, these appear low and clinical implementation of phage therapy is warranted in order to capitalise on their therapeutic benefits.

6.7. Study progressions and limitations

Whilst this thesis has made substantial progress in characterising two distinct phages from wastewater and breastmilk samples, several limitations to the study design and execution are acknowledged. The first lies in the isolation approach. Given evidence suggesting the presence of *S. aureus* phages in farmyard / agricultural environments, it may have been advantageous to extend the search for phages to these sources rather than attempt to optimise enrichment techniques for wastewater [1]. However, the selection of phages more active against agricultural strains remains uncertain, albeit unlikely since *S. aureus* phages tend to exhibit a broad range of activity regardless of isolation strain [172, 209]. Another limitation was in the use of a transposon-based library that hindered the application of widely used programs such as PhageTerm [221] to identify the definitive ends of bacteriophage genomes [159]. Future sequencing efforts employing different library preparation methods may be required address this. Nevertheless, in this thesis reordered phage genomes utilising the small terminase subunits appeared complete and aligned well with closely related genomes (Figures 4.8 and 4.9), showing expected sizes very similar to their closest relatives (Table 4.3). Furthermore, bacterial sequencing was conducted on the host bacteria for Koomba kaat 1 and Biyabeda mokiny 1 phages using a hybrid sequencing approach with long and short reads to resolve the genomes into a single contig. Finally, the lack of bacterial sequencing data to accompany the host range panel may also limit the understanding of phage specificity in relation to bacterial diversity, however these can be incorporated into future experimental designs. Overall, these limitations do not adversely affect the quality of data generated within this thesis nor the interpretation of its findings, namely that phages could be isolated, retain effective

concentrations when aerosolised, and do not prompt acute inflammation or cytotoxicity *in vitro* or *in vivo*.

6.8. Contributions to the field

In conclusion, the data presented in this thesis demonstrate that phages have the potential to treat respiratory tract infections caused by *S. aureus* bacteria including MRSA variants without causing major onsets of inflammation or cytotoxicity. In addition, Koomba kaat 1 and Biyabeda mokiny 1 were stable and retained their infective capabilities when aerosolised. Whilst their isolation from environmental and clinical sources was not without its difficulties; these phages demonstrate broad ranges of activity and are predicted to be polyvalent phages with multiple RBPs. Moreover, when assessed for signs of contamination from the host propagating strain, phage samples produced using propagation strains SA01 and SA09 were deemed to be safe, this is an important consideration for *S. aureus* phages specifically. The development of scalable, high throughput pipelines for genomic safety characterisations demonstrates that the timely characterisation of phages from the environment is possible and may streamline future characterisations of phages. The use of containerised applications (such as genome assembly and annotation pipelines utilised using a docker container) ensure that the numerous processes required to analyse genomics data are held accountable and are reproducible in an easily traceable manner. The demonstration of safety within the animal model used also provides insights towards the inflammatory potential of phages when applied directly to the airways within a therapeutically relevant treatment regime. Overall, the data reported may help to provide the preclinical safety assurances required to enable the use of these phages within clinical trials.

Appendix A:

9 December 2015

Clinical Prof. Francis Lannigan
School of Surgery, M704,
University of Western Australia
35 Stirling Highway
CRAWLEY WA 6009

Dear Professor Lannigan,

Re: WA Epithelial Research Program for Childhood Respiratory Diseases
(Our ref No: 901)

Thank you for your reply of the 4 December 2015, addressing the queries raised by the Scientific Review Sub-Committee (SRC). The SRC has reviewed your reply out of session and your proposed research program was tabled at the recent St John of God Health Care (SJGHC) Human Research Ethics Committee (HREC) meeting on 9 December 2015.

I am pleased to advise that your research program has been granted ethical approval as satisfying the ethical requirements set out in the National Health and Medical Research Council's National Statement on Ethical Conduct in Human Research (NHMRC, 2007) ("the National Statement"), in particular Section 3.2 "Databanks" and Section 3.4.3 "Prospective collection of human biospecimens for research." The Committee notes that for all future individual research studies conducted within this research program, these will undergo separate HREC review principally to ensure that the studies are a satisfactory use of the biospecimens collected as part of the research program.

This ethical approval is inclusive of the following research program documentation:

1. Original Study Protocol submitted to the SJGHC HREC on 30 October 2015
2. ERP Kids Information Brochure Version 1.1 St John of God Hospital dated October 2015.
3. The three Participant Consent Forms (ie Medical Research Consent on behalf of Child, Medical Research Assent, and Medical Research Consent) - recorded on the Surface Pro as part of the paper light system of recruiting.
4. WA Epithelial Research Program For Childhood Lung Disease Version 1.1 St John of God Subiaco Hospital dated October 2015.
5. EPR Audit Sheet Version 1.1 St John of God Hospital dated October 2015.

This study approval is granted for a time frame from the date of this approval letter to 22 January 2028. Should an extension of this timeframe be required, then you must seek continued approval from the Committee *before* the expiry of this time period. .../2

You are reminded that this letter constitutes **ethical approval only**. You must not commence this project at SJGHC until separate authorisation from SJGHC has been obtained.

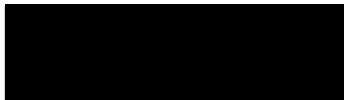
The Committee is a HREC that is constituted and operates in accordance with the National Statement. In line with the National Statement requirements, researchers need to keep the Committee and the institution (specifically, St John of God Subiaco Hospital) promptly and regularly informed on the progress of their approved research including:

1. any adverse events or unexpected outcomes that may affect continued ethical approval of the research program.
2. any proposed changes in the research protocol.
3. when the research program is completed or abandoned.

The Committee would also appreciate receiving *at a minimum an annual* progress report, as well as a final report on the research program results and/or any subsequent publications.

I wish you well with your research program.

Yours sincerely



Clinical Professor Dr Simon Dimmitt

Chairman

St John of God Health Care Human Research Ethics Committee

Enc.

- cc. Ms Liz Starcevich, Telethon Kids Institute (via email)
Dr Anthony Kicic, Telethon Kids Institute (via email)
Dr Luke Garratt, Telethon Kids Institute (via email)
Adjunct A/Professor Nik Zeps, Research Director, SJG Subiaco Hospital (via email)

**ST JOHN OF GOD HEALTH CARE HUMAN RESEARCH ETHICS
COMMITTEE MEMBERSHIP**

NAME	CORE MEMBER	SEX	APPOINTMENT	POSITION
Clinical Professor Simon Dimmitt	Core	M	Chair (with suitable experience whose other responsibilities will not impair the HREC's capacity to carry out its obligations under the National Statement).	Consultant Physician, General & Cardiovascular Medicine (accredited to St John of God Health Care)
Ms Tracey Piani	Core	F	Member with knowledge of and current experience in the professional care, counselling or treatment of humans (ie medical practitioner, clinical psychologist, social worker, nurse as appropriate)	Deputy Director of Nursing, St John of God Midland Public & Private Hospitals
Fr Joe Parkinson	Core	M	Member who performs a pastoral care role in a community for example an Aboriginal Elder, a minister of religion	Minister of Religion; Bioethicist, Director L. J. Goody Bioethics Centre
Mr Eric Heenan	Core	M	Member who is a lawyer, and where possible who is not engaged to advise the institution	Retired Supreme Court Judge, WA
Dr Janie Brown	Core	F	Member with current research experience that is relevant to research proposals to be considered at the meetings.	Nursing and Midwifery Research Coordinator, St John of God Subiaco Hospital
Sr Leonie O'Brien	Core	F	Laywoman who has no affiliation with the institution and does not currently engage in medical, scientific, legal or academic work.	Mercy Sister
Professor Sally Sandover	Core	F	Member with current research experience that is relevant to research proposals to be considered at the meetings.	Academic Co-ordinator Carrick Support Initiative, UWA Co-ordinator Regional Programs & PBL Consultant, University of WA
Mr Hamish Milne	Core	M	Layman who has no affiliation with the institution and does not currently engage in medical, scientific, legal or academic work	Self-employed Consultant
Mr Patrick O'Connor		M	Community member with expert knowledge in clinical psychology	Senior Clinical Psychologist, Health Dept WA (mental health services) and Clinical Psychologist, Hillarys Medical Centre
Mr Jeffrey Williams		M	Hospital Representative. Expert knowledge in Quality and Risk Management, public hospital management.	Director of Nursing, St John of God Midland Public & Private Hospitals
Mr Colin Keogh		M	Hospital Representative. Expert knowledge in Mission and culture.	Director of Mission, St John of God Murdoch Hospital
Ms Mary Rigby		F	Hospital Representative. Expert knowledge in nursing, particularly in palliative care & oncology.	Ward Nurse Manager, St John of God Subiaco Hospital

The St John of God Health Care Human Research Ethics Committee is a Human Research Ethics Committee that is constituted and operates in accordance with the National Health and Medical Research Council's National Statement on Ethical Conduct in Human Research (2007).

Date of Ethics Committee Meeting: _9 December 2015_Chairman's Signature: 

Appendix B:



Curtin University

Research Office at Curtin

GPO Box U1987
Perth Western Australia 6845

Telephone +61 8 9266 7863
Facsimile +61 8 9266 3793
Web research.curtin.edu.au

26-Feb-2019

Name: Anthony Kicic
Department/School: School of Public Health
Email: Anthony.Kicic@curtin.edu.au

Dear Anthony Kicic

RE: Reciprocal ethics approval
Approval number: HRE2019-0086

Thank you for your application submitted to the Human Research Ethics Office for the project WA Epithelial Research Program for Childhood Respiratory Diseases.

Your application has been approved by the Curtin University Human Research Ethics Committee (HREC) through a reciprocal approval process with the lead HREC.

The lead HREC for this project has been identified as St John of God Health Care Human Research Ethics Committee.

Approval number from the lead HREC is noted as 901.

The Curtin University Human Research Ethics Office approval number for this project is **HRE2019-0086**. Please use this number in all correspondence with the Curtin University Ethics Office regarding this project.

Approval is granted for a period of one year from to **22-Jan-2028**. Continuation of approval will be granted on an annual basis following submission of an annual report.

Personnel authorised to work on this project:

Name	Role
Kicic, Anthony	CI

You must comply with the lead HREC's reporting requirements and conditions of approval. You must also:

- Keep the Curtin University Ethics Office informed of submissions to the lead HREC, and of the review outcomes for those submissions
- Conduct your research according to the approved proposal
- Report to the lead HREC anything that might warrant review of the ethics approval for the project
- Submit an annual progress report to the Curtin University Ethics Office on or before the anniversary of approval, and a completion report on completion of the project. These can be the same reports submitted to the lead HREC.
- Personnel working on this project must be adequately qualified by education, training and experience for their role, or supervised
- Personnel must disclose any actual or potential conflicts of interest, including any financial or other interest or affiliation, that bears on this project
- Data and primary materials must be managed in accordance with the [Western Australian University Sector Disposal Authority \(WAUSDA\)](#) and the [Curtin University Research Data and Primary Materials policy](#)
- Where practicable, results of the research should be made available to the research participants in a timely and clear manner
- The Curtin University Ethics Office may conduct audits on a portion of approved projects.

This letter constitutes ethical approval only. This project may not proceed until you have met all of the Curtin University research governance requirements.

Should you have any queries regarding consideration of your project, please contact the Ethics Support Officer for your faculty or the Ethics Office at hrec@curtin.edu.au or on 9266 2784.

Yours sincerely



Amy Bowater
Ethics, Team Lead

Appendix C:



Research Office at Curtin

GPO Box U1987
Perth Western Australia 6845

Telephone +61 8 9266 7863
Facsimile +61 8 9266 3793
Web research.curtin.edu.au

11-Apr-2022

Name: Anthony Kicic
Department/School: School of Public Health
Email: Anthony.Kicic@curtin.edu.au

Dear Anthony Kicic

RE: Amendment approval
Approval number: HRE2019-0086

Thank you for submitting an amendment request to the Human Research Ethics Office for the project **RECIPROCAL - WA Epithelial Research Program for Childhood Respiratory Diseases**.

Your amendment request has been reviewed and the review outcome is: **Approved**

The amendment approval number is HRE2019-0086-01 approved on 11-Apr-2022.

The following amendments were approved:

Addition of Denby Evans, Joshua James Iszatt, Michelle Schwager and Andrew Vaitekenas to the project team.

Condition of Approval

It is the responsibility of the Chief Investigator to ensure that any activity undertaken under this project adheres to the latest available advice from the Government or the University regarding COVID-19.

Any special conditions noted in the original approval letter still apply.

Standard conditions of approval

1. Research must be conducted according to the approved proposal
2. Report in a timely manner anything that might warrant review of ethical approval of the project including:
 - proposed changes to the approved proposal or conduct of the study
 - unanticipated problems that might affect continued ethical acceptability of the project
 - major deviations from the approved proposal and/or regulatory guidelines
 - serious adverse events
3. Amendments to the proposal must be approved by the Human Research Ethics Office before they are implemented (except where an amendment is undertaken to eliminate an immediate risk to participants)
4. An annual progress report must be submitted to the Human Research Ethics Office on or before the anniversary of approval and a completion report submitted on completion of the project
5. Personnel working on this project must be adequately qualified by education, training and experience for their role, or supervised
6. Personnel must disclose any actual or potential conflicts of interest, including any financial or other interest or affiliation, that bears on this project
7. Changes to personnel working on this project must be reported to the Human Research Ethics Office
8. Data and primary materials must be retained and stored in accordance with the [Western Australian University Sector Disposal Authority \(WAUSDA\)](#) and the [Curtin University Research Data and Primary Materials policy](#)
9. Where practicable, results of the research should be made available to the research participants in a timely and clear manner
10. Unless prohibited by contractual obligations, results of the research should be disseminated in a manner that will allow public scrutiny; the Human Research Ethics Office must be informed of any constraints on publication

11. Ethics approval is dependent upon ongoing compliance of the research with the [Australian Code for the Responsible Conduct of Research](#), the [National Statement on Ethical Conduct in Human Research](#), applicable legal requirements, and with Curtin University policies, procedures and governance requirements
12. The Human Research Ethics Office may conduct audits on a portion of approved projects.

Should you have any queries regarding consideration of your project, please contact the Ethics Support Officer for your faculty or the Ethics Office at hrec@curtin.edu.au or on 9266 2784.

Yours sincerely



Amy Bowater
Ethics, Team Lead

Appendix D:



ANIMAL ETHICS COMMITTEE APPROVAL LETTER

A/Professor Alexander Larcombe
Telethon Kids Institute
Via E-mail: alexander.larcombe@telethonkids.org.au

Dear A/Professor Larcombe

Animal Ethics Committee Number: AEC #P2267

Project Title: profiling of bacteriophage in mice

Approval Period: 21 April 2023 to 30 April 2026

Approved Animals:

Animals Strain	Number Requested	Number Approved
C57BL/6J (7 - 8 weeks) mice	504	504
TOTAL	504	504

Thank you for submitting your revisions and/or clarifications for the above project, which were requested by the Animal Ethics Committee (AEC) at the 17 April 2023 Meeting. On behalf of the AEC, I am pleased to inform you that your application for this project has been approved to proceed.

The approval of this project is subject to the conditions and continued ethical approval of the AEC, and your compliance with the [Animal Welfare Act 2002](#), [Australian Code for the Care and Use of Animals for Scientific Purposes, 8th Edition 2013 \(Code\)](#), and the [Licence to use animals for scientific purposes](#).

General Conditions:

The following general conditions apply to this research project, and acceptance of AEC approval will be deemed to be an acceptance of these conditions by all researchers involved in the research project. The Principal Investigator (PI) is responsible for:

- 1 Ensuring appropriate and safe housing is available for the animals as determined by the Bioresources Manager and the Animal Welfare Officer (AWO).
- 2 Ensuring that all regulated approvals, permits and clearances have been obtained prior to undertaking any research on this project.
- 3 Supervising their team and taking ultimate responsibility for all matters related to the welfare of their animals. If you have any concerns regarding animal wellbeing or welfare, please immediately notify the AWO at awo@telethonkids.org.au
- 4 Ensuring that records of the monitoring, care and experimental use of animals are maintained, and respective details properly recorded in the project monitoring sheet(s) and available to all people involved in animal care (see Code 2.4.30 - 2.4.33; 3.1.20 – 3.1.22). Records must be legible and sufficiently detailed to verify that the wellbeing of animals has been monitored as agreed and to allow review and critical investigation of Adverse Events.
- 5 Maintaining records of the care and use of animals and providing to the AEC an Annual Report and State Government Annual Animal Use Statistics for the approved project (see Code 2.4.32 and 2.4.34). Reports are due in January of each year.



Northern Entrance
Perth Children's Hospital
15 Hospital Avenue
Nedlands WA 6009

PO Box 855,
West Perth WA 6872

ABN 86 009 278 755

T | 61 8 6319 1000

E | info@telethonkids.org.au

W | telethonkids.org.au

Proudly supported by the
people of Western Australia

Telethon

Discover. Prevent. Cure.



- 6 Ensuring the project has made provisions to allow for potential interruptions to experiments, due to the impacts of COVID-19 restrictions. PIs and their teams must adhere to COVID updates and guidelines as directed by the Institute.
- 7 Submitting an Amendment to the AEC for any changes to the project and ensuring approval is given in writing, before proceeding with any changes. This includes discontinuation, termination, or modification for any reason (e.g. personnel, source of animals, animal numbers, location of animals, protocol, and experimental procedures).
- 8 Considering animal welfare issues in accordance with the Code, at every step in the evolution of their protocol, with a focus on any areas of additional impost and strategies to manage and monitor them. The PI should contact the AWO for advice as appropriate.
- 9 Reporting immediately to the AWO, Adverse Events, unexpected deaths or unplanned euthanasia, illness and injuries, and subsequent completion of the Adverse Event form. It is a requirement of the Code that when an animal dies unexpectedly, or is euthanased due to unforeseen complications, an autopsy should be performed by a person with appropriate qualifications and/or experience.
- 10 Ensuring aseptic technique is used for recovery surgical procedures in animals (Code 3.3.16 (ii)). Animals that have undergone surgical procedures must be supported and safeguarded by using aseptic procedures if the animal is expected to recover.

If you have any queries, please contact the Animal Ethics Office at aeo@telethonkids.org.au

The AEC wish you every success for your research project.

Yours sincerely



Kristy Le May
AEC Chair
Telethon Kids Institute

Appendix E:



Curtin University

Research Office at Curtin

GPO Box U1987
Perth Western Australia 6845

Telephone +61 8 9266 7863

Facsimile +61 8 9266 3793

Web research.curtin.edu.au

05-Jul-2023

Name: Alexander Larcombe
Department/School: Curtin School of Population Health
Email: Alexander.Larcombe@curtin.edu.au

Dear Alexander Larcombe

RE: Reciprocal ethics approval
Approval number: ARE2023-15

Thank you for submitting your application to the Animal Ethics Office for the project **RECIPROCAL - Safety profiling of bacteriophage in mice**.

Your application for reciprocal approval was reviewed by the Curtin University Animal Ethics Committee at their meeting on .

Your application was **noted** by the Animal Ethics Committee.

The lead AEC for this project has been identified as **Telethon Kids Institute Animal Ethics Committee**

Approval number from the lead AEC is noted as **P2267**

The Curtin University Animal Research Ethics Office approval number for this project is **ARE2023-15**. Please use this number in all correspondence with the Curtin University Ethics Office regarding this project.

Approval is granted from **05-Jul-2023** to **30-Apr-2026**.

Standard conditions of approval

- An Annual Progress Report must be submitted to the Ethics Office annually, on the anniversary of approval.
- An Annual Animal Use Report that captures the relevant details regarding the number of animals used in the preceding year i.e. 1 January to 31 December must be submitted before 31 January of the following year.
- Any amendments to the approved protocol must be submitted to the Ethics Office.
- A Completion Report must be submitted to the Ethics Office on completion of the project.
- Should any animal(s) experience an adverse or unexpected outcome resulting from the experimentation, the AEC is to be notified in writing immediately.
- Please ensure that you quote the Animal Ethics Committee approval number whenever you order animals for this project. Note also that an AEC approval number must be displayed on the cage(s)/aquaria etc used to house/maintain animals during an approved activity.
- If the results of this research will be published, citations should state: "All experiments were performed according to the Australian Code of Practice for the care and use of animals for scientific purposes".

Special Conditions of Approval

This letter constitutes ethical approval only. This project may not proceed until you have met all of the Curtin University research governance requirements.

Should you have any queries regarding consideration of your project, please contact the Ethics Officer at aec@curtin.edu.au or on 9266

2784.

Yours sincerely



Dr Ricky Latou
Chair, Animal Ethics Committee

Appendix F:



Government of Western Australia
North Metropolitan Health Service
Women and Newborn Health Service



12/11/2018

Prof Karen Simmer
NCCU
Level 1, A Block
KEMH, 374 Bagot Road
SUBIACO WA 6009

Dear Prof Simmer

RE: 2055EW - AMENDMENT OF TRIAL APPROVAL
HUMAN RESEARCH ETHICS COMMITTEE (HREC)
HREC Ref 2055EW
Study Expiry Date 2/10/2018
Study Title Characterisation of Milk and Preterm birth

The application for amendment to this project was approved by the Women and Newborn Health Service Human Research Ethics Committee on 6/11/2018.

The approved amendments and documents are listed below:

Addition of a site: Telethon Kids Institute
Extension application to 2.10.20

You must forward a copy of this letter to all Principal Investigators involved in this project and to your institution.

Please note that all requirements of the original ethical approval for this project still apply.

Should you wish to discuss this matter, please contact Research Ethics and Office on 9340 1667 or kemhethics@health.wa.gov.au

The Research Ethics and Governance Office wishes you every continued success in your research.

Please quote the above trial number 2055EW on all correspondence associated with this trial.

Yours sincerely


Prof Jeffrey Keelan
DEPUTY CHAIR
WNHS ETHICS COMMITTEE

* The Ethics Committee is constituted, and operates in accordance with the National Health and Medical Research Council's National Statement on Ethical Conduct in Research Involving Humans

Appendix G:

G1. BMP1 annotations

<i>CDS</i>	<i>Len_t</i> <i>h(bp)</i>	<i>PHRO</i> <i>G</i>	<i>Product label</i>	<i>Category</i>
<i>phage_EJ5</i> <i>P_00001</i>	411	phrog_ 1063	terminase small subunit	head and packaging
<i>phage_EJ5</i> <i>P_00002</i>	1818	phrog_ 675	terminase large subunit	head and packaging
<i>phage_EJ5</i> <i>P_00003</i>	822	phrog_ 1917	virion structural protein	head and packaging
<i>phage_EJ5</i> <i>P_00004</i>	480	phrog_ 1116	hypothetical protein	unknown function
<i>phage_EJ5</i> <i>P_00005</i>	1212	phrog_ 3094	hypothetical protein	unknown function
<i>phage_EJ5</i> <i>P_00006</i>	285	phrog_ 3937	hypothetical protein	unknown function
<i>phage_EJ5</i> <i>P_00007</i>	381	phrog_ 1108	portal protein	head and packaging
<i>phage_EJ5</i> <i>P_00008</i>	1692	phrog_ 15361	portal protein	head and packaging
<i>phage_EJ5</i> <i>P_00009</i>	774	phrog_ 1028	head maturation protease	head and packaging
<i>phage_EJ5</i> <i>P_00010</i>	957	phrog_ 1133	hypothetical protein	unknown function
<i>phage_EJ5</i> <i>P_00011</i>	1392	phrog_ 752	major head protein	head and packaging
<i>phage_EJ5</i> <i>P_00012</i>	297	phrog_ 1205	hypothetical protein	unknown function
<i>phage_EJ5</i> <i>P_00013</i>	909	phrog_ 772	tail fiber protein	tail
<i>phage_EJ5</i> <i>P_00014</i>	879	phrog_ 1004	virion structural protein	head and packaging
<i>phage_EJ5</i> <i>P_00015</i>	621	phrog_ 1127	hypothetical protein	unknown function
<i>phage_EJ5</i> <i>P_00016</i>	837	phrog_ 1000	hypothetical protein	unknown function
<i>phage_EJ5</i> <i>P_00017</i>	216	phrog_ 1151	hypothetical protein	unknown function
<i>phage_EJ5</i> <i>P_00018</i>	1764	phrog_ 279	tail sheath	tail
<i>phage_EJ5</i> <i>P_00019</i>	429	phrog_ 985	virion structural protein	head and packaging
<i>phage_EJ5</i> <i>P_00020</i>	141	phrog_ 2701	hypothetical protein	unknown function
<i>phage_EJ5</i> <i>P_00021</i>	291	phrog_ 12287	hypothetical protein	unknown function
<i>phage_EJ5</i> <i>P_00022</i>	459	phrog_ 1905	hypothetical protein	unknown function
<i>phage_EJ5</i> <i>P_00023</i>	195	phrog_ 4320	hypothetical protein	unknown function
<i>phage_EJ5</i> <i>P_00024</i>	153	phrog_ 16917	hypothetical protein	unknown function
<i>phage_EJ5</i> <i>P_00025</i>	312	phrog_ 2754	virion structural protein	head and packaging
<i>phage_EJ5</i> <i>P_00026</i>	456	phrog_ 1038	tail assembly chaperone	tail
<i>phage_EJ5</i> <i>P_00027</i>	537	phrog_ 1316	RNA polymerase beta subunit	DNA, RNA and nucleotide metabolism

<i>phage_EJ5</i> <i>P_00028</i>	4056	phrog_1047	tail associated lysin	tail
<i>phage_EJ5</i> <i>P_00029</i>	2427	phrog_1015	tail protein with lysin activity	tail
<i>phage_EJ5</i> <i>P_00030</i>	888	phrog_2677	tail protein with lysin activity	tail
<i>phage_EJ5</i> <i>P_00031</i>	2547	phrog_2204	glycerophosphoryl diester phosphodiesterase	other
<i>phage_EJ5</i> <i>P_00032</i>	792	phrog_1011	virion structural protein	head and packaging
<i>phage_EJ5</i> <i>P_00033</i>	525	phrog_1073	hypothetical protein	unknown function
<i>phage_EJ5</i> <i>P_00034</i>	705	phrog_975	baseplate protein	tail
<i>phage_EJ5</i> <i>P_00035</i>	1047	phrog_6	baseplate protein	tail
<i>phage_EJ5</i> <i>P_00036</i>	2565	phrog_2386	virion structural protein	head and packaging
<i>phage_EJ5</i> <i>P_00037</i>	522	phrog_1394	virion structural protein	head and packaging
<i>phage_EJ5</i> <i>P_00038</i>	3459	phrog_877	hypothetical protein	unknown function
<i>phage_EJ5</i> <i>P_00039</i>	159	phrog_1074	hypothetical protein	unknown function
<i>phage_EJ5</i> <i>P_00040</i>	1923	phrog_2665	virion structural protein	head and packaging
<i>phage_EJ5</i> <i>P_00041</i>	375	phrog_2671	tail fiber protein	tail
<i>phage_EJ5</i> <i>P_00042</i>	1377	phrog_2691	tail fiber protein	tail
<i>phage_EJ5</i> <i>P_00043</i>	1749	phrog_14619	DNA helicase	DNA, RNA and nucleotide metabolism
<i>phage_EJ5</i> <i>P_00044</i>	1614	phrog_1098	HTH DNA binding protein	DNA, RNA and nucleotide metabolism
<i>phage_EJ5</i> <i>P_00045</i>	1443	phrog_19	DnaB-like replicative helicase	DNA, RNA and nucleotide metabolism
<i>phage_EJ5</i> <i>P_00046</i>	1026	phrog_100	SbcD-like subunit of palindrome specific endonuclease	DNA, RNA and nucleotide metabolism
<i>phage_EJ5</i> <i>P_00047</i>	378	phrog_2773	hypothetical protein	unknown function
<i>phage_EJ5</i> <i>P_00048</i>	1920	phrog_77	SbcC-like subunit of palindrome specific endonuclease	DNA, RNA and nucleotide metabolism
<i>phage_EJ5</i> <i>P_00049</i>	582	phrog_59	HNH endonuclease	DNA, RNA and nucleotide metabolism
<i>phage_EJ5</i> <i>P_00050</i>	597	phrog_1070	anti-sigma factor	moron, auxiliary metabolic gene and host takeover
<i>phage_EJ5</i> <i>P_00051</i>	1068	phrog_47	DNA primase	DNA, RNA and nucleotide metabolism
<i>phage_EJ5</i> <i>P_00052</i>	438	phrog_1291	hypothetical protein	unknown function
<i>phage_EJ5</i> <i>P_00053</i>	453	phrog_1095	hypothetical protein	unknown function
<i>phage_EJ5</i> <i>P_00054</i>	609	phrog_244	RusA-like Holliday junction resolvase	DNA, RNA and nucleotide metabolism
<i>phage_EJ5</i> <i>P_00055</i>	393	phrog_883	flavodoxin	moron, auxiliary metabolic gene and host takeover
<i>phage_EJ5</i> <i>P_00056</i>	2115	phrog_84	ribonucleoside-diphosphate reductase large subunit	DNA, RNA and nucleotide metabolism
<i>phage_EJ5</i> <i>P_00057</i>	1050	phrog_86	ribonucleoside diphosphate reductase small subunit	DNA, RNA and nucleotide metabolism
<i>phage_EJ5</i> <i>P_00058</i>	330	phrog_2797	hypothetical protein	unknown function

<i>phage_EJ5</i> <i>P_00059</i>	321	nan	hypothetical protein	
<i>phage_EJ5</i> <i>P_00060</i>	597	phrog_1054	hypothetical protein	unknown function
<i>phage_EJ5</i> <i>P_00061</i>	306	phrog_379	DNA binding protein	DNA, RNA and nucleotide metabolism
<i>phage_EJ5</i> <i>P_00062</i>	873	phrog_4008	DNA polymerase	DNA, RNA and nucleotide metabolism
<i>phage_EJ5</i> <i>P_00063</i>	513	phrog_2340	endonuclease	DNA, RNA and nucleotide metabolism
<i>phage_EJ5</i> <i>P_00064</i>	2331	phrog_17	DNA polymerase	DNA, RNA and nucleotide metabolism
<i>phage_EJ5</i> <i>P_00065</i>	243	phrog_3621	hypothetical protein	unknown function
<i>phage_EJ5</i> <i>P_00066</i>	483	phrog_1069	hypothetical protein	unknown function
<i>phage_EJ5</i> <i>P_00067</i>	1272	phrog_2672	hypothetical protein	unknown function
<i>phage_EJ5</i> <i>P_00068</i>	1257	phrog_97	UvsX-like recombinase	other
<i>phage_EJ5</i> <i>P_00069</i>	354	phrog_1089	hypothetical protein	unknown function
<i>phage_EJ5</i> <i>P_00070</i>	663	phrog_1025	RNA polymerase sigma factor	transcription regulation
<i>phage_EJ5</i> <i>P_00071</i>	633	phrog_1240	Ig domain containing protein	other
<i>phage_EJ5</i> <i>P_00072</i>	513	phrog_341	major tail protein	tail
<i>phage_EJ5</i> <i>P_00073</i>	228	phrog_341	major tail protein	tail
<i>phage_EJ5</i> <i>P_00074</i>	261	phrog_2673	hypothetical protein	unknown function
<i>phage_EJ5</i> <i>P_00075</i>	756	phrog_2721	hypothetical protein	unknown function
<i>phage_EJ5</i> <i>P_00076</i>	1251	phrog_284	exonuclease	DNA, RNA and nucleotide metabolism
<i>phage_EJ5</i> <i>P_00077</i>	369	phrog_2892	hypothetical protein	unknown function
<i>phage_EJ5</i> <i>P_00078</i>	312	phrog_3644	hypothetical protein	unknown function
<i>phage_EJ5</i> <i>P_00079</i>	537	phrog_1080	hypothetical protein	unknown function
<i>phage_EJ5</i> <i>P_00080</i>	768	phrog_984	hypothetical protein	unknown function
<i>phage_EJ5</i> <i>P_00081</i>	447	phrog_2356	hypothetical protein	unknown function
<i>phage_EJ5</i> <i>P_00082</i>	864	phrog_1113	hypothetical protein	unknown function
<i>phage_EJ5</i> <i>P_00083</i>	732	phrog_1007	hypothetical protein	unknown function
<i>phage_EJ5</i> <i>P_00084</i>	459	phrog_1104	virion structural protein	head and packaging
<i>phage_EJ5</i> <i>P_00085</i>	444	phrog_1303	DNA binding protein	DNA, RNA and nucleotide metabolism
<i>phage_EJ5</i> <i>P_00086</i>	705	phrog_2726	hypothetical protein	unknown function
<i>phage_EJ5</i> <i>P_00087</i>	399	phrog_2863	hypothetical protein	unknown function
<i>phage_EJ5</i> <i>P_00088</i>	243	phrog_3157	hypothetical protein	unknown function
<i>phage_EJ5</i> <i>P_00089</i>	558	phrog_5958	hypothetical protein	unknown function

<i>phage_EJ5</i> <i>P_00090</i>	177	phrog_3664	DNA sliding clamp inhibitor; arrest of <i>S.aureus</i> DNA synthesis	DNA, RNA and nucleotide metabolism
<i>phage_EJ5</i> <i>P_00091</i>	252	phrog_6867	hypothetical protein	unknown function
<i>phage_EJ5</i> <i>P_00092</i>	234	phrog_6850	hypothetical protein	unknown function
<i>phage_EJ5</i> <i>P_00093</i>	645	phrog_3854	ribulose-1;5-bisphosphate carboxylase/oxygenase small subunit	moron, auxiliary metabolic gene and host takeover
<i>phage_EJ5</i> <i>P_00094</i>	249	phrog_4009	hypothetical protein	unknown function
<i>phage_EJ5</i> <i>P_00095</i>	177	phrog_3524	hypothetical protein	unknown function
<i>phage_EJ5</i> <i>P_00096</i>	297	phrog_3128	hypothetical protein	unknown function
<i>phage_EJ5</i> <i>P_00097</i>	183	phrog_3640	membrane protein	moron, auxiliary metabolic gene and host takeover
<i>phage_EJ5</i> <i>P_00098</i>	369	phrog_3669	hypothetical protein	unknown function
<i>phage_EJ5</i> <i>P_00099</i>	348	phrog_2988	hypothetical protein	unknown function
<i>phage_EJ5</i> <i>P_00100</i>	279	phrog_3804	hypothetical protein	unknown function
<i>phage_EJ5</i> <i>P_00101</i>	306	phrog_3143	hypothetical protein	unknown function
<i>phage_EJ5</i> <i>P_00102</i>	351	phrog_3752	hypothetical protein	unknown function
<i>phage_EJ5</i> <i>P_00103</i>	603	phrog_4208	HNH endonuclease	DNA, RNA and nucleotide metabolism
<i>phage_EJ5</i> <i>P_00104</i>	180	phrog_3701	hypothetical protein	unknown function
<i>phage_EJ5</i> <i>P_00105</i>	411	phrog_1486	membrane protein	moron, auxiliary metabolic gene and host takeover
<i>phage_EJ5</i> <i>P_00106</i>	294	phrog_32014	hypothetical protein	unknown function
<i>phage_EJ5</i> <i>P_00107</i>	288	phrog_1486	membrane protein	moron, auxiliary metabolic gene and host takeover
<i>phage_EJ5</i> <i>P_00108</i>	117	phrog_4580	transcription factor	transcription regulation
<i>phage_EJ5</i> <i>P_00109</i>	321	phrog_4584	carboxypeptidase	other
<i>phage_EJ5</i> <i>P_00110</i>	666	phrog_14215	hypothetical protein	unknown function
<i>phage_EJ5</i> <i>P_00111</i>	306	phrog_654	hypothetical protein	unknown function
<i>phage_EJ5</i> <i>P_00112</i>	405	phrog_6562	hypothetical protein	unknown function
<i>phage_EJ5</i> <i>P_00113</i>	237	phrog_7553	hypothetical protein	unknown function
<i>phage_EJ5</i> <i>P_00114</i>	528	phrog_547	phosphoesterase	other
<i>phage_EJ5</i> <i>P_00115</i>	309	phrog_7962	hypothetical protein	unknown function
<i>phage_EJ5</i> <i>P_00116</i>	180	phrog_4743	hypothetical protein	unknown function
<i>phage_EJ5</i> <i>P_00117</i>	264	phrog_4418	hypothetical protein	unknown function
<i>phage_EJ5</i> <i>P_00118</i>	318	phrog_4081	hypothetical protein	unknown function
<i>phage_EJ5</i> <i>P_00119</i>	681	phrog_4650	hypothetical protein	unknown function

<i>phage_EJ5</i> <i>P_00120</i>	204	phrog_7235	hypothetical protein	unknown function
<i>phage_EJ5</i> <i>P_00121</i>	159	phrog_4430	hypothetical protein	unknown function
<i>phage_EJ5</i> <i>P_00122</i>	225	phrog_7618	hypothetical protein	unknown function
<i>phage_EJ5</i> <i>P_00123</i>	201	phrog_3453	hypothetical protein	unknown function
<i>phage_EJ5</i> <i>P_00124</i>	291	phrog_4096	hypothetical protein	unknown function
<i>phage_EJ5</i> <i>P_00125</i>	309	phrog_1099	hypothetical protein	unknown function
<i>phage_EJ5</i> <i>P_00126</i>	909	phrog_619	ribose-phosphate pyrophosphokinase	other
<i>phage_EJ5</i> <i>P_00127</i>	1470	phrog_448	nicotinamide phosphoribosyl transferase	other
<i>phage_EJ5</i> <i>P_00128</i>	246	phrog_4028	hypothetical protein	unknown function
<i>phage_EJ5</i> <i>P_00129</i>	393	phrog_3847	hypothetical protein	unknown function
<i>phage_EJ5</i> <i>P_00130</i>	198	phrog_4340	hypothetical protein	unknown function
<i>phage_EJ5</i> <i>P_00131</i>	294	phrog_654	hypothetical protein	unknown function
<i>phage_EJ5</i> <i>P_00132</i>	312	phrog_3224	hypothetical protein	unknown function
<i>phage_EJ5</i> <i>P_00133</i>	240	phrog_11635	hypothetical protein	unknown function
<i>phage_EJ5</i> <i>P_00134</i>	156	phrog_13028	hypothetical protein	unknown function
<i>phage_EJ5</i> <i>P_00135</i>	345	phrog_19859	transcriptional regulator	transcription regulation
<i>phage_EJ5</i> <i>P_00136</i>	390	phrog_15759	hypothetical protein	unknown function
<i>phage_EJ5</i> <i>P_00137</i>	306	phrog_14594	hypothetical protein	unknown function
<i>phage_EJ5</i> <i>P_00138</i>	237	nan	hypothetical protein	
<i>phage_EJ5</i> <i>P_00139</i>	228	phrog_11002	hypothetical protein	unknown function
<i>phage_EJ5</i> <i>P_00140</i>	354	phrog_10962	hypothetical protein	unknown function
<i>phage_EJ5</i> <i>P_00141</i>	174	nan	hypothetical protein	
<i>phage_EJ5</i> <i>P_00142</i>	384	phrog_11628	hypothetical protein	unknown function
<i>phage_EJ5</i> <i>P_00143</i>	171	phrog_14278	membrane protein	moron, auxiliary metabolic gene and host takeover
<i>phage_EJ5</i> <i>P_00144</i>	237	phrog_12287	hypothetical protein	unknown function
<i>phage_EJ5</i> <i>P_00145</i>	300	phrog_654	hypothetical protein	unknown function
<i>phage_EJ5</i> <i>P_00146</i>	186	phrog_3204	hypothetical protein	unknown function
<i>phage_EJ5</i> <i>P_00147</i>	324	phrog_654	hypothetical protein	unknown function
<i>phage_EJ5</i> <i>P_00148</i>	294	phrog_654	hypothetical protein	unknown function
<i>phage_EJ5</i> <i>P_00149</i>	255	phrog_1099	hypothetical protein	unknown function
<i>phage_EJ5</i> <i>P_00150</i>	240	phrog_1099	hypothetical protein	unknown function

<i>phage_EJ5</i> <i>P_00151</i>	348	phrog_3522	hypothetical protein	unknown function
<i>phage_EJ5</i> <i>P_00152</i>	339	phrog_3077	hypothetical protein	unknown function
<i>phage_EJ5</i> <i>P_00153</i>	309	phrog_2601	hypothetical protein	unknown function
<i>phage_EJ5</i> <i>P_00154</i>	285	phrog_3164	hypothetical protein	unknown function
<i>phage_EJ5</i> <i>P_00155</i>	255	phrog_22949	hypothetical protein	unknown function
<i>phage_EJ5</i> <i>P_00156</i>	159	phrog_3325	TreN-like membrane protein	other
<i>phage_EJ5</i> <i>P_00157</i>	270	phrog_9817	hypothetical protein	unknown function
<i>phage_EJ5</i> <i>P_00158</i>	309	phrog_32750	hypothetical protein	unknown function
<i>phage_EJ5</i> <i>P_00159</i>	327	phrog_3276	hypothetical protein	unknown function
<i>phage_EJ5</i> <i>P_00160</i>	402	phrog_3543	hypothetical protein	unknown function
<i>phage_EJ5</i> <i>P_00161</i>	222	phrog_8721	hypothetical protein	unknown function
<i>phage_EJ5</i> <i>P_00162</i>	138	phrog_10435	hypothetical protein	unknown function
<i>phage_EJ5</i> <i>P_00163</i>	165	phrog_6946	hypothetical protein	unknown function
<i>phage_EJ5</i> <i>P_00164</i>	237	phrog_3480	hypothetical protein	unknown function
<i>phage_EJ5</i> <i>P_00165</i>	285	phrog_4534	hypothetical protein	unknown function
<i>phage_EJ5</i> <i>P_00166</i>	264	phrog_11460	hypothetical protein	unknown function
<i>phage_EJ5</i> <i>P_00167</i>	174	phrog_3789	hypothetical protein	unknown function
<i>phage_EJ5</i> <i>P_00168</i>	270	phrog_3549	hypothetical protein	unknown function
<i>phage_EJ5</i> <i>P_00169</i>	252	phrog_23311	hypothetical protein	unknown function
<i>phage_EJ5</i> <i>P_00170</i>	237	phrog_2884	hypothetical protein	unknown function
<i>phage_EJ5</i> <i>P_00171</i>	264	phrog_16296	hypothetical protein	unknown function
<i>phage_EJ5</i> <i>P_00172</i>	192	phrog_4249	hypothetical protein	unknown function
<i>phage_EJ5</i> <i>P_00173</i>	249	phrog_21704	membrane protein	moron, auxiliary metabolic gene and host takeover
<i>phage_EJ5</i> <i>P_00174</i>	483	phrog_3619	hypothetical protein	unknown function
<i>phage_EJ5</i> <i>P_00175</i>	432	phrog_2349	hypothetical protein	unknown function
<i>phage_EJ5</i> <i>P_00176</i>	543	phrog_4045	hypothetical protein	unknown function
<i>phage_EJ5</i> <i>P_00177</i>	489	phrog_1017	hypothetical protein	unknown function
<i>phage_EJ5</i> <i>P_00178</i>	399	phrog_3857	hypothetical protein	unknown function
<i>phage_EJ5</i> <i>P_00179</i>	708	phrog_246	NinI-like serine-threonine phosphatase	other
<i>phage_EJ5</i> <i>P_00180</i>	549	phrog_2948	hypothetical protein	unknown function
<i>phage_EJ5</i> <i>P_00181</i>	219	phrog_3686	hypothetical protein	unknown function

<i>phage_EJ5</i> <i>P_00182</i>	195	phrog_3950	hypothetical protein	unknown function
<i>phage_EJ5</i> <i>P_00183</i>	738	phrog_3464	nucleotidyltransferase	DNA, RNA and nucleotide metabolism
<i>phage_EJ5</i> <i>P_00184</i>	105	phrog_5230	hypothetical protein	unknown function
<i>phage_EJ5</i> <i>P_00185</i>	240	phrog_3697	hypothetical protein	unknown function
<i>phage_EJ5</i> <i>P_00186</i>	390	phrog_2164	hypothetical protein	unknown function
<i>phage_EJ5</i> <i>P_00187</i>	174	phrog_3504	hypothetical protein	unknown function
<i>phage_EJ5</i> <i>P_00188</i>	483	phrog_3319	hypothetical protein	unknown function
<i>phage_EJ5</i> <i>P_00189</i>	543	phrog_3635	hypothetical protein	unknown function
<i>phage_EJ5</i> <i>P_00190</i>	534	phrog_3702	hypothetical protein	unknown function
<i>phage_EJ5</i> <i>P_00191</i>	165	phrog_152	RinB-like transcriptional activator	transcription regulation
<i>phage_EJ5</i> <i>P_00192</i>	279	phrog_3751	membrane protein	moron, auxiliary metabolic gene and host takeover
<i>phage_EJ5</i> <i>P_00193</i>	846	phrog_1909	hypothetical protein	unknown function
<i>phage_EJ5</i> <i>P_00194</i>	1119	phrog_249	porphyrin biosynthesis	moron, auxiliary metabolic gene and host takeover
<i>phage_EJ5</i> <i>P_00195</i>	327	phrog_2861	hypothetical protein	unknown function
<i>phage_EJ5</i> <i>P_00196</i>	417	phrog_2708	nucleotide kinase	other
<i>phage_EJ5</i> <i>P_00197</i>	303	phrog_715	MazG-like pyrophosphatase	other
<i>phage_EJ5</i> <i>P_00198</i>	189	phrog_3048	hypothetical protein	unknown function
<i>phage_EJ5</i> <i>P_00199</i>	162	phrog_2966	hypothetical protein	unknown function
<i>phage_EJ5</i> <i>P_00200</i>	2052	phrog_3200	hypothetical protein	unknown function
<i>phage_EJ5</i> <i>P_00201</i>	264	phrog_2811	virion structural protein	head and packaging
<i>phage_EJ5</i> <i>P_00202</i>	174	phrog_1274	lysM motif protein	lysis
<i>phage_EJ5</i> <i>P_00203</i>	579	phrog_2642	hypothetical protein	unknown function
<i>phage_EJ5</i> <i>P_00204</i>	627	phrog_1817	nucleoside 2-deoxyribosyltransferase	DNA, RNA and nucleotide metabolism
<i>phage_EJ5</i> <i>P_00205</i>	225	phrog_3093	hypothetical protein	unknown function
<i>phage_EJ5</i> <i>P_00206</i>	741	phrog_170	PhoH-like phosphate starvation-inducible	other
<i>phage_EJ5</i> <i>P_00207</i>	615	phrog_2995	hypothetical protein	unknown function
<i>phage_EJ5</i> <i>P_00208</i>	426	phrog_531	Rnase H	DNA, RNA and nucleotide metabolism
<i>phage_EJ5</i> <i>P_00209</i>	192	phrog_2706	hypothetical protein	unknown function
<i>phage_EJ5</i> <i>P_00210</i>	642	phrog_2896	hypothetical protein	unknown function
<i>phage_EJ5</i> <i>P_00211</i>	231	nan	hypothetical protein	unknown function
<i>phage_EJ5</i> <i>P_00212</i>	228	phrog_2770	hypothetical protein	unknown function

<i>phage_EJ5</i> <i>P_00213</i>	693	phrog_3310	transglycosylase	other
<i>phage_EJ5</i> <i>P_00214</i>	795	phrog_200	lipoprotein	other
<i>phage_EJ5</i> <i>P_00215</i>	309	phrog_3667	hypothetical protein	unknown function
<i>phage_EJ5</i> <i>P_00216</i>	1488	phrog_635	endolysin	lysis
<i>phage_EJ5</i> <i>P_00217</i>	504	phrog_962	holin	lysis
<i>phage_EJ5</i> <i>P_00218</i>	186	phrog_987	hypothetical protein	unknown function
<i>phage_EJ5</i> <i>P_00219</i>	72	nan	tRNA-Trp	
<i>phage_EJ5</i> <i>P_00220</i>	73	nan	tRNA-Phe	
<i>phage_EJ5</i> <i>P_00221</i>	76	nan	tRNA-Asp	
<i>phage_EJ5</i> <i>P_00222</i>	219	phrog_1257	ribosome associated inhibitor A; zinc finger domain protein	moron, auxiliary metabolic gene and host takeover
<i>phage_EJ5</i> <i>P_00223</i>	210	phrog_1215	hypothetical protein	unknown function
<i>phage_EJ5</i> <i>P_00224</i>	333	phrog_937	hemolysin	other
<i>phage_EJ5</i> <i>P_00225</i>	327	phrog_1481	hypothetical protein	unknown function
<i>phage_EJ5</i> <i>P_00226</i>	387	phrog_3395	membrane protein	moron, auxiliary metabolic gene and host takeover

G2. P1 annotations

<i>CDS</i>	<i>Length h(bp)</i>	<i>PHRO G</i>	<i>Product label</i>	<i>Category</i>
<i>phage_KW_93_00001</i>	411	phrog_1063	terminase small subunit	head and packaging
<i>phage_KW_93_00002</i>	351	phrog_9315	terminase large subunit	head and packaging
<i>phage_KW_93_00003</i>	771	phrog_559	HNH endonuclease	DNA, RNA and nucleotide metabolism
<i>phage_KW_93_00004</i>	1461	phrog_675	terminase large subunit	head and packaging
<i>phage_KW_93_00005</i>	822	phrog_1917	virion structural protein	head and packaging
<i>phage_KW_93_00006</i>	480	phrog_1116	hypothetical protein	unknown function
<i>phage_KW_93_00007</i>	1212	phrog_3094	hypothetical protein	unknown function
<i>phage_KW_93_00008</i>	342	phrog_3937	hypothetical protein	unknown function
<i>phage_KW_93_00009</i>	381	phrog_1108	portal protein	head and packaging
<i>phage_KW_93_00010</i>	1692	phrog_15361	portal protein	head and packaging
<i>phage_KW_93_00011</i>	774	phrog_1028	head maturation protease	head and packaging
<i>phage_KW_93_00012</i>	957	phrog_1133	hypothetical protein	unknown function
<i>phage_KW_93_00013</i>	1392	phrog_752	major head protein	head and packaging
<i>phage_KW_93_00014</i>	210	phrog_1205	hypothetical protein	unknown function
<i>phage_KW_93_00015</i>	909	phrog_772	tail fiber protein	tail
<i>phage_KW_93_00016</i>	879	phrog_1004	virion structural protein	head and packaging
<i>phage_KW_93_00017</i>	621	phrog_1127	hypothetical protein	unknown function
<i>phage_KW_93_00018</i>	837	phrog_1000	hypothetical protein	unknown function
<i>phage_KW_93_00019</i>	216	phrog_1151	hypothetical protein	unknown function
<i>phage_KW_93_00020</i>	1764	phrog_279	tail sheath	tail
<i>phage_KW_93_00021</i>	429	phrog_985	virion structural protein	head and packaging
<i>phage_KW_93_00022</i>	141	phrog_2701	hypothetical protein	unknown function
<i>phage_KW_93_00023</i>	291	phrog_12287	hypothetical protein	unknown function
<i>phage_KW_93_00024</i>	459	phrog_1905	hypothetical protein	unknown function
<i>phage_KW_93_00025</i>	153	phrog_16917	hypothetical protein	unknown function
<i>phage_KW_93_00026</i>	312	phrog_2754	virion structural protein	head and packaging
<i>phage_KW_93_00027</i>	456	phrog_1038	tail assembly chaperone	tail
<i>phage_KW_93_00028</i>	537	phrog_1316	RNA polymerase beta subunit	DNA, RNA and nucleotide metabolism
<i>phage_KW_93_00029</i>	4056	phrog_1047	tail associated lysin	tail

<i>phage_KW</i> 93_00030	2427	phrog_1015	tail protein with lysin activity	tail
<i>phage_KW</i> 93_00031	888	phrog_2677	tail protein with lysin activity	tail
<i>phage_KW</i> 93_00032	2547	phrog_2204	glycerophosphoryl diester phosphodiesterase	other
<i>phage_KW</i> 93_00033	792	phrog_1011	virion structural protein	head and packaging
<i>phage_KW</i> 93_00034	525	phrog_1073	hypothetical protein	unknown function
<i>phage_KW</i> 93_00035	705	phrog_975	baseplate protein	tail
<i>phage_KW</i> 93_00036	1047	phrog_6	baseplate protein	tail
<i>phage_KW</i> 93_00037	2565	phrog_2386	virion structural protein	head and packaging
<i>phage_KW</i> 93_00038	522	phrog_1394	virion structural protein	head and packaging
<i>phage_KW</i> 93_00039	3459	phrog_877	hypothetical protein	unknown function
<i>phage_KW</i> 93_00040	159	phrog_1074	hypothetical protein	unknown function
<i>phage_KW</i> 93_00041	1923	phrog_2665	virion structural protein	head and packaging
<i>phage_KW</i> 93_00042	375	phrog_2671	tail fiber protein	tail
<i>phage_KW</i> 93_00043	1476	phrog_2691	tail fiber protein	tail
<i>phage_KW</i> 93_00044	1749	phrog_14619	DNA helicase	DNA, RNA and nucleotide metabolism
<i>phage_KW</i> 93_00045	1614	phrog_1098	HTH DNA binding protein	DNA, RNA and nucleotide metabolism
<i>phage_KW</i> 93_00046	1443	phrog_19	DnaB-like replicative helicase	DNA, RNA and nucleotide metabolism
<i>phage_KW</i> 93_00047	1026	phrog_100	SbcD-like subunit of palindrome specific endonuclease	DNA, RNA and nucleotide metabolism
<i>phage_KW</i> 93_00048	378	phrog_2773	hypothetical protein	unknown function
<i>phage_KW</i> 93_00049	1920	phrog_77	SbcC-like subunit of palindrome specific endonuclease	DNA, RNA and nucleotide metabolism
<i>phage_KW</i> 93_00050	597	phrog_1070	anti-sigma factor	moron, auxiliary metabolic gene and host takeover
<i>phage_KW</i> 93_00051	1068	phrog_47	DNA primase	DNA, RNA and nucleotide metabolism
<i>phage_KW</i> 93_00052	339	phrog_1291	hypothetical protein	unknown function
<i>phage_KW</i> 93_00053	453	phrog_1095	hypothetical protein	unknown function
<i>phage_KW</i> 93_00054	609	phrog_244	RusA-like Holliday junction resolvase	DNA, RNA and nucleotide metabolism
<i>phage_KW</i> 93_00055	393	phrog_883	flavodoxin	moron, auxiliary metabolic gene and host takeover
<i>phage_KW</i> 93_00056	2115	phrog_84	ribonucleoside-diphosphate reductase large subunit	DNA, RNA and nucleotide metabolism
<i>phage_KW</i> 93_00057	1050	phrog_86	ribonucleoside diphosphate reductase small subunit	DNA, RNA and nucleotide metabolism
<i>phage_KW</i> 93_00058	330	phrog_2797	hypothetical protein	unknown function
<i>phage_KW</i> 93_00059	321	nan	hypothetical protein	
<i>phage_KW</i> 93_00060	597	phrog_1054	hypothetical protein	unknown function

<i>phage_KW</i> 93_00061	306	phrog_379	DNA binding protein	DNA, RNA and nucleotide metabolism
<i>phage_KW</i> 93_00062	3219	phrog_17	DNA polymerase	DNA, RNA and nucleotide metabolism
<i>phage_KW</i> 93_00063	243	phrog_3621	hypothetical protein	unknown function
<i>phage_KW</i> 93_00064	483	phrog_1069	hypothetical protein	unknown function
<i>phage_KW</i> 93_00065	1272	phrog_2672	hypothetical protein	unknown function
<i>phage_KW</i> 93_00066	1257	phrog_97	UvsX-like recombinase	other
<i>phage_KW</i> 93_00067	354	phrog_1089	hypothetical protein	unknown function
<i>phage_KW</i> 93_00068	663	phrog_1025	RNA polymerase sigma factor	transcription regulation
<i>phage_KW</i> 93_00069	633	phrog_1240	Ig domain containing protein	other
<i>phage_KW</i> 93_00070	513	phrog_341	major tail protein	tail
<i>phage_KW</i> 93_00071	228	phrog_341	major tail protein	tail
<i>phage_KW</i> 93_00072	261	phrog_2673	hypothetical protein	unknown function
<i>phage_KW</i> 93_00073	756	phrog_2721	hypothetical protein	unknown function
<i>phage_KW</i> 93_00074	1251	phrog_284	exonuclease	DNA, RNA and nucleotide metabolism
<i>phage_KW</i> 93_00075	369	phrog_2892	hypothetical protein	unknown function
<i>phage_KW</i> 93_00076	312	phrog_3644	hypothetical protein	unknown function
<i>phage_KW</i> 93_00077	537	phrog_1080	hypothetical protein	unknown function
<i>phage_KW</i> 93_00078	768	phrog_984	hypothetical protein	unknown function
<i>phage_KW</i> 93_00079	447	phrog_2356	hypothetical protein	unknown function
<i>phage_KW</i> 93_00080	864	phrog_1113	hypothetical protein	unknown function
<i>phage_KW</i> 93_00081	732	phrog_1007	hypothetical protein	unknown function
<i>phage_KW</i> 93_00082	459	phrog_1104	virion structural protein	head and packaging
<i>phage_KW</i> 93_00083	444	phrog_1303	DNA binding protein	DNA, RNA and nucleotide metabolism
<i>phage_KW</i> 93_00084	705	phrog_2726	hypothetical protein	unknown function
<i>phage_KW</i> 93_00085	399	phrog_2863	hypothetical protein	unknown function
<i>phage_KW</i> 93_00086	243	phrog_3157	hypothetical protein	unknown function
<i>phage_KW</i> 93_00087	558	phrog_5958	hypothetical protein	unknown function
<i>phage_KW</i> 93_00088	177	phrog_3664	DNA sliding clamp inhibitor; arrest of S.aureus DNA synthesis	DNA, RNA and nucleotide metabolism
<i>phage_KW</i> 93_00089	252	phrog_6867	hypothetical protein	unknown function
<i>phage_KW</i> 93_00090	234	phrog_6850	hypothetical protein	unknown function

<i>phage_KW</i> <i>93_00091</i>	645	phrog_ 3854	ribulose-1;5-bisphosphate carboxylase/oxygenase small subunit	moron, auxiliary metabolic gene and host takeover
<i>phage_KW</i> <i>93_00092</i>	249	phrog_ 4009	hypothetical protein	unknown function
<i>phage_KW</i> <i>93_00093</i>	180	phrog_ 3524	hypothetical protein	unknown function
<i>phage_KW</i> <i>93_00094</i>	297	phrog_ 3128	hypothetical protein	unknown function
<i>phage_KW</i> <i>93_00095</i>	183	phrog_ 3640	membrane protein	moron, auxiliary metabolic gene and host takeover
<i>phage_KW</i> <i>93_00096</i>	369	phrog_ 3669	hypothetical protein	unknown function
<i>phage_KW</i> <i>93_00097</i>	348	phrog_ 2988	hypothetical protein	unknown function
<i>phage_KW</i> <i>93_00098</i>	279	phrog_ 3804	hypothetical protein	unknown function
<i>phage_KW</i> <i>93_00099</i>	306	phrog_ 3143	hypothetical protein	unknown function
<i>phage_KW</i> <i>93_00100</i>	351	phrog_ 3752	hypothetical protein	unknown function
<i>phage_KW</i> <i>93_00101</i>	603	phrog_ 4208	HNH endonuclease	DNA, RNA and nucleotide metabolism
<i>phage_KW</i> <i>93_00102</i>	180	phrog_ 3701	hypothetical protein	unknown function
<i>phage_KW</i> <i>93_00103</i>	411	phrog_ 1486	membrane protein	moron, auxiliary metabolic gene and host takeover
<i>phage_KW</i> <i>93_00104</i>	294	phrog_ 32014	hypothetical protein	unknown function
<i>phage_KW</i> <i>93_00105</i>	243	phrog_ 22787	membrane protein	moron, auxiliary metabolic gene and host takeover
<i>phage_KW</i> <i>93_00106</i>	114	phrog_ 4580	transcription factor	transcription regulation
<i>phage_KW</i> <i>93_00107</i>	267	phrog_ 4584	carboxypeptidase	other
<i>phage_KW</i> <i>93_00108</i>	306	phrog_ 654	hypothetical protein	unknown function
<i>phage_KW</i> <i>93_00109</i>	402	phrog_ 6562	hypothetical protein	unknown function
<i>phage_KW</i> <i>93_00110</i>	237	phrog_ 7553	hypothetical protein	unknown function
<i>phage_KW</i> <i>93_00111</i>	528	phrog_ 547	phosphoesterase	other
<i>phage_KW</i> <i>93_00112</i>	309	phrog_ 7962	hypothetical protein	unknown function
<i>phage_KW</i> <i>93_00113</i>	180	phrog_ 4743	hypothetical protein	unknown function
<i>phage_KW</i> <i>93_00114</i>	264	phrog_ 4418	hypothetical protein	unknown function
<i>phage_KW</i> <i>93_00115</i>	318	phrog_ 4081	hypothetical protein	unknown function
<i>phage_KW</i> <i>93_00116</i>	681	phrog_ 4650	hypothetical protein	unknown function
<i>phage_KW</i> <i>93_00117</i>	204	phrog_ 7235	hypothetical protein	unknown function
<i>phage_KW</i> <i>93_00118</i>	159	phrog_ 4430	hypothetical protein	unknown function
<i>phage_KW</i> <i>93_00119</i>	225	phrog_ 7618	hypothetical protein	unknown function
<i>phage_KW</i> <i>93_00120</i>	201	phrog_ 3453	hypothetical protein	unknown function

<i>phage_KW</i> 93_00121	291	phrog_4096	hypothetical protein	unknown function
<i>phage_KW</i> 93_00122	309	phrog_1099	hypothetical protein	unknown function
<i>phage_KW</i> 93_00123	909	phrog_619	ribose-phosphate pyrophosphokinase	other
<i>phage_KW</i> 93_00124	1470	phrog_448	nicotinamide phosphoribosyl transferase	other
<i>phage_KW</i> 93_00125	246	phrog_4028	hypothetical protein	unknown function
<i>phage_KW</i> 93_00126	393	phrog_3847	hypothetical protein	unknown function
<i>phage_KW</i> 93_00127	198	phrog_4340	hypothetical protein	unknown function
<i>phage_KW</i> 93_00128	294	phrog_654	hypothetical protein	unknown function
<i>phage_KW</i> 93_00129	312	phrog_3224	hypothetical protein	unknown function
<i>phage_KW</i> 93_00130	300	phrog_7070	hypothetical protein	unknown function
<i>phage_KW</i> 93_00131	240	phrog_11635	hypothetical protein	unknown function
<i>phage_KW</i> 93_00132	156	phrog_13028	hypothetical protein	unknown function
<i>phage_KW</i> 93_00133	345	phrog_19859	transcriptional regulator	transcription regulation
<i>phage_KW</i> 93_00134	333	phrog_4637	hypothetical protein	unknown function
<i>phage_KW</i> 93_00135	447	phrog_15759	hypothetical protein	unknown function
<i>phage_KW</i> 93_00136	1095	phrog_4538	hypothetical protein	unknown function
<i>phage_KW</i> 93_00137	171	phrog_14278	membrane protein	moron, auxiliary metabolic gene and host takeover
<i>phage_KW</i> 93_00138	306	phrog_12287	hypothetical protein	unknown function
<i>phage_KW</i> 93_00139	300	phrog_654	hypothetical protein	unknown function
<i>phage_KW</i> 93_00140	186	phrog_3204	hypothetical protein	unknown function
<i>phage_KW</i> 93_00141	324	phrog_654	hypothetical protein	unknown function
<i>phage_KW</i> 93_00142	294	phrog_654	hypothetical protein	unknown function
<i>phage_KW</i> 93_00143	255	phrog_1099	hypothetical protein	unknown function
<i>phage_KW</i> 93_00144	240	phrog_1099	hypothetical protein	unknown function
<i>phage_KW</i> 93_00145	348	phrog_3522	hypothetical protein	unknown function
<i>phage_KW</i> 93_00146	339	phrog_3077	hypothetical protein	unknown function
<i>phage_KW</i> 93_00147	309	phrog_2601	hypothetical protein	unknown function
<i>phage_KW</i> 93_00148	285	phrog_3164	hypothetical protein	unknown function
<i>phage_KW</i> 93_00149	180	phrog_29935	hypothetical protein	unknown function
<i>phage_KW</i> 93_00150	222	phrog_8721	hypothetical protein	unknown function
<i>phage_KW</i> 93_00151	138	phrog_10435	hypothetical protein	unknown function

<i>phage_KW</i> 93_00152	165	phrog_ 6946	hypothetical protein	unknown function
<i>phage_KW</i> 93_00153	237	phrog_ 3480	hypothetical protein	unknown function
<i>phage_KW</i> 93_00154	285	phrog_ 4534	hypothetical protein	unknown function
<i>phage_KW</i> 93_00155	168	phrog_ 5861	hypothetical protein	unknown function
<i>phage_KW</i> 93_00156	264	phrog_ 11460	hypothetical protein	unknown function
<i>phage_KW</i> 93_00157	174	phrog_ 3789	hypothetical protein	unknown function
<i>phage_KW</i> 93_00158	270	phrog_ 3549	hypothetical protein	unknown function
<i>phage_KW</i> 93_00159	180	phrog_ 4863	hypothetical protein	unknown function
<i>phage_KW</i> 93_00160	237	phrog_ 2884	hypothetical protein	unknown function
<i>phage_KW</i> 93_00161	246	phrog_ 11889	hypothetical protein	unknown function
<i>phage_KW</i> 93_00162	555	phrog_ 98	hypothetical protein	unknown function
<i>phage_KW</i> 93_00163	255	phrog_ 4355	hypothetical protein	unknown function
<i>phage_KW</i> 93_00164	192	phrog_ 4249	hypothetical protein	unknown function
<i>phage_KW</i> 93_00165	486	phrog_ 3619	hypothetical protein	unknown function
<i>phage_KW</i> 93_00166	126	phrog_ 15772	hypothetical protein	unknown function
<i>phage_KW</i> 93_00167	465	phrog_ 19882	hypothetical protein	unknown function
<i>phage_KW</i> 93_00168	432	phrog_ 2349	hypothetical protein	unknown function
<i>phage_KW</i> 93_00169	495	phrog_ 1017	hypothetical protein	unknown function
<i>phage_KW</i> 93_00170	405	phrog_ 3857	hypothetical protein	unknown function
<i>phage_KW</i> 93_00171	702	phrog_ 246	NinI-like serine-threonine phosphatase	other
<i>phage_KW</i> 93_00172	549	phrog_ 2948	hypothetical protein	unknown function
<i>phage_KW</i> 93_00173	219	phrog_ 3686	hypothetical protein	unknown function
<i>phage_KW</i> 93_00174	195	phrog_ 3950	hypothetical protein	unknown function
<i>phage_KW</i> 93_00175	738	phrog_ 3464	nucleotidyltransferase	DNA, RNA and nucleotide metabolism
<i>phage_KW</i> 93_00176	105	phrog_ 5230	hypothetical protein	unknown function
<i>phage_KW</i> 93_00177	228	phrog_ 3697	hypothetical protein	unknown function
<i>phage_KW</i> 93_00178	387	phrog_ 2164	hypothetical protein	unknown function
<i>phage_KW</i> 93_00179	174	phrog_ 3504	hypothetical protein	unknown function
<i>phage_KW</i> 93_00180	483	phrog_ 3319	hypothetical protein	unknown function
<i>phage_KW</i> 93_00181	543	phrog_ 3635	hypothetical protein	unknown function
<i>phage_KW</i> 93_00182	531	phrog_ 3702	hypothetical protein	unknown function

<i>phage_KW</i> 93_00183	165	phrog_152	RinB-like transcriptional activator	transcription regulation
<i>phage_KW</i> 93_00184	276	phrog_3751	membrane protein	moron, auxiliary metabolic gene and host takeover
<i>phage_KW</i> 93_00185	846	phrog_1909	hypothetical protein	unknown function
<i>phage_KW</i> 93_00186	1119	phrog_249	porphyrin biosynthesis	moron, auxiliary metabolic gene and host takeover
<i>phage_KW</i> 93_00187	327	phrog_2861	hypothetical protein	unknown function
<i>phage_KW</i> 93_00188	417	phrog_2708	nucleotide kinase	other
<i>phage_KW</i> 93_00189	621	phrog_374	HNH endonuclease	DNA, RNA and nucleotide metabolism
<i>phage_KW</i> 93_00190	315	phrog_715	MazG-like pyrophosphatase	other
<i>phage_KW</i> 93_00191	189	phrog_3048	hypothetical protein	unknown function
<i>phage_KW</i> 93_00192	162	phrog_2966	hypothetical protein	unknown function
<i>phage_KW</i> 93_00193	2052	phrog_3200	hypothetical protein	unknown function
<i>phage_KW</i> 93_00194	264	phrog_2811	virion structural protein	head and packaging
<i>phage_KW</i> 93_00195	174	phrog_1274	lysM motif protein	lysis
<i>phage_KW</i> 93_00196	579	phrog_2642	hypothetical protein	unknown function
<i>phage_KW</i> 93_00197	627	phrog_1817	nucleoside 2-deoxyribosyltransferase	DNA, RNA and nucleotide metabolism
<i>phage_KW</i> 93_00198	225	phrog_3093	hypothetical protein	unknown function
<i>phage_KW</i> 93_00199	921	phrog_8446	HNH endonuclease	DNA, RNA and nucleotide metabolism
<i>phage_KW</i> 93_00200	180	phrog_374	HNH endonuclease	DNA, RNA and nucleotide metabolism
<i>phage_KW</i> 93_00201	756	phrog_170	PhoH-like phosphate starvation-inducible	other
<i>phage_KW</i> 93_00202	576	phrog_2995	hypothetical protein	unknown function
<i>phage_KW</i> 93_00203	426	phrog_531	Rnase H	DNA, RNA and nucleotide metabolism
<i>phage_KW</i> 93_00204	192	phrog_2706	hypothetical protein	unknown function
<i>phage_KW</i> 93_00205	642	phrog_2896	hypothetical protein	unknown function
<i>phage_KW</i> 93_00206	231	nan	hypothetical protein	
<i>phage_KW</i> 93_00207	228	phrog_2770	hypothetical protein	unknown function
<i>phage_KW</i> 93_00208	693	phrog_3310	transglycosylase	other
<i>phage_KW</i> 93_00209	384	nan	hypothetical protein	
<i>phage_KW</i> 93_00210	636	phrog_374	HNH endonuclease	DNA, RNA and nucleotide metabolism
<i>phage_KW</i> 93_00211	792	phrog_200	lipoprotein	other
<i>phage_KW</i> 93_00212	309	phrog_3667	hypothetical protein	unknown function
<i>phage_KW</i> 93_00213	1488	phrog_635	endolysin	lysis

<i>phage_KW</i> 93_00214	504	phrog_962	holin	lysis
<i>phage_KW</i> 93_00215	186	phrog_987	hypothetical protein	unknown function
<i>phage_KW</i> 93_00216	73	nan	tRNA-Phe	
<i>phage_KW</i> 93_00217	76	nan	tRNA-Asp	
<i>phage_KW</i> 93_00218	219	phrog_1257	ribosome associated inhibitor A; zinc finger domain protein	moron, auxiliary metabolic gene and host takeover
<i>phage_KW</i> 93_00219	210	phrog_1215	hypothetical protein	unknown function
<i>phage_KW</i> 93_00220	333	phrog_937	hemolysin	other
<i>phage_KW</i> 93_00221	327	phrog_1481	hypothetical protein	unknown function
<i>phage_KW</i> 93_00222	387	phrog_3395	membrane protein	moron, auxiliary metabolic gene and host takeover

G3: P7 annotations

<i>CDS</i>	<i>Length h(bp)</i>	<i>PHRO G</i>	<i>Product label</i>	<i>Category</i>
<i>phage_WY3 Z_00001</i>	414	phrog_ 1063	terminase small subunit	head and packaging
<i>phage_WY3 Z_00002</i>	369	phrog_ 9315	terminase large subunit	head and packaging
<i>phage_WY3 Z_00003</i>	168	phrog_ 34048	terminase large subunit	head and packaging
<i>phage_WY3 Z_00004</i>	99	nan	hypothetical protein	
<i>phage_WY3 Z_00005</i>	1194	phrog_ 675	terminase large subunit	head and packaging
<i>phage_WY3 Z_00006</i>	921	phrog_ 559	HNH endonuclease	DNA, RNA and nucleotide metabolism
<i>phage_WY3 Z_00007</i>	162	nan	hypothetical protein	
<i>phage_WY3 Z_00008</i>	801	phrog_ 1917	virion structural protein	head and packaging
<i>phage_WY3 Z_00009</i>	177	phrog_ 3863	hypothetical protein	unknown function
<i>phage_WY3 Z_00010</i>	480	phrog_ 1116	hypothetical protein	unknown function
<i>phage_WY3 Z_00011</i>	885	phrog_ 3094	hypothetical protein	unknown function
<i>phage_WY3 Z_00012</i>	360	phrog_ 3937	hypothetical protein	unknown function
<i>phage_WY3 Z_00013</i>	366	phrog_ 1108	portal protein	head and packaging
<i>phage_WY3 Z_00014</i>	1686	phrog_ 15361	portal protein	head and packaging
<i>phage_WY3 Z_00015</i>	774	phrog_ 1028	head maturation protease	head and packaging
<i>phage_WY3 Z_00016</i>	951	phrog_ 1133	hypothetical protein	unknown function
<i>phage_WY3 Z_00017</i>	1392	phrog_ 752	major head protein	head and packaging
<i>phage_WY3 Z_00018</i>	234	phrog_ 1205	hypothetical protein	unknown function
<i>phage_WY3 Z_00019</i>	909	phrog_ 772	tail fiber protein	tail
<i>phage_WY3 Z_00020</i>	876	phrog_ 1004	virion structural protein	head and packaging
<i>phage_WY3 Z_00021</i>	621	phrog_ 1127	hypothetical protein	unknown function
<i>phage_WY3 Z_00022</i>	837	phrog_ 1000	hypothetical protein	unknown function
<i>phage_WY3 Z_00023</i>	207	phrog_ 1151	hypothetical protein	unknown function
<i>phage_WY3 Z_00024</i>	1761	phrog_ 279	tail sheath	tail
<i>phage_WY3 Z_00025</i>	360	phrog_ 985	virion structural protein	head and packaging
<i>phage_WY3 Z_00026</i>	987	phrog_ 7140	intron encoded nuclease	DNA, RNA and nucleotide metabolism
<i>phage_WY3 Z_00027</i>	144	phrog_ 2701	hypothetical protein	unknown function
<i>phage_WY3 Z_00028</i>	450	phrog_ 1905	hypothetical protein	unknown function
<i>phage_WY3 Z_00029</i>	309	phrog_ 2754	virion structural protein	head and packaging

<i>phage_WY3</i> <i>Z_00030</i>	417	phrog_1038	tail assembly chaperone	tail
<i>phage_WY3</i> <i>Z_00031</i>	444	phrog_1316	RNA polymerase beta subunit	DNA, RNA and nucleotide metabolism
<i>phage_WY3</i> <i>Z_00032</i>	2994	phrog_1047	tail associated lysin	tail
<i>phage_WY3</i> <i>Z_00033</i>	870	phrog_10341	endolysin	lysis
<i>phage_WY3</i> <i>Z_00034</i>	825	phrog_8949	hypothetical protein	unknown function
<i>phage_WY3</i> <i>Z_00035</i>	2433	phrog_1015	tail protein with lysin activity	tail
<i>phage_WY3</i> <i>Z_00036</i>	891	phrog_2677	tail protein with lysin activity	tail
<i>phage_WY3</i> <i>Z_00037</i>	2457	phrog_2204	glycerophosphoryl diester phosphodiesterase	other
<i>phage_WY3</i> <i>Z_00038</i>	852	phrog_1011	virion structural protein	head and packaging
<i>phage_WY3</i> <i>Z_00039</i>	522	phrog_1073	hypothetical protein	unknown function
<i>phage_WY3</i> <i>Z_00040</i>	705	phrog_975	baseplate protein	tail
<i>phage_WY3</i> <i>Z_00041</i>	1047	phrog_6	baseplate protein	tail
<i>phage_WY3</i> <i>Z_00042</i>	2703	phrog_2386	virion structural protein	head and packaging
<i>phage_WY3</i> <i>Z_00043</i>	522	phrog_1394	virion structural protein	head and packaging
<i>phage_WY3</i> <i>Z_00044</i>	3459	phrog_877	hypothetical protein	unknown function
<i>phage_WY3</i> <i>Z_00045</i>	171	phrog_1074	hypothetical protein	unknown function
<i>phage_WY3</i> <i>Z_00046</i>	1914	phrog_2665	virion structural protein	head and packaging
<i>phage_WY3</i> <i>Z_00047</i>	357	phrog_2671	tail fiber protein	tail
<i>phage_WY3</i> <i>Z_00048</i>	1365	phrog_2691	tail fiber protein	tail
<i>phage_WY3</i> <i>Z_00049</i>	456	phrog_14619	DNA helicase	DNA, RNA and nucleotide metabolism
<i>phage_WY3</i> <i>Z_00050</i>	1314	phrog_9690	DNA helicase	DNA, RNA and nucleotide metabolism
<i>phage_WY3</i> <i>Z_00051</i>	1587	phrog_1098	HTH DNA binding protein	DNA, RNA and nucleotide metabolism
<i>phage_WY3</i> <i>Z_00052</i>	1440	phrog_19	DnaB-like replicative helicase	DNA, RNA and nucleotide metabolism
<i>phage_WY3</i> <i>Z_00053</i>	258	phrog_11461	hypothetical protein	unknown function
<i>phage_WY3</i> <i>Z_00054</i>	246	phrog_12198	hypothetical protein	unknown function
<i>phage_WY3</i> <i>Z_00055</i>	111	phrog_6025	DNA methyltransferase	other
<i>phage_WY3</i> <i>Z_00056</i>	477	phrog_67	DNA methyltransferase	other
<i>phage_WY3</i> <i>Z_00057</i>	249	phrog_9725	hypothetical protein	unknown function
<i>phage_WY3</i> <i>Z_00058</i>	690	phrog_67	DNA methyltransferase	other
<i>phage_WY3</i> <i>Z_00059</i>	1032	phrog_100	SbcD-like subunit of palindrome specific endonuclease	DNA, RNA and nucleotide metabolism
<i>phage_WY3</i> <i>Z_00060</i>	267	phrog_2773	hypothetical protein	unknown function

<i>phage_WY3</i> <i>Z_00061</i>	1935	phrog_77	SbcC-like subunit of palindrome specific endonuclease	DNA, RNA and nucleotide metabolism
<i>phage_WY3</i> <i>Z_00062</i>	594	phrog_1070	anti-sigma factor	moron, auxiliary metabolic gene and host takeover
<i>phage_WY3</i> <i>Z_00063</i>	1077	phrog_47	DNA primase	DNA, RNA and nucleotide metabolism
<i>phage_WY3</i> <i>Z_00064</i>	309	phrog_1291	hypothetical protein	unknown function
<i>phage_WY3</i> <i>Z_00065</i>	462	phrog_1095	hypothetical protein	unknown function
<i>phage_WY3</i> <i>Z_00066</i>	609	phrog_244	RusA-like Holliday junction resolvase	DNA, RNA and nucleotide metabolism
<i>phage_WY3</i> <i>Z_00067</i>	1338	phrog_86	ribonucleoside diphosphate reductase small subunit	DNA, RNA and nucleotide metabolism
<i>phage_WY3</i> <i>Z_00068</i>	2652	phrog_12229	ribonucleotide reductase	DNA, RNA and nucleotide metabolism
<i>phage_WY3</i> <i>Z_00069</i>	327	phrog_2797	hypothetical protein	unknown function
<i>phage_WY3</i> <i>Z_00070</i>	321	nan	hypothetical protein	
<i>phage_WY3</i> <i>Z_00071</i>	603	phrog_1054	hypothetical protein	unknown function
<i>phage_WY3</i> <i>Z_00072</i>	303	phrog_379	DNA binding protein	DNA, RNA and nucleotide metabolism
<i>phage_WY3</i> <i>Z_00073</i>	3750	phrog_4008	DNA polymerase	DNA, RNA and nucleotide metabolism
<i>phage_WY3</i> <i>Z_00074</i>	645	phrog_2081	HNH endonuclease	DNA, RNA and nucleotide metabolism
<i>phage_WY3</i> <i>Z_00075</i>	657	phrog_5995	DNA polymerase	DNA, RNA and nucleotide metabolism
<i>phage_WY3</i> <i>Z_00076</i>	483	phrog_1069	hypothetical protein	unknown function
<i>phage_WY3</i> <i>Z_00077</i>	369	phrog_24838	hypothetical protein	unknown function
<i>phage_WY3</i> <i>Z_00078</i>	1170	phrog_2672	hypothetical protein	unknown function
<i>phage_WY3</i> <i>Z_00079</i>	234	phrog_8290	RecA or Sak4, length ?	other
<i>phage_WY3</i> <i>Z_00080</i>	1026	phrog_97	UvsX-like recombinase	other
<i>phage_WY3</i> <i>Z_00081</i>	354	phrog_1089	hypothetical protein	unknown function
<i>phage_WY3</i> <i>Z_00082</i>	660	phrog_1025	RNA polymerase sigma factor	transcription regulation
<i>phage_WY3</i> <i>Z_00083</i>	750	phrog_1240	Ig domain containing protein	other
<i>phage_WY3</i> <i>Z_00084</i>	513	phrog_341	major tail protein	tail
<i>phage_WY3</i> <i>Z_00085</i>	213	phrog_341	major tail protein	tail
<i>phage_WY3</i> <i>Z_00086</i>	255	phrog_2673	hypothetical protein	unknown function
<i>phage_WY3</i> <i>Z_00087</i>	771	phrog_2721	hypothetical protein	unknown function
<i>phage_WY3</i> <i>Z_00088</i>	1254	phrog_284	exonuclease	DNA, RNA and nucleotide metabolism
<i>phage_WY3</i> <i>Z_00089</i>	330	phrog_2892	hypothetical protein	unknown function
<i>phage_WY3</i> <i>Z_00090</i>	534	phrog_1080	hypothetical protein	unknown function
<i>phage_WY3</i> <i>Z_00091</i>	762	phrog_984	hypothetical protein	unknown function

<i>phage_WY3</i> <i>Z_00092</i>	507	phrog_2356	hypothetical protein	unknown function
<i>phage_WY3</i> <i>Z_00093</i>	855	phrog_1113	hypothetical protein	unknown function
<i>phage_WY3</i> <i>Z_00094</i>	732	phrog_1007	hypothetical protein	unknown function
<i>phage_WY3</i> <i>Z_00095</i>	459	phrog_1104	virion structural protein	head and packaging
<i>phage_WY3</i> <i>Z_00096</i>	438	phrog_1303	DNA binding protein	DNA, RNA and nucleotide metabolism
<i>phage_WY3</i> <i>Z_00097</i>	636	phrog_2726	hypothetical protein	unknown function
<i>phage_WY3</i> <i>Z_00098</i>	399	phrog_2863	hypothetical protein	unknown function
<i>phage_WY3</i> <i>Z_00099</i>	261	phrog_3157	hypothetical protein	unknown function
<i>phage_WY3</i> <i>Z_00100</i>	264	phrog_13266	hypothetical protein	unknown function
<i>phage_WY3</i> <i>Z_00101</i>	285	phrog_3128	hypothetical protein	unknown function
<i>phage_WY3</i> <i>Z_00102</i>	294	phrog_2988	hypothetical protein	unknown function
<i>phage_WY3</i> <i>Z_00103</i>	315	phrog_3143	hypothetical protein	unknown function
<i>phage_WY3</i> <i>Z_00104</i>	246	phrog_13794	hypothetical protein	unknown function
<i>phage_WY3</i> <i>Z_00105</i>	495	phrog_13381	hypothetical protein	unknown function
<i>phage_WY3</i> <i>Z_00106</i>	657	phrog_923	hypothetical protein	unknown function
<i>phage_WY3</i> <i>Z_00107</i>	552	phrog_11752	hypothetical protein	unknown function
<i>phage_WY3</i> <i>Z_00108</i>	207	phrog_3453	hypothetical protein	unknown function
<i>phage_WY3</i> <i>Z_00109</i>	720	phrog_923	hypothetical protein	unknown function
<i>phage_WY3</i> <i>Z_00110</i>	258	phrog_13842	hypothetical protein	unknown function
<i>phage_WY3</i> <i>Z_00111</i>	402	phrog_17473	hypothetical protein	unknown function
<i>phage_WY3</i> <i>Z_00112</i>	732	phrog_923	hypothetical protein	unknown function
<i>phage_WY3</i> <i>Z_00113</i>	315	phrog_13526	hypothetical protein	unknown function
<i>phage_WY3</i> <i>Z_00114</i>	297	phrog_19178	hypothetical protein	unknown function
<i>phage_WY3</i> <i>Z_00115</i>	546	phrog_9084	homing endonuclease	DNA, RNA and nucleotide metabolism
<i>phage_WY3</i> <i>Z_00116</i>	624	phrog_4538	hypothetical protein	unknown function
<i>phage_WY3</i> <i>Z_00117</i>	402	phrog_467	hypothetical protein	unknown function
<i>phage_WY3</i> <i>Z_00118</i>	222	phrog_16365	hypothetical protein	unknown function
<i>phage_WY3</i> <i>Z_00119</i>	207	phrog_13453	nuclease	DNA, RNA and nucleotide metabolism
<i>phage_WY3</i> <i>Z_00120</i>	186	phrog_3204	hypothetical protein	unknown function
<i>phage_WY3</i> <i>Z_00121</i>	240	phrog_6981	hypothetical protein	unknown function
<i>phage_WY3</i> <i>Z_00122</i>	201	phrog_17940	hypothetical protein	unknown function

<i>phage_WY3</i> <i>Z_00123</i>	339	phrog_16583	hypothetical protein	unknown function
<i>phage_WY3</i> <i>Z_00124</i>	339	phrog_18429	hypothetical protein	unknown function
<i>phage_WY3</i> <i>Z_00125</i>	309	phrog_9163	hypothetical protein	unknown function
<i>phage_WY3</i> <i>Z_00126</i>	402	phrog_1486	membrane protein	moron, auxiliary metabolic gene and host takeover
<i>phage_WY3</i> <i>Z_00127</i>	360	phrog_12588	hypothetical protein	unknown function
<i>phage_WY3</i> <i>Z_00128</i>	747	phrog_24081	hypothetical protein	unknown function
<i>phage_WY3</i> <i>Z_00129</i>	210	phrog_21987	hypothetical protein	unknown function
<i>phage_WY3</i> <i>Z_00130</i>	309	phrog_13773	hypothetical protein	unknown function
<i>phage_WY3</i> <i>Z_00131</i>	624	phrog_923	hypothetical protein	unknown function
<i>phage_WY3</i> <i>Z_00132</i>	282	phrog_1709	hypothetical protein	unknown function
<i>phage_WY3</i> <i>Z_00133</i>	408	phrog_12518	hypothetical protein	unknown function
<i>phage_WY3</i> <i>Z_00134</i>	315	phrog_2601	hypothetical protein	unknown function
<i>phage_WY3</i> <i>Z_00135</i>	156	phrog_15099	hypothetical protein	unknown function
<i>phage_WY3</i> <i>Z_00136</i>	234	phrog_10311	hypothetical protein	unknown function
<i>phage_WY3</i> <i>Z_00137</i>	147	phrog_17700	hypothetical protein	unknown function
<i>phage_WY3</i> <i>Z_00138</i>	147	phrog_3325	TreN-like membrane protein	other
<i>phage_WY3</i> <i>Z_00139</i>	342	phrog_8830	hypothetical protein	unknown function
<i>phage_WY3</i> <i>Z_00140</i>	225	phrog_3549	hypothetical protein	unknown function
<i>phage_WY3</i> <i>Z_00141</i>	345	phrog_8830	hypothetical protein	unknown function
<i>phage_WY3</i> <i>Z_00142</i>	567	phrog_17429	hypothetical protein	unknown function
<i>phage_WY3</i> <i>Z_00143</i>	102	nan	hypothetical protein	
<i>phage_WY3</i> <i>Z_00144</i>	180	phrog_2884	hypothetical protein	unknown function
<i>phage_WY3</i> <i>Z_00145</i>	399	phrog_8847	hypothetical protein	unknown function
<i>phage_WY3</i> <i>Z_00146</i>	522	phrog_20169	membrane protein	moron, auxiliary metabolic gene and host takeover
<i>phage_WY3</i> <i>Z_00147</i>	384	phrog_301	secreted protein	other
<i>phage_WY3</i> <i>Z_00148</i>	393	phrog_2884	hypothetical protein	unknown function
<i>phage_WY3</i> <i>Z_00149</i>	393	phrog_98	hypothetical protein	unknown function
<i>phage_WY3</i> <i>Z_00150</i>	189	phrog_2532	hypothetical protein	unknown function
<i>phage_WY3</i> <i>Z_00151</i>	405	phrog_467	hypothetical protein	unknown function
<i>phage_WY3</i> <i>Z_00152</i>	531	phrog_2948	hypothetical protein	unknown function
<i>phage_WY3</i> <i>Z_00153</i>	561	phrog_2981	hypothetical protein	unknown function

<i>phage_WY3</i> <i>Z_00154</i>	393	phrog_4178	major tail protein	tail
<i>phage_WY3</i> <i>Z_00155</i>	225	phrog_12286	hypothetical protein	unknown function
<i>phage_WY3</i> <i>Z_00156</i>	786	phrog_14652	DNA binding protein	DNA, RNA and nucleotide metabolism
<i>phage_WY3</i> <i>Z_00157</i>	363	phrog_452	endonuclease	DNA, RNA and nucleotide metabolism
<i>phage_WY3</i> <i>Z_00158</i>	3219	phrog_19864	hypothetical protein	unknown function
<i>phage_WY3</i> <i>Z_00159</i>	180	phrog_19864	hypothetical protein	unknown function
<i>phage_WY3</i> <i>Z_00160</i>	141	nan	hypothetical protein	
<i>phage_WY3</i> <i>Z_00161</i>	324	phrog_2861	hypothetical protein	unknown function
<i>phage_WY3</i> <i>Z_00162</i>	417	phrog_2708	nucleotide kinase	other
<i>phage_WY3</i> <i>Z_00163</i>	186	phrog_3048	hypothetical protein	unknown function
<i>phage_WY3</i> <i>Z_00164</i>	162	phrog_2966	hypothetical protein	unknown function
<i>phage_WY3</i> <i>Z_00165</i>	2040	phrog_3200	hypothetical protein	unknown function
<i>phage_WY3</i> <i>Z_00166</i>	264	phrog_2811	virion structural protein	head and packaging
<i>phage_WY3</i> <i>Z_00167</i>	174	phrog_1274	lysM motif protein	lysis
<i>phage_WY3</i> <i>Z_00168</i>	624	phrog_2642	hypothetical protein	unknown function
<i>phage_WY3</i> <i>Z_00169</i>	594	phrog_1817	nucleoside 2-deoxyribosyltransferase	DNA, RNA and nucleotide metabolism
<i>phage_WY3</i> <i>Z_00170</i>	2301	phrog_8238	RNA ligase	DNA, RNA and nucleotide metabolism
<i>phage_WY3</i> <i>Z_00171</i>	399	phrog_23790	hypothetical protein	unknown function
<i>phage_WY3</i> <i>Z_00172</i>	603	phrog_2995	hypothetical protein	unknown function
<i>phage_WY3</i> <i>Z_00173</i>	264	phrog_3093	hypothetical protein	unknown function
<i>phage_WY3</i> <i>Z_00174</i>	426	phrog_25616	Rnase H	DNA, RNA and nucleotide metabolism
<i>phage_WY3</i> <i>Z_00175</i>	189	phrog_2706	hypothetical protein	unknown function
<i>phage_WY3</i> <i>Z_00176</i>	639	phrog_2896	hypothetical protein	unknown function
<i>phage_WY3</i> <i>Z_00177</i>	216	phrog_8	transcriptional regulator	transcription regulation
<i>phage_WY3</i> <i>Z_00178</i>	222	phrog_2770	hypothetical protein	unknown function
<i>phage_WY3</i> <i>Z_00179</i>	759	phrog_12367	endolysin	lysis
<i>phage_WY3</i> <i>Z_00180</i>	918	phrog_833	endolysin	lysis
<i>phage_WY3</i> <i>Z_00181</i>	501	phrog_962	holin	lysis
<i>phage_WY3</i> <i>Z_00182</i>	189	phrog_987	hypothetical protein	unknown function
<i>phage_WY3</i> <i>Z_00183</i>	216	phrog_1257	ribosome associated inhibitor A; zinc finger domain protein	moron, auxiliary metabolic gene and host takeover
<i>phage_WY3</i> <i>Z_00184</i>	216	phrog_1215	hypothetical protein	unknown function

<i>phage_WY3</i> <i>Z_00185</i>	333	phrog_ 937	hemolysin	other
<i>phage_WY3</i> <i>Z_00186</i>	333	phrog_ 1481	hypothetical protein	unknown function
<i>phage_WY3</i> <i>Z_00187</i>	231	phrog_ 5547	membrane protein	moron, auxiliary metabolic gene and host takeover

G4: P15 annotations

<i>CDS</i>	<i>Length (bp)</i>	<i>PHROG</i>	<i>Product label</i>	<i>Category</i>
<i>phage_UQ8W_00001</i>	495	phrog_15 95	terminase small subunit	head and packaging
<i>phage_UQ8W_00002</i>	1212	phrog_2	terminase large subunit	head and packaging
<i>phage_UQ8W_00003</i>	1479	phrog_64	portal protein	head and packaging
<i>phage_UQ8W_00004</i>	981	phrog_11 5	minor head protein	head and packaging
<i>phage_UQ8W_00005</i>	597	phrog_19 4	head scaffolding protein	head and packaging
<i>phage_UQ8W_00006</i>	825	phrog_54 4	major head protein	head and packaging
<i>phage_UQ8W_00007</i>	327	phrog_39 0	Arc-like repressor	transcription regulation
<i>phage_UQ8W_00008</i>	315	phrog_11 61	head-tail adaptor	connector
<i>phage_UQ8W_00009</i>	336	nan	hypothetical protein	
<i>phage_UQ8W_00010</i>	513	phrog_5	tail completion or Neck1 protein	connector
<i>phage_UQ8W_00011</i>	438	phrog_17 6	tail terminator	connector
<i>phage_UQ8W_00012</i>	561	phrog_23 8	major tail protein	tail
<i>phage_UQ8W_00013</i>	495	phrog_31 021	tail assembly chaperone	tail
<i>phage_UQ8W_00014</i>	342	phrog_31 021	tail assembly chaperone	tail
<i>phage_UQ8W_00015</i>	2970	phrog_37 657	hypothetical protein	unknown function
<i>phage_UQ8W_00016</i>	936	phrog_28 208	tail protein	tail
<i>phage_UQ8W_00017</i>	1887	phrog_66 3	minor head protein	head and packaging
<i>phage_UQ8W_00018</i>	1899	phrog_28 7	minor tail protein	tail
<i>phage_UQ8W_00019</i>	1824	phrog_17 192	hypothetical protein	unknown function
<i>phage_UQ8W_00020</i>	378	phrog_30 0	tail fiber protein	tail
<i>phage_UQ8W_00021</i>	177	phrog_23 700	hypothetical protein	unknown function
<i>phage_UQ8W_00022</i>	300	phrog_27 6	hypothetical protein	unknown function
<i>phage_UQ8W_00023</i>	1875	phrog_75 9	tail associated cell-wall hydrolase	other
<i>phage_UQ8W_00024</i>	1173	phrog_11 25	tail fiber protein	tail
<i>phage_UQ8W_00025</i>	396	phrog_12 62	hypothetical protein	unknown function
<i>phage_UQ8W_00026</i>	438	phrog_96 2	holin	lysis
<i>phage_UQ8W_00027</i>	1446	phrog_63 5	endolysin	lysis
<i>phage_UQ8W_00028</i>	312	phrog_79 19	hypothetical protein	unknown function
<i>phage_UQ8W_00029</i>	384	phrog_70 90	hypothetical protein	unknown function

<i>phage_UQ8W_00030</i>	1047	phrog_1	integrase	integration and excision
<i>phage_UQ8W_00031</i>	180	phrog_2033	excisionase	integration and excision
<i>phage_UQ8W_00032</i>	933	phrog_2039	hypothetical protein	unknown function
<i>phage_UQ8W_00033</i>	639	phrog_4	transcriptional repressor	transcription regulation
<i>phage_UQ8W_00034</i>	255	phrog_8	transcriptional regulator	transcription regulation
<i>phage_UQ8W_00035</i>	882	phrog_12047	ParB-like partition nuclease	DNA, RNA and nucleotide metabolism
<i>phage_UQ8W_00036</i>	768	phrog_1033	ParB-like partition protein	DNA, RNA and nucleotide metabolism
<i>phage_UQ8W_00037</i>	171	phrog_1534	hypothetical protein	unknown function
<i>phage_UQ8W_00038</i>	210	phrog_3240	hypothetical protein	unknown function
<i>phage_UQ8W_00039</i>	186	phrog_8	transcriptional regulator	transcription regulation
<i>phage_UQ8W_00040</i>	753	phrog_15968	anti-repressor	transcription regulation
<i>phage_UQ8W_00041</i>	666	phrog_7948	hypothetical protein	unknown function
<i>phage_UQ8W_00042</i>	222	phrog_989	hypothetical protein	unknown function
<i>phage_UQ8W_00043</i>	261	phrog_401	hypothetical protein	unknown function
<i>phage_UQ8W_00044</i>	222	phrog_946	hypothetical protein	unknown function
<i>phage_UQ8W_00045</i>	780	phrog_32104	hypothetical protein	unknown function
<i>phage_UQ8W_00046</i>	555	phrog_378	single strand DNA binding protein	DNA, RNA and nucleotide metabolism
<i>phage_UQ8W_00047</i>	666	phrog_398	hypothetical protein	unknown function
<i>phage_UQ8W_00048</i>	780	phrog_99	HNH endonuclease	DNA, RNA and nucleotide metabolism
<i>phage_UQ8W_00049</i>	804	phrog_1163	hypothetical protein	unknown function
<i>phage_UQ8W_00050</i>	774	phrog_50	DnaC-like helicase loader	DNA, RNA and nucleotide metabolism
<i>phage_UQ8W_00051</i>	159	phrog_809	transcriptional regulator	transcription regulation
<i>phage_UQ8W_00052</i>	222	phrog_433	hypothetical protein	unknown function
<i>phage_UQ8W_00053</i>	405	phrog_190	Holliday junction resolvase	DNA, RNA and nucleotide metabolism
<i>phage_UQ8W_00054</i>	186	phrog_299	hypothetical protein	unknown function
<i>phage_UQ8W_00055</i>	372	phrog_201	Panton-Valentine leukocidin	DNA, RNA and nucleotide metabolism
<i>phage_UQ8W_00056</i>	249	phrog_258	virulence associated	other
<i>phage_UQ8W_00057</i>	372	phrog_742	acetyltransferase	other
<i>phage_UQ8W_00058</i>	537	phrog_31995	hypothetical protein	unknown function
<i>phage_UQ8W_00059</i>	207	phrog_278	transcriptional regulator	transcription regulation
<i>phage_UQ8W_00060</i>	204	phrog_1616	hypothetical protein	unknown function

<i>phage_UQ8W_00061</i>	237	phrog_55 5	hypothetical protein	unknown function
<i>phage_UQ8W_00062</i>	390	phrog_30 1	secreted protein	other
<i>phage_UQ8W_00063</i>	174	phrog_15 2	RinB-like transcriptional activator	transcription regulation
<i>phage_UQ8W_00064</i>	402	phrog_10 58	hypothetical protein	unknown function

G5: P29 annotations

<i>CDS</i>	<i>Length (bp)</i>	<i>PHROG</i>	<i>Product label</i>	<i>Category</i>
<i>phage_71VF_00001</i>	495	phrog_15 95	terminase small subunit	head and packaging
<i>phage_71VF_00002</i>	1212	phrog_2	terminase large subunit	head and packaging
<i>phage_71VF_00003</i>	1479	phrog_64	portal protein	head and packaging
<i>phage_71VF_00004</i>	981	phrog_11 5	minor head protein	head and packaging
<i>phage_71VF_00005</i>	597	phrog_19 4	head scaffolding protein	head and packaging
<i>phage_71VF_00006</i>	825	phrog_54 4	major head protein	head and packaging
<i>phage_71VF_00007</i>	327	phrog_39 0	Arc-like repressor	transcription regulation
<i>phage_71VF_00008</i>	315	phrog_11 61	head-tail adaptor	connector
<i>phage_71VF_00009</i>	336	nan	hypothetical protein	
<i>phage_71VF_00010</i>	414	phrog_5	tail completion or Neck1 protein	connector
<i>phage_71VF_00011</i>	438	phrog_17 6	tail terminator	connector
<i>phage_71VF_00012</i>	561	phrog_23 8	major tail protein	tail
<i>phage_71VF_00013</i>	495	phrog_31 021	tail assembly chaperone	tail
<i>phage_71VF_00014</i>	342	phrog_31 021	tail assembly chaperone	tail
<i>phage_71VF_00015</i>	2970	phrog_37 657	hypothetical protein	unknown function
<i>phage_71VF_00016</i>	936	phrog_28 208	tail protein	tail
<i>phage_71VF_00017</i>	1887	phrog_66 3	minor head protein	head and packaging
<i>phage_71VF_00018</i>	1899	phrog_28 7	minor tail protein	tail
<i>phage_71VF_00019</i>	1824	phrog_17 192	hypothetical protein	unknown function
<i>phage_71VF_00020</i>	378	phrog_30 0	tail fiber protein	tail
<i>phage_71VF_00021</i>	177	phrog_23 700	hypothetical protein	unknown function
<i>phage_71VF_00022</i>	300	phrog_27 6	hypothetical protein	unknown function
<i>phage_71VF_00023</i>	1875	phrog_75 9	tail associated cell-wall hydrolase	other
<i>phage_71VF_00024</i>	1239	phrog_11 25	tail fiber protein	tail
<i>phage_71VF_00025</i>	396	phrog_12 62	hypothetical protein	unknown function
<i>phage_71VF_00026</i>	276	phrog_26 3	holin	lysis
<i>phage_71VF_00027</i>	1413	phrog_48 9	endolysin	lysis
<i>phage_71VF_00028</i>	558	phrog_61 49	hypothetical protein	unknown function
<i>phage_71VF_00029</i>	186	phrog_15 29	hypothetical protein	unknown function

<i>phage_71VF_00030</i>	1392	phrog_95	integrase	integration and excision
<i>phage_71VF_00031</i>	504	phrog_40 37	hypothetical protein	unknown function
<i>phage_71VF_00032</i>	186	phrog_51 92	hypothetical protein	unknown function
<i>phage_71VF_00033</i>	147	phrog_63 85	hypothetical protein	unknown function
<i>phage_71VF_00034</i>	711	phrog_4	transcriptional repressor	transcription regulation
<i>phage_71VF_00035</i>	240	nan	hypothetical protein	
<i>phage_71VF_00036</i>	444	phrog_84 7	anti-repressor Ant	transcription regulation
<i>phage_71VF_00037</i>	144	phrog_12 63	hypothetical protein	unknown function
<i>phage_71VF_00038</i>	210	phrog_23 66	hypothetical protein	unknown function
<i>phage_71VF_00039</i>	714	phrog_46 3	anti-repressor	transcription regulation
<i>phage_71VF_00040</i>	93	nan	hypothetical protein	
<i>phage_71VF_00041</i>	261	phrog_40 1	hypothetical protein	unknown function
<i>phage_71VF_00042</i>	480	phrog_25 3	Mu Gam-like end protection	DNA, RNA and nucleotide metabolism
<i>phage_71VF_00043</i>	639	phrog_23 24	Erf-like ssDNA annealing protein	DNA, RNA and nucleotide metabolism
<i>phage_71VF_00044</i>	429	phrog_44	single strand DNA binding protein	DNA, RNA and nucleotide metabolism
<i>phage_71VF_00045</i>	675	phrog_39 8	hypothetical protein	unknown function
<i>phage_71VF_00046</i>	117	phrog_10 049	hypothetical protein	unknown function
<i>phage_71VF_00047</i>	858	phrog_22 32	hypothetical protein	unknown function
<i>phage_71VF_00048</i>	810	phrog_42 8	replication initiation protein	DNA, RNA and nucleotide metabolism
<i>phage_71VF_00049</i>	780	phrog_50	DnaC-like helicase loader	DNA, RNA and nucleotide metabolism
<i>phage_71VF_00050</i>	159	phrog_80 9	transcriptional regulator	transcription regulation
<i>phage_71VF_00051</i>	222	phrog_43 3	hypothetical protein	unknown function
<i>phage_71VF_00052</i>	408	phrog_14 0	RusA-like Holliday junction resolvase	DNA, RNA and nucleotide metabolism
<i>phage_71VF_00053</i>	186	phrog_29 9	hypothetical protein	unknown function
<i>phage_71VF_00054</i>	363	phrog_20 1	Panton-Valentine leukocidin	DNA, RNA and nucleotide metabolism
<i>phage_71VF_00055</i>	255	phrog_16 89	nucleotide kinase	other
<i>phage_71VF_00056</i>	243	phrog_25 8	virulence associated	other
<i>phage_71VF_00057</i>	207	phrog_12 41	hypothetical protein	unknown function
<i>phage_71VF_00058</i>	405	phrog_24 347	hypothetical protein	unknown function
<i>phage_71VF_00059</i>	195	phrog_25 32	hypothetical protein	unknown function
<i>phage_71VF_00060</i>	453	phrog_22 346	hypothetical protein	unknown function

<i>phage_71VF_00061</i>	504	phrog_8205	hypothetical protein	unknown function
<i>phage_71VF_00062</i>	108	nan	hypothetical protein	
<i>phage_71VF_00063</i>	252	phrog_266	hypothetical protein	unknown function
<i>phage_71VF_00064</i>	174	phrog_3898	hypothetical protein	unknown function
<i>phage_71VF_00065</i>	162	phrog_4872	hypothetical protein	unknown function
<i>phage_71VF_00066</i>	528	phrog_31995	hypothetical protein	unknown function
<i>phage_71VF_00067</i>	288	phrog_2334	transcriptional regulator	transcription regulation
<i>phage_71VF_00068</i>	237	phrog_555	hypothetical protein	unknown function
<i>phage_71VF_00069</i>	387	phrog_301	secreted protein	other
<i>phage_71VF_00070</i>	174	phrog_152	RinB-like transcriptional activator	transcription regulation
<i>phage_71VF_00071</i>	402	phrog_1058	hypothetical protein	unknown function

G6: P30 annotations

<i>CDS</i>	<i>Length (bp)</i>	<i>PHROG</i>	<i>Product label</i>	<i>Category</i>
<i>phage_IPDA_00001</i>	495	phrog_1595	terminase small subunit	head and packaging
<i>phage_IPDA_00002</i>	1212	phrog_2	terminase large subunit	head and packaging
<i>phage_IPDA_00003</i>	1479	phrog_64	portal protein	head and packaging
<i>phage_IPDA_00004</i>	981	phrog_115	minor head protein	head and packaging
<i>phage_IPDA_00005</i>	597	phrog_194	head scaffolding protein	head and packaging
<i>phage_IPDA_00006</i>	825	phrog_544	major head protein	head and packaging
<i>phage_IPDA_00007</i>	327	phrog_390	Arc-like repressor	transcription regulation
<i>phage_IPDA_00008</i>	315	phrog_1161	head-tail adaptor	connector
<i>phage_IPDA_00009</i>	336	nan	hypothetical protein	
<i>phage_IPDA_00010</i>	414	phrog_5	tail completion or Neck1 protein	connector
<i>phage_IPDA_00011</i>	438	phrog_176	tail terminator	connector
<i>phage_IPDA_00012</i>	561	phrog_238	major tail protein	tail
<i>phage_IPDA_00013</i>	495	phrog_31021	tail assembly chaperone	tail
<i>phage_IPDA_00014</i>	342	phrog_31021	tail assembly chaperone	tail
<i>phage_IPDA_00015</i>	2970	phrog_37657	hypothetical protein	unknown function
<i>phage_IPDA_00016</i>	936	phrog_28208	tail protein	tail
<i>phage_IPDA_00017</i>	1887	phrog_663	minor head protein	head and packaging
<i>phage_IPDA_00018</i>	1899	phrog_287	minor tail protein	tail
<i>phage_IPDA_00019</i>	1824	phrog_17192	hypothetical protein	unknown function
<i>phage_IPDA_00020</i>	378	phrog_300	tail fiber protein	tail
<i>phage_IPDA_00021</i>	177	phrog_23700	hypothetical protein	unknown function
<i>phage_IPDA_00022</i>	300	phrog_276	hypothetical protein	unknown function
<i>phage_IPDA_00023</i>	1875	phrog_759	tail associated cell-wall hydrolase	other
<i>phage_IPDA_00024</i>	1239	phrog_1125	tail fiber protein	tail
<i>phage_IPDA_00025</i>	396	phrog_1262	hypothetical protein	unknown function
<i>phage_IPDA_00026</i>	276	phrog_263	holin	lysis
<i>phage_IPDA_00027</i>	1413	phrog_489	endolysin	lysis
<i>phage_IPDA_00028</i>	558	phrog_6149	hypothetical protein	unknown function
<i>phage_IPDA_00029</i>	186	phrog_1529	hypothetical protein	unknown function
<i>phage_IPDA_00030</i>	1392	phrog_95	integrase	integration and excision
<i>phage_IPDA_00031</i>	504	phrog_4037	hypothetical protein	unknown function

<i>phage_IPDA_00032</i>	186	phrog_5192	hypothetical protein	unknown function
<i>phage_IPDA_00033</i>	147	phrog_6385	hypothetical protein	unknown function
<i>phage_IPDA_00034</i>	711	phrog_4	transcriptional repressor	transcription regulation
<i>phage_IPDA_00035</i>	240	nan	hypothetical protein	
<i>phage_IPDA_00036</i>	444	phrog_847	anti-repressor Ant	transcription regulation
<i>phage_IPDA_00037</i>	144	phrog_1263	hypothetical protein	unknown function
<i>phage_IPDA_00038</i>	210	phrog_2366	hypothetical protein	unknown function
<i>phage_IPDA_00039</i>	714	phrog_463	anti-repressor	transcription regulation
<i>phage_IPDA_00040</i>	93	nan	hypothetical protein	
<i>phage_IPDA_00041</i>	261	phrog_401	hypothetical protein	unknown function
<i>phage_IPDA_00042</i>	480	phrog_253	Mu Gam-like end protection	DNA, RNA and nucleotide metabolism
<i>phage_IPDA_00043</i>	639	phrog_2324	Erf-like ssDNA annealing protein	DNA, RNA and nucleotide metabolism
<i>phage_IPDA_00044</i>	429	phrog_44	single strand DNA binding protein	DNA, RNA and nucleotide metabolism
<i>phage_IPDA_00045</i>	675	phrog_398	hypothetical protein	unknown function
<i>phage_IPDA_00046</i>	117	phrog_10049	hypothetical protein	unknown function
<i>phage_IPDA_00047</i>	858	phrog_2232	hypothetical protein	unknown function
<i>phage_IPDA_00048</i>	909	phrog_428	replication initiation protein	DNA, RNA and nucleotide metabolism
<i>phage_IPDA_00049</i>	780	phrog_50	DnaC-like helicase loader	DNA, RNA and nucleotide metabolism
<i>phage_IPDA_00050</i>	159	phrog_809	transcriptional regulator	transcription regulation
<i>phage_IPDA_00051</i>	222	phrog_433	hypothetical protein	unknown function
<i>phage_IPDA_00052</i>	408	phrog_140	RusA-like Holliday junction resolvase	DNA, RNA and nucleotide metabolism
<i>phage_IPDA_00053</i>	186	phrog_299	hypothetical protein	unknown function
<i>phage_IPDA_00054</i>	363	phrog_201	Panton-Valentine leukocidin	DNA, RNA and nucleotide metabolism
<i>phage_IPDA_00055</i>	255	phrog_1689	nucleotide kinase	other
<i>phage_IPDA_00056</i>	243	phrog_258	virulence associated	other
<i>phage_IPDA_00057</i>	207	phrog_1241	hypothetical protein	unknown function
<i>phage_IPDA_00058</i>	405	phrog_24347	hypothetical protein	unknown function
<i>phage_IPDA_00059</i>	195	phrog_2532	hypothetical protein	unknown function

<i>phage_IPDA_00060</i>	453	phrog_22346	hypothetical protein	unknown function
<i>phage_IPDA_00061</i>	504	phrog_8205	hypothetical protein	unknown function
<i>phage_IPDA_00062</i>	108	nan	hypothetical protein	
<i>phage_IPDA_00063</i>	252	phrog_266	hypothetical protein	unknown function
<i>phage_IPDA_00064</i>	174	phrog_3898	hypothetical protein	unknown function
<i>phage_IPDA_00065</i>	162	phrog_4872	hypothetical protein	unknown function
<i>phage_IPDA_00066</i>	528	phrog_31995	hypothetical protein	unknown function
<i>phage_IPDA_00067</i>	288	phrog_2334	transcriptional regulator	transcription regulation
<i>phage_IPDA_00068</i>	237	phrog_555	hypothetical protein	unknown function
<i>phage_IPDA_00069</i>	387	phrog_301	secreted protein	other
<i>phage_IPDA_00070</i>	174	phrog_152	RinB-like transcriptional activator	transcription regulation
<i>phage_IPDA_00071</i>	402	phrog_1058	hypothetical protein	unknown function

G7: P38 annotations

<i>CDS</i>	<i>Length</i> <i>h</i> <i>(bp)</i>	<i>PHR</i> <i>OG</i>	<i>Product label</i>	<i>Start</i> <i>art</i>	<i>End</i> <i>d</i>	<i>Category</i>	<i>Strand</i> <i>d</i>
<i>phage_VT</i> <i>HP_0000</i> 1	306	phrog _361	terminase small subunit	1	30 6	head and packaging	+
<i>phage_VT</i> <i>HP_0000</i> 2	1692	phrog _9	terminase large subunit	29 6	19 87	head and packaging	+
<i>phage_VT</i> <i>HP_0000</i> 3	1239	phrog _12	portal protein	19 92	32 30	head and packaging	+
<i>phage_VT</i> <i>HP_0000</i> 4	774	phrog _94	head maturation protease	32 14	39 87	head and packaging	+
<i>phage_VT</i> <i>HP_0000</i> 5	1209	phrog _10	major head protein	39 54	51 62	head and packaging	+
<i>phage_VT</i> <i>HP_0000</i> 6	279	phrog _40	head-tail adaptor Ad1	52 31	55 09	connector	+
<i>phage_VT</i> <i>HP_0000</i> 7	333	phrog _25	head closure Hc1	55 21	58 53	connector	+
<i>phage_VT</i> <i>HP_0000</i> 8	402	phrog _5	tail completion or Neck1 protein	58 50	62 51	connector	+
<i>phage_VT</i> <i>HP_0000</i> 9	396	phrog _78	tail terminator	62 52	66 47	connector	+
<i>phage_VT</i> <i>HP_0001</i> 0	642	phrog _88	major tail protein	66 82	73 23	tail	+
<i>phage_VT</i> <i>HP_0001</i> 1	456	phrog _341	major tail protein	74 15	78 70	tail	+
<i>phage_VT</i> <i>HP_0001</i> 2	351	phrog _187	head-tail adaptor	79 28	82 78	connector	+
<i>phage_VT</i> <i>HP_0001</i> 3	159	phrog _567	hypothetical protein	83 20	84 78	unknown function	+
<i>phage_VT</i> <i>HP_0001</i> 4	6201	phrog _4070	tail length tape measure protein	84 92	14 69	tail	+
<i>phage_VT</i> <i>HP_0001</i> 5	825	phrog _2952 9	hypothetical protein	14 69 2	15 51 6	unknown function	+
<i>phage_VT</i> <i>HP_0001</i> 6	1584	phrog _326	tail protein with endopeptidase domain protein	15 52 5	17 10 8	other	+
<i>phage_VT</i> <i>HP_0001</i> 7	291	phrog _574	hypothetical protein	17 10 8	17 39 8	unknown function	+
<i>phage_VT</i> <i>HP_0001</i> 8	1911	phrog _287	minor tail protein	17 41 4	19 32 4	tail	+
<i>phage_VT</i> <i>HP_0001</i> 9	1500	phrog _257	minor tail protein	19 29 1	20 79 0	tail	+

<i>phage_VT</i> <i>HP_0002</i> 0	390	phrog _300	tail fiber protein	20 79 0	21 17 9	tail	+
<i>phage_VT</i> <i>HP_0002</i> 1	165	phrog _134	hypothetical protein	21 17 2	21 33 6	unknown function	+
<i>phage_VT</i> <i>HP_0002</i> 2	300	phrog _276	hypothetical protein	21 38 2	21 68 1	unknown function	+
<i>phage_VT</i> <i>HP_0002</i> 3	303	phrog _263	holin	21 81 7	22 11 9	lysis	+
<i>phage_VT</i> <i>HP_0002</i> 4	1455	phrog _489	endolysin	22 13 0	23 58 4	lysis	+
<i>phage_VT</i> <i>HP_0002</i> 5	1206	phrog _1	integrase	24 42 9	25 63 4	integration and excision	-
<i>phage_VT</i> <i>HP_0002</i> 6	615	phrog _716	Na/K ATPase	25 76 0	26 37 4	other	+
<i>phage_VT</i> <i>HP_0002</i> 7	126	phrog _787	hypothetical protein	26 37 1	26 49 6	unknown function	-
<i>phage_VT</i> <i>HP_0002</i> 8	396	phrog _1776	hypothetical protein	26 60 8	27 00 3	unknown function	-
<i>phage_VT</i> <i>HP_0002</i> 9	435	phrog _1759	hypothetical protein	27 03 2	27 46 6	unknown function	-
<i>phage_VT</i> <i>HP_0003</i> 0	471	phrog _87	metallo-protease	27 48 4	27 95 4	other	-
<i>phage_VT</i> <i>HP_0003</i> 1	330	phrog _2967	transcriptional regulator	27 95 8	28 28 7	transcription regulation	-
<i>phage_VT</i> <i>HP_0003</i> 2	192	nan	hypothetical protein	28 44 8	28 63 9		+
<i>phage_VT</i> <i>HP_0003</i> 3	177	phrog _1534	hypothetical protein	28 72 3	28 89 9	unknown function	+
<i>phage_VT</i> <i>HP_0003</i> 4	240	phrog _2641	hypothetical protein	28 89 6	29 13 5	unknown function	-
<i>phage_VT</i> <i>HP_0003</i> 5	216	phrog _640	hypothetical protein	29 18 2	29 39 7	unknown function	+
<i>phage_VT</i> <i>HP_0003</i> 6	264	phrog _534	DNA binding protein	29 42 2	29 68 5	DNA, RNA and nucleotide metabolism	+
<i>phage_VT</i> <i>HP_0003</i> 7	213	phrog _2182	hypothetical protein	29 95 1	30 16 3	unknown function	+
<i>phage_VT</i> <i>HP_0003</i> 8	261	phrog _401	hypothetical protein	30 14 4	30 40 4	unknown function	+
<i>phage_VT</i> <i>HP_0003</i> 9	363	phrog _408	hypothetical protein	30 41 8	30 78 0	unknown function	+

<i>phage_VT</i> <i>HP_0004</i> 0	1167	phrog _69	exonuclease	30 77 7	31 94 3	DNA, RNA and nucleotide metabolism	+
<i>phage_VT</i> <i>HP_0004</i> 1	558	phrog _112	Gp2.5-like ssDNA binding protein and ssDNA annealing protein	31 96 9	32 52 6	DNA, RNA and nucleotide metabolism	+
<i>phage_VT</i> <i>HP_0004</i> 2	1953	phrog _1028 5	DNA polymerase	32 59 4	34 54 6	DNA, RNA and nucleotide metabolism	+
<i>phage_VT</i> <i>HP_0004</i> 3	186	phrog _299	hypothetical protein	34 55 9	34 74 4	unknown function	+
<i>phage_VT</i> <i>HP_0004</i> 4	402	phrog _201	Panton-Valentine leukocidin	34 74 4	35 14 5	DNA, RNA and nucleotide metabolism	+
<i>phage_VT</i> <i>HP_0004</i> 5	258	phrog _1689	nucleotide kinase	35 14 5	35 40 2	other	+
<i>phage_VT</i> <i>HP_0004</i> 6	201	phrog _987	hypothetical protein	35 40 5	35 60 5	unknown function	+
<i>phage_VT</i> <i>HP_0004</i> 7	243	phrog _258	virulence associated	35 62 0	35 86 2	other	+
<i>phage_VT</i> <i>HP_0004</i> 8	207	phrog _1241	hypothetical protein	35 87 6	36 08 2	unknown function	+
<i>phage_VT</i> <i>HP_0004</i> 9	405	phrog _2434 7	hypothetical protein	36 08 5	36 48 9	unknown function	+
<i>phage_VT</i> <i>HP_0005</i> 0	348	phrog _2434 7	hypothetical protein	36 48 6	36 83 3	unknown function	+
<i>phage_VT</i> <i>HP_0005</i> 1	309	phrog _1034	hypothetical protein	36 83 0	37 13 8	unknown function	+
<i>phage_VT</i> <i>HP_0005</i> 2	243	phrog _266	hypothetical protein	37 13 1	37 37 3	unknown function	+
<i>phage_VT</i> <i>HP_0005</i> 3	531	phrog _3199 5	hypothetical protein	37 43 3	37 96 3	unknown function	+
<i>phage_VT</i> <i>HP_0005</i> 4	207	phrog _278	transcriptional regulator	38 00 0	38 20 6	transcription regulation	+
<i>phage_VT</i> <i>HP_0005</i> 5	204	phrog _1122	hypothetical protein	38 20 3	38 40 6	unknown function	+
<i>phage_VT</i> <i>HP_0005</i> 6	237	phrog _555	hypothetical protein	38 39 9	38 63 5	unknown function	+
<i>phage_VT</i> <i>HP_0005</i> 7	390	phrog _301	secreted protein	38 62 5	39 01 4	other	+
<i>phage_VT</i> <i>HP_0005</i> 8	153	phrog _152	RinB-like transcriptional activator	39 01 1	39 16 3	transcription regulation	+
<i>phage_VT</i> <i>HP_0005</i> 9	201	phrog _4426	hypothetical protein	39 23 1	39 43 1	unknown function	+

<i>phage_VT</i> <i>HP_0006</i> 0	2448	phrog _256	DNA helicase	39 48 3	41 93 0	DNA, RNA and nucleotide metabolism	+
<i>phage_VT</i> <i>HP_0006</i> 1	291	phrog _93	endonuclease	42 27 1	42 56 1	DNA, RNA and nucleotide metabolism	+
<i>phage_VT</i> <i>HP_0006</i> 2	1368	phrog _62	DNA helicase	42 54 2	43 90 9	DNA, RNA and nucleotide metabolism	+
<i>phage_VT</i> <i>HP_0006</i> 3	438	phrog _36	transcriptional regulator	43 92 2	44 35 9	transcription regulation	+
<i>phage_VT</i> <i>HP_0006</i> 4	315	phrog _119	HNH endonuclease	44 51 6	44 83 0	DNA, RNA and nucleotide metabolism	+

Appendix H:

Table X: WAERP ID and participant demographics.

WAERP ID	Age at collection	Atopy	Sex	Past wheeze	Past asthma
121N	7.47	Non-atopic	Female	No	No
128N	4.76	Non-atopic	Male	No	No
98N	5.69	Non-atopic	Female	No	No
105N	8.47	Non-atopic	Female	No	No
222N	4.94	Non-atopic	Male	No	No
224N	6.81	Non-atopic	Male	No	No

References:

1. Mattila, S., P. Ruotsalainen, and M. Jalasvuori, *On-Demand Isolation of Bacteriophages Against Drug-Resistant Bacteria for Personalized Phage Therapy*. *Front Microbiol*, 2015. **6**: p. 1271.
2. Mendelson, M., et al., *Antibiotic resistance has a language problem*. *Nature*, 2017. **545**(7652): p. 23-25.
3. Mendelson, M., M. Sharland, and M. Mpundu, *Antibiotic resistance: calling time on the 'silent pandemic'*. *JAC Antimicrob Resist*, 2022. **4**(2): p. dlac016.
4. Heled, Y., A.S. Rutschman, and L. Vertinsky, *The problem with relying on profit-driven models to produce pandemic drugs*. *J Law Biosci*, 2020. **7**(1): p. lsa060.
5. Charani, E., et al., *Behavior change strategies to influence antimicrobial prescribing in acute care: a systematic review*. *Clin Infect Dis*, 2011. **53**(7): p. 651-62.
6. Kosiyaporn, H., et al., *Surveys of knowledge and awareness of antibiotic use and antimicrobial resistance in general population: A systematic review*. *PLoS One*, 2020. **15**(1): p. e0227973.
7. Van Katwyk, S.R., et al., *Adopting a Global AMR Target within the Pandemic Instrument Will Act as a Catalyst for Action*. *J Law Med Ethics*, 2022. **50**(S2): p. 64-70.
8. Prestinaci, F., P. Pezzotti, and A. Pantosti, *Antimicrobial resistance: a global multifaceted phenomenon*. *Pathog Glob Health*, 2015. **109**(7): p. 309-18.
9. Boucher, H.W., et al., *Bad bugs, no drugs: no ESKAPE! An update from the Infectious Diseases Society of America*. *Clinical Infectious Diseases*, 2009. **48**(1): p. 1-12.
10. O'Neill, J., *Tackling a Crisis for the Health and Wealth of Nations*. Review on Antimicrobial Resistance, 2014.
11. O'Neill, J., *Tackling Drug-Resistant Infections Globally: Final Report and Recommendations*. Review on Antimicrobial Resistance, 2016.
12. Collaborators, G.L., *Estimates of the global, regional, and national morbidity, mortality, and aetiologies of lower respiratory tract infections in 195 countries: a systematic analysis for the Global Burden of Disease Study 2015*. *Lancet Infect Dis*, 2017. **17**(11): p. 1133-1161.
13. Cassini, A., et al., *Attributable deaths and disability-adjusted life-years caused by infections with antibiotic-resistant bacteria in the EU and the European Economic Area in 2015: a population-level modelling analysis*. *Lancet Infect Dis*, 2019. **19**(1): p. 56-66.
14. Antimicrobial Resistance, C., *Global burden of bacterial antimicrobial resistance in 2019: a systematic analysis*. *Lancet*, 2022. **399**(10325): p. 629-655.
15. Pariente, N. and P.B.S. Editors, *The antimicrobial resistance crisis needs action now*. *PLoS Biol*, 2022. **20**(11): p. e3001918.
16. Freire, M.P., et al., *Impact of COVID-19 on healthcare-associated infections: Antimicrobial consumption does not follow antimicrobial resistance*. *Clinics (Sao Paulo)*, 2023. **78**: p. 100231.
17. CDC, *COVID-19: U.S. Impact on Antimicrobial Resistance*. 2022.
18. Mulani, M.S., et al., *Emerging Strategies to Combat ESKAPE Pathogens in the Era of Antimicrobial Resistance: A Review*. *Front Microbiol*, 2019. **10**: p. 539.
19. Pendleton, J.N., S.P. Gorman, and B.F. Gilmore, *Clinical relevance of the ESKAPE pathogens*. *Expert Rev Anti Infect Ther*, 2013. **11**(3): p. 297-308.
20. Spernovasilis, N., et al., *Epidemics and pandemics: Is human overpopulation the elephant in the room?* *Ethics Med Public Health*, 2021. **19**: p. 100728.
21. Browne, A.J., et al., *Global antibiotic consumption and usage in humans, 2000-18: a spatial modelling study*. *Lancet Planet Health*, 2021. **5**(12): p. e893-e904.
22. Mulchandani, R., et al., *Global trends in antimicrobial use in food-producing animals: 2020 to 2030*. *PLOS Glob Public Health*, 2023. **3**(2): p. e0001305.
23. Asokan, G.V., et al., *WHO Global Priority Pathogens List: A Bibliometric Analysis of Medline-PubMed for Knowledge Mobilization to Infection Prevention and Control Practices in Bahrain*. *Oman Med J*, 2019. **34**(3): p. 184-193.
24. Dolecek, C., et al., *Drug-resistant bacterial infections: We need urgent action and investment that focus on the weakest link*. *PLoS Biol*, 2022. **20**(11): p. e3001903.

25. WHO *Guiding principles for pathogen genome data sharing*. Geneva: World Health Organization, 2022.
26. Ball, M., M. Hossain, and D. Padalia, *Anatomy, Airway*, in *StatPearls*. 2023: Treasure Island (FL) ineligible companies. Disclosure: Mohammad Hossain declares no relevant financial relationships with ineligible companies. Disclosure: Devang Padalia declares no relevant financial relationships with ineligible companies.
27. *Global Health Estimates 2019: Deaths by Cause, Age, Sex, by Country and by Region, 2000-2019*. 2020(Geneva, World Health Organisation; 2020).
28. Chang, R.Y.K., et al., *Phage therapy for respiratory infections*. *Adv Drug Deliv Rev*, 2018. **133**: p. 76-86.
29. Morris, Z.S., S. Wooding, and J. Grant, *The answer is 17 years, what is the question: understanding time lags in translational research*. *J R Soc Med*, 2011. **104**(12): p. 510-20.
30. Azoulay, E., et al., *Diagnosis of severe respiratory infections in immunocompromised patients*. *Intensive Care Med*, 2020. **46**(2): p. 298-314.
31. Pragman, A.A., J.P. Berger, and B.J. Williams, *Understanding persistent bacterial lung infections: clinical implications informed by the biology of the microbiota and biofilms*. *Clin Pulm Med*, 2016. **23**(2): p. 57-66.
32. De Rose, V., et al., *Airway Epithelium Dysfunction in Cystic Fibrosis and COPD*. *Mediators Inflamm*, 2018. **2018**: p. 1309746.
33. Elborn, J.S., *Cystic fibrosis*. *The Lancet*, 2016. **388**(10059): p. 2519-2531.
34. Middleton, P.G., et al., *Elexacaftor-Tezacaftor-Ivacaftor for Cystic Fibrosis with a Single Phe508del Allele*. *N Engl J Med*, 2019. **381**(19): p. 1809-1819.
35. Chaudary, N., *Triplet CFTR modulators: future prospects for treatment of cystic fibrosis*. *Ther Clin Risk Manag*, 2018. **14**: p. 2375-2383.
36. Elborn, J.S., *Cystic fibrosis*. *Lancet*, 2016. **388**(10059): p. 2519-2531.
37. Tang, X.X., et al., *Acidic pH increases airway surface liquid viscosity in cystic fibrosis*. *J. Clin. Investig.*, 2016. **126**(3): p. 879-891.
38. Boucher, R.C., *Muco-Obstructive Lung Diseases*. *N Engl J Med*, 2019. **380**(20): p. 1941-1953.
39. Mathieu, E., et al., *Paradigms of Lung Microbiota Functions in Health and Disease, Particularly, in Asthma*. *Front Physiol*, 2018. **9**: p. 1168.
40. Clunes, M.T. and R.C. Boucher, *Cystic Fibrosis: The Mechanisms of Pathogenesis of an Inherited Lung Disorder*. *Drug Discov Today Dis Mech*, 2007. **4**(2): p. 63-72.
41. Courtney, J.M., M. Ennis, and J.S. Elborn, *Cytokines and inflammatory mediators in cystic fibrosis*. *J Cyst Fibros*, 2004. **3**(4): p. 223-31.
42. Esposito, S., et al., *Antimicrobial Treatment of Staphylococcus aureus in Patients With Cystic Fibrosis*. *Front Pharmacol*, 2019. **10**: p. 849.
43. Kumaran, D., et al., *Does Treatment Order Matter? Investigating the Ability of Bacteriophage to Augment Antibiotic Activity against Staphylococcus aureus Biofilms*. *Front Microbiol*, 2018. **9**: p. 127.
44. Rosenfeld, M., O. Rayner, and A.R. Smyth, *Prophylactic anti-staphylococcal antibiotics for cystic fibrosis*. *Cochrane Database Syst Rev*, 2020. **9**(9): p. CD001912.
45. Stutman, H.R., et al., *Antibiotic prophylaxis in infants and young children with cystic fibrosis: a randomized controlled trial*. *J Pediatr*, 2002. **140**(3): p. 299-305.
46. Caudri, D., et al., *The association between Staphylococcus aureus and subsequent bronchiectasis in children with cystic fibrosis*. *J Cyst Fibros*, 2018. **17**(4): p. 462-469.
47. Foster, T.J., *Antibiotic resistance in Staphylococcus aureus. Current status and future prospects*. *FEMS Microbiol Rev*, 2017. **41**(3): p. 430-449.
48. Foster, T.J., *Immune evasion by staphylococci*. *Nat Rev Microbiol*, 2005. **3**(12): p. 948-58.
49. Hoppe, J.E. and S.D. Sagel, *Shifting Landscape of Airway Infection in Early Cystic Fibrosis*. *Am J Respir Crit Care Med*, 2019. **200**(5): p. 528-529.
50. de Kraker, M.E.A., et al., *Mortality and Hospital Stay Associated with Resistant Staphylococcus aureus and Escherichia coli Bacteremia: Estimating the Burden of Antibiotic Resistance in Europe*. *PLOS Medicine*, 2011. **8**(10): p. e1001104.

51. Howden, B.P., A.Y. Peleg, and T.P. Stinear, *The evolution of vancomycin intermediate Staphylococcus aureus (VISA) and heterogenous-VISA*. *Infect Genet Evol*, 2014. **21**: p. 575-82.
52. Shariati, A., et al., *Global prevalence and distribution of vancomycin resistant, vancomycin intermediate and heterogeneously vancomycin intermediate Staphylococcus aureus clinical isolates: a systematic review and meta-analysis*. *Sci Rep*, 2020. **10**(1): p. 12689.
53. Li, G., M.J. Walker, and D.M.P. De Oliveira, *Vancomycin Resistance in Enterococcus and Staphylococcus aureus*. *Microorganisms*, 2022. **11**(1).
54. Liang, J., et al., *Resistance and Molecular Characteristics of Methicillin-Resistant Staphylococcus aureus and Heterogeneous Vancomycin-Intermediate Staphylococcus aureus*. *Infect Drug Resist*, 2023. **16**: p. 379-388.
55. Partridge, S.R., et al., *Mobile Genetic Elements Associated with Antimicrobial Resistance*. *Clin Microbiol Rev*, 2018. **31**(4).
56. Burian, M., et al., *Temporal expression of adhesion factors and activity of global regulators during establishment of Staphylococcus aureus nasal colonization*. *J Infect Dis*, 2010. **201**(9): p. 1414-21.
57. Burian, M., C. Wolz, and C. Goerke, *Regulatory adaptation of Staphylococcus aureus during nasal colonization of humans*. *PLoS One*, 2010. **5**(4): p. e10040.
58. Bleul, L., P. Francois, and C. Wolz, *Two-Component Systems of S. aureus: Signaling and Sensing Mechanisms*. *Genes (Basel)*, 2021. **13**(1).
59. Poudel, S., et al., *Revealing 29 sets of independently modulated genes in Staphylococcus aureus, their regulators, and role in key physiological response*. *Proc Natl Acad Sci U S A*, 2020. **117**(29): p. 17228-17239.
60. Burian, M., C. Wolz, and A.S. Yazdi, *Transcriptional adaptation of staphylococci during colonization of the authentic human environment: An overview of transcriptomic changes and their relationship to physiological conditions*. *Front Cell Infect Microbiol*, 2022. **12**: p. 1062329.
61. Dastgheyb, S.S. and M. Otto, *Staphylococcal adaptation to diverse physiologic niches: an overview of transcriptomic and phenotypic changes in different biological environments*. *Future Microbiol*, 2015. **10**(12): p. 1981-95.
62. Delaune, A., et al., *The WalkR system controls major staphylococcal virulence genes and is involved in triggering the host inflammatory response*. *Infect Immun*, 2012. **80**(10): p. 3438-53.
63. Long, D.R., et al., *Polyclonality, Shared Strains, and Convergent Evolution in Chronic Cystic Fibrosis Staphylococcus aureus Airway Infection*. *Am J Respir Crit Care Med*, 2021. **203**(9): p. 1127-1137.
64. Breuer, O., et al., *Changing Prevalence of Lower Airway Infections in Young Children with Cystic Fibrosis*. *American Journal of Respiratory and Critical Care Medicine*, 2019. **200**(5): p. 590-599.
65. Esposito, S., et al., *New Antibiotics for Staphylococcus aureus Infection: An Update from the World Association of Infectious Diseases and Immunological Disorders (WAidid) and the Italian Society of Anti-Infective Therapy (SITA)*. *Antibiotics (Basel)*, 2023. **12**(4).
66. Iskandar, K., et al., *Antibiotic Discovery and Resistance: The Chase and the Race*. *Antibiotics (Basel)*, 2022. **11**(2).
67. Clegg, J., et al., *Staphylococcus aureus Vaccine Research and Development: The Past, Present and Future, Including Novel Therapeutic Strategies*. *Front Immunol*, 2021. **12**: p. 705360.
68. Fattom, A., et al., *Efficacy profile of a bivalent Staphylococcus aureus glycoconjugated vaccine in adults on hemodialysis: Phase III randomized study*. *Hum Vaccin Immunother*, 2015. **11**(3): p. 632-41.
69. Fattom, A.I., et al., *Development of StaphVAX, a polysaccharide conjugate vaccine against S. aureus infection: from the lab bench to phase III clinical trials*. *Vaccine*, 2004. **22**(7): p. 880-7.

70. Boyle-Vavra, S., et al., *USA300 and USA500 clonal lineages of Staphylococcus aureus do not produce a capsular polysaccharide due to conserved mutations in the cap5 locus*. mBio, 2015. **6**(2).
71. Hassanzadeh, H., et al., *Efficacy of a 4-Antigen Staphylococcus aureus Vaccine in Spinal Surgery: The STaphylococcus aureus suRgical Inpatient Vaccine Efficacy (STRIVE) Randomized Clinical Trial*. Clin Infect Dis, 2023. **77**(2): p. 312-320.
72. Scully, I.L., et al., *Performance of a Four-Antigen Staphylococcus aureus Vaccine in Preclinical Models of Invasive S. aureus Disease*. Microorganisms, 2021. **9**(1).
73. Dryla, A., et al., *Comparison of antibody repertoires against Staphylococcus aureus in healthy individuals and in acutely infected patients*. Clin Diagn Lab Immunol, 2005. **12**(3): p. 387-98.
74. Karazum, H. and S.K. Datta, *Adaptive Immunity Against Staphylococcus aureus*. Curr Top Microbiol Immunol, 2017. **409**: p. 419-439.
75. Wang, X., et al., *Release of Staphylococcus aureus extracellular vesicles and their application as a vaccine platform*. Nat Commun, 2018. **9**(1): p. 1379.
76. Choi, S.J., et al., *Active Immunization with Extracellular Vesicles Derived from Staphylococcus aureus Effectively Protects against Staphylococcal Lung Infections, Mainly via Th1 Cell-Mediated Immunity*. PLoS One, 2015. **10**(9): p. e0136021.
77. de Vor, L., et al., *Human monoclonal antibodies against Staphylococcus aureus surface antigens recognize in vitro and in vivo biofilm*. Elife, 2022. **11**.
78. Ragle, B.E. and J. Bubeck Wardenburg, *Anti-alpha-hemolysin monoclonal antibodies mediate protection against Staphylococcus aureus pneumonia*. Infect Immun, 2009. **77**(7): p. 2712-8.
79. Schaffer, A.C., et al., *Immunization with Staphylococcus aureus clumping factor B, a major determinant in nasal carriage, reduces nasal colonization in a murine model*. Infect Immun, 2006. **74**(4): p. 2145-53.
80. Brown, A.F., et al., *Staphylococcus aureus Colonization: Modulation of Host Immune Response and Impact on Human Vaccine Design*. Front Immunol, 2014. **4**: p. 507.
81. Verkaik, N.J., et al., *Heterogeneity of the humoral immune response following Staphylococcus aureus bacteremia*. Eur J Clin Microbiol Infect Dis, 2010. **29**(5): p. 509-18.
82. Buckley, P.T., et al., *Multivalent human antibody-centyrin fusion protein to prevent and treat Staphylococcus aureus infections*. Cell Host Microbe, 2023. **31**(5): p. 751-765 e11.
83. Yu, X.Q., et al., *Safety, Tolerability, and Pharmacokinetics of MEDI4893, an Investigational, Extended-Half-Life, Anti-Staphylococcus aureus Alpha-Toxin Human Monoclonal Antibody, in Healthy Adults*. Antimicrob Agents Chemother, 2017. **61**(1).
84. Vanamala, K., et al., *Novel approaches for the treatment of methicillin-resistant Staphylococcus aureus: Using nanoparticles to overcome multidrug resistance*. Drug Discov Today, 2021. **26**(1): p. 31-43.
85. Brown, A.N., et al., *Nanoparticles functionalized with ampicillin destroy multiple-antibiotic-resistant isolates of Pseudomonas aeruginosa and Enterobacter aerogenes and methicillin-resistant Staphylococcus aureus*. Appl Environ Microbiol, 2012. **78**(8): p. 2768-74.
86. Xie, S., et al., *Biodegradable nanoparticles for intracellular delivery of antimicrobial agents*. J Control Release, 2014. **187**: p. 101-17.
87. Chakraborty, S.P., P. Pramanik, and S. Roy, *In vitro dose and duration dependent approaches for the assessment of ameliorative effects of nanoconjugated vancomycin against Staphylococcus aureus infection induced oxidative stress in murine peritoneal macrophages*. Microb Pathog, 2016. **91**: p. 74-84.
88. Chakraborty, S.P., et al., *In vitro antimicrobial activity of nanoconjugated vancomycin against drug resistant Staphylococcus aureus*. Int J Pharm, 2012. **436**(1-2): p. 659-76.
89. Pires, D.P., et al., *Phage therapy as an alternative or complementary strategy to prevent and control biofilm-related infections*. Curr Opin Microbiol, 2017. **39**: p. 48-56.
90. Wittebole, X., S. De Roock, and S.M. Opal, *A historical overview of bacteriophage therapy as an alternative to antibiotics for the treatment of bacterial pathogens*. Virulence, 2014. **5**(1): p. 226-35.

91. Gainey, A.B., et al., *Combining bacteriophages with cefiderocol and meropenem/vaborbactam to treat a pan-drug resistant Achromobacter species infection in a pediatric cystic fibrosis patient*. *Pediatr Pulmonol*, 2020.
92. Law, N., et al., *Successful adjunctive use of bacteriophage therapy for treatment of multidrug-resistant Pseudomonas aeruginosa infection in a cystic fibrosis patient*. *Infection*, 2019. **47**(4): p. 665-668.
93. Petrovic Fabijan, A., et al., *Safety of bacteriophage therapy in severe Staphylococcus aureus infection*. *Nat Microbiol*, 2020. **5**(3): p. 465-472.
94. Ng, R.N., et al., *Overcoming Challenges to Make Bacteriophage Therapy Standard Clinical Treatment Practice for Cystic Fibrosis*. *Front Microbiol*, 2020. **11**: p. 593988.
95. Hoe, S., et al., *Respirable bacteriophages for the treatment of bacterial lung infections*. *J Aerosol Med Pulm Drug Deliv*, 2013. **26**(6): p. 317-35.
96. Wienhold, S.M., J. Lienau, and M. Witzenrath, *Towards Inhaled Phage Therapy in Western Europe*. *Viruses*, 2019. **11**(3).
97. Trend, S., et al., *The potential of phage therapy in cystic fibrosis: Essential human-bacterial-phage interactions and delivery considerations for use in Pseudomonas aeruginosa-infected airways*. *J Cyst Fibros*, 2017. **16**(6): p. 663-670.
98. Wang, X., et al., *Prospects of Inhaled Phage Therapy for Combatting Pulmonary Infections*. *Front Cell Infect Microbiol*, 2021. **11**: p. 758392.
99. Abatangelo, V., et al., *Broad-range lytic bacteriophages that kill Staphylococcus aureus local field strains*. *PLoS One*, 2017. **12**(7): p. e0181671.
100. Furfaro, L.L., M.S. Payne, and B.J. Chang, *Bacteriophage Therapy: Clinical Trials and Regulatory Hurdles*. *Front Cell Infect Microbiol*, 2018. **8**: p. 376.
101. Melo, L.D.R., et al., *Phage therapy efficacy: a review of the last 10 years of preclinical studies*. *Crit Rev Microbiol*, 2020. **46**(1): p. 78-99.
102. Moller, A.G., R.A. Petit, 3rd, and T.D. Read, *Species-Scale Genomic Analysis of Staphylococcus aureus Genes Influencing Phage Host Range and Their Relationships to Virulence and Antibiotic Resistance Genes*. *mSystems*, 2022. **7**(1): p. e0108321.
103. Doron, S., et al., *Systematic discovery of antiphage defense systems in the microbial pangenome*. *Science*, 2018. **359**(6379).
104. Merabishvili, M., et al., *Quality-controlled small-scale production of a well-defined bacteriophage cocktail for use in human clinical trials*. *PLoS One*, 2009. **4**(3): p. e4944.
105. Lehman, S.M., et al., *Design and Preclinical Development of a Phage Product for the Treatment of Antibiotic-Resistant Staphylococcus aureus Infections*. *Viruses*, 2019. **11**(1).
106. McCallin, S., et al., *Current State of Compassionate Phage Therapy*. *Viruses*, 2019. **11**(4).
107. Kutateladze, M. and R. Adamia, *Phage therapy experience at the Eliava Institute*. *Med Mal Infect*, 2008. **38**(8): p. 426-30.
108. Rhoads, D.D., et al., *Bacteriophage therapy of venous leg ulcers in humans: results of a phase I safety trial*. *J Wound Care*, 2009. **18**(6): p. 237-8, 240-3.
109. Wright, A., et al., *A controlled clinical trial of a therapeutic bacteriophage preparation in chronic otitis due to antibiotic-resistant Pseudomonas aeruginosa; a preliminary report of efficacy*. *Clin Otolaryngol*, 2009. **34**(4): p. 349-57.
110. Jurczak-Kurek, A., et al., *Biodiversity of bacteriophages: morphological and biological properties of a large group of phages isolated from urban sewage*. *Sci Rep*, 2016. **6**: p. 34338.
111. Gonzalez-Menendez, E., et al., *Comparative analysis of different preservation techniques for the storage of Staphylococcus phages aimed for the industrial development of phage-based antimicrobial products*. *PLoS One*, 2018. **13**(10): p. e0205728.
112. Lubowska, N., et al., *Characterization of the Three New Kayviruses and Their Lytic Activity Against Multidrug-Resistant Staphylococcus aureus*. *Microorganisms*, 2019. **7**(10).
113. Van Norman, G.A., *Drugs, Devices, and the FDA: Part I: An Overview of Approval Processes for Drugs*. *JACC Basic Transl Sci*, 2016. **1**(3): p. 170-179.

114. Chang, R.Y.K., et al., *Storage stability of inhalable phage powders containing lactose at ambient conditions*. Int J Pharm, 2019. **560**: p. 11-18.
115. Kim, H.Y., et al., *Bacteriophage-Delivering Hydrogels: Current Progress in Combating Antibiotic Resistant Bacterial Infection*. Antibiotics (Basel), 2021. **10**(2).
116. Astudillo, A., et al., *Nebulization effects on structural stability of bacteriophage PEV 44*. Eur J Pharm Biopharm, 2018. **125**: p. 124-130.
117. Leung, S.S.Y., et al., *Jet nebulization of bacteriophages with different tail morphologies - Structural effects*. Int J Pharm, 2019. **554**: p. 322-326.
118. Semler, D.D., et al., *Aerosol phage therapy efficacy in Burkholderia cepacia complex respiratory infections*. Antimicrob Agents Chemother, 2014. **58**(7): p. 4005-13.
119. Chang, R.Y., et al., *Production of highly stable spray dried phage formulations for treatment of Pseudomonas aeruginosa lung infection*. Eur J Pharm Biopharm, 2017. **121**: p. 1-13.
120. Leung, S.S.Y., et al., *Effects of storage conditions on the stability of spray dried, inhalable bacteriophage powders*. Int J Pharm, 2017. **521**(1-2): p. 141-149.
121. Chang, R.Y.K., et al., *Proof-of-Principle Study in a Murine Lung Infection Model of Antipseudomonal Activity of Phage PEV20 in a Dry-Powder Formulation*. Antimicrob Agents Chemother, 2018. **62**(2).
122. Trend, S., et al., *Use of a Primary Epithelial Cell Screening Tool to Investigate Phage Therapy in Cystic Fibrosis*. Front Pharmacol, 2018. **9**: p. 1330.
123. Ling, K.M., S.M. Stick, and A. Kicic, *Pulmonary bacteriophage and cystic fibrosis airway mucus: friends or foes?* Front Med (Lausanne), 2023. **10**: p. 1088494.
124. Borin, J.M., et al., *Comparison of bacterial suppression by phage cocktails, dual-receptor generalists, and coevolutionarily trained phages*. Evol Appl, 2023. **16**(1): p. 152-162.
125. Chadha, P., O.P. Katare, and S. Chhibber, *In vivo efficacy of single phage versus phage cocktail in resolving burn wound infection in BALB/c mice*. Microbial Pathogenesis, 2016. **99**: p. 68-77.
126. Lin, Y., et al., *Synergy of nebulized phage PEV20 and ciprofloxacin combination against Pseudomonas aeruginosa*. International journal of pharmaceutics, 2018. **551**(1-2): p. 158-165.
127. Chin, W.H., et al., *Bacteriophages evolve enhanced persistence to a mucosal surface*. Proc Natl Acad Sci U S A, 2022. **119**(27): p. e2116197119.
128. Carroll-Portillo, A. and H.C. Lin, *Exploring Mucin as Adjunct to Phage Therapy*. Microorganisms, 2021. **9**(3).
129. Ren, H., N.P. Birch, and V. Suresh, *An Optimised Human Cell Culture Model for Alveolar Epithelial Transport*. PLoS One, 2016. **11**(10): p. e0165225.
130. Garratt, L.W., et al., *Determinants of culture success in an airway epithelium sampling program of young children with cystic fibrosis*. Exp Lung Res, 2014. **40**(9): p. 447-59.
131. Martinovich, K.M., et al., *Conditionally reprogrammed primary airway epithelial cells maintain morphology, lineage and disease specific functional characteristics*. Sci Rep, 2017. **7**(1): p. 17971.
132. Looi, K., et al., *Effect of human rhinovirus infection on airway epithelium tight junction protein disassembly and transepithelial permeability*. Exp Lung Res, 2016. **42**(7): p. 380-395.
133. Cafora, M., et al., *Phages as immunomodulators and their promising use as anti-inflammatory agents in a cfr loss-of-function zebrafish model*. J Cyst Fibros, 2020.
134. Forrest, O.A., et al., *Frontline Science: Pathological conditioning of human neutrophils recruited to the airway milieu in cystic fibrosis*. J Leukoc Biol, 2018. **104**(4): p. 665-675.
135. Lepper, P.M., et al., *Clinical implications of antibiotic-induced endotoxin release in septic shock*. Intensive Care Med, 2002. **28**(7): p. 824-33.
136. Prazak, J., et al., *Benefits of Aerosolized Phages for the Treatment of Pneumonia Due to Methicillin-Resistant Staphylococcus aureus: An Experimental Study in Rats*. J Infect Dis, 2022. **225**(8): p. 1452-1459.

137. Valente, L.G., et al., *Searching for synergy: combining systemic daptomycin treatment with localised phage therapy for the treatment of experimental pneumonia due to MRSA*. BMC Res Notes, 2021. **14**(1): p. 381.
138. Dufour, N., et al., *The Lysis of Pathogenic Escherichia coli by Bacteriophages Releases Less Endotoxin Than by beta-Lactams*. Clin Infect Dis, 2017. **64**(11): p. 1582-1588.
139. Dufour, N., et al., *Phage Therapy of Pneumonia Is Not Associated with an Overstimulation of the Inflammatory Response Compared to Antibiotic Treatment in Mice*. Antimicrob Agents Chemother, 2019. **63**(8).
140. Jeon, J. and D. Yong, *Two Novel Bacteriophages Improve Survival in Galleria mellonella Infection and Mouse Acute Pneumonia Models Infected with Extensively Drug-Resistant Pseudomonas aeruginosa*. Appl Environ Microbiol, 2019. **85**(9).
141. Wang, Z., et al., *SLPW: A Virulent Bacteriophage Targeting Methicillin-Resistant Staphylococcus aureus In vitro and In vivo*. Front Microbiol, 2016. **7**: p. 934.
142. Prazak, J., et al., *Bacteriophages Improve Outcomes in Experimental Staphylococcus aureus Ventilator-associated Pneumonia*. Am J Respir Crit Care Med, 2019. **200**(9): p. 1126-1133.
143. Huff, W.E., et al., *Evaluation of aerosol spray and intramuscular injection of bacteriophage to treat an Escherichia coli respiratory infection*. Poult Sci, 2003. **82**(7): p. 1108-12.
144. Carmody, L.A., et al., *Efficacy of bacteriophage therapy in a model of Burkholderia cenocepacia pulmonary infection*. J Infect Dis, 2010. **201**(2): p. 264-71.
145. Morello, E., et al., *Pulmonary bacteriophage therapy on Pseudomonas aeruginosa cystic fibrosis strains: first steps towards treatment and prevention*. PLoS One, 2011. **6**(2): p. e16963.
146. Fothergill, J.L., et al., *Pseudomonas aeruginosa adaptation in the nasopharyngeal reservoir leads to migration and persistence in the lungs*. Nat Commun, 2014. **5**: p. 4780.
147. Muller, S., et al., *Poorly Cross-Linked Peptidoglycan in MRSA Due to mecA Induction Activates the Inflammasome and Exacerbates Immunopathology*. Cell Host Microbe, 2015. **18**(5): p. 604-12.
148. Alemayehu, D., et al., *Bacteriophages phiMR299-2 and phiNH-4 can eliminate Pseudomonas aeruginosa in the murine lung and on cystic fibrosis lung airway cells*. mBio, 2012. **3**(2): p. e00029-12.
149. Nir-Paz, R., et al., *Successful Treatment of Antibiotic-resistant, Poly-microbial Bone Infection With Bacteriophages and Antibiotics Combination*. Clin Infect Dis, 2019. **69**(11): p. 2015-2018.
150. Secor, P.R., et al., *Effect of acute predation with bacteriophage on intermicrobial aggression by Pseudomonas aeruginosa*. PLoS One, 2017. **12**(6): p. e0179659.
151. Park, K., K.E. Cha, and H. Myung, *Observation of inflammatory responses in mice orally fed with bacteriophage T7*. J Appl Microbiol, 2014. **117**(3): p. 627-33.
152. Jault, P., et al., *Efficacy and tolerability of a cocktail of bacteriophages to treat burn wounds infected by Pseudomonas aeruginosa (PhagoBurn): a randomised, controlled, double-blind phase 1/2 trial*. Lancet Infect Dis, 2019. **19**(1): p. 35-45.
153. Junge, S., et al., *Factors Associated with Worse Lung Function in Cystic Fibrosis Patients with Persistent Staphylococcus aureus*. PLoS One, 2016. **11**(11): p. e0166220.
154. Breuer, O., et al., *Changing Prevalence of Lower Airway Infections in Young Children with Cystic Fibrosis*. Am J Respir Crit Care Med, 2019. **200**(5): p. 590-599.
155. Hommes, J.W. and B.G.J. Surewaard, *Intracellular Habitation of Staphylococcus aureus: Molecular Mechanisms and Prospects for Antimicrobial Therapy*. Biomedicines, 2022. **10**(8).
156. Idrees, M., et al., *Staphylococcus aureus Biofilm: Morphology, Genetics, Pathogenesis and Treatment Strategies*. Int J Environ Res Public Health, 2021. **18**(14).
157. Philipson, C.W., et al., *Characterizing Phage Genomes for Therapeutic Applications*. Viruses, 2018. **10**(4).
158. Glonti, T. and J.P. Pirnay, *In Vitro Techniques and Measurements of Phage Characteristics That Are Important for Phage Therapy Success*. Viruses, 2022. **14**(7).

159. Turner, D., et al., *Phage Annotation Guide: Guidelines for Assembly and High-Quality Annotation*. Phage (New Rochelle), 2021. **2**(4): p. 170-182.
160. Turner, D., A.M. Kropinski, and E.M. Adriaenssens, *A Roadmap for Genome-Based Phage Taxonomy*. Viruses, 2021. **13**(3).
161. Millard, A.S. and Andrew, *Phage Genome Annotation: Where to Begin and End*. PHAGE, 2021. **2**(4): p. 183-193.
162. Abedon, S., *Phage therapy pharmacology: calculating phage dosing*. Adv Appl Microbiol, 2011. **77**: p. 1-40.
163. Loc-Carrillo, C. and S.T. Abedon, *Pros and cons of phage therapy*. Bacteriophage, 2011. **1**(2): p. 111-114.
164. Liu, D., et al., *The Safety and Toxicity of Phage Therapy: A Review of Animal and Clinical Studies*. Viruses, 2021. **13**(7).
165. Doub, J.B., et al., *Salvage Bacteriophage Therapy for a Chronic MRSA Prosthetic Joint Infection*. Antibiotics (Basel), 2020. **9**(5).
166. Gilbey, T., et al., *Adjunctive bacteriophage therapy for prosthetic valve endocarditis due to Staphylococcus aureus*. Med J Aust, 2019. **211**(3): p. 142-143 e1.
167. Jakociune, D. and A. Moodley, *A Rapid Bacteriophage DNA Extraction Method*. Methods Protoc, 2018. **1**(3).
168. Kutter, E., *Phage Host Range and Efficiency of Plating*, in *Bacteriophages: Methods and Protocols, Volume 1: Isolation, Characterization, and Interactions*, M.R.J. Clokie and A.M. Kropinski, Editors. 2009, Humana Press: Totowa, NJ. p. 141-149.
169. Todaro, G.J. and H. Green, *Quantitative studies of the growth of mouse embryo cells in culture and their development into established lines*. J Cell Biol, 1963. **17**(2): p. 299-313.
170. Gordillo Altamirano, F.L. and J.J. Barr, *Phage Therapy in the Postantibiotic Era*. Clinical microbiology reviews, 2019. **32**(2): p. e00066-18.
171. Clokie, M.R., et al., *Phages in nature*. Bacteriophage, 2011. **1**(1): p. 31-45.
172. Han, J.E., et al., *Isolation and characterization of a Myoviridae bacteriophage against Staphylococcus aureus isolated from dairy cows with mastitis*. Res Vet Sci, 2013. **95**(2): p. 758-63.
173. Khan Mirzaei, M. and A.S. Nilsson, *Isolation of phages for phage therapy: a comparison of spot tests and efficiency of plating analyses for determination of host range and efficacy*. PLoS One, 2015. **10**(3): p. e0118557.
174. Rasool, M.H., et al., *Isolation, Characterization, and Antibacterial Activity of Bacteriophages Against Methicillin-Resistant Staphylococcus aureus in Pakistan*. Jundishapur J Microbiol, 2016. **9**(10): p. e36135.
175. Wintachai, P., et al., *Isolation and Characterization of a Phage Infecting Multidrug-Resistant Acinetobacter baumannii in A549 Alveolar Epithelial Cells*. Viruses, 2022. **14**(11): p. 2561.
176. Batinovic, S., et al., *Bacteriophages in Natural and Artificial Environments*. Pathogens, 2019. **8**(3).
177. Ottawa, K., et al., *Abundance, diversity, and dynamics of viruses on microorganisms in activated sludge processes*. Microb Ecol, 2007. **53**(1): p. 143-52.
178. Rihtman, B., et al., *Assessing Illumina technology for the high-throughput sequencing of bacteriophage genomes*. PeerJ, 2016. **4**: p. e2055.
179. Lin, B., J. Hui, and H. Mao, *Nanopore Technology and Its Applications in Gene Sequencing*. Biosensors (Basel), 2021. **11**(7).
180. Rhoads, A. and K.F. Au, *PacBio Sequencing and Its Applications*. Genomics Proteomics Bioinformatics, 2015. **13**(5): p. 278-89.
181. Bankevich, A., et al., *SPAdes: a new genome assembly algorithm and its applications to single-cell sequencing*. J Comput Biol, 2012. **19**(5): p. 455-77.
182. Afiahayati, K. Sato, and Y. Sakakibara, *MetaVelvet-SL: an extension of the Velvet assembler to a de novo metagenomic assembler utilizing supervised learning*. DNA research : an international journal for rapid publication of reports on genes and genomes, 2015. **22**(1): p. 69-77.
183. Wick, R.R., et al., *Unicycler: Resolving bacterial genome assemblies from short and long sequencing reads*. PLOS Computational Biology, 2017. **13**(6): p. e1005595.

184. Christie, G.E. and T. Dokland, *Pirates of the Caudovirales*. Virology, 2012. **434**(2): p. 210-21.
185. Hawkins, N.C., et al., *Shape shifter: redirection of prolate phage capsid assembly by staphylococcal pathogenicity islands*. Nat Commun, 2021. **12**(1): p. 6408.
186. Schneider, C.A., W.S. Rasband, and K.W. Eliceiri, *NIH Image to ImageJ: 25 years of image analysis*. Nat Methods, 2012. **9**(7): p. 671-5.
187. Bushnell, B., J. Rood, and E. Singer, *BBMerge - Accurate paired shotgun read merging via overlap*. PLoS One, 2017. **12**(10): p. e0185056.
188. . 2010.
189. Nayfach, S., et al., *CheckV assesses the quality and completeness of metagenome-assembled viral genomes*. Nat Biotechnol, 2021. **39**(5): p. 578-585.
190. Ladner, J.T., et al., *Standards for sequencing viral genomes in the era of high-throughput sequencing*. mBio, 2014. **5**(3): p. e01360-14.
191. Cook, R., et al., *INrastructure for a PHAge REference Database: Identification of Large-Scale Biases in the Current Collection of Cultured Phage Genomes*. Phage (New Rochelle), 2021. **2**(4): p. 214-223.
192. Camacho, C., et al., *BLAST+: architecture and applications*. BMC Bioinformatics, 2009. **10**: p. 421.
193. Seemann, T., *Prokka: rapid prokaryotic genome annotation*. Bioinformatics, 2014. **30**(14): p. 2068-9.
194. Terzian, P., et al., *PHROG: families of prokaryotic virus proteins clustered using remote homology*. NAR Genom Bioinform, 2021. **3**(3): p. lqab067.
195. Strancar, V., et al., *Isolation and in vitro characterization of novel S. epidermidis phages for therapeutic applications*. Front Cell Infect Microbiol, 2023. **13**: p. 1169135.
196. Beamud, B., et al., *Genetic determinants of host tropism in Klebsiella phages*. Cell Rep, 2023. **42**(2): p. 112048.
197. Torsten, S., *Abricate*. 2023.
198. Feldgarden, M., et al., *AMRFinderPlus and the Reference Gene Catalog facilitate examination of the genomic links among antimicrobial resistance, stress response, and virulence*. Sci Rep, 2021. **11**(1): p. 12728.
199. Feldgarden, M., et al., *Validating the AMRFinder Tool and Resistance Gene Database by Using Antimicrobial Resistance Genotype-Phenotype Correlations in a Collection of Isolates*. Antimicrob Agents Chemother, 2019. **63**(11).
200. Turner, D., et al., *Abolishment of morphology-based taxa and change to binomial species names: 2022 taxonomy update of the ICTV bacterial viruses subcommittee*. Arch Virol, 2023. **168**(2): p. 74.
201. de Gier, C., et al., *PCV7- and PCV10-Vaccinated Otitis-Prone Children in New Zealand Have Similar Pneumococcal and Haemophilus influenzae Densities in Their Nasopharynx and Middle Ear*. Vaccines (Basel), 2019. **7**(1).
202. Montgomery, S., *Extraction of high molecular weight DNA from nasal lining fluid*. protocols.io, 2023.
203. Kolmogorov, M., et al., *Assembly of long, error-prone reads using repeat graphs*. Nat Biotechnol, 2019. **37**(5): p. 540-546.
204. Walker, B.J., et al., *Pilon: an integrated tool for comprehensive microbial variant detection and genome assembly improvement*. PLoS One, 2014. **9**(11): p. e112963.
205. Deghorain, M. and L. Van Melderen, *The Staphylococci phages family: an overview*. Viruses, 2012. **4**(12): p. 3316-35.
206. Parks, D.H., et al., *CheckM: assessing the quality of microbial genomes recovered from isolates, single cells, and metagenomes*. Genome Res, 2015. **25**(7): p. 1043-55.
207. Ajuebor, J., et al., *Comparison of Staphylococcus Phage K with Close Phage Relatives Commonly Employed in Phage Therapeutics*. Antibiotics (Basel), 2018. **7**(2).
208. Ramesh, N., et al., *Effect of various bacteriological media on the plaque morphology of Staphylococcus and Vibrio phages*. Access Microbiology, 2019. **1**(4): p. e000036.
209. Gonzalez-Menendez, E., et al., *Optimizing Propagation of Staphylococcus aureus Infecting Bacteriophage vB_SauM-phiIPLA-RODI on Staphylococcus xylosoy Using Response Surface Methodology*. Viruses, 2018. **10**(4).

210. Coombs, G.W., et al., *Diversity of bacteriophages encoding Panton-Valentine leukocidin in temporally and geographically related Staphylococcus aureus*. PLoS One, 2020. **15**(2): p. e0228676.
211. Kuntova, L., et al., *Staphylococcus aureus Prophage-Encoded Protein Causes Abortive Infection and Provides Population Immunity against Kayviruses*. mBio, 2023. **14**(2): p. e0249022.
212. Peng, C., et al., *Silviavirus phage MR003 displays a broad host range against methicillin-resistant Staphylococcus aureus of human origin*. Appl Microbiol Biotechnol, 2019. **103**(18): p. 7751-7765.
213. Tabassum, R., et al., *TSP, a virulent Podovirus, can control the growth of Staphylococcus aureus for 12 h*. Sci Rep, 2022. **12**(1): p. 10008.
214. Cui, Z., et al., *Characterization and complete genome of the virulent Myoviridae phage JD007 active against a variety of Staphylococcus aureus isolates from different hospitals in Shanghai, China*. Virol J, 2017. **14**(1): p. 26.
215. Leskinen, K., et al., *Characterization of vB_SauM-fRuSau02, a Twort-Like Bacteriophage Isolated from a Therapeutic Phage Cocktail*. Viruses, 2017. **9**(9).
216. Bin Jang, H., et al., *Taxonomic assignment of uncultivated prokaryotic virus genomes is enabled by gene-sharing networks*. Nat Biotechnol, 2019. **37**(6): p. 632-639.
217. Kitamura, N., et al., *Characterization of two newly isolated Staphylococcus aureus bacteriophages from Japan belonging to the genus Silviavirus*. Arch Virol, 2020. **165**(10): p. 2355-2359.
218. Nirmal Kumar, G.P., et al., *Use of prophage free host for achieving homogenous population of bacteriophages: new findings*. Virus Res, 2012. **169**(1): p. 182-7.
219. Moller, A.G., J.A. Lindsay, and T.D. Read, *Determinants of Phage Host Range in Staphylococcus Species*. Appl Environ Microbiol, 2019. **85**(11).
220. Russell, D.A., *Sequencing, Assembling, and Finishing Complete Bacteriophage Genomes*. Methods Mol Biol, 2018. **1681**: p. 109-125.
221. Garneau, J.R., et al., *PhageTerm: a tool for fast and accurate determination of phage termini and packaging mechanism using next-generation sequencing data*. Sci Rep, 2017. **7**(1): p. 8292.
222. Kelly, D., et al., *Prevention of Staphylococcus aureus biofilm formation and reduction in established biofilm density using a combination of phage K and modified derivatives*. Lett Appl Microbiol, 2012. **54**(4): p. 286-91.
223. Kelly, D., et al., *Development of a broad-host-range phage cocktail for biocontrol*. Bioeng Bugs, 2011. **2**(1): p. 31-7.
224. Hyman, P., *Phages for Phage Therapy: Isolation, Characterization, and Host Range Breadth*. Pharmaceuticals (Basel), 2019. **12**(1).
225. Labiris, N.R. and M.B. Dolovich, *Pulmonary drug delivery. Part I: physiological factors affecting therapeutic effectiveness of aerosolized medications*. Br J Clin Pharmacol, 2003. **56**(6): p. 588-99.
226. Neopane, P., et al., *In vitro biofilm formation by Staphylococcus aureus isolated from wounds of hospital-admitted patients and their association with antimicrobial resistance*. Int J Gen Med, 2018. **11**: p. 25-32.
227. Katoh, K. and D.M. Standley, *MAFFT multiple sequence alignment software version 7: improvements in performance and usability*. Mol Biol Evol, 2013. **30**(4): p. 772-80.
228. Shannon, P., et al., *Cytoscape: a software environment for integrated models of biomolecular interaction networks*. Genome Res, 2003. **13**(11): p. 2498-504.
229. Elnaggar, A., et al., *ProtTrans: Toward Understanding the Language of Life Through Self-Supervised Learning*. IEEE Trans Pattern Anal Mach Intell, 2022. **44**(10): p. 7112-7127.
230. Boeckeaerts, D., et al., *Identification of Phage Receptor-Binding Protein Sequences with Hidden Markov Models and an Extreme Gradient Boosting Classifier*. Viruses, 2022. **14**(6).
231. Soding, J., A. Biegert, and A.N. Lupas, *The HHpred interactive server for protein homology detection and structure prediction*. Nucleic Acids Res, 2005. **33**(Web Server issue): p. W244-8.

232. Takeuchi, I., et al., *The Presence of Two Receptor-Binding Proteins Contributes to the Wide Host Range of Staphylococcal Twort-Like Phages*. Appl Environ Microbiol, 2016. **82**(19): p. 5763-74.
233. Kaneko, J., et al., *Identification of ORF636 in phage phiSLT carrying Panton-Valentine leukocidin genes, acting as an adhesion protein for a poly(glycerophosphate) chain of lipoteichoic acid on the cell surface of Staphylococcus aureus*. J Bacteriol, 2009. **191**(14): p. 4674-80.
234. Steinegger, M. and J. Soding, *MMseqs2 enables sensitive protein sequence searching for the analysis of massive data sets*. Nat Biotechnol, 2017. **35**(11): p. 1026-1028.
235. Shimoyama, Y., *pyGenomeViz: A genome visualization python package for comparative genomics*. 2022.
236. Moller, A.G., et al., *Genes Influencing Phage Host Range in Staphylococcus aureus on a Species-Wide Scale*. mSphere, 2021. **6**(1).
237. Zhang, M., et al., *The Life Cycle Transitions of Temperate Phages: Regulating Factors and Potential Ecological Implications*. Viruses, 2022. **14**(9).
238. Cairns, B.J., et al., *Quantitative models of in vitro bacteriophage-host dynamics and their application to phage therapy*. PLoS Pathog, 2009. **5**(1): p. e1000253.
239. Hsieh, S.E., et al., *Wide host range and strong lytic activity of Staphylococcus aureus lytic phage Stau2*. Appl Environ Microbiol, 2011. **77**(3): p. 756-61.
240. Kolenda, C., et al., *Phage Therapy against Staphylococcus aureus: Selection and Optimization of Production Protocols of Novel Broad-Spectrum Silviavirus Phages*. Pharmaceutics, 2022. **14**(9).
241. Save, J., et al., *Bacteriophages Combined With Subtherapeutic Doses of Flucloxacillin Act Synergistically Against Staphylococcus aureus Experimental Infective Endocarditis*. J Am Heart Assoc, 2022. **11**(3): p. e023080.
242. Jurado, A., et al., *Understanding the Mechanisms That Drive Phage Resistance in Staphylococci to Prevent Phage Therapy Failure*. Viruses, 2022. **14**(5).
243. Abdallah, K., A. Tharwat, and R. Gharieb, *High efficacy of a characterized lytic bacteriophage in combination with thyme essential oil against multidrug-resistant Staphylococcus aureus in chicken products*. Iran J Vet Res, 2021. **22**(1): p. 24-32.
244. Jonczyk-Matysiak, E., et al., *Factors determining phage stability/activity: challenges in practical phage application*. Expert Rev Anti Infect Ther, 2019. **17**(8): p. 583-606.
245. Jonczyk, E., et al., *The influence of external factors on bacteriophages--review*. Folia Microbiol (Praha), 2011. **56**(3): p. 191-200.
246. Vandenneuvel, D., et al., *Feasibility of spray drying bacteriophages into respirable powders to combat pulmonary bacterial infections*. Eur J Pharm Biopharm, 2013. **84**(3): p. 578-82.
247. Liu, K., et al., *Impact of relative humidity and collection media on mycobacteriophage D29 aerosol*. Appl Environ Microbiol, 2012. **78**(5): p. 1466-72.
248. Alves, D.R., et al., *Combined use of bacteriophage K and a novel bacteriophage to reduce Staphylococcus aureus biofilm formation*. Appl Environ Microbiol, 2014. **80**(21): p. 6694-703.
249. Rees, P.J. and B.A. Fry, *The morphology of staphylococcal bacteriophage K and DNA metabolism in infected Staphylococcus aureus*. J Gen Virol, 1981. **53**(Pt 2): p. 293-307.
250. Le Guellec, S., et al., *Administration of Bacteriophages via Nebulization during Mechanical Ventilation: In Vitro Study and Lung Deposition in Macaques*. Viruses, 2023. **15**(3).
251. Guillon, A., et al., *Inhaled bacteriophage therapy in a porcine model of pneumonia caused by Pseudomonas aeruginosa during mechanical ventilation*. Br J Pharmacol, 2021. **178**(18): p. 3829-3842.
252. Bodner, K., A.L. Melkonian, and M.W. Covert, *The Enemy of My Enemy: New Insights Regarding Bacteriophage-Mammalian Cell Interactions*. Trends Microbiol, 2020.
253. Bernheim, A. and R. Sorek, *The pan-immune system of bacteria: antiviral defence as a community resource*. Nat Rev Microbiol, 2020. **18**(2): p. 113-119.
254. Broniewski, J.M., et al., *The effect of phage genetic diversity on bacterial resistance evolution*. ISME J., 2020. **14**(3): p. 828-836.

255. Coulter, L.B., et al., *Effect of bacteriophage infection in combination with tobramycin on the emergence of resistance in Escherichia coli and Pseudomonas aeruginosa biofilms*. *Viruses*, 2014. **6**(10): p. 3778-3786.
256. Drilling, A.J., et al., *Long-Term Safety of Topical Bacteriophage Application to the Frontal Sinus Region*. *Front Cell Infect Microbiol*, 2017. **7**: p. 49.
257. Labrie, S.J., J.E. Samson, and S. Moineau, *Bacteriophage resistance mechanisms*. *Nat. Rev. Microbiol.*, 2010. **8**(5): p. 317-27.
258. Moulton-Brown, C.E. and V.-P. Friman, *Rapid evolution of generalized resistance mechanisms can constrain the efficacy of phage–antibiotic treatments*. *Evolutionary Applications*, 2018. **11**(9): p. 1630-1641.
259. Oechslin, F., *Resistance Development to Bacteriophages Occurring during Bacteriophage Therapy*. *Viruses*, 2018. **10**(7).
260. Wright, R.C.T., et al., *Cross-resistance is modular in bacteria–phage interactions*. *PLoS Biol.*, 2018. **16**(10): p. e2006057.
261. Sunagar, R., S.A. Patil, and R.K. Chandrakanth, *Bacteriophage therapy for Staphylococcus aureus bacteremia in streptozotocin-induced diabetic mice*. *Res Microbiol*, 2010. **161**(10): p. 854-60.
262. Shivshetty, N., et al., *Experimental protection of diabetic mice against Lethal P. aeruginosa infection by bacteriophage*. *Biomed Res Int*, 2014. **2014**: p. 793242.
263. Villarroel, J., et al., *HostPhinder: A Phage Host Prediction Tool*. *Viruses*, 2016. **8**(5).
264. Versoza, C.J. and S.P. Pfeifer, *Computational Prediction of Bacteriophage Host Ranges*. *Microorganisms*, 2022. **10**(1).
265. Aggarwal, S., et al., *An ensemble method for prediction of phage-based therapy against bacterial infections*. *Front Microbiol*, 2023. **14**: p. 1148579.
266. De Soyza, A., et al., *Developing an international Pseudomonas aeruginosa reference panel*. *MicrobiologyOpen*, 2013. **2**(6): p. 1010-1023.
267. Moreland, R., et al., *Complete Genome Sequence of Staphylococcus aureus Myophage Maine*. *Microbiol Resour Announc*, 2019. **8**(40).
268. D'Souza, R., et al., *Complete Genome Sequence of Broad-Host-Range Staphylococcus aureus Myophage ESa1*. *Microbiol Resour Announc*, 2020. **9**(30).
269. Senevirathne, A., et al., *Complete genome sequence analysis of a novel Staphylococcus phage StAPI and proposal of a new species in the genus Silviavirus*. *Arch Virol*, 2017. **162**(7): p. 2145-2148.
270. Flores, V., et al., *Comparative genomic analysis of Pseudomonas aeruginosa phage PaMx25 reveals a novel siphovirus group related to phages infecting hosts of different taxonomic classes*. *Arch. Virol.*, 2017. **162**(8): p. 2345-2355.
271. Jamal, M., et al., *Characterization of Siphoviridae phage Z and studying its efficacy against multidrug-resistant Klebsiella pneumoniae planktonic cells and biofilm*. *J Med Microbiol*, 2015. **64**(Pt 4): p. 454-462.
272. Zund, M., et al., *What Lies Beneath? Taking the Plunge into the Murky Waters of Phage Biology*. *mSystems*, 2023. **8**(1): p. e0080722.
273. Kebriaei, R., et al., *Optimization of Phage-Antibiotic Combinations against Staphylococcus aureus Biofilms*. *Microbiol Spectr*, 2023. **11**(3): p. e0491822.
274. Hietala, V., et al., *The Removal of Endo- and Enterotoxins From Bacteriophage Preparations*. *Front Microbiol*, 2019. **10**: p. 1674.
275. Estrella, L.A., et al., *Characterization of novel Staphylococcus aureus lytic phage and defining their combinatorial virulence using the OmniLog(R) system*. *Bacteriophage*, 2016. **6**(3): p. e1219440.
276. Guo, Y., et al., *Characterization of Two Pseudomonas aeruginosa Viruses vB_PaeM_SCUT-S1 and vB_PaeM_SCUT-S2*. *Viruses*, 2019. **11**(4): p. 318.
277. Chan, H.K. and R.Y.K. Chang, *Inhaled Delivery of Anti-Pseudomonas Phages to Tackle Respiratory Infections Caused by Superbugs*. *J Aerosol Med Pulm Drug Deliv*, 2022. **35**(2): p. 73-82.
278. Chow, M.Y.T., et al., *Pharmacokinetics and Time-Kill Study of Inhaled Antipseudomonal Bacteriophage Therapy in Mice*. *Antimicrob Agents Chemother*, 2020. **65**(1).

279. Regulski, K., P. Champion-Arnaud, and J. Gabard, *Bacteriophage manufacturing: From early twentieth-century processes to current GMP*, in *Bacteriophages: Biology, Technology, Therapy*, D.R. Harper, et al., Editors. 2018, Springer International Publishing: Cham. p. 1-31.
280. Bretaudeau, L., et al., *Good Manufacturing Practice (GMP) Compliance for Phage Therapy Medicinal Products*. *Front Microbiol*, 2020. **11**: p. 1161.
281. Pabary, R., et al., *Antipseudomonal Bacteriophage Reduces Infective Burden and Inflammatory Response in Murine Lung*. *Antimicrob Agents Chemother*, 2016. **60**(2): p. 744-51.
282. Takemura-Uchiyama, I., et al., *Experimental phage therapy against lethal lung-derived septicemia caused by Staphylococcus aureus in mice*. *Microbes Infect*, 2014. **16**(6): p. 512-7.
283. Ngassam-Tchamba, C., et al., *In vitro and in vivo assessment of phage therapy against Staphylococcus aureus causing bovine mastitis*. *J Glob Antimicrob Resist*, 2020. **22**: p. 762-770.
284. Shi, Y., et al., *Safety and Efficacy of a Phage, kpsk3, in an in vivo Model of Carbapenem-Resistant Hypermucoviscous Klebsiella pneumoniae Bacteremia*. *Front Microbiol*, 2021. **12**: p. 613356.
285. Ujmajuridze, A., et al., *Adapted Bacteriophages for Treating Urinary Tract Infections*. *Front Microbiol*, 2018. **9**: p. 1832.
286. Duplessis, C., et al., *Refractory Pseudomonas bacteremia in a 2-year-old sterilized by bacteriophage therapy*. *J. Pediatric. Infect. Dis. Soc.*, 2018. **7**(3): p. 253-256.
287. Fong, S.A., et al., *Activity of bacteriophages in removing biofilms of Pseudomonas aeruginosa isolates from chronic rhinosinusitis patients*. *Front. Cell. Infect. Microbiol.*, 2017. **7**: p. 418-418.
288. Drilling, A., et al., *Safety and efficacy of topical bacteriophage and ethylenediaminetetraacetic acid treatment of Staphylococcus aureus infection in a sheep model of sinusitis*. *Int Forum Allergy Rhinol*, 2014. **4**(3): p. 176-86.
289. Chung, K.M., S.C. Nang, and S.S. Tang, *The Safety of Bacteriophages in Treatment of Diseases Caused by Multidrug-Resistant Bacteria*. *Pharmaceuticals (Basel)*, 2023. **16**(10).
290. Brix, A., et al., *Animal Models to Translate Phage Therapy to Human Medicine*. *International journal of molecular sciences*, 2020. **21**(10): p. 3715.
291. Chang, R.Y.K., et al., *Proof-of-Principle Study in a Murine Lung Infection Model of Antipseudomonal Activity of Phage PEV20 in a Dry-Powder Formulation*. *Antimicrobial Agents and Chemotherapy*, 2018. **62**(2): p. e01714-17.
292. Izadpanah, M. and H. Khalili, *Antibiotic regimens for treatment of infections due to multidrug-resistant Gram-negative pathogens: An evidence-based literature review*. *J Res Pharm Pract*, 2015. **4**(3): p. 105-14.
293. Kahl, B.C., et al., *agr-dependent bacterial interference has no impact on long-term colonization of Staphylococcus aureus during persistent airway infection of cystic fibrosis patients*. *J Clin Microbiol*, 2003. **41**(11): p. 5199-201.
294. Kicic, A., et al., *Intrinsic biochemical and functional differences in bronchial epithelial cells of children with asthma*. *Am J Respir Crit Care Med*, 2006. **174**(10): p. 1110-8.
295. Alphons Gwatimba, Y.K., *BIMANA*. 2023.
296. Kumar, P., A. Nagarajan, and P.D. Uchil, *Analysis of Cell Viability by the Lactate Dehydrogenase Assay*. *Cold Spring Harb Protoc*, 2018. **2018**(6).
297. Sutanto, E.N., et al., *Innate inflammatory responses of pediatric cystic fibrosis airway epithelial cells*. *American Journal of Respiratory Cell and Molecular Biology*, 2011. **44**(6): p. 761-767.
298. Landwehr, K.R., et al., *Respiratory Health Effects of In Vivo Sub-Chronic Diesel and Biodiesel Exhaust Exposure*. *Int J Mol Sci*, 2023. **24**(6).
299. *The jamovi project*. [computer software], 2023(jamovi (Version 2.3)).
300. Team, R.C., *R: A language and environment for statistical computing*. R Foundation for Statistical Computing, Vienna, Austria, 2022.
301. Virtanen, P., et al., *SciPy 1.0: fundamental algorithms for scientific computing in Python*. *Nat Methods*, 2020. **17**(3): p. 261-272.

302. Zhang, L., et al., *Staphylococcus aureus* Bacteriophage Suppresses LPS-Induced Inflammation in MAC-T Bovine Mammary Epithelial Cells. *Front Microbiol*, 2018. **9**: p. 1614.
303. Kiedrowski, M.R., et al., *Development of an in vitro colonization model to investigate Staphylococcus aureus interactions with airway epithelia*. *Cell Microbiol*, 2016. **18**(5): p. 720-32.
304. Kiedrowski, M.R., et al., *Staphylococcus aureus* Biofilm Growth on Cystic Fibrosis Airway Epithelial Cells Is Enhanced during Respiratory Syncytial Virus Coinfection. *mSphere*, 2018. **3**(4).
305. Murphy, M.P., et al., *The in vitro host cell immune response to bovine-adapted Staphylococcus aureus varies according to bacterial lineage*. *Sci Rep*, 2019. **9**(1): p. 6134.
306. O'Brien, G.J., et al., *Staphylococcus aureus* enterotoxins induce IL-8 secretion by human nasal epithelial cells. *Respir Res*, 2006. **7**(1): p. 115.
307. Yao, L., F.D. Lowy, and J.W. Berman, *Interleukin-8 gene expression in Staphylococcus aureus-infected endothelial cells*. *Infect Immun*, 1996. **64**(8): p. 3407-9.
308. Chekabab, S.M., et al., *Staphylococcus aureus* Inhibits IL-8 Responses Induced by *Pseudomonas aeruginosa* in Airway Epithelial Cells. *PLoS One*, 2015. **10**(9): p. e0137753.
309. Trend, S., et al., *Use of a primary epithelial cell screening tool to investigate phage therapy in cystic fibrosis*. *Frontiers in Pharmacology*, 2018. **9**(1330).
310. Skronska-Wasek, W., et al., *Polarized cytokine release from airway epithelium differentially influences macrophage phenotype*. *Mol Immunol*, 2021. **132**: p. 142-149.
311. Pezzulo, A.A., et al., *The air-liquid interface and use of primary cell cultures are important to recapitulate the transcriptional profile of in vivo airway epithelia*. *Am J Physiol Lung Cell Mol Physiol*, 2011. **300**(1): p. L25-31.
312. Shan, J., et al., *Bacteriophages are more virulent to bacteria with human cells than they are in bacterial culture; insights from HT-29 cells*. *Sci Rep*, 2018. **8**(1): p. 5091.
313. Shen, G.H., et al., *Isolation and characterization of phikm18p, a novel lytic phage with therapeutic potential against extensively drug resistant *Acinetobacter baumannii**. *PLoS One*, 2012. **7**(10): p. e46537.
314. Khan Mirzaei, M., et al., *Morphologically Distinct *Escherichia coli* Bacteriophages Differ in Their Efficacy and Ability to Stimulate Cytokine Release In Vitro*. *Front Microbiol*, 2016. **7**: p. 437.
315. Gangell, C., et al., *Inflammatory responses to individual microorganisms in the lungs of children with cystic fibrosis*. *Clin. Infect. Dis.*, 2011. **53**(5): p. 425-32.
316. Keiser, N.W., et al., *Defective innate immunity and hyperinflammation in newborn cystic fibrosis transmembrane conductance regulator-knockout ferret lungs*. *Am J Respir Cell Mol Biol*, 2015. **52**(6): p. 683-94.
317. Chmiel, J.F. and P.B. Davis, *State of the art: why do the lungs of patients with cystic fibrosis become infected and why can't they clear the infection?* *Respir Res*, 2003. **4**(1): p. 8.
318. Hector, A., et al., *Microbial colonization and lung function in adolescents with cystic fibrosis*. *Journal of Cystic Fibrosis*, 2016. **15**(3): p. 340-349.
319. Barr, J.J., et al., *Bacteriophage adhering to mucus provide a non-host-derived immunity*. *Proc Natl Acad Sci U S A*, 2013. **110**(26): p. 10771-6.
320. Rothschild-Rodriguez, D., et al., *Phage-encoded carbohydrate-interacting proteins in the human gut*. *Front Microbiol*, 2022. **13**: p. 1083208.
321. Fraser, J.S., K.L. Maxwell, and A.R. Davidson, *Immunoglobulin-like domains on bacteriophage: weapons of modest damage?* *Curr Opin Microbiol*, 2007. **10**(4): p. 382-7.
322. Huang, J., et al., *Salmonella phage CKT1 significantly relieves the body weight loss of chicks by normalizing the abnormal intestinal microbiome caused by hypervirulent *Salmonella Pullorum**. *Poult Sci*, 2022. **101**(3): p. 101668.
323. Han, B.G., et al., *Markers of glycemic control in the mouse: comparisons of 6-h- and overnight-fasted blood glucoses to Hb A1c*. *Am J Physiol Endocrinol Metab*, 2008. **295**(4): p. E981-6.

324. Casimir, G.J., et al., *The Acid-Base Balance and Gender in Inflammation: A Mini-Review*. Front Immunol, 2018. **9**: p. 475.
325. Bouda, J., et al., *Blood acid-base and plasma electrolyte values in healthy ostriches: the effect of age and sex*. Res Vet Sci, 2009. **87**(1): p. 26-8.
326. Huaux, F., et al., *A profibrotic function of IL-12p40 in experimental pulmonary fibrosis*. J Immunol, 2002. **169**(5): p. 2653-61.
327. Fernandes de Souza, W.D., et al., *Lung Inflammation Induced by Inactivated SARS-CoV-2 in C57BL/6 Female Mice Is Controlled by Intranasal Instillation of Vitamin D*. Cells, 2023. **12**(7).
328. Eisfeld, A.J., et al., *C57BL/6J and C57BL/6NJ Mice Are Differentially Susceptible to Inflammation-Associated Disease Caused by Influenza A Virus*. Front Microbiol, 2018. **9**: p. 3307.
329. Oz, H.H., et al., *Recruited monocytes/macrophages drive pulmonary neutrophilic inflammation and irreversible lung tissue remodeling in cystic fibrosis*. Cell Rep, 2022. **41**(11): p. 111797.
330. Waters, E.M., et al., *Phage therapy is highly effective against chronic lung infections with Pseudomonas aeruginosa*. Thorax, 2017. **72**(7): p. 666-667.
331. Pillarisetti, N., et al., *Infection, inflammation and lung function decline in infants with cystic fibrosis*. Am. J. Respir. Crit. Care Med., 2011. **184**(1): p. 75-81.
332. Cooper, A.M. and S.A. Khader, *IL-12p40: an inherently agonistic cytokine*. Trends Immunol, 2007. **28**(1): p. 33-8.
333. Mitchell, C., et al., *IFN-gamma acts on the airway epithelium to inhibit local and systemic pathology in allergic airway disease*. J Immunol, 2011. **187**(7): p. 3815-20.
334. Malaviya, R., et al., *Repeated exposure of house dust mite induces progressive airway inflammation in mice: Differential roles of CCL17 and IL-13*. Pharmacol Res Perspect, 2021. **9**(3): p. e00770.
335. Zarcone, M.C., et al., *Cellular response of mucociliary differentiated primary bronchial epithelial cells to diesel exhaust*. Am J Physiol Lung Cell Mol Physiol, 2016. **311**(1): p. L111-23.
336. Lambert, A.L., et al., *Ultrafine carbon black particles enhance respiratory syncytial virus-induced airway reactivity, pulmonary inflammation, and chemokine expression*. Toxicol Sci, 2003. **72**(2): p. 339-46.
337. Hatfull, G.F. and R.W. Hendrix, *Bacteriophages and their genomes*. Curr Opin Virol, 2011. **1**(4): p. 298-303.
338. Chibani, C.M., et al., *Classifying the Unclassified: A Phage Classification Method*. Viruses, 2019. **11**(2).
339. Brix, A., et al., *Animal Models to Translate Phage Therapy to Human Medicine*. Int J Mol Sci, 2020. **21**(10).
340. Weber-Dabrowska, B., et al., *Bacteriophage Procurement for Therapeutic Purposes*. Front Microbiol, 2016. **7**: p. 1177.
341. Pirnay, J.P., et al., *The Magistral Phage*. Viruses, 2018. **10**(2).
342. Zaczek, M., et al., *Phage Therapy in Poland - a Centennial Journey to the First Ethically Approved Treatment Facility in Europe*. Front Microbiol, 2020. **11**: p. 1056.
343. Capparelli, R., et al., *Experimental phage therapy against Staphylococcus aureus in mice*. Antimicrob Agents Chemother, 2007. **51**(8): p. 2765-73.
344. Oduor, J.M.O., et al., *Experimental phage therapy against haematogenous multi-drug resistant Staphylococcus aureus pneumonia in mice*. Afr J Lab Med, 2016. **5**(1): p. 435.
345. Moraru, C., A. Varsani, and A.M. Kropinski, *VIRIDIC-A Novel Tool to Calculate the Intergenomic Similarities of Prokaryote-Infecting Viruses*. Viruses, 2020. **12**(11).
346. Martinez de Tejada, G., et al., *Lipoproteins/peptides are sepsis-inducing toxins from bacteria that can be neutralized by synthetic anti-endotoxin peptides*. Sci Rep, 2015. **5**: p. 14292.
347. Schooley, R.T., et al., *Development and Use of Personalized Bacteriophage-Based Therapeutic Cocktails To Treat a Patient with a Disseminated Resistant Acinetobacter baumannii Infection*. Antimicrob Agents Chemother, 2017. **61**(10).
348. Rubalskii, E., et al., *Bacteriophage Therapy for Critical Infections Related to Cardiothoracic Surgery*. Antibiotics (Basel), 2020. **9**(5).

349. Ahmad-Mansour, N., et al., *Staphylococcus aureus* Toxins: An Update on Their Pathogenic Properties and Potential Treatments. *Toxins* (Basel), 2021. **13**(10).
350. Matsuzaki, S., et al., *Experimental protection of mice against lethal Staphylococcus aureus infection by novel bacteriophage phi MR11*. *J Infect Dis*, 2003. **187**(4): p. 613-24.
351. Kissner, T.L., et al., *Staphylococcal enterotoxin A induction of pro-inflammatory cytokines and lethality in mice is primarily dependent on MyD88*. *Immunology*, 2010. **130**(4): p. 516-26.
352. Janik, E., et al., *Biological Toxins as the Potential Tools for Bioterrorism*. *Int J Mol Sci*, 2019. **20**(5).
353. Jerome, G., *Prophage in Phage Manufacturing: Is the Risk Overrated Compared to Other Therapies or Food?* *Antibiotics* (Basel), 2020. **9**(8).
354. Suh, G.A., et al., *Considerations for the Use of Phage Therapy in Clinical Practice*. *Antimicrob Agents Chemother*, 2022. **66**(3): p. e0207121.
355. Gibson, S.B., et al., *Constructing and Characterizing Bacteriophage Libraries for Phage Therapy of Human Infections*. *Front Microbiol*, 2019. **10**: p. 2537.
356. Hitchcock, N.M., et al., *Current Clinical Landscape and Global Potential of Bacteriophage Therapy*. *Viruses*, 2023. **15**(4).
357. Aslam, S., et al., *Early clinical experience of bacteriophage therapy in 3 lung transplant recipients*. *Am. J. Transplant.*, 2019. **19**(9): p. 2631-2639.
358. Kutter, E., et al., *Phage therapy in clinical practice: treatment of human infections*. *Curr Pharm Biotechnol*, 2010. **11**(1): p. 69-86.
359. Luong, T., A.C. Salabarria, and D.R. Roach, *Phage Therapy in the Resistance Era: Where Do We Stand and Where Are We Going?* *Clin Ther*, 2020. **42**(9): p. 1659-1680.
360. Strathdee, S.A., et al., *Phage therapy: From biological mechanisms to future directions*. *Cell*, 2023. **186**(1): p. 17-31.
361. Liu, J., et al., *Evaluation of Potential ARG Packaging by Two Environmental T7-Like Phage during Phage-Host Interaction*. *Viruses*, 2020. **12**(10).
362. Eyer, L., et al., *Structural protein analysis of the polyvalent staphylococcal bacteriophage 812*. *Proteomics*, 2007. **7**(1): p. 64-72.
363. Glowacka-Rutkowska, A., et al., *The Ability of Lytic Staphylococcal Podovirus vB_SauP_phiAGO1.3 to Coexist in Equilibrium With Its Host Facilitates the Selection of Host Mutants of Attenuated Virulence but Does Not Preclude the Phage Antistaphylococcal Activity in a Nematode Infection Model*. *Front Microbiol*, 2018. **9**: p. 3227.
364. Löffler, B., et al., *Staphylococcus aureus panton-valentine leukocidin is a very potent cytotoxic factor for human neutrophils*. *PLoS Pathog*, 2010. **6**(1): p. e1000715.
365. Mirdita, M., et al., *ColabFold: making protein folding accessible to all*. *Nat Methods*, 2022. **19**(6): p. 679-682.
366. Mavrich, T.N., et al., *pdm_utils: a SEA-PHAGES MySQL phage database management toolkit*. *Bioinformatics*, 2021. **37**(16): p. 2464-2466.
367. Lamine, J.G., R.J. DeJong, and S.M. Nelesen, *PhamDB: a web-based application for building Phamerator databases*. *Bioinformatics*, 2016. **32**(13): p. 2026-8.
368. Kazmierczak, Z., A. Gorski, and K. Dabrowska, *Facing antibiotic resistance: Staphylococcus aureus phages as a medical tool*. *Viruses*, 2014. **6**(7): p. 2551-70.
369. Zhang, B., et al., *Interactions between Jumbo Phage SA1 and Staphylococcus: A Global Transcriptomic Analysis*. *Microorganisms*, 2022. **10**(8).
370. Abd-Allah, I.M., et al., *An Anti-MRSA Phage From Raw Fish Rinse: Stability Evaluation and Production Optimization*. *Front Cell Infect Microbiol*, 2022. **12**: p. 904531.
371. Mishra, A.K., et al., *Isolation, characterization and therapeutic potential assessment of bacteriophages virulent to Staphylococcus aureus associated with goat mastitis*. *Iran J Vet Res*, 2014. **15**(4): p. 320-5.
372. Young, G.R., et al., *Optimisation and Application of a Novel Method to Identify Bacteriophages in Maternal Milk and Infant Stool Identifies Host-Phage Communities Within Preterm Infant Gut*. *Front Pediatr*, 2022. **10**: p. 856520.

373. Borin, J.M., et al., *Coevolutionary phage training leads to greater bacterial suppression and delays the evolution of phage resistance*. Proc Natl Acad Sci U S A, 2021. **118**(23).
374. O'Flaherty, S., et al., *Potential of the polyvalent anti-Staphylococcus bacteriophage K for control of antibiotic-resistant staphylococci from hospitals*. Appl Environ Microbiol, 2005. **71**(4): p. 1836-42.
375. Weigele, P. and E.A. Raleigh, *Biosynthesis and Function of Modified Bases in Bacteria and Their Viruses*. Chem Rev, 2016. **116**(20): p. 12655-12687.
376. Tisza, M.J., et al., *Roving methyltransferases generate a mosaic epigenetic landscape and influence evolution in Bacteroides fragilis group*. Nat Commun, 2023. **14**(1): p. 4082.
377. Li, P.E., et al., *Enabling the democratization of the genomics revolution with a fully integrated web-based bioinformatics platform*. Nucleic Acids Res, 2017. **45**(1): p. 67-80.
378. Turner, N.A., et al., *Methicillin-resistant Staphylococcus aureus: an overview of basic and clinical research*. Nat Rev Microbiol, 2019. **17**(4): p. 203-218.
379. Xia, G. and C. Wolz, *Phages of Staphylococcus aureus and their impact on host evolution*. Infect Genet Evol, 2014. **21**: p. 593-601.
380. Arndt, D., et al., *PHASTER: a better, faster version of the PHAST phage search tool*. Nucleic Acids Res, 2016. **44**(W1): p. W16-21.
381. Deutsch, D.R., et al., *Extra-Chromosomal DNA Sequencing Reveals Episomal Prophages Capable of Impacting Virulence Factor Expression in Staphylococcus aureus*. Front Microbiol, 2018. **9**: p. 1406.
382. Dedrick, R.M., et al., *Engineered bacteriophages for treatment of a patient with a disseminated drug-resistant Mycobacterium abscessus*. Nat Med, 2019. **25**(5): p. 730-733.
383. Dams, D., et al., *Engineering of receptor-binding proteins in bacteriophages and phage tail-like bacteriocins*. Biochem Soc Trans, 2019. **47**(1): p. 449-460.
384. Latka, A., et al., *Engineering the Modular Receptor-Binding Proteins of Klebsiella Phages Switches Their Capsule Serotype Specificity*. mBio, 2021. **12**(3).
385. Dunne, M., et al., *Reprogramming Bacteriophage Host Range through Structure-Guided Design of Chimeric Receptor Binding Proteins*. Cell Reports, 2019. **29**(5): p. 1336-1350.e4.
386. Assad-Garcia, N., et al., *Cross-Genus "Boot-Up" of Synthetic Bacteriophage in Staphylococcus aureus by Using a New and Efficient DNA Transformation Method*. Appl Environ Microbiol, 2022. **88**(3): p. e0148621.
387. Brettin, T., et al., *RASTtk: a modular and extensible implementation of the RAST algorithm for building custom annotation pipelines and annotating batches of genomes*. Sci Rep, 2015. **5**: p. 8365.
388. Nami, Y., N. Imeni, and B. Panahi, *Application of machine learning in bacteriophage research*. BMC Microbiol, 2021. **21**(1): p. 193.
389. Loewa, A., J.J. Feng, and S. Hedtrich, *Human disease models in drug development*. Nat Rev Bioeng, 2023: p. 1-15.
390. Gray, M., S. Guido, and A. Kugadas, *Editorial: The use of large animal models to improve pre-clinical translational research*. Front Vet Sci, 2022. **9**: p. 1086912.
391. Hockenberry, A.J. and C.O. Wilke, *BACPHLIP: predicting bacteriophage lifestyle from conserved protein domains*. PeerJ, 2021. **9**: p. e11396.
392. Ren, J., et al., *VirFinder: a novel k-mer based tool for identifying viral sequences from assembled metagenomic data*. Microbiome, 2017. **5**(1): p. 69.
393. Yves Briers, D.B., Michiel Stock, Jesus Oteo-Gonzalez, Rafael Sanjuan, Pilar Dominigo-Calap, Bernard De Baets, *Actionable prediction of Klebsiella phage-host specificity at the subspecies level*. 2023.
394. Styles, K.M., A.T. Brown, and A.P. Sagona, *A Review of Using Mathematical Modeling to Improve Our Understanding of Bacteriophage, Bacteria, and Eukaryotic Interactions*. Front Microbiol, 2021. **12**: p. 724767.
395. Storey, J., et al., *A Structured Approach to Optimizing Animal Model Selection for Human Translation: The Animal Model Quality Assessment*. ILAR J, 2021. **62**(1-2): p. 66-76.

396. Dominguez-Oliva, A., et al., *The Importance of Animal Models in Biomedical Research: Current Insights and Applications*. Animals (Basel), 2023. **13**(7).
397. Stoehr, L.C., et al., *Assessment of a panel of interleukin-8 reporter lung epithelial cell lines to monitor the pro-inflammatory response following zinc oxide nanoparticle exposure under different cell culture conditions*. Part Fibre Toxicol, 2015. **12**: p. 29.
398. Battin, C., et al., *A human monocytic NF-kappaB fluorescent reporter cell line for detection of microbial contaminants in biological samples*. PLoS One, 2017. **12**(5): p. e0178220.
399. Young, M.J., et al., *Phage Therapy for Diabetic Foot Infection: A Case Series*. Clin Ther, 2023. **45**(8): p. 797-801.
400. Van Nieuwenhuysse, B., et al., *A Case of In Situ Phage Therapy against Staphylococcus aureus in a Bone Allograft Polymicrobial Biofilm Infection: Outcomes and Phage-Antibiotic Interactions*. Viruses, 2021. **13**(10).
401. Ferriol-Gonzalez, C. and P. Domingo-Calap, *Phages for Biofilm Removal*. Antibiotics (Basel), 2020. **9**(5).
402. Azeredo, J., P. Garcia, and Z. Drulis-Kawa, *Targeting biofilms using phages and their enzymes*. Curr Opin Biotechnol, 2021. **68**: p. 251-261.
403. Dakheel, K.H., et al., *Genomic analyses of two novel biofilm-degrading methicillin-resistant Staphylococcus aureus phages*. BMC Microbiol, 2019. **19**(1): p. 114.
404. Schlafer, S. and R.L. Meyer, *Confocal microscopy imaging of the biofilm matrix*. J Microbiol Methods, 2017. **138**: p. 50-59.
405. Kong, C., et al., *Suppression of Staphylococcus aureus biofilm formation and virulence by a benzimidazole derivative, UM-C162*. Sci Rep, 2018. **8**(1): p. 2758.
406. Bano, S., et al., *Biofilms as Battlefield Armor for Bacteria against Antibiotics: Challenges and Combating Strategies*. Microorganisms, 2023. **11**(10).
407. Archer, N.K., et al., *Staphylococcus aureus biofilms: properties, regulation, and roles in human disease*. Virulence, 2011. **2**(5): p. 445-59.
408. Jean-Pierre, V., et al., *Biofilm Formation by Staphylococcus aureus in the Specific Context of Cystic Fibrosis*. Int J Mol Sci, 2022. **24**(1).
409. Kreisel, K., et al., *Risk factors for recurrence in patients with Staphylococcus aureus infections complicated by bacteremia*. Diagn Microbiol Infect Dis, 2006. **55**(3): p. 179-84.
410. Kolenda, C., et al., *Evaluation of the Activity of a Combination of Three Bacteriophages Alone or in Association with Antibiotics on Staphylococcus aureus Embedded in Biofilm or Internalized in Osteoblasts*. Antimicrob Agents Chemother, 2020. **64**(3).
411. Li, J., H. Zheng, and S.S.Y. Leung, *Potential of bacteriophage therapy in managing Staphylococcus aureus infections during chemotherapy for lung cancer patients*. Sci Rep, 2023. **13**(1): p. 9534.
412. Chatterjee, K., et al., *Doxorubicin cardiomyopathy*. Cardiology, 2010. **115**(2): p. 155-62.
413. Fong, K., et al., *How Broad Is Enough: The Host Range of Bacteriophages and Its Impact on the Agri-Food Sector*. Phage (New Rochelle), 2021. **2**(2): p. 83-91.
414. Aljayoussi, G., et al., *Pharmacokinetic-Pharmacodynamic modelling of intracellular Mycobacterium tuberculosis growth and kill rates is predictive of clinical treatment duration*. Sci Rep, 2017. **7**(1): p. 502.
415. Donnellan, S., et al., *Intracellular Pharmacodynamic Modeling Is Predictive of the Clinical Activity of Fluoroquinolones against Tuberculosis*. Antimicrob Agents Chemother, 2019. **64**(1).
416. Payne, R.J., D. Phil, and V.A. Jansen, *Phage therapy: the peculiar kinetics of self-replicating pharmaceuticals*. Clin Pharmacol Ther, 2000. **68**(3): p. 225-30.
417. Roach, D.R., et al., *Synergy between the host immune system and bacteriophage is essential for successful phage therapy against an acute respiratory pathogen*. Cell Host & Microbe, 2017. **22**(1): p. 38-47.e4.
418. Ooi, M.L., et al., *Safety and Tolerability of Bacteriophage Therapy for Chronic Rhinosinusitis Due to Staphylococcus aureus*. JAMA Otolaryngol Head Neck Surg, 2019. **145**(8): p. 723-729.

419. Oechslin, F., et al., *Synergistic interaction between phage therapy and antibiotics clears Pseudomonas aeruginosa infection in endocarditis and reduces virulence*. J. Infect. Dis., 2016. **215**(5): p. 703-712.
420. Li, N., et al., *Characterization of Phage Resistance and Their Impacts on Bacterial Fitness in Pseudomonas aeruginosa*. Microbiol Spectr, 2022. **10**(5): p. e0207222.
421. Torres-Barcelo, C., *Phage Therapy Faces Evolutionary Challenges*. Viruses, 2018. **10**(6).
422. Goldfarb, T., et al., *BREX is a novel phage resistance system widespread in microbial genomes*. EMBO J, 2015. **34**(2): p. 169-83.
423. Ofir, G., et al., *DISARM is a widespread bacterial defence system with broad anti-phage activities*. Nat Microbiol, 2018. **3**(1): p. 90-98.
424. Rohde, C., et al., *Expert Opinion on Three Phage Therapy Related Topics: Bacterial Phage Resistance, Phage Training and Prophages in Bacterial Production Strains*. Viruses, 2018. **10**(4).